

General Disclaimer

One or more of the Following Statements may affect this Document

- This document has been reproduced from the best copy furnished by the organizational source. It is being released in the interest of making available as much information as possible.
- This document may contain data, which exceeds the sheet parameters. It was furnished in this condition by the organizational source and is the best copy available.
- This document may contain tone-on-tone or color graphs, charts and/or pictures, which have been reproduced in black and white.
- This document is paginated as submitted by the original source.
- Portions of this document are not fully legible due to the historical nature of some of the material. However, it is the best reproduction available from the original submission.

(NASA-CR-159462) INTERACTIVE MULTI-MODE
BLADE IMPACT ANALYSIS Final Report, Jan.
1976 - Aug. 1977 and Feb. 1978 - Aug. 1978
(Hamilton Standard, Windsor Locks, Conn.)

N79-17858

301 p HC A16/MF A01

Unclas
CSCI 21E G3/07 16096

PREFACE

Contained in this report is the theoretical methodology used in developing an analysis for the response of blades subjected to soft-body impacts and a description of the computer program that was developed using the theory as its basis. This work was conducted at Hamilton Standard, Division of United Technologies Corporation, Windsor Locks, Connecticut, under NASA Lewis Research Center Contract No. NAS3-20091. The analysis was based upon three fields of study. The development of the modal equations was carried out by Messrs. W. W. Westervelt and N. E. Houtz. The development of the equations used for the missile model, based on studies of 2-dimensional and 3-dimensional fluid jets, was carried out by Dr. R. W. Cornell. The development of the interactive equations, geometry, general methodology and computer program was carried out by Mr. A. Alexander.

This program is an outgrowth of two analyses that were previously developed for the purpose of studying problems of a similar nature: a 3-mode beam impact analysis and a multi-mode beam impact analysis. The program utilizes an improved missile model that is interactively coupled with blade motion, which is more consistent with observation. It takes into account local deformation at the impact area, blade camber effects and the spreading of the impacted missile mass on the blade surface. In addition, it accomodates plate-type mode shapes. The analysis represents a significant improvement in the development of the methodology for evaluating potential fan blade materials with regard to foreign object impact resistance.

The work was monitored by Dr. C. C. Chamis of NASA Lewis Research Center and was conducted during the periods January 1976 to August 1977 and February 1978 to July 1978.

TABLE OF CONTENTS

<u>SECTION</u>		<u>PAGE</u>
I	INTRODUCTION AND SUMMARY	1
	1.1 Background	1
	1.2 Objectives and Approach	1
	1.3 Summary and Conclusions	2
II	THEORY AND MATHEMATICAL FORMULATION	5
	2.1 Missile and Blade Geometry	5
	2.1.1 Planform Reference Frame	5
	2.1.2 In Plane/Out of Plane Reference Frame	6
	2.1.3 Blade and Missile Coordinates	6
	2.1.4 Impact Coordinates	10
	2.1.5 Relative Impact Velocity and Angle	11
	2.2 Development of an Improved Missile Model	12
	2.2.1 Definition of an Oblique Angle Impact of a Fluid Jet on a Surface	19
	2.2.2 Location of Forward and Backwash Flow Area Faces	22
	2.2.3 Pressure Distribution	24
	2.2.4 Effect of Blade Camber on Pressure	25
	2.3 Modal Analysis	28
	2.4 Basic Problem Flow Diagram	34
III	COMPUTER PROGRAM DESCRIPTION	35
	Correlation Between Theoretical and Coded Variables	36
	3.1 Main	37
	3.1.1 Input Variables	37
	3.1.2 Problem Initialization	38
	3.1.3 Printout of Initial Conditions	41
	3.1.4 Time Step Increment Entry Point	41

TABLE OF CONTENTS

<u>SECTION</u>	<u>PAGE</u>
3.1.5 Blade Chord Angle and Blade Segment Angles	41
3.1.6 Forward and Aft Points of Missile Sections	42
3.1.7 Missile-Blade Contact Points	42
3.1.8 Time Step Size	46
3.1.9 Relative Impact Velocity and Angle, and Adjusted Time Step Size	46
3.1.10 Impacting Missile Section Length	47
3.1.11 Node Pressures Due to Initial Impact	47
3.1.12 Node Pressures Resulting from Impacts During Previous Time Steps	48
3.1.13 In Plane and Out of Plane Node Forces	48
3.1.14 Modal Analysis	50
3.1.15 Time Update, Data Output, Return to 800 for Next Time Step	51
3.2 P3D-3D Pressure Distribution Integration	52
3.2.1 Input Variables	52
3.2.2 Discussion	52
3.3 LAMBDA - Iteration Solution for λ_2^1	52
3.3.1 Input Variables	52
3.3.2 Discussion	53
3.4 CAMBER - Calculation of Pressure Effects Due to Blade Curvature	54
3.4.1 Input Variables	54
3.4.2 Discussion	54
3.5 REGION - Determination of Blade Curvature Region	55
3.5.1 Input Variables	55
3.5.2 Discussion	56

TABLE OF CONTENTS

<u>SECTION</u>	<u>PAGE</u>
3.6 INCURV - Calculation of the Inverse of the Curvature Radius Corresponding to Region JCI	56
3.6.1 Input Variables	56
3.6.2 Discussion	56
3.7 PRESUR - Pressure Over a Node	56
3.7.1 Input Variables	56
3.7.2 2-D Pressure	57
3.7.3 3-D Pressure	57
3.7.4 Camber Effects	58
3.8 MODAL - Calculation of the Blade Response to the Loads on the Blade During A Time Step	58
3.8.1 Input Variables	58
3.8.2 Discussion	58
3.9 PRINTP - Pressure Distribution Printout	60
3.9.1 Input Variables	60
3.9.2 Discussion	60
3.10 PRINTV- Displacement and Stress Output Data Arrangement and Storage	60
3.10.1 Input Variables	60
3.10.2 Discussion	61
3.11 PRINTR - Displacement and Stress Printout	62
3.11.1 Input Variables	62
3.11.2 Discussion	62
3.12 PINIT - Initial Impact Force	62
3.12.1 Input Variables	62
3.12.2 Formation of Impacting Missile Portion	63
3.12.3 Impact Location, Relative Velocity and Relative Angle of Incidence	63

TABLE OF CONTENTS

<u>SECTION</u>	<u>PAGE</u>
3.12.4 Coefficients Associated With the Fluid Jet Model	64
3.12.5 Impact Force and Equivalent Pressure	64
3.13 Detailed Flow Diagrams	65
3.13.1 MAIN	66
3.13.2 P3D	77
3.13.3 LAMBDA	80
3.13.4 CAMBER	81
3.13.5 REGION	82
3.13.6 INCURV	83
3.13.7 PRESUR	84
3.13.8 MODAL	85
3.13.9 PINIT	86
IV INSTRUCTIONS ON THE USE OF THE PROGRAM	89
4.1 Problem Definition	89
4.2 Missile Description	91
4.3 Modal Data	92
4.4 Blade Description	95
4.5 Output	96
4.5.1 Pressure Distribution	96
4.5.2 Poor Convergence in Subroutine LAMBDA	96
4.5.3 Displacement and Stress	97
V DEMONSTRATION PROBLEMS	98
5.1 Impacts on Rigid Plates	98
5.2 30-Degree Impact of a 1 LB Sphere on a Flat Plate Simulated Q-Fan Blade	99
5.3 Recommendations	102
REFERENCES	103
BIBLIOGRAPHY	107
TABLES	109
APPENDICES	155

LIST OF TABLES

<u>TABLE NO.</u>		<u>PAGE</u>
I	EXPERIMENTAL IMPACT DATA	109
II	RELATIONSHIPS FOR 2D, 3D AND GENERAL SYMMETRICAL MISSILE MODELS	110
III	PRESSURE RATIOS FOR 25, 45 AND 90 DEGREE IMPACTS OF CYLINDRICAL MISSILES ON RIGID PLATES	111
IV	INPUT DATA TO MMBI PROGRAM FOR ANALYSIS OF 30 DEGREE IMPACT OF A 1 LB. SPHERICAL MISSILE	112
 <u>APPENDIX A</u>		
IA	PEAK PRESSURE AND ELAPSED TIME AT PEAK PRESSURE	157

LIST OF FIGURES

<u>FIGURE NO.</u>		<u>PAGE</u>
1	BLADE FACE MAPPED OUT ON PLANFORM PLANE	119
2	BLADE CROSS SECTION IN IP-OOP FRAME	120
3	BLADE SEGMENTS IN IP-OOP FRAME	121
4	MISSILE SECTIONS IN IP-OOP FRAME	122
5	MISSILE DEFINITION	123
6	INITIAL MISSILE AND BLADE GEOMETRY	124
7	MISSILE AND BLADE GEOMETRY DURING TIMES OF IMPACT	125
8	DETERMINATION OF BLADE SEGMENT TO BE HIT	126
9	TWO-DIMENSIONAL JET MISSILE PER SCHACH	127
10	STREAMFORM FOR 2D JET PER SCHACH	128
11	PRESSURE DISTRIBUTION FOR 2D JET - MEASURED, SCHACH AND APPROXIMATIONS	129
12	PRESSURE AND VELOCITY DISTRIBUTIONS FOR 60° IMPINGEMENT OF A 2D JET - SCHACH AND APPROXIMATIONS	130
13	PRESSURE DISTRIBUTIONS FOR A 15° 2D JET - SCHACH AND APPROXIMATIONS	131
14	LOCATIONS FOR A 2D JET OF IMPACT FORCE AND STAGNATION POINT - SCHACH AND APPROXIMATIONS	132
15	3D JET MISSILE MODEL PER SCHACH	133
16	PRESSURE DISTRIBUTION FOR A 3D JET - MEASURED AND SCHACH'S THEORY	134
17	NORMAL IMPINGEMENT OF A 3D JET - PRESSURE, STREAMFORM AND VELOCITY DISTRIBUTIONS (THEORY AND TEST)	135
18	3D JET LOCATIONS OF IMPACT FORCE AND STAGNATION POINT	136
19	VARYING MULTI-SEGMENT MISSILE	137
20	APPROXIMATION OF GENERAL SHAPED MISSILE FROM 2D AND 3D JETS	138
21	APPROXIMATED STREAMFORM PARAMETERS	139

LIST OF FIGURES (CONTINUED)

<u>FIGURE NO.</u>		<u>PAGE</u>
22	PATH AND LOCATION OF AN ELEMENTAL VOLUME OF FLUID	140
23	INITIAL AND FINAL FORM OF AN IMPACTING MISSILE PORTION	141
24	GENERAL IMPACTED MISSILE MASS DISTRIBUTION	142
25	SPREAD OF IMPACTED MISSILE MASS DISTRIBUTION WITH TIME	143
26	ELEMENTAL MASS VOLUME TRAVERSING A CURVED SURFACE	144
27	BLADE CAMBER CURVATURE GEOMETRY	145
28	MISSILE MODEL USED FOR IMPACTS ON RIGID TARGETS	146
29	PRESSURE DISTRIBUTION FOR 25° IMPACT ON RIGID TARGET - MEASURED AND MMBI RESULTS	147
30	PRESSURE DISTRIBUTION FOR 45° IMPACT ON RIGID TARGET - MEASURED AND MMBI RESULTS	148
31	PRESSURE DISTRIBUTION FOR 90° IMPACT ON RIGID TARGET - MEASURED AND MMBI RESULTS	149
32	FLAT PLATE SIMULATED Q-FAN BLADE MODEL	150
33	SIDE VIEW OF SPHERICAL MISSILE MODEL	151
34	CROSS SECTION OF SPHERICAL MISSILE MODEL	152
35	FLATWISE DISPLACEMENT RESPONSE OF SIMULATED Q-FAN BLADE - MEASURED AND MMBI RESULTS	153
36	TWIST RESPONSE OF SIMULATED Q-FAN BLADE - MEASURED AND MMBI RESULTS	154
 <u>APPENDIX A</u>		
1A	MODEL DISCRETIZATION FOR A TWO-DIMENSIONAL ELLIPTICAL FLUID MISSILE INTERSECTING A RIGID FLAT SURFACE	158
2A	AVERAGE IMPACT PRESSURE OVER THE IMPACTED SURFACE VS TIME	159

<u>FIGURE NO.</u>		<u>PAGE</u>
	<u>APPENDIX B</u>	
1B	APPROXIMATE 2D MISSILE	161
2B	APPROXIMATE 3D JET MISSILE	162
3B	PRESSURE ELLIPSE DIMENSIONS AND OFFSET OF IMPACT FORCE . . .	164
	<u>APPENDIX D</u>	
1D	DISTANCE OF RESULTANT LOAD FROM STAGNATION POINT FOR 3D IMPACTING JET MISSILE	170
	<u>APPENDIX E</u>	
1E	CORRECTION FACTORS FOR SPREADING AND PRESSURE LOADING FOR GENERAL, SYMMETRICAL JET MISSILE	175

APPENDICES

<u>APPENDIX</u>	<u>PAGE</u>
A - Spring-Mass Elemental Missile Model	155
B - Uniform Pressure, 2D & 3D Oblique Impacting Jet Missiles	160
C - Approximation for 2D Oblique Impacting Jet Missile. . .	165
D - Approximate 3D Oblique Impacting Jet Missile	167
E - General Symmetrical 3D, Oblique Impacting Jet Missile .	171
F - Supplementary Relationships for General Missile Model .	176
G - Listing of Computer Output Results for Demonstration Problem 5.2	180
H - Compiled Listing of Source Program and Subroutines. . .	252

NOMENCLATURE

- IP - Refers to the in-plane direction.
- OOP - Refers to the out-of-plane direction.
- \vec{V}_n - Directional vector on blade in the IP-OOP system. (length)
- A_n - Scalar length between nodes n and $n+1$ on the blade. (length)
- x_n, y_n - IP and OOP coordinates of a node on the blade. (length)
- θ_n - Angle between the IP axis and vector \vec{V}_n . (radians)
- \vec{U}_K - Directional vector along the missile length in the IP-OOP system. (length)
- B_K - Scalar length of vector \vec{U}_K . (length)
- x_K, y_K - IP and OOP coordinates of a point of the missile. (length)
- α_0 - Initial impact angle between the missile and blade chord. (radians)
- β - Angle between the vector \vec{U}_K and the IP axis. (radians)
- v_n - Magnitude of the velocity at node n of the blade. (length/time)
- ω_n - Magnitude of angular velocity of blade segment n about node n . (radians/time)
- v_n - Magnitude of relative missile velocity in the direction of \vec{V}_n . (length/time)
- v_K - Magnitude of relative missile velocity in the direction of \vec{U}_K . (length/time)
- v_i - Magnitude of relative impact velocity. (length/time)
- x_i, y_i - IP and OOP coordinates of the center of impact on the blade. (length)
- v_0 - Magnitude of missile velocity relative to the IP-OOP system. (length/time)
- α_K - Relative impact angle between missile and blade. (radians)
- ℓ - Distance measured from the location of the center of force of the impact to the point on the blade where the stream flow can be considered to be parallel to the surface of the blade. (length)

- f - Distance between the stagnation pressure point and the location of the center of force of impact. (length)
- g - Distance between the point of intersection of the missile center-line and the blade and the stagnation point. (length)
- a - Thickness of the missile. (length)
- λ_1 - Distance between the center of force of the impact and the initial position of the boundary defining the void formed on the positive side of the flow stream. (length)
- λ_2 - Distance between the center of force of the impact and the initial position of the boundary defining the void formed on the negative side of the flow stream. (length)
- P_0 - Stagnation pressure = $\frac{1}{2}\rho V^2$ (force/(length)²)
- ρ - Mass density of the missile. (mass/(length)³)
- γ_1 - Pressure decay constant in the positive side of the flow stream.
- γ_2 - Pressure decay constant in the negative side of the flow stream.
- P_1 - Pressure in the positive side of the flow stream. (force/(length)²)
- P_2 - Pressure in the negative side of the flow stream. (force/(length)²)
- $\{\phi\}_i$ - Displacement vector describing the i^{th} mode shape. (length)
- $\{S\}_i$ - Stress vector containing the chordwise, radial and shear components of stress for the i^{th} mode shape. (force/length)²)
- m_i - i^{th} modal mass (mass)
- β_i - Critical damping ratio associated with the i^{th} mode.
- q_i - Generalized coordinate associated with the i^{th} mode.
- ω_{oi} - Characteristic natural frequency of the i^{th} mode. (radians/time)
- ω - Damped natural frequency for the i^{th} mode. (radians/time)

SECTION I

INTRODUCTION AND SUMMARY

1.1 BACKGROUND

The availability of an accurate and reliable method for the impact analysis of aircraft engine fan blades can play a major part in designing these blades for FOD (Foreign Object Damage) resistance and in assessing new materials for blade applications. Over the past several years Hamilton Standard has developed under company funding two modal analysis methods based upon beam models. Improvements and extensions of these computerized methods, one of which is a Three Mode Model and the other a more sophisticated and comprehensive Multi-Mode Model, provide the basis for the present program.

1.2 OBJECTIVES AND APPROACH

The purpose of the Multi-Mode Blade Impact (MMBI) computer program described herein is to provide the analyst with a tool that enables him to study the transient effects of soft body impacts on blades exhibiting characteristic coupled modes. Included within this purpose are three major objectives:

- a) The development of a consistent missile model
- b) The ability of the program to model the spreading impacted missile mass with respect to time.
- c) To provide information on deformations, pressure distribution and stresses at the impact region of the blade, as well as over the entire blade.

The approach used in developing a missile model was based upon theoretical and experimental information associated with incident fluid jets on surfaces. The model is a general, symmetrical 3-dimensional fluid jet which is approximated by taking into account the combined effects of 2-dimensional and 3-dimensional fluid jets.

The spreading missile mass is modeled as an expanding oval consisting of a 2-dimensional streamform at its center and a 3-dimensional streamform at its outer limits.

With respect to the blade the program utilizes a 2-dimensional surface with mode shapes consisting of the coupled plate modes of vibration associated with the blade. By including the higher modes of the blade in the program, local deformations and stresses can be determined in the impact area.

1.3 SUMMARY AND CONCLUSIONS

The MMBI program is based upon a theoretical and experimental analysis of incident 2-dimensional and 3-dimensional fluid jets combined with the methods of modal response analysis. The geometrical representation of the problem is based upon 2 right-handed systems of reference. The entire surface of the blade is represented on a 2-dimensional planform model of the blade face upon which the pressure and impacted missile mass distribution is mapped out. The interaction between the missile and blade is represented in a 2-dimensional reference frame defined by the rotational axis of the blade and an axis lying in the plane of rotation. For consistency the program uses the methods of vector analysis to determine the missile and blade locations throughout the duration of the problem. The solution for blade response during each time step interval is obtained from a closed form solution of the uncoupled modal equations of the system, using the results of the previous time step as initial conditions.

During the impact event the blade and missile interaction program accounts for the following effects:

- a) local perturbations on relative impact angle and velocity
due to blade response
- b) initial and ending effects of the missile forward and aft shape
- c) pressure variations due to the blade face curvature.

The program provides an efficient method of analyzing the response of blades subjected to soft body impacts at a minimal cost to the user. Such problems as time step size, missile size variation, blade load variation and the spreading of the missile mass on the blade surface with time are handled as entirely internal problems to the program. The outputs available to the user include:

- 1) Pressure distribution variation with respect to time.
- 2) Gross blade displacements with respect to time.
- 3) Local deformations of the blade surface at the impact area.
- 4) Gross blade stresses with respect to time.
- 5) Local stresses at the impact area.

Detailed verification of the program is described in Sections 5.1 and 5.2 where results are presented for several cases that were analyzed using the MMBI program and compared with test data. The program was first used to analyze impacts of cylindrical missiles on rigid plates for 25, 45 and 90-degree impact angles. These runs were primarily a check on the computed pressure distribution and the spreading of the missile with respect to time. Within the accuracy of the test data, the program was able to predict both the shape and magnitude of the pressure distribution, corresponding to the three angles and, in general, showed good correlation with test.

The program was then used to analyze the response of a simulated blade subjected to a 600 ft/sec, 30-degree leading edge impact by a 1 pound, 3.75 inch diameter spherical missile. The blade consisted of a rigid, steel plate bolted onto a titanium spar. Comparison with test results obtained for the same problem show good correlation for the displacement of the blade. With respect to the blade twist, test data was available for angular motion at the blade tip while the MMBI program outputs this data at the impact

radius of the blade. A direct correlation for response of the blade in twist was therefore difficult, however a comparison of the response duration showed good agreement with test. In addition, by considering the modal aspects of the blade, the differences between test data at the blade tip versus calculated results at the impact radius are readily explained.

The results obtained for the demonstration problems presented in this report are encouraging. However, a full evaluation of the capabilities of the program should include a case which involves the effects of blade camber and local deformations at the impact area. Data for this case is available from tests performed by Hamilton Standard on missile impacts of the 3A Q-Fan Demo Blade under NASA Contract No. NAS3-17837.

SECTION II

THEORY AND MATHEMATICAL FORMULATION

The problem of multi-mode blade impact analysis can be organized into three separate phases:

1. - Definition of missile and blade geometry
2. - Definition of missile and load distribution
3. - Modal response of the blade.

Phase 1 involves an interaction with the results of Phase 3 so that the problem geometry can be updated at the end of each time step. Phase 2 consists of a further breakdown into three subcases:

- 2a. - Definition of a fluid jet impinging on a surface at an oblique angle.
- 2b. - Distribution of pressures at the nodal points describing the blade.
- 2c. - Effect of blade camber on pressure.

In Section 2.4 is a diagram depicting the basic problem flow, the details of which are discussed below.

2.1 MISSILE AND BLADE GEOMETRY

The MMBI program uses two geometric reference frames to develop the problem geometry.

2.1.1 Planform Reference Frame

To describe the distribution of the impacted missile mass on the blade face, the three dimensional surface of the face is mapped onto a flat plane (Fig. 1). The blade is untwisted and laid out on the plane such that the curved distance between adjacent points on the three-dimensional surface is preserved. Chordwise distance along the blade is taken along the abscissa and radial distance is taken along the ordinate. During each time step, the center of impact and stagnation pressure points are located on the planform representation of the blade face and the spreading missile mass is mapped out relative to these two points (Section 2.2.2).

2.1.2 In Plane (IP) / Out of Plane (OOP) Reference Frame

This reference system lies in a plane whose normal is parallel to the radial axis of the blade such that the coordinate system is a right-handed one, with the rotational axis of the blade taken as the ordinate (Out-Of-Plane or OOP axis) and the abscissa lying in the plane of rotation (In-Plane or IP axis) (Fig. 2). The contour of the blade face at the impact radial station is represented in this coordinate system by straight line segments connecting the nodes that lie on the surface of the face along the impact radial station.

2.1.3 Blade and Missile Coordinates

Each blade segment n is represented by a vector \vec{V}_n to establish the orientation of the surface between nodes n and $n+1$ relative to the IP-OOP system; see Fig. 3.

$$\vec{V}_n = A_n [\cos(\theta_n) \vec{ii} + \sin(\theta_n) \vec{jj}] \quad 2.1.3(a)$$

where A_n is the length of segment $(n, n+1)$ and is given by

$$A_n = \sqrt{(x_{n+1} - x_n)^2 + (y_{n+1} - y_n)^2}$$

and $\cos(\theta_n) = (x_{n+1} - x_n) / A_n$

$$\sin(\theta_n) = (y_{n+1} - y_n) / A_n$$

x represents the IP coordinate of a node

y represents the OOP coordinate of a node

\vec{ii} and \vec{jj} are unit vectors in the IP and OOP directions respectively.

Next, the forward and aft ends of the missile are located relative to the blade. The missile is sliced along its length into six sections (Fig. 4). Each missile section κ is described by a vector \vec{U}_κ of length B_κ and angle β relative to the IP axis. From Fig. 4

$$\vec{U}_\kappa = B_\kappa [\cos(\beta) \vec{ii} + \sin(\beta) \vec{jj}] \quad 2.1.3(b)$$

$$B_\kappa = \text{Length of missile section } \kappa = \sqrt{(x_\kappa - x'_\kappa)^2 + (y_\kappa - y'_\kappa)^2} \quad 2.1.3(c)$$

$$\cos(\beta) = (x_{\kappa} - x'_{\kappa}) / B_{\kappa}$$

$$\sin(\beta) = (y_{\kappa} - y'_{\kappa}) / B_{\kappa}$$

Initially, the points (x_{κ}, y_{κ}) and $(x'_{\kappa}, y'_{\kappa})$ are determined from input data. Referring to Figs. 2 and 5, the user inputs the parameters:

x_0 = IP coordinate of the missile centerline impact point

y_0 = OOP coordinate of the missile centerline impact point

α_0 = initial impact angle relative to blade chord line

R_{κ} = radial distance from missile centerline to centerline of missile section κ

r_{κ} = thickness of missile section κ

B_{κ} = length of missile section

D_{κ} = offset (toward the aft end of the missile) of the front face of missile section κ relative to the forward most point of the missile at the missile centerline

W_{κ} = width of missile section κ

*Note that $R_{\kappa} < 0$ for sections to the left of the centerline.

The initial blade chord angle, θ_0 , can now be calculated from the relation:

$$\theta_0 = \cos^{-1} \left[\frac{(x_{t.e.} - x_{l.e.})}{\sqrt{(x_{t.e.} - x_{l.e.})^2 + (y_{t.e.} - y_{l.e.})^2}} \right] \quad 2.1.3(d)$$

where: $x_{t.e.}$, $y_{t.e.}$ refer to the IP and OOP coordinates of the trailing edge.

and $x_{l.e.}$, $y_{l.e.}$ refer to the IP and OOP coordinates of the leading edge at the impact radial station (Fig. 6).

Note that there is a restriction that θ_0 be greater than 0 degrees and less than or equal to 90 degrees.

The absolute missile angle, β , is defined by

$$\beta = \theta_0 - \alpha_0 \quad 2.1.3(e)$$

For each missile section κ the coordinates, (x_κ, y_κ) and (x'_κ, y'_κ) of the forward and aft ends are given by

$$x_\kappa = x_0 + R_\kappa \sin(\beta) - D_\kappa \cos(\beta)$$

$$y_\kappa = y_0 - R_\kappa \cos(\beta) - D_\kappa \sin(\beta)$$

2.1.3(f)

$$x'_\kappa = x_\kappa - B_\kappa \cos(\beta)$$

$$y'_\kappa = y_\kappa - B_\kappa \sin(\beta)$$

For times greater than zero the points (x_κ, y_κ) and (x'_κ, y'_κ) are dependent on the missile velocity, the total time elapsed during the previous time step and the amount of missile section length that has impacted on the blade during the previous time step, Fig. 7. Assuming that at time t the forward and aft coordinates of missile section κ are given by $(x_{\kappa t}, y_{\kappa t})$ and $(x'_{\kappa t}, y'_{\kappa t})$, and that the missile velocity relative to the IP-OOP frame is V , the aft end of section κ moves forward by an amount $V\Delta t$, where Δt is the size of the time step. The coordinates of the aft point at time $t+\Delta t$ are given by:

$$x'_{\kappa}(t+\Delta t) = x'_{\kappa t} + V\Delta t \cos(\beta)$$

$$y'_{\kappa}(t+\Delta t) = y'_{\kappa t} + V\Delta t \sin(\beta)$$

2.1.3(g)

If, during the time t and $t+\Delta t$, a portion δ_κ of section κ impacted on the blade, then the length of section κ at time $t+\Delta t$ is

$$B_\kappa(t+\Delta t) = B_{\kappa t} - \delta_\kappa$$

and the coordinates of the forward point for section κ are given by

$$x_{\kappa(t+\Delta t)} = x_{\kappa t} + (V\Delta t - \delta_\kappa) \cos(\beta)$$

2.1.3(h)

$$y_{\kappa(t+\Delta t)} = y_{\kappa t} + (V\Delta t - \delta_\kappa) \sin(\beta)$$

By updating the length of missile section κ at the end of each time step, in the same manner described above, the missile size can be continuously reduced throughout the duration of impact.

Once the locations of the forward and aft points of missile section κ are established, the blade segment that is impacted by section κ can be determined as well as the IP and OOP coordinates of the impact. From Fig. 8 define the vectors

$$\begin{aligned}\vec{A}_\kappa &= (x_{n+1} - x'_\kappa) \vec{U} + (y_{n+1} - y'_\kappa) \vec{J} \\ \vec{A}'_\kappa &= (x_n - x'_\kappa) \vec{U} + (y_n - y'_\kappa) \vec{J} \\ \vec{B}_\kappa &= (x_\kappa - x_{n+1}) \vec{U} + (y_\kappa - y_{n+1}) \vec{J} \\ \vec{B}'_\kappa &= (x_\kappa - x_n) \vec{U} + (y_\kappa - y_n) \vec{J}\end{aligned}\tag{2.1.3(i)}$$

Using the expression 2.1.3(b) for \vec{U}_κ the following cross products are performed:

$$\begin{aligned}\vec{U}_\kappa \times \vec{A} &= C_\kappa \vec{z} \\ \vec{A}'_\kappa \times \vec{U}_\kappa &= C'_\kappa \vec{z}\end{aligned}\tag{2.1.3(j)}$$

where C_κ and C'_κ are scalar quantities and \vec{z} is a unit vector perpendicular to the IP-OOP plane. Observing the right-hand rule for cross products and referring to Fig. 8, it can be seen that a line passing through the points (x_κ, y_κ) and (x'_κ, y'_κ) will also pass between the nodes n and $n+1$ if both C_κ and C'_κ are greater than or equal to zero. This criterion is used to establish the blade segment that will be hit by missile section κ during a time step.

Furthermore, from the cross product:

$$\vec{B}_\kappa \times \vec{B}'_\kappa = D_\kappa \vec{z}\tag{2.1.3(k)}$$

(where D_κ is a scalar), it is seen that for:

$D_K > 0$: point (x_K, y_K) is behind the blade and the missile position will have to be adjusted by moving it aft along its centerline.

$D_K = 0$: point (x_K, y_K) is in contact with the blade.

$D_K < 0$: point (x_K, y_K) is in front of the blade and the missile position will have to be adjusted by moving it forward along its centerline.

2.1.4 Impact Coordinates

The location of the impact point for each missile section is determined by performing cross-products on vectors lying along the missile length and blade segment direction, respectively. A unit vector lying in the direction of the missile length is given by

$$\vec{K}_K = \cos(\beta) \vec{i} + \sin(\beta) \vec{j} \quad 2.1.4(a)$$

The vector \vec{L}_K which lies in the direction of the missile length between the point (x_K, y_K) and the impact point $(x_{iK}, y_{iK})_K$ is given by

$$\vec{L}_K = (x_K - x_{iK}) \vec{i} + (y_K - y_{iK}) \vec{j} \quad 2.1.4(b)$$

Performing the cross-product between \vec{L}_K and \vec{K}_K and noting that the two vectors are colinear results in the expression

$$(x_K - x_{iK}) \sin(\beta) - (y_K - y_{iK}) \cos(\beta) = 0 \quad 2.1.4(c)$$

In a similar manner consider the unit vector \vec{N}_n and the vector \vec{R}_n where

$$\begin{aligned} \vec{N}_n &= \cos(\theta_n) \vec{i} + \sin(\theta_n) \vec{j} \\ \vec{R}_n &= (x_{iK} - x_n) \vec{i} + (y_{iK} - y_n) \vec{j} \end{aligned} \quad 2.1.4(d)$$

Both of these vectors lie in the direction of blade segment n. Performing the cross-product between \vec{R}_n and \vec{N}_n results in the second expression involving (x_{iK}, y_{iK}) , i.e.

$$(x_{iK} - x_n) \sin(\theta_n) - (y_{iK} - y_n) \cos(\theta_n) = 0 \quad 2.1.4(e)$$

Solving equations 2.1.4(c) and (e) for x_{ik} and performing some trigonometric manipulations results in

$$x_{ik} = \frac{[(y_k - y_n) \cos(\beta) - x_k \sin(\beta)] \cos(\theta_n) + x_n \sin(\theta_n) \cos(\beta)}{\sin(\theta_n - \beta)} \quad 2.1.4(f)$$

Substitution of the result from 2.1.4(f) into either 2.1.4(c) or 2.1.4(e) will yield the value for y_{ik} .

2.1.5 Relative Velocity Impact and Angle

Consider the blade segment n with velocity vectors \vec{v}_n at node n and \vec{v}_{n+1} at node n+1 given by

$$\begin{aligned} \vec{v}_n &= \dot{x}_n \vec{u} + \dot{y}_n \vec{j} \\ \vec{v}_{n+1} &= \dot{x}_{n+1} \vec{u} + \dot{y}_{n+1} \vec{j} \end{aligned} \quad 2.1.5(a)$$

where the dot signifies the first derivative with respect to time. The angular velocity ω_n of blade segment n about node n is given by

$$\omega_n = \frac{\dot{x}_{n+1} - \dot{x}_n}{y_{n+1} - y_n} = \frac{\dot{y}_{n+1} - \dot{y}_n}{x_{n+1} - x_n} \quad 2.1.5(b)$$

The IP and OOP velocity components for a point (x_i, y_i) lying on blade segment n between nodes n and n+1, are given by

$$\begin{aligned} \dot{x}_i &= \dot{x}_n - (y_i - y_n) \omega_n \\ \dot{y}_i &= \dot{y}_n + (x_i - x_n) \omega_n \end{aligned} \quad 2.1.5(c)$$

$$\vec{v}_i = \dot{x}_i \vec{u} + \dot{y}_i \vec{j} \quad \text{or} \quad 2.1.5(d)$$

where \vec{v}_i is the velocity vector of point (x_i, y_i) . The component of \vec{v}_i in the direction of the missile length is determined from the dot product of 2.1.5(d) with the unit vector given by 2.1.4(a), i.e.

$$v_k = \dot{x}_i \cos(\beta) + \dot{y}_i \sin(\beta) \quad 2.1.5(e)$$

Similarly, using the first of the expressions 2.1.4(d), the magnitude of

the velocity for point (x_i, y_i) in the direction of blade segment n is given by:

$$v_n = \dot{x}_i \cos(\theta_n) + \dot{y}_i \sin(\theta_n) \quad 2.1.5(f)$$

The components of the relative impact velocity for missile section

κ impacting at point (x_i, y_i) are therefore given by

$$\begin{aligned} \dot{X}_\kappa &= (V_o - V_\kappa) \cos(\beta) - V_n \cos(\theta_n) \\ \dot{Y}_\kappa &= (V_o - V_\kappa) \sin(\beta) - V_n \sin(\theta_n) \end{aligned} \quad 2.1.5(g)$$

where V_o is the velocity of the missile relative to the IP-OOP frame.

From the dot product of the vector with components given by 2.1.5(g) and the unit vector in the direction of blade segment n , the relative impact angle, α_κ , is given by:

$$\alpha_\kappa = \cos^{-1} \left[\frac{\dot{X}_\kappa \cos(\theta_n) + \dot{Y}_\kappa \sin(\theta_n)}{\sqrt{(\dot{X}_\kappa)^2 + (\dot{Y}_\kappa)^2}} \right] \quad 2.1.5(h)$$

where the quantity $\sqrt{(\dot{X}_\kappa)^2 + (\dot{Y}_\kappa)^2}$ is the magnitude of the relative impact velocity.

2.2 DEVELOPMENT OF AN IMPROVED MISSILE MODEL

Experimental impact tests using birds show that they behave essentially as a fluid during impact; see Reference 4. However, in view of the short length of the missile, it would also be desirable for the model to account for the transient effects caused by the beginning and ending of the missile.

A literature search was conducted with the hope that an existing solution could be found for one or both of the above problems; see references and bibliography. Analytical solutions for the steady state, cylindrical case of a 90° jet and near 90° jet impinging on a flat surface and for the steady state two-dimensional

case of an angled jet impinging on a flat surface, were found in the literature; see References 5 and 6 and Reference 7, respectively. Several papers were found on the numerical solution of the transient/steady state case for cylinders and spheres impacting rigid plates at 90° ; see References 8 and 9. However, no solution was found for either the general case of a steady state or the transient/steady state fluid missile impacting obliquely on a flat plate. Several papers actually commented about the lack of such a general solution; see for example References 10 and 11. Numerous papers and reports were found dealing with both steady state transient oblique incidence of fluid jets, which could be used for a data base and for evaluating any analytical results; see References 6, 7 and 11 through 16. A summary of the scope and information available from these tests is given in Table I.

Because no general solution of the jet impact problem was found, the following five possible approaches for developing a missile model were considered:

1. Develop an empirical model based on available test data
2. Develop a three-dimensional analysis of an incompressible inviscid jet of fluid
3. Develop a finite element transient/steady state solution
4. Develop a finite difference transient/steady state analysis of liquid droplets
5. Develop a transient/steady state analysis based on a spring-mass model

The first approach was considered one of last resort and would be difficult to do without a theoretical basis. The development of a rigorous hydrodynamic model of an incompressible jet impinging on a flat plate did not appear feasible considering the comments in the literature. The labor and coding complexity required to develop a finite element solution was beyond the scope of the present program; see Reference 17. The finite difference program COMCAM

for the impact of liquid droplets looked promising, see Reference 14; however, at present the program handles only normal impacts and, therefore, would have to be generalized for the oblique impacts analyzed by the MMBI program. The fifth approach of developing a three-dimensional transient/steady state analysis of a compressible, inviscid liquid slug using a spring-mass model appeared to be the most amenable approach and, therefore, was pursued.

The development of the analysis of the spring-beam missile model was performed by Dr. Brice N. Cassenti of UTRC and is given in Appendix A. In this approach the finite fluid slug of arbitrary configuration is broken into discrete blocks. The pressure, volume, and position of each block is tracked as a function of time. The momentum equations are satisfied by summing the forces acting on each face and the conservation of mass is enforced by making the mass of each block a constant function of time. The analysis was programmed, and several two-dimensional impact cases with various degrees of grid fineness and various impact angles were run. The initial results from this approach look very promising, giving reasonable values of the back flow, the initial uniaxial impact pressure peak ($\rho_0 C_0 V_0$ - Hugoniot), and the later steady state flow pressure. However, during the period of steady pressure the solution tends to be unstable. To rectify this stability problem and to improve the accuracy of the model required time and funding beyond the scope of the initial contract. A planning document to cover this additional effort as a supplement to the present contract was sent to NASA-Lewis in early February, 1977.

In the meantime, some approximate steady state two and three-dimensional fluid jet missile models were developed. Both of these crude models assumed a constant pressure of $1/2 \rho V^2 \sin^2 \theta$ over the effective impact area, which was based on the

low angle test results given in Reference 4. The derivations of these two approximate analyses are given in Appendix B. Later, it was discovered that the test results in Reference 4 were in error even for low impingement angles, so that the assumption of a constant pressure over the impact area was not a good approximation and resulted in poor correlation with test results; see Figure 11.

In January 1977, two German papers by Schach, References 5 & 7, were obtained which pertained to the two-dimensional oblique impacting jet and the three-dimensional cylindrical oblique impacting jet. The former case was solved by conformal transformation and the latter case, although not solved, was shown to have certain characteristics which agreed with experimental test results. Based on these two papers and References 5, 7 and 12, approximate analyses were developed which agreed well with the available test data. Originally it was planned to use these more rigorous analytical models in place of the above crude models for only the 3D Blade Impact Analysis (References 1 and 2), but because the supplemental funding for completing the spring-mass model did not materialize, it was decided to use it also for the MMBI analysis.

Two-Dimensional Oblique Impacting Jet

Although many papers and texts, for example Reference 18, give the elementary hydrodynamic solution for the flow split and center of force for a two-dimensional jet obliquely impinging on a flat plate, Schach's solution, Reference 7, is the only known general solution from which the complete boundary, pressure and velocity distributions can be calculated.

Figure 9 summarizes Schach's expressions for calculating the pressure and velocity distribution, and the locations of center of force and stagnation pressure for a two-dimensional jet missile. The calculated streamform and pressure distributions for various impingement angles are given in Figures 10 and 11. For very small

impingement angles α_0 , which are of prime importance, Schach's solution places the location of the stagnation pressure point outside of the jet envelope. Also, the total impingement load on the plate appears to be greater than it should be for small impingement angles; see Figure 13. It is believed this is a result of his approach of deriving the location of the stagnation point based upon points on the jet boundary for which the value of the conjugate velocity vector is $w = \text{Expe}(-i\alpha_0/2)$. Because of these apparent deficiencies in Schach's solution, an approximate model was developed based on an exponential pressure distribution; see Appendix C. This model satisfies all the hydrodynamic load and moment criteria, but places the stagnation pressure location at the edge of the jet for very small impingement angles.

Figure 11 compares the pressure distributions derived by Schach, the original crude constant pressure approximation given in Appendix B, and the exponential approximation given in Appendix C. Figure 12 presents a comparison of pressure and velocity distributions given by Schach's solution and the two approximations for a 60° impingement angle, and shows the exponential approximation correlates very well. Figure 13 presents a comparison between the Schach's solution and the exponential approximation for a 15° impingement angle, and shows reasonable agreement except for the location of the stagnation pressure. Figure 14 presents a comparison of the centers of force, e/a , and stagnation pressure, g/a , for both analyses. For small impingement angles the center of force occurs at the edge of the jet; however, for Schach's solution the distance of the stagnation pressure point to the center of force, f/a , goes to $(\ln 4)/\pi$ rather than zero, so that the stagnation pressure occurs outside the jet. Figure 14 shows this does not occur for the approximate solution. It is possible to make the location of the stagnation pressure for the exponential approximation match Schach's values; however, the resulting exponential coefficients below 22° become illogical. It is also possible to define the exponential approximation so that it fits Schach's

solution more exactly for the higher impingement angles; see Appendix C and Figure 14. However, because the improvement is minor, the extra complication of the more refined approximation was not deemed worth it.

Three-Dimensional Oblique Impacting Jet

There appears to be no general solution for a cylindrical jet obliquely impinging on a flat plate. However, a solution by Schach was found for 90° impingement; see Reference 7. Reference 5 by Schach presents some concepts and test results which could be used to develop an approximate analysis for the general case of a cylindrical jet obliquely impinging on a flat plate. This concept follows the same general approach given in Appendix B, but assumes a more realistic form of pressure distribution rather than a constant pressure distribution. Appendix D gives the development of this approximate 3D jet analysis, which assumes that the flow is radial from the stagnation point. This assumption has been essentially substantiated by tests; see Reference 5. Figure 15 depicts the nomenclature for a cylindrical jet impinging at an angle on a flat plate. Schach solves for the squashing and spreading of the jet based on the assumption that the fluid in each sector of the jet remains in the deflected sector.

Figure 16 gives a comparison between the measured pressure distribution given in Reference 5 for a 60° impingement angle and that given by the approximate theory developed in Appendix D. The theory matches the test results extremely well for all azimuth positions. The theory was checked by applying it to the normal or 90° impingement case for which there is a theoretical solution, see Reference 7, and test measurements, see Reference 12. Figure 17 compares the results from the approximate theory given herein and the results in these two references with regard to squashing thickness, velocity, and pressure distributions. Again, the approximate theory is found to agree very well with measure-

ment and the formal theory. Figure 18 presents a comparison of the centers of force, e/r , and stagnation pressure, g/r , for both test and the approximate analysis. The correlation is excellent as far as there are test results, i.e. 30° up to 90° .

General Three-Dimensional Oblique Impacting Jet

Although missiles impacting blades are of arbitrary shape, they can be usually depicted approximately as either an ellipsoid or a cylinder. However, because of the impacting angle, the finite length, and the orientation of the missile with respect to the impacted airfoil surface of the blade, the simple 3D jet representation given above cannot be used directly to represent the missile. Instead, the missile must be approximated by a combination of a 2D jet and a 3D jet; see Appendix E. The shape, and therefore, combination of 2 and 3D jets will vary with time because of the end effects of the missile; see Figure 19.

For the MMBI Analysis the impacting section of the missile is assumed to consist of a 2D jet in the center bounded by halves of a 3D jet; see Figure 20. As the front of the missile progressively impinges on the airfoil the impacting area and shape grows and changes. For a cylindrical missile, the approximation given in Figure 20 degenerates to a cylinder once the end effect is passed. If the missile is a slice of a cylinder or bird, the approximation requires that the spanwise width be a constant, so that the spanwise planform of each parallel division must be a rectangle; see Figure 20.

The location of the impact force and stagnation centers are assumed to be the weighted average of those for the 2D and 3D jets making up the particular cross-section. The resulting pressure loading and squashing thickness distributions are

modified values of the corresponding 2D and 3D jet results, so that there is no discontinuity between the two; see Appendix E. The former is done on an incremental load basis, whereas the latter is done on an incremental fluid area basis. Because of the tying together of the 2D and 3D jet results in the analysis, the squashing and spreading action of the 3D jet with distance from the stagnation point will force the 2D deflected thickness to decrease and spread with distance. However, the simple approach given in Appendix E for tying the 2D and 3D jets together assumes a constant modified thickness and pressure spanwise across the 2D jet, which is probably not correct; however, it is doubtful that the error introduced by this assumption is significant. Table II summarizes the expressions for defining the general jet missile based on those for the 2D and 3D jet missiles.

2.2.1 Definition of an Oblique Angle Impact of a Fluid Jet on a Surface

In order to use the equations developed in Appendices C, D and E and listed in Table II it is necessary to locate the frontal flow area faces of the 2-D jet in both the positive and negative sides of the fluid jet split (Fig. 21). This first requires a knowledge of the curved surfaces formed by the portions of the incident jet during their transitions onto the impacted surface. The approximation made here is that the curvatures take the form of a portion of a circular cylindrical surface.

From Fig. 21, define the radii:

R_1 = Radius of the arc drawn from the point of flow separation, O, to the point A_+ tangent to the impacted surface on the positive side of the jet split.

R_2 = Radius of the arc drawn from the point of flow separation to the point A, tangent to the impacted surface on the negative side of the jet split.

R = Radius of the arc drawn from the point of flow separation to the stagnation point, S.P., on the impacted surface. Note that the center of this arc lies on the plane of the impacted surface.

It is also noted that the arcs defined by radii R_1 , R_2 and R are tangent to the line O-F drawn through the point of flow separation parallel to the jet center-line. The angle subtended by the arc defined by R_1 is equal to α , the impact angle, and the bisector of this angle passes through the point F. From Fig.21

$$\begin{aligned} \ell &= R_1 \tan(\alpha/2) = R_2 \cot(\alpha/2) \\ R &= R_2 \left(1 + \frac{1}{\cos \alpha}\right) \\ R \sin \alpha + \ell \cos \alpha &= R + g - \frac{a}{2} \cot \alpha \end{aligned} \quad 2.2.1(a)$$

From Table II, equation 8, the distance g , between the impact center point C and the stagnation point is given by

$$g = \frac{a}{2} \left[\cot(\alpha) + \frac{2\ell}{a} \left(1 - \frac{2\alpha}{\pi}\right) \sin(\alpha) \right] \quad 2.2.1(b)$$

where a is the jet thickness.

Substitution of the right-hand side of the second of expressions 2.2.1(a) and the right-hand side of 2.2.1(b) into the third expression of 2.2.1(a) and collecting terms yields

$$\ell \cos(\alpha) + \ell [\sin(\alpha) - 1] \left[1 + \frac{1}{\cos(\alpha)}\right] \tan\left(\frac{\alpha}{2}\right) = \frac{14a}{9} \left(1 - \frac{2\alpha}{\pi}\right) \sin(\alpha) \quad 2.2.1(c)$$

Using the trigonometric identities

$$\tan\left(\frac{\alpha}{2}\right) = \frac{\sin(\alpha)}{1+\cos(\alpha)} = \frac{1-\cos(\alpha)}{\sin(\alpha)}$$

$$\sin^2(\alpha) + \cos^2(\alpha) = 1$$

$$\cos(\alpha) = \sin\left(\frac{\pi}{2} - \alpha\right)$$

in 2.2.1(c) yields for ℓ

$$\ell = \frac{28a}{9\pi} \left(\frac{\pi}{2} - \alpha\right) \frac{\sin(\alpha)[1+\sin(\alpha)]}{\sin\left(\frac{\pi}{2} - \alpha\right)} \quad 2.2.1(d)$$

Note that

$$\lim_{\alpha \rightarrow \frac{\pi}{2}} \left[\frac{(\pi/2 - \alpha)}{\sin(\pi/2 - \alpha)} \right] = 1$$

Using 2.2.1(d) in 2.2.1(a), expressions for R_1 and R_2 in terms of the initial incident jet thickness, a , and the impact angle α , can be obtained. Assuming now that the incident jet velocity is V_0 and referring to Fig. 22, it is observed that an elemental volume located at point P, which lies on the positive portion of the fluid jet along the line Q-F, will travel a distance $d = V_0 t$ during the time interval t . However, once the elemental volume has passed the point of flow separation, it will travel a distance S along the arc defined by radius R_1 . The angle subtended by S is given by

$$\phi = \frac{S}{R_1} \quad 2.2.1(e)$$

where

$$S = \ell + \frac{a}{2} \frac{\cos^2(\alpha)}{\sin(\alpha)} \quad 2.2.1(f)$$

The location of the elemental volume after time t , relative to the position of the point F is calculated from:

$$\lambda_1 = \ell - R_1 \sin(\alpha - \phi) \quad 2.2.1(g)$$

It is important to note that the location of the center of force of the impact is at the point F.

2.2.2 Location of Forward and Backwash Flow Area Faces

It has been assumed throughout the development of the relations in Section 2.2.1, that the flow conditions are steady state and that the incident jet stream is continuous. In the MMBI program the missile is portioned into streams of finite lengths $V_I \Delta t_I$ where:

V_I = Incident stream velocity

Δt_I = Time step length

From Fig. 23 note that the point P_t , located at the backstream face of the jet, a distance $V_I \Delta t_I$ from the incident face at the beginning of the time increment, will travel to the point $P_{t+\Delta t_I}$ at the end of the time interval. The location on the positive flow side of $P_{t+\Delta t_I}$, relative to the center of force F, is obtained from 2.2.1(g). In order to locate at time $t+\Delta t_I$ the elemental volume that originated on the negative side of the flow at point P_t in the beginning of the time interval, the moment of forces about the point F is calculated. Since F is the location of the center of force, the moment about this point must be zero and an expression can be derived for λ_2 , the distance between the center of force and the position on the negative flow side, of the elemental volume at time $t+\Delta t_I$. From the summary of equations listed in Table II:

Pressure on the positive side of the flow

$$P_1 = P_0 e^{-(x/\lambda_1)} (2 - e^{-(x/\lambda_1)}) \quad 2.2.2(a)$$

Pressure on the negative side of the flow

$$P_2 = P_0 e^{(x/\lambda_2)} (2 - e^{(x/\lambda_2)}) \quad 2.2.2(b)$$

where P_0 is the stagnation pressure, and γ_1 and γ_2 are decay constants in the positive and negative sides of the flow, respectively. Note that since x is

measured from the stagnation point it is necessary to use the value

$$\lambda_1' = \lambda_1 + f \quad 2.2.2(c)$$

where f is the distance between the stagnation point and the center of force.

From Table II

$$f = \frac{14a}{9} \left(1 - \frac{2\alpha}{\pi}\right) \sin(\alpha) \quad 2.2.2(d)$$

Integrating the moment due to P_1 between the limits λ_1' and $\lambda_1' + V_I \Delta t_I$ gives:

$$\begin{aligned} \frac{M(\lambda_1')}{P_0 b} = & \frac{\gamma_1}{4} e^{-\left(\frac{2\lambda_1'}{\delta_1}\right)} \left\{ e^{-2\left(\frac{\delta_I}{\delta_1}\right)} \left[2(\lambda_1' + \delta_I) + \delta_1 \right] - 2\lambda_1' + \delta_1 \right\} \\ & + 2\gamma_1 e^{-\left(\frac{\lambda_1'}{\delta_1}\right)} \left[(\lambda_1' + \delta_1) \left(1 - e^{-\left(\frac{\delta_I}{\delta_1}\right)} \right) - \delta_I e^{-\left(\frac{\delta_I}{\delta_1}\right)} \right] + 2f\gamma_1 \left[e^{-\left(\frac{\lambda_1'}{\delta_1}\right)} \left(e^{-\left(\frac{\delta_I}{\delta_1}\right)} - 1 \right) - \frac{1}{4} e^{-2\left(\frac{\lambda_1'}{\delta_1}\right)} \left(e^{-\left(\frac{\delta_I}{\delta_1}\right)} - 1 \right) \right] \end{aligned} \quad 2.2.2(e)$$

where $\delta_I = V_I \Delta t_I$

P_0 = stagnation pressure

b = width of flow

Similarly, for P_2

$$\begin{aligned} \frac{M(\lambda_2')}{P_0 b} = & \frac{\gamma_2}{4} e^{-2\left(\frac{\lambda_2'}{\delta_2}\right)} \left\{ e^{2\left(\frac{\delta_I}{\delta_2}\right)} \left[2(\lambda_2' + \delta_I) + \delta_2 \right] - (2\lambda_2' + \delta_2) \right\} \\ & + 2\gamma_2 e^{-\left(\frac{\lambda_2'}{\delta_2}\right)} \left[(\lambda_2' + \delta_2) \left(1 - e^{-\left(\frac{\delta_I}{\delta_2}\right)} \right) - \delta_I e^{-\left(\frac{\delta_I}{\delta_2}\right)} \right] - 2f\gamma_2 \left[e^{-\left(\frac{\lambda_2'}{\delta_2}\right)} \left(e^{-\left(\frac{\delta_I}{\delta_2}\right)} - 1 \right) - \frac{1}{4} e^{-2\left(\frac{\lambda_2'}{\delta_2}\right)} \left(e^{-\left(\frac{\delta_I}{\delta_2}\right)} - 1 \right) \right] \end{aligned} \quad 2.2.2(f)$$

where $\lambda_2' = \lambda_2 - f$

Equating the right-hand sides of 2.2.2(e) and 2.2.2(f) will yield an expression

in terms of λ_2' . The MMBI program uses the Newton-Raphson numerical iteration

method to obtain a solution for λ_2' . Consider the function $F(\lambda_2')$ defined by

$$F(\lambda_2') = M(\lambda_2') - M(\lambda_1') = 0 \quad 2.2.2(g)$$

As a first approximation assume F is a linear function such that

$$\frac{dF(p_1)}{d\lambda'_2} = \frac{F(p_1)}{p_1 - p_2}$$

2.2.2(h)

where p_1 is an initial first guess for λ'_2 and p_2 is the desired value necessary to make F equal to zero. Solving for p_2

$$p_2 = p_1 - \frac{F(p_1)}{\frac{dF(p_1)}{d\lambda'_2}}$$

2.2.2(i)

If p_2 is indeed the solution for which $F=0$ then a second trial, p_3 in the equation

$$p_3 = p_2 - \frac{F(p_2)}{\frac{dF(p_2)}{d\lambda'_2}}$$

yield a value that is equal to p_2 . In general this is not the case since F is not truly linear. However, p_3 will be a better approximation for λ'_2 (i.e., p_3 will make $F(p_3)$ closer to zero than $F(p_2)$). By successively applying the above technique the solution for 2.2.2(g) can be obtained to any desired accuracy.

2.2.3 Pressure Distribution

As described in Appendix E an impacting missile is composed of 2 subdivisions, a 2-D and 3-D fluid jet. Figure 24 depicts the general model with the 2-D uniform flow spreading outward from the point lying a distance $\frac{\lambda'_2 - \lambda'_1}{2}$ from the stagnation point and the 3-D portion of the flow spreading radially outward from points A and B. The location of the points A and B is determined by a consideration of Fig. 24. Since the impact is assumed to be symmetrical about the impact centerline, the points A and B are located a distance $\frac{w-a}{2}$ above and below the impact centerline where

w = total missile portion width
and $\frac{a}{2}$ = the radius of the outer extremes of the missile portion which is equal to one half the missile portion thickness.

The rate of spreading of the forward and backwash flow area faces is taken equal to the impact velocity. Figure 25 illustrates the scheme used in depicting the spread of the impacted missile mass with time. Note that at the instant the aft end of the missile portion reaches the impacted surface, a void of width $\lambda_1' - \lambda_2'$ occurs, centered about the point $\frac{\lambda_1' + \lambda_2'}{2}$ from the stagnation point. For times after the void appears the spreading mass takes the form of an oval ring expanding with time at the rate of the impact velocity. The pressure distribution is obtained from equations 2.2.2(a) and (b) for the 2-D portion of the spreading mass. The pressure distribution for the 3-D portion of the mass distribution is determined from the pressure relation in Table II for a 3-D jet.

$$P_3 = P_0 e^{-(r/\gamma_3)^2} [2 - e^{-(r/\gamma_3)^2}]$$

where γ_3 is a decay coefficient associated with the 3D jet. The MMBI program determines the load on the blade at any instant in two ways. At the instant of impact the initial force is calculated by integrating the pressure over the oval area defined by the 2-D boundaries

(S.P. - λ_2') (negative flow side)

and (S.P. + λ_1') (positive flow side)

where S.P. is the location of the stagnation pressure point, and the 3-D boundaries defined by the radius

$$\frac{\lambda_1' + \lambda_2'}{2} \quad (\text{See Fig. 24})$$

For time increments after the initial impact of the missile portion, the blade loads are determined by multiplying the pressure over each node of the blade by an effective nodal area as described in Section 3.1.11.

2.2.4 Effect of Blade Camber on Pressure

As the spreading impacted missile mass traverses the blade it encounters an additional acceleration due to the curvature of the surface. The effect of this acceleration is to produce an

additional pressure normal to the blade surface. Consider an elemental volume of mass traveling across the blade with velocity V_M (Fig. 26). If the instantaneous radius of curvature is R , then the force on the center of gravity of the mass is

$$F_{c.g.} = \frac{M V_M^2}{R} \quad 2.2.4(a)$$

where M = total mass of the elemental volume. Assuming that the mass has a thickness T_M , length dL_M , density ρ_M and is of unit width, the mass of the element can be expressed as

$$M = \rho_M T_M dL_M \quad 2.2.4(b)$$

Substituting 2.2.4(b) into 2.2.4(a) and dividing through by dL_M results in an expression for the pressure on the blade:

$$P_{\text{camber}} = \frac{F_{c.g.}}{dL_M} = \frac{M T_M V_M^2}{R} \quad 2.2.4(c)$$

In order to determine the radius of curvature, the MMBI program divides the blade surface into discrete regions of curvature along the chordwise direction. Referring to the description of blade geometry in Section 2.1.3 and to Fig. 27, the midpoints of the blade segments are calculated and then used to establish the bounds of each curvature region. For the blade segments at the leading and trailing edges the program uses the leading and trailing edge node points rather than the midpoints of the segments. Given blade segments n and $n+1$ with nodes n and $n+1$ for segment n , and nodes $n+1$ and $n+2$ for blade segment $n+1$, the midpoint coordinates are determined from

$$\begin{aligned} x_m &= x_n + [A_n \cos(\theta_n)]/2 \\ y_m &= y_n + [A_n \sin(\theta_n)]/2 \\ x_{m+1} &= x_{n+1} + [A_{n+1} \cos(\theta_{n+1})]/2 \\ y_{m+1} &= y_{n+1} + [A_{n+1} \sin(\theta_{n+1})]/2 \end{aligned} \quad 2.2.4(d)$$

where $x_n, y_n, x_{n+1}, y_{n+1}, A_n, A_{n+1}, \theta_n$ and θ_{n+1} are as defined in Section 2.1.3. Considering a circular arc that passes through the points m and $m+1$ such that it is tangent to the blade segments passing through these midpoints, the chordal length of the arc is

$$D_{\text{chord}} = \sqrt{(x_m - x_{m+1})^2 + (y_m - y_{m+1})^2} \quad 2.2.4(e)$$

The angle subtended by the arc is equal to the difference of the blade segment angles, i.e.

$$\Delta\phi = \theta_{n+1} - \theta_n$$

The radius of curvature is therefore given by

$$R = \frac{D_{\text{chord}}}{2 \sin(\Delta\phi/2)} \quad 2.2.4(f)$$

Substitution of this value in 2.2.4(c) gives the pressure at node $n+1$ due to the mass passing over it.

2.3 MODAL ANALYSIS

Consider a representation of the blade with n nodes such that the vector

$$V(x) = \{V\} = [V_1 \ V_2 \ V_3 \ \dots \ V_n] \quad 2.3.1(a)$$

contains the out-of-plane displacements as represented by a lumped mass model of r masses. Similarly, the in-plane displacements can be represented by W .

The total displacement vector can be represented by the function

$$\{\phi\}_i = \begin{Bmatrix} V_i \\ W_i \\ \theta_i \end{Bmatrix} \quad 2.3.1(b)$$

where ϕ is a $2n$ vector. Thus ϕ represents the mode shape of the blade and if this mode shape corresponds to the eigenvector of the system for mode i and they are normalized to a maximum of unity for the highest component, the function is denoted ϕ_i .

Corresponding to each displacement mode shape eigenvector is a stress mode shape eigenvector, $\{S\}_i$, which represents the chordwise, radial and shear stress components at the location of each node for mode i .

The modal mass m_i is defined as

$$m_i = \{\phi_i\}^T [M_p] \{\phi_i\} \quad 2.3.1(c)$$

where the superscript T refers to the transpose matrix operation and M_p represents the mass matrix of the structure. The subscript p refers to the system physical points used to simulate a given property. The mass matrix $[M_p]$ is

$$[M_p] = \begin{bmatrix} m & & \\ & m & \\ & & 1 \end{bmatrix}$$

If the mass matrix is diagonal, then Equation (3) becomes

$$\{m_i\} = [M_p] \{\phi_i\}^2$$

2.3.1(d)

The loads must be transformed from physical points to the generalized coordinates corresponding to the mode shapes. This is accomplished by the equation

$$\{P_i\} = \{\phi_i\}^T \{P_p\}$$

and

$$\{P_p\} = [P_{iv} \ P_{iw} \ P_{ie}]^T$$

2.3.1(e)

The use of normal modes provides an uncoupled set of differential equations for each mode. This is because the modes are orthogonal.

The equations of motion for the i th mode are

$$m_i \ddot{q}_i + b_i \dot{q}_i + k_i q_i = P_i(t)$$

or

$$\ddot{q}_i + 2\beta_i \dot{q}_i + \omega_{oi}^2 q_i = \frac{1}{m_i} P_i$$

2.3.1(f)

where q_i is the generalized coordinate and

$$\beta_i = \frac{b_i}{2m_i}, \quad \omega_{oi}^2 = \frac{k_i}{m_i}$$

The dots refer to time derivatives of the generalized coordinate. The general solution of Equation (7) is

$$q_i = F q_{i0} + G \dot{q}_{i0} + \frac{1}{m_i} \int_{t_n}^t G(t-\tau) P_i(\tau) d\tau \quad 2.3.1(g)$$

The functions F and G are combinations of the homogeneous solution

$$q_i(t) = e^{(-\beta_i \pm \sqrt{\beta_i^2 - \omega_{oi}^2})(t-t_n)} \quad 2.3.1(h)$$

which satisfy the initial conditions for unit values of the displacement and velocity. For the case of underdamped oscillations, F and G can be calculated by the equations

$$\begin{aligned} F &= e^{-\beta_i h} \left(\cos \omega h + \frac{\beta_i}{\omega} \sin \omega h \right) \\ G &= \frac{1}{\omega} e^{-\beta_i h} \sin \omega h \end{aligned} \quad 2.3.1(i)$$

where $\omega^2 = (\omega_{oi}^2 - \beta_i^2)$ and h is the time increment defined by $(t-t_n)$. The velocities are also required and are given by the expressions

$$\begin{aligned} F' &= -\frac{\omega_{oi}^2}{\omega} e^{-\beta_i h} \sin \omega h \\ G' &= e^{-\beta_i h} \left(\cos \omega h - \frac{\beta_i}{\omega} \sin \omega h \right) \end{aligned} \quad 2.3.1(j)$$

The remaining term of Equation 2.3.1(g) is a convolution or Duhammel integral, the solution of which, assuming P_i varies linearly with time, can be evaluated

by the expressions

$$g_i = A P_{i,n} + B P_{i,n+1}$$

2.3.1(k)

$$\dot{g}_i = A' P_{i,n} + B' P_{i,n+1}$$

The values of the coefficients of Equations 2.3.1(k) are given by the expressions

$$A = \frac{1}{h K_i \omega} \left\{ e^{-\beta_i h} \left[\left(\frac{\omega^2 - \beta_i^2}{\omega_{oi}^2} - h \beta_i \right) \sin \omega h \right. \right.$$

2.3.1(l)

$$\left. - \left(\frac{2 \omega \beta_i}{\omega_{oi}^2} + h \omega \right) \cos \omega h \right] + \frac{2 \beta_i \omega}{\omega_{oi}^2} \right\}$$

$$B = \frac{1}{h K_i \omega} \left\{ e^{-\beta_i h} \left[- \left(\frac{\omega^2 - \beta_i^2}{\omega_{oi}^2} \right) \sin \omega h + \frac{2 \omega \beta_i}{\omega_{oi}^2} \cos \omega h \right] \right.$$

2.3.1(m)

$$\left. + \omega h - \frac{2 \beta_i \omega}{\omega_{oi}^2} \right\}$$

$$A' = \frac{1}{h K \omega} \left\{ e^{-\beta h} [(\beta + h \omega_o^2) \sin \omega h + \omega \cos \omega h] - \omega \right\} \quad 2.3.1(n)$$

$$B' = \frac{1}{h K \omega} \left\{ -e^{-\beta h} [\beta \sin \omega h + \omega \cos \omega h] + \omega \right\}$$

where $K = \omega_o^2 M_i$

If the generalized force is constant over the time interval h , the generalized displacement and velocity as given by Equations 2.3.1(k) reduce to,

$$q_i = \bar{A} P_{i,n} \quad \text{and} \quad \dot{q}_i = \bar{B} P_{i,n} \quad 2.3.1(o)$$

where

$$\bar{A} = \frac{1}{K \omega} \left\{ e^{-\beta h} [-\beta \sin \omega h + \omega \cos \omega h] + \omega \right\}$$

$$\bar{B} = \frac{1}{K \omega} e^{-\beta h} \omega_o^2 \sin \omega h$$

Thus if $P_{i,n} = P_{i, n+1}$ the total solution at the end of the time period is

$$q_{i, n+1} = F q_{i, n} + G \dot{q}_{i, n} + \bar{A} P_{i, n}$$

$$\dot{q}_{i, n+1} = F' q_{i, n} + G' \dot{q}_{i, n} + \bar{B} P_{i, n} \quad 2.3.1(p)$$

and the coefficients are given by Equations 2.3.1 (i), (j), and (o).

Assuming that at time zero the in-plane and out-of-plane coordinates of the nodes are contained in the $2n$ vector

$$\{X_0\} = \begin{Bmatrix} X_1 & X_2 & X_3 & \cdots & X_n \\ Y_1 & Y_2 & Y_3 & \cdots & Y_n \end{Bmatrix}$$

and the initial chordwise, radial and shear stress components at the nodes are contained in the $3n$ vector

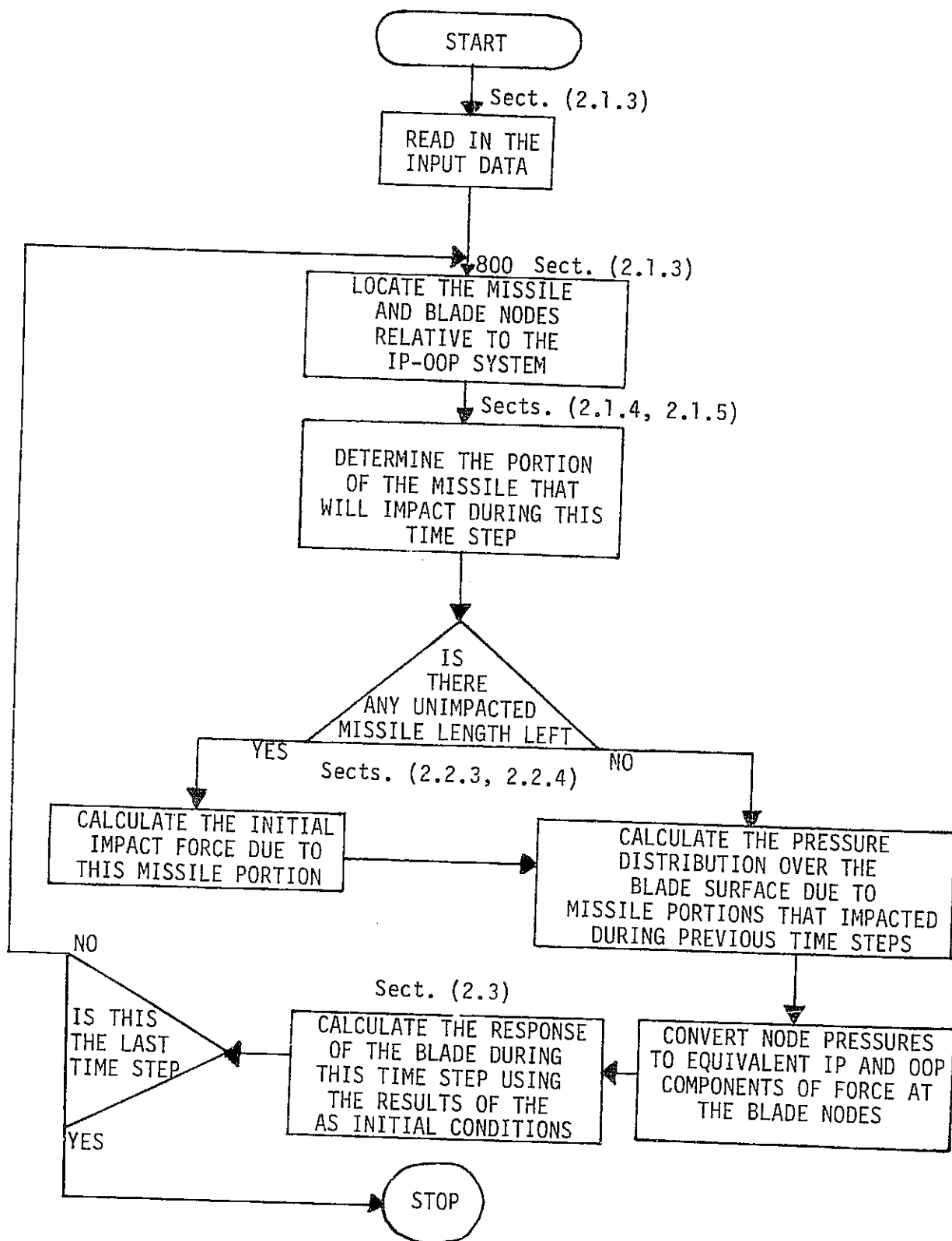
$$\{\sigma_0\} = \begin{Bmatrix} \sigma_{c1} & \sigma_{c2} & \sigma_{c3} & \cdots & \sigma_{cn} \\ \sigma_{r1} & \sigma_{r2} & \sigma_{r3} & \cdots & \sigma_{rn} \\ \tau_1 & \tau_2 & \tau_3 & \cdots & \tau_n \end{Bmatrix}$$

the coordinates and stress components at the end of the time period are given by

$$\{X\} = \{X_0\} + \sum_i q_i \{\phi\}_i \quad 2.3.1 \text{ (q)}$$

$$\{\sigma\} = \{\sigma_0\} + \sum_i q_i \{S\}_i \quad 2.3.1 \text{ (r)}$$

2.4 BASIC PROBLEM FLOW DIAGRAM



SECTION III

COMPUTER PROGRAM DESCRIPTION

The MMBI program consists of a main routine and eleven subroutines. In Section 3.13 are the flow diagrams associated with each routine which are summarized below and discussed in detail in the following sections.

MAIN - Input data is read in; initial conditions for the problem are calculated; the geometrical position and shape of the missile and blade are determined; the length of the time step is determined; the total force on the blade during each time step is distributed among the nodes; and the position is determined for the nodes describing the blade cross section in the in-plane out-of-plane reference frame at the end of each time step.

P3D - Calculates the instantaneous force imparted to the blade by the 3-D jet part of the missile portion that impacts during a particular time step.

LAMBDA - Calculates the distance between the stagnation point and the boundary of the void formed on the backwash side of the fluid flow at the end of the time step during which the missile portion impacted.

CAMBER - Calculates the thickness of the impacted missile mass passing over a node on the blade and the pressure effect due to the curved surface at the node.

REGION - Determines which radius of curvature is to be used for the calculation of pressure effects due to camber.

INCURV - Calculates the inverse of the radius of curvature at a particular node located on the blade surface.

PRESUR - Maps the pressure distribution on the blade and calculates the pressure over each node of the blade during every time step.

MODAL - Calculates the modal coefficients during each time step, the total displacement at every node relative to its position at time zero, and the three components of stress at every node.

PRINTP - Prints the pressures at the nodes falling within the impacted mass distribution during a particular time step.

PRINTV - Sets up the format for, and stores the displacement and stress output data to be printed at the end of the run.

PRINTR - Prints the displacements and stresses at the nodes chosen by the user for the time steps chosen by the user.

PINIT - Calculates the combined shape of the missile portion impacting during a time step, the impact parameters associated with the missile portion, the combined instantaneous impact force due to the 2-D and 3-D parts of the model, and distributes the force as equivalent pressures at the nearest two nodes to the center of force of the impact.

CORRELATION BETWEEN THEORETICAL AND CODED VARIABLES

<u>Equation</u>	<u>Computer</u>	<u>Units</u>
x_n	XO	length
y_n	YO	length
θ_n	THETA	radians
x_k	X	length
y_k	Y	length
α_o	THETAO	radians
β	BETA	radians
v_n	VEL	length/time
ω_n	OMEGA	radians/time
v_n	VB	length/time
V_k	VI	length/time
v	VR	length/time
x_i	XI	length
y_i	YI	length
v_o	V	length/time
α_k	ALPHA	radians
ℓ	AL	length
f	F	length
g	GLJ	length
a	RM	length
λ_1	LAND11	length
λ_2	LAND21	length
P_o	PO	force/(length) ²
ρ	DEN	mass/(length) ³
γ_1	GAMMA1	-----
γ_2	GAMMA2	-----
P_1, P_2	PRSS	force/(length) ²
$\{\phi\}$	PH2	length
$\{S\}$	SH2	force/(length) ²
m_i	VMI	mass
β_i	BET	-----
q_i	QI	-----
ω_{oi}	WO	radians/time
ω	WI	radians/time

3.1 MAIN

3.1.1 Input Variables

- a) V - Missile velocity relative to in plane-out of plane reference frame.
- b) RIMP - Radius of blade at which impact occurs.
- c) TSTØP - Total time duration for which the analysis is to be performed.
- d) ALPHAO - Initial angle between missile and blade chord. This angle is measured positive counterclockwise in the in plane-out of plane reference frame from the centerline of the missile to the blade chord.
- e) XOCL, YOCL - In plane and out of plane coordinates for the intersection of the forward point of the missile at its centerline and the blade face.
- f) NR - Total number of radial stations describing the blade.
- g) NN - Total number of nodes describing the blade.
- h) NM - Total number of blade modes used in the analysis.
- i) NVA - Total number of sections dividing up the missile along its length.
- j) IPDEL - Number of time steps between each printout of deflections and stresses. Once the missile is entirely on the blade (i.e., there is no more unimpacted missile length) the pressures at the blade nodes are printed only every IPDEL time step. While there is still unimpacted missile length, the node pressures are printed during each time step.
- k) DEN - Mass density of missile.
- l) ISYM - Flag to signal whether missile is symmetric⁽⁰⁾ or unsymmetric⁽¹⁾
- m) RL(M) - Radial distance between missile centerline and centerline of missile section M.
- n) RM(M) - Thickness of missile section M.
- o) CL(M) - Length of missile section M.
- p) DELTL(M) - Offset from forward point of the missile at the centerline to the forward point of missile section M (positive toward rear of missile).
- q) WM(M) - Width of missile section M.

- r) MAX(I3) - Total number of nodes at radial station I3.
- s) NJ3(I3) - Index of chordwise node at each radial station I3 where deflection and stress output is desired. The program automatically outputs deflections and stresses at the leading edge and trailing edge nodes of each radial station. The number NJ3 may be anything from 1 to MAX of each radial station.
- t) VM(I6) - Modal mass associated with each mode I6.
- u) DR(I6) - Modal damping ratio associated with each mode I6.
- v) WØ(I6) - Modal frequency associated with each mode I6 (radians/second).
- w) PH2(J6, K6, I6) - In-plane (J6 = 1) and Out-of-plane (J6 = 2) displacements associated with each node K6 for each mode I6.
- x) SH2(J6, K6, I6) - Extensional (J6 = 1, 2) and shear (J6 = 3) stresses associated with each node (K6) for each mode I6.
- y) YNØDE(I3), XNØDE(I3, J3) - Radial coordinate and chordwise coordinate at radial station I3 of node J3 describing the blade geometry in the planform reference frame.
- z) XØ(JC), YØ(JC) - Initial in-plane and out-of-plane coordinates of nodes JC describing the blade face curvature at the impact radial station in the in-plane/out-of-plane reference frame. The number of XØ, YØ pairs must be the same as the value for MAX at the corresponding radial station.

3.1.2 Problem Initialization

a) Modal Parameters:

The modal coefficients, Q and QD, for each mode I6, for example, are set to zero. The program then sets the numerically highest modal frequency into array element HIMØDE(NM) and the lowest modal frequency into array element HIMØDE(1).

From the modal mass, VMI(I6) the modal stiffness VKI(I6) can be calculated as $VKI(I6) = [VMI(I6)] \times [WØ(I6)]^2$ 3.1.2 (a)

Furthermore, the modal decay constant is given by

$$BET(I6) = [DR(I6)] \times [W\phi(I6)] \quad 3.1.2 (b)$$

and the effective damped modal frequency, $WI(I6)$, is calculated from

$$WI(I6) = \sqrt{[W\phi(I6)]^2 - [BET(I6)]^2} \quad 3.1.2 (c)$$

b) Effective Pressure Area at Nodes:

For each node at radial station $I3$ and chordwise station $J3$, for example, the chordwise distance between the two closest neighboring nodes on the same radial station is given by

$$XR - XL = [XN\phi DE(I3, J3 + 1)] - [XN\phi DE(I3, J3 - 1)]$$

and for the radial distance between the two closest neighboring nodes above and below radial station $I3$

$$RA - RB = [YN\phi DE(I3 + 1)] - [YN\phi DE(I3 - 1)]$$

The area $AAN\phi DE(I3, J3)$ is thus given by

$$AAN\phi DE(I3, J3) = [XR - XL] \times [RA - RB]/4$$

If the node should lie on either the lowest radial station or the highest radial station, then the value of $YN\phi DE(I3)$ is used instead of $YN\phi DE(I3-1)$ or $YN\phi DE(I3 + 1)$ respectively. Similarly, if the node lies on one of the blade edges, then the value of $YN\phi DE(I3, J3)$ is substituted for $XN\phi DE(I3, J3 - 1)$ in the case of the leading edge and for $XN\phi DE(I3, J3 + 1)$ in the case of the trailing edge.

c) Correspondence between planform and in-plane/out-of-plane geometry.

The program sets variables $NSTAT$ and $NSTAF$ equal to the number of nodes at the impact radial station and the number of blade segments at the impact radial station respectively. Array XM is then set up with its elements equal to the $XN\phi DE(I7, J3)$ values corresponding to the nodes at the impact radial station, $I7$. Thus, $XM(1)$ is the chordwise coordinate on the planform geometry corresponding to the leading edge node at the impact radial station, with coordinates $X\phi(1)$, $Y\phi(1)$ in the in-plane/out-of-plane reference frame. Using the values of XM , the blade is now

divided up into NSTAF-1 regions of curvature. The bounds of each curvature region are defined by the mid-points between adjacent chordwise points X_M . Thus, the first curvature region will lie between $X_M(1)$ and the mid-point of $X_M(2)$ and $X_M(3)$. The second curvature region lies between the mid-point of $X_M(2)$ and $X_M(3)$ and the mid-point of $X_M(3)$ and $X_M(4)$. The last curvature region lies between the mid-point of $X_M(NSTAT-2)$ and $X_M(NSTAT-1)$ and the point $X_M(NSTAT)$. The values of these mid-points are stored in arrays XCEN1 and XCEN2 where XCEN1(JC) is the beginning of curvature region JC and XCEN2(JC) marks the end of curvature region JC and the beginning of curvature region (JC + 1).

d) In-plane/out-of-plane blade coordinates X_0 , Y_0 :

The elements of arrays X_0 and Y_0 are assigned the corresponding values of the elements in arrays $X\emptyset$ and $Y\emptyset$. The program updates the blade coordinates in arrays X_0 and Y_0 at the end of each time step.

e) Time step index I is set equal to zero and absolute TIME is set equal to zero. These variables are updated after every time step.

f) Displacement and stress print flag - ITPRNT:

ITPRNT is initially set equal to one. Further on in the program, a comparison is made between the values of I and ITPRNT. If they are equal, then the program stores the displacement and stress output data for time step I. ITPRNT is then incremented by IPDEL (see 3.1.1(k) and 3.10.2).

g) IFV - Free vibration flag:

Initially IFV is set equal to zero. When the blade is no longer in contact with any missile mass (i.e., all node pressures are zero), IFV will be set to 1. This will trigger the program to alter its normal solution run in order to save time as will be discussed further on in the narrative. (Sect. 3.1.15)

h) IFSLD - Shallow impact angle flag:

Normally IFSLD is set to zero. If during a particular time step the impact angle is less than one tenth of a degree, IFSLD is set to 1. The remainder of the unimpacted missile length is assumed to slide onto the blade and no further impact analysis will be performed.

i) IIFLG - Zero impact length flag:

IIFLG is initially set to zero. When the length of the missile has reduced to zero during the impact stage of the program, IIFLG is set to 1. This will cause the program to skip calculations involving initial impact.

3.1.3 Printout of Initial Conditions

The program prints the following data:

- a) Initial planform and in-plane/out-of-plane blade geometry.
- b) Initial thickness, length, width and offset of each missile section.
- c) The modal frequency, modal mass, modal stiffness and modal damping ratio for each mode to be used in the analysis.
- d) Missile velocity, initial impact angle, missile density, in plane and out of plane coordinates of the center of impact and the impact radius.

3.1.4 Time Step Increment Entry Point

The point of the program where time stepping begins is denoted by statement number 800. Each time the program returns to this point, the index I is incremented by 1.

3.1.5 Blade Chord Angle, Missile Angle and Blade Segment Angles

The blade chord angle THETA0 and missile angle BETA are calculated using the relations 2.1.3(d) and 2.1.3(e). For each blade segment JC, in the in-plane/out-of-plane reference frame, the angle with respect to the in-plane axis is determined by using the expressions 2.1.3(a). The sign of the angle is determined by comparing the difference $[Y0(JC + 1) - Y0(JC)]$ with zero. If the difference is negative, then THETA(JC) is negative.

3.1.6 Forward and Aft Points of Missile Sections

Using the value of BETA and the relations 2.1.3(f), the coordinates of the forward and aft points of each missile section L are calculated for the first time step. For I greater than 1, the relations 2.1.3(g) and 2.1.3(h) are used. The X and Y coordinates of the forward point of missile section L are assigned respectively to array elements X(L) and Y(L). Similarly, for the aft point of missile section L, the X and Y coordinates are assigned to array elements X1(L) and Y1(L) respectively.

The remaining unimpacted length of each missile section L is calculated for I greater than 1. Assigned to array element VDT(L, I-1) is the amount of length of missile section L that impacted on the blade during time step I-1. The remaining unimpacted length (CL(L)) is obtained by subtracting the value of VDT(L, I-1) from the length of missile section L. When the remaining length is less than or equal to one percent of the length at the beginning of time step I-1 the program considers this length to be effectively zero.

This is necessary in order to avoid infinite looping due to computer roundoff error in the calculation of VDT. When CL(L) is zero, an array flag, II(L) is set to a value of 2 signaling the program that missile section L will no longer be involved in the impact calculations.

3.1.7 Missile - Blade Contact Points

To find the blade segment that is impacted by missile section L during time step I, the program uses the relations 2.1.3(j). If the missile section is not aiming at any blade segments during a time step, then a flag IHIT(L) is set to zero and the program moves to the next missile section. When a blade segment JC is established as the one to be impacted by missile section L, the program then uses equation 2.1.3(k) to determine where the forward point of the section is relative to the blade. Furthermore, IHIT(L) is assigned the value JC and a flag IBACK(L) is established such that its value is zero if the missile section is in front of the blade and 1 if the missile section is in back of the blade.

The program now checks the shallowness of the impact angle. If the impact angle is less than 1.7×10^{-3} radians (approximately one tenth of a degree) the missile section is considered to be sliding on the blade.

a) Sliding - If missile section L is sliding, then a flag ISLIDE(L) is set equal to 1. The program now determines whether the blade segment angle THETA(JC) is close to 90 degrees. If THETA(JC) is within $\pm 1.7 \times 10^{-3}$ radians of $\pi/2$ then the out of plane coordinate of the impact point YI(L) is set equal to the out of plane coordinate Y(L) and the in plane coordinate of the impact point is calculated from

$$XI(L) = [Y(L) - YO(JC)] \times \cot^{-1} [THETA(JC)] + XO(JC) \quad 3.1.7 (a)$$

If THETA(JC) is not close to $\pi/2$, then the program sets the in plane coordinate of the impact point XI(L) equal to X(L) and determines the out-of-plane coordinate of the impact point from

$$YI(L) = [X(L) - XO(JC)] \times \tan^{-1} [THETA(JC)] + YO(JC) \quad 3.1.7 (b)$$

The parameter XNEAR(L) is now assigned the value of XM(JC) in order to establish the location of the impact on the planform geometry. In addition, since the missile section is sliding on the blade, the distance between the forward point of section L and its impact point is set equal to zero in array element DFB(L). The chordwise distance DELTA(L) from the node corresponding to XM(JC) to the impact point is now calculated from

$$DELTA(L) = [XI(L) - XO(JC)]^2 + [YI(L) - YO(JC)]^2$$

Because of the arbitrary manner of assigning the value of Y(L) to YI(L) or X(L) to XI(L) it is possible that the impact point can be close enough to node (JC + 1) so that the impact can be considered to occur on blade segment JC + 1 rather than JC. This condition is indicated, for THETA(JC) less than zero when YI(L) is less than YO(JC + 1), and for THETA(JC) greater than zero when YI(L) is greater than YO(JC + 1). If either of these conditions occurs, the program assigns:

$$\begin{aligned}
XI(L) &= XO(JC + 1) \\
YI(L) &= YO(JC + 1) \\
XNEAR(L) &= XM(JC + 1) \\
IHIT(L) &= (JC + 1) \\
ISLIDE(L) &= 0 \\
\text{and } DELTA(L) &= 0.
\end{aligned}$$

Note that in this case, the impact point does not lie exactly on the centerline connecting the forward and aft points of missile section L. Instead of using the distance between the points $[X(L), Y(L)]$ and $[XI(L), YI(L)]$ for $DFB(L)$, the program calculates the projected distance in the direction of the missile centerline, i.e.

$$DFB(L) = [X(L) - XI(L)]^2 + [Y(L) - YI(L)]^2 \quad 3.1.7 (c)$$

Now the angle between the missile centerline and the line joining the impact point and forward point is calculated:

$$DALPHA = \cos^{-1} [X(L) - XI(L)] / DFB(L) \quad 3.1.7 (d)$$

The projected distance is then given by

$$DFB(L) = [DFB(L)] \times \cos [BETA - DALPHA] \quad 3.1.7 (e)$$

However, if $DFB(L)$, as calculated in equation 3.1.7 (c), is less than 1×10^{-5} , the program arbitrarily assigns $DFB(L)$ a value of zero. In order to locate the center of impact of missile section L on the planform geometry, one more parameter, $GAMMA(L)$, must be calculated. This is the chordwise location of the impact point on the planform geometry, i.e.,

$$GAMMA(L) = XNEAR(L) + DELTA(L) \quad 3.1.7 (f)$$

b) Impact angle is not shallow

In this case, the program uses the relation 2.1.3 (f) to calculate the impact coordinate $XI(L)$. If $THETA(JC)$ is within $\pm 1.7 \times 10^3$ of $\pi/2$ then $YI(L)$ is determined by equation 2.1.3 (c). Otherwise, $YI(L)$ is calculated by equation 2.1.3 (e).

In addition, the program calculates

$$XNEAR(L) = XM(JC)$$

$$DELTA(L) = [XO(JC) - XI(L)]^2 + [YO(JC) - YI(L)]^2$$

$$DFB(L) = [XI(L) - X(L)]^2 + [YI(L) - Y(L)]^2$$

$$\text{and } GAMMA(L) = XNEAR(L) + DELTA(L)$$

After all missile sections have been analyzed, the program examines Flag IT to determine the direction that the missile will have to be moved in order to locate the initial contact points between the missile and blade for time step I. If it is greater than zero then the program is signaled to move the missile rearward so that all forward points of the missile sections are in front of the blade. In addition, stored in array element DMAX(IT) is the distance that the missile will have to be moved back.

If IT is equal to zero then the program is signaled that all forward points are in front of the blade and the smallest distance, DFB, is stored in array element SDFB(NVA). Thus, depending on the value of IT, for each missile section

if IT>0

$$X(L) = X(L) - [DMAX(IT)] [\cos(BETA)]$$

$$Y(L) = Y(L) - [DMAX(IT)] [\sin(BETA)]$$

if IT=0

$$X(L) = X(L) + [SDFB(NVA)] [\cos(BETA)]$$

$$Y(L) = Y(L) + [SDFB(NVA)] [\sin(BETA)]$$

The adjusted values of the elements of DFB are now recalculated using the relation 3.1.7 (c). As a final step, the program assigns to the Flag II(L) for each missile section L a value of 1 or 0 depending upon

whether the forward point is in contact with the blade ($DFB(L)=0.$) or not ($DFB(L)=0.$).

3.1.8 Time Step Size

Using the values assigned to the elements of $HIMODE$ (Section 3.1.2A), an initial time step size $CNST$ is calculated. If IFV is equal to 1, (Section 3.1.2G) then the program calculates a time step that is one tenth the period associated with $HIMODE(NM)$, i.e.

$$CNST=2\pi/(10 \times [HIMODE(NM)]) \quad 3.1.8 (a)$$

If IFB is equal to 0 (free vibration), then

$$CNST=2\pi/(10 \times [HIMODE(I)]) \quad 3.1.8 (b)$$

The value of $CNST$ is assigned to variable DT .

3.1.9 Relative Impact Velocity and Angle, and Adjusted Time Step Size

Using the relations in Section 2.1.4 the relative impact velocity $VR(L,I)$ and relative impact angle $ALPHA(L)$ are calculated for missile section L . By dividing the remaining unimpacted section length $CL(L)$, for sections with $II(L)=1$, by the corresponding relative impact velocity $VR(L,I)$, the time that it would take to impact the remaining length, $DT1$, is determined. Comparing $DT1$ to DT , if $DT1$ is smaller than DT , then DT is assigned the value $DT1$.

If $II(L)=0$, the program calculates the time that it would take missile section L to traverse the distance $DFB(L)$ and assigns this value to $DT1$. If $DT1$ is less than DT but greater than $DT/2$, then DT is assigned the value $DT1$. If $DT1$ is less than $DT/2$, then the program assumes that section L will impact during this time step and sets $II(L)=1$. Note that the length of the time step will remain unchanged for this case.

3.1.10 Impacting Missile Section Length

The length of the missile section L that will impact during the time step I, $VDT(L,I)$, is now calculated. For missile sections having $IHIT(L)=0$ (section 3.1.7) or $II(L)=2$ (missile section has completely impacted already) or $II(L)=0$, $VDT(L,I)$ is assigned a value of zero.

Otherwise VDT is calculated from

$$VDT(L,I)=[VR(L,I)] \times [DT]-DFB(L) \quad 3.1.9 (a)$$

3.1.11 Node Pressures Due to Initial Impact

The program checks the values assigned to flags IFSLD and IIFLG (items H and I of 3.1.2). If either of these flags has a value of 1, the program will skip this calculation. If both IFSLD and IIFLG are different from 1, the program calls subroutine PINIT to calculate the initial impact parameters and forces associated with the impact of the missile sections hitting the blade during time step I. Among the variables outputted by subroutine PINIT are arrays NA(I) and ITSLD(I), which are used as signals by MAIN in determining the values of IFSLD and IIFLG. The value of NA(I) corresponds to the number of missile sections impacting the blade during time step I. If the value of ITSLD(I) is other than 7, then the program is signaled that the remainder of the missile is sliding on the blade. When $NA(I)=0$ and $ITSLD(I)=7$, the program sets $IIFLG=1$ and assigns variable KFIN the value $I-1$ meaning that the last impact occurred during the previous time step. When $NA(I)=0$ and $ITSLD(I)$ is less than 7, the program sets $IFSLD=1$ and variable $KFIN=I-1$. For time steps with $NA(I)$ greater than zero the program sets $KFIN=I$. Until either IFSLD or IIFLG are set equal to 1 each time step has associated with it impact parameters describing the size and shape of the portion of the missile that impacted during that time step. KFIN is used as an index for the array parameters associated with impacts from time steps 1 through KFIN.

3.1.12 Node Pressures Resulting from Impacts that Occurred During

Previous Time Steps

As described in Section 3.2.3 the distribution of an impacted portion of the missile takes the form of an expanding oval ring. For missile portions that have impacted the blade during a previous time step the program calculates the average size of the ring during the present time step. For the 2-D portion of the ring the location of the inner boundaries of the distributed mass in the negative and positive sides of the flow, relative to the centerline of the expanding ring, is calculated by adding half the amount of expansion during this time step (impact velocity times half the time step) to the location of these inner boundaries as of the end of the previous time step. This value is assigned to variable DIST(K) for the missile portion that impacted during a previous time step K. For the 3-D portion of the distribution the value of DIST(K) will be used as the average position of the inner radius during this time step. The program now calls subroutine PRESUR to distribute the pressure at the blade nodes that lie within the distribution.

For a missile portion that has impacted on the blade during the present time step the program calculates the initial size of the oval ring but does not call subroutine PRESUR since the node pressures have already been calculated in subroutine PINIT.

3.1.13 In-Plane and Out-of-Plane Node Forces

The pressures distributed among the nodes are now converted to in-plane and out-of-plane components of the equivalent forces at the nodes. The elements of array PRSS contain the values of the pressures at the nodes. For example, PRSS(I3,J3) represents the pressure at the J3 node along the row located

at the radial station I3. From Section 3.1.2B the elements of array AANODE(I3,J3) contain the effective areas of the nodes. The components of the force at a particular node are evaluated by using the blade segment angles in array THETA (Section 3.1.5). Since the blade segment angle of blade segment (JC) at the impact radial station (I7) is contained in array element THETA(JC), the relative angle of the blade segment containing a particular node (J3) at any other radial station (I3) is calculated as follows:

At the impact radial station, segment (JC) represents a portion of the blade chord equal to $[XM(JC+1) - XM(JC)]/[XM(NSTAT) - XM(1)]$. For the radial station (I3) a corresponding width is equal to the above ratio times the total chord width at radial station (I3), or

$$WIDTH = \frac{[XM(JC+1) - XM(JC)] \cdot [XNODE(I3,LIM) - XNODE(I3,1)]}{[XM(NSTAT) - XM(1)]}$$

The program now assigns to variable CAMLIM an initial value equal to the chordwise coordinate of the leading edge node at radial station (I3), i.e.

$$CAMLIM = XNODE(I3,1)$$

Next, variable WIDTH is calculated using

$$XM(JC) = XM(1)$$

$$\text{and } XM(JC+1) = XM(2)$$

If node (I3,J3) falls within the range CAMLIM and (CAMLIM + WIDTH), then THETA(JC) is assigned to variable ANGLE which is used to calculate the components of force. If node (I3,J3) does not fall within the range, CAMLIM is increased by WIDTH and the process is repeated with

$$XM(2) = XM(JC)$$

$$\text{and } XM(3) = XM(JC+1) \text{ in 3.1.11(a)}$$

When the range CAMLIM and (CAMLIM + WIDTH) is found to contain node (I3,J3), the program now calculates the components of force at the node from the equations:

$$\begin{aligned} \text{PIF}\text{ØRC}(\text{I3},\text{J3}) &= [\text{PRSS}(\text{I3},\text{J3})] \cdot [\text{AAN}\text{ØDE}(\text{I3},\text{J3})] \cdot [\text{Sin}(\text{ANGLE})] \\ \text{PØF}\text{ØRC}(\text{I3},\text{J3}) &= -[\text{PRSS}(\text{I3},\text{J3})] \cdot [\text{AAN}\text{ØDE}(\text{I3},\text{J3})] \cdot [\text{Cos}(\text{ANGLE})] \end{aligned}$$

where

PIFØRC(I3,J3) is the in-plane force component

and PØFØRC(I3,J3) is the out-of-plane force component at node (I3,J3).

Referring to items W and X in section (3.1.1), note that the modal displacements and stresses at the nodes are stored in arrays that have a different method of indexing nodes and components. In order to achieve consistency between the arrays PH2, SH2 and the node forces the program assigns the in-plane and out-of-plane components of force to array PP(I5,1) and PP(I5,2) such that (I5) corresponds to the node being referred by (I5) in PH2(J6,I5,M) and SH2(J6,I5,7). The index (J6)= 1 refers to in-plane and (J6)= 2 refers to out-of-plane components. In addition, the value of the index in array (PP) referring to the leading edge node at the impact radial station is assigned to variable (I8) so that the velocities and displacements of the nodes at this radial station can be readily referenced. The program also algebraically sums the values of the elements of (PP) and assigns the total to variable (FV). (FV) will be used as a flag to determine when to set IFV equal to 1 (see item G under section 3.1.2).

3.1.14 Modal Analysis

The modal analysis that determines the response of the blade to the force distribution at the nodes is performed by calling subroutine MØDAL. Among the variables output by subroutine MØDAL is the array DEF(J6,K6) containing the in-plane (J6 = 1) and out-of-plane (J6 = 2) displacements of the nodes relative to their coordinates at time zero. Using the value of (I8) referred to in section (3.1.12) the program calculates the in-plane and out-of-plane coordinates of the blade nodes along the impact centerline from the relations

$$XO(JB) = X\phi(JB) + DEF(1,I9)$$

$$YO(JB) = Y\phi(JB) + DEF(2,I9)$$

where (JB) refers to the chordwise index of the node at the impact radial station and (I9) is the corresponding index relative to variable (I8).

3.1.15 Time Update, Data Output, Return to 800 for Next Time Step

The program now calculates the total elapsed time by adding the value of (DT) (sections 3.1.8 and 3.1.9) to the previous value in variable TIME. In order to determine whether the entire length of the missile has impacted, the total number of missile sections having either (II) = 2 (section 3.1.6) or IHIT = 0 (section 3.1.7) are summed, and the value assigned to variable (III). The program now calls subroutine PRINTV to store the displacement and stress output data for this time step if any of the following conditions are satisfied.

- A - This is the first time step (I = 1)
- B - TIME is greater than TSTOP (item C of section 3.1.1)
- C - I equals ITPRNT (section 3.1.2F)

In addition, if the value of (III) is equal to the total number of missile sections, the program will call subroutine PRINTP to print the pressure distribution for this time step. If (III) is less than the total number of missile sections (NVA), the program calls PRINTP whether the conditions A, B or C are satisfied or not. Next, the value assigned to variable (FV) (section 3.1.13) is compared to zero. If (FV) = 0 the program is triggered to set (IFV) = 1. The value assigned to variable TIME is now compared to TSTOP. If time is less than TSTOP the program returns to statement 800 to start a new time step. If TIME is greater than or equal to TSTOP the program calls subroutine PRINTR as a final step. PRINTR prints the displacement and stress output data for time steps selected by the user.

3.2 P3D - 3D PRESSURE DISTRIBUTION INTEGRATION

3.2.1 Input Variables

- a) A - Thickness of the missile portion impacting the blade.
- b) ALPHA - Impact angle
- c) P \emptyset - Stagnation pressure
- d) GAMDA1, GAMDA2 - Parameters used to define the limits of the 3D pressure distribution. (See discussion on the variables λ_1' and λ_2' in Sections 2.2.2 and 2.2.3)

3.2.2 Discussion

This subroutine performs a numerical integration of the pressure distribution associated with the 3D portion of the distributed impacted missile mass. The shape of the distribution is formed by a semi-circle of radius $[GAMDA1 + GAMDA2]/2$. The routine arbitrarily sets the number of integration points to 1352, and evaluates the integral using a 2-dimensional grid formed by these points.

Given a rhombic area with corners at points (x, y) , $(x+\Delta x, y)$, $(x, y+\Delta y)$ and $(x+\Delta x, y+\Delta y)$, the integral of the pressure over this area is given by

$$\int P da = \frac{\Delta x \Delta y}{6} [P(x, y) + 2P(x + \Delta x, y) + 2P(x, y + \Delta y) + P(x + \Delta x, y + \Delta y)] \quad 3.2.2(a)$$

where P is the pressure distribution. The value of the integral for the entire semi-circular region is approximated by summing the integrals of the individual discreet areas over the entire system. The value of the integral is assigned to variable TL \emptyset AD.

3.3 LAMBDA - ITERATION SOLUTION FOR λ_2'

3.3.1 Input variables

- a) GAMDA1 - Variable λ_1' in Section 2.2.2
- b) DEL - Amount of missile portion impacting the blade during the time step of interest.
- c) G1, G2 - 2D jet pressure distribution decay parameters in the positive and negative sides of the flow separation respectively.
- d) F - Distance between the stagnation pressure point and the location of the center of force.
- e) I - Time step increment number.
- f) ALPHA - Impact angle
- g) ISPLT - Flag determining the impact direction. If ISPLT=1 the flow in the positive side is toward the trailing edge. If ISPLT=-1 the flow is in the direction of the leading edge.
- h) SP - Location of the stagnation pressure point relative to the planform geometry coordinate system.
- i) X1,X2 - Location of the leading edge and trailing edge nodes, respectively, relative to the planform geometry system.

3.3.2 Iteration Solution for λ_2'

The methodology used to obtain a value for λ_2' is described in Section 2.2.2. The routine attempts to solve for λ_2' in 200 iteration steps using the Newton Raphson Method. If after that point, convergence to one-tenth of a percent accuracy for the solution has not been achieved, the routine prints a warning message to the user and returns to the calling program. Since the equations used by the routine involve exponential terms, the program is instructed to skip the analysis if the absolute value of the argument is greater than 20. In addition, the value of λ_2' for this case is arbitrarily set equal to zero. This approximation is not inconsistent since large absolute values of the arguments in the exponential functions represents a shallow impact angle such that the majority of the flow will be in the positive direction of the stream separation.

The value for λ_2' is assigned to variable BESTL.

3.4 CAMBER - CALCULATION OF PRESSURE EFFECTS DUE TO BLADE CURVATURE

3.4.1 Input Variables

- a) XNØDE, YNØDE - Planform geometry coordinates of a node.
- b) A, B - Radial coordinate of the limiting bounds for the 2-D portion of the spreading missile mass in the planform geometry system
- c) ISPLIT - see 3.3.1(g)
- d) RM - Thickness of the impacted missile portion that is associated with this portion of mass distribution.
- e) ALPHA - Impact angle
- f) SPP - (See 3.3.1(h))
- g) VDT - See 3.1.6
- h) CØSFEE - Angle with respect to x axis, defined by a line connecting a node at coordinates (XNØDE, YNØDE) and the point located at coordinates $x = \text{SPP}$ and $y = \begin{cases} A & \text{if } YNØDE \geq A \\ B & \text{if } YNØDE \leq B \end{cases}$ in the planform geometry system.
- i) VR - Relative impact velocity
- j) DEN - Missile density
- k) NSTAT - Number of chordwise stations at the impact radial station.
- l) DIST - See Section 3.1.11.

3.4.2 Discussion

This subroutine calculates the average thickness of mass traversing the node located at planform coordinates (XNØDE, YNØDE), and, through subroutines REGION and INCURV, it calculates the pressure over the node due to blade curvature. For a mass element in the negative side of the flow separation, the thickness for the 2D portion is approximated by

$$\text{THICK} = \text{RM} * [1 - \text{Cos}(\text{ALPHA})] / 2$$

3.4.2(a)

and in the positive side by

$$THICK = RM * [1 + \cos(\alpha)] / 2 \quad 3.4.2(b)$$

For the 3D flow portion the mass thickness is determined from the assumption that the average thickness varies inversely with the ratio of the cross sectional area of the 3D portion of the unimpacted missile to the area of the distributed 3D impacted mass, i.e.

$$H_{3D} = \frac{(THICK_{3D})_{IMPACTED}}{VDT} = \frac{\pi(RM)^2}{\pi [(DIST+VDT)^2 - (DIST)^2]} \quad 3.4.2(c)$$

Assuming now that the thickness varies linearly with angle along the mean radius of the distribution, an expression for the thickness of mass over a node lying within the 3D portion of the distribution is written as

$$THICK = (H_{3D}) \left[1 + \cos(\alpha) - \frac{2\cos(\alpha)}{\pi} \cos^{-1}(\cos \theta) \right] \quad 3.4.2(d)$$

Referring to the discussion in Section 2.2.4, the routine now calls subroutine REGION to determine which curvature region of the blade the node with coordinates (XNODE, YNODE) lies within. Assigning this value to variable (JC1), subroutine INCURV is called to determine the value of the inverse of the radius of curvature for the curvature region corresponding to (JC1). Using this value in variable (PI) the pressure due to blade curvature is calculated using equation 2.2.4(c) and assigned to variable PRESSC.

3.5 REGION - DETERMINATION OF BLADE CURVATURE REGION

3.5.1 Input variables

- a) XNODE - See 3.4.1(a)
- b) NSTAT - See 3.4.1(a)
- c) XCEN1, XCEN2 - Arrays containing the planform x-coordinates of the bounds of the discrete curvature regions (see 2.2.4 and 3.1.2(c)).

3.5.2 Discussion

This subroutine determines which blade curvature region, as defined by XCEN1 and XCEN2, the coordinate XNODE of a node lies within. The index of the correct region is assigned to variable JC1.

3.6 INCURV - CALCULATION OF THE INVERSE OF THE CURVATURE RADIUS CORRESPONDING TO REGION JC1

3.6.1 Input Variables -

- a) JC1 - see 3.4.2
- b) XO,YO - Arrays containing the in-plane and out-of-plane coordinates of the blade cross section nodes during the time step of interest
- c) THETA - Array containing the relative angles between the blade segments and the in-plane axis during the time step of interest.

3.6.2 Discussion

Using the equations and methodology described in Section 2.2.4, the inverse of the blade curvature radius is calculated and assigned to variable P1.

3.7 PRESUR - PRESSURE OVER A NODE

3.7.1 Input variables -

- a) NR - Number of radial stations
- b) A,B - see 3.4.1(b)
- c) DIST - see Section 3.1.11
- d) ISPLIT - see 3.3.1(g)
- e) SPP - see 3.3.1(h)
- f) SPP1 - Planform x coordinate for the center of the oval distribution of mass associated with this impacted portion of the missile.
- g) VDT - see 3.1.6
- h) GAMMA1, GAMMA2 - Exponential decay constants in the positive and negative flow directions respectively.

- i) PO - Stagnation Pressure
- j) RM - see 3.4.1(d)
- k) ALPHA - Impact angle associated with this missile portion.
- l) VR - Impact velocity associated with this missile portion
- m) DEN - Missile density
- n) NSTAT - see 3.4.1(k)
- o) IIFLG - see 3.1.2(I)
- p) XNODE, YNODE - see 3.4.1(a)
- q) MAX - Array containing the number of chordwise nodes at each radial station

3.7.2 2D Pressure

The 2D pressure region associated with an impacted missile portion is bounded chordwise by the planform coordinates:

SPPl - (DIST + VDT) for the negative flow side
and SPPl + (DIST + VDT) for the positive flow side.

For the radial bounds, the 2-D portion extends between planform radial coordinates B and A. In addition, for the distribution consisting of a void (see Section 2.2.3) the inner chordwise bounds of the distribution are SPPl-DIST in the negative side and SPPl + DIST in the positive side of the flow. Having located the boundaries of the 2-D portion of the impacted mass the routine determines which nodes fall within this region and calculates the pressure accordingly. The value of this pressure is assigned to array element PRESS(I3, J3) corresponding to the node located in radial station I3 and chordwise station J3.

3.7.3 3D Pressure

The bounds of the 3D portion of the distributed mass are determined by semi-circles of radius (DIST + VDT) centered about the coordinates

(SPPl, B) for the portion below the centerline
and (SPPl, A) for the portion above the centerline,

For the inner bound due to the formation of a void, the radius is taken as DIST. Similar to the 2D portion described in 3.7.2, the pressure is determined for nodes falling within the bound of the 3D distribution and the value assigned to array element PRESS (I3, J3).

3.7.4 Camber Effects

The routine now calls subroutine CAMBER to calculate the additional pressure over a node due to blade curvature. The output value of the camber pressure, stored in variable PRESSC, is added to the value in PRESS (I3, J3). Array PRESS will be used in subroutine PRINTP further on in the program to print the pressure distribution. For use in the calculation of nodal loads as described in Section 3.1.12, the program assigns the values in PRESS to corresponding elements in array PRSS. However, for nodes I3, J3 corresponding to the void of a mass distribution, the element PRSS (I3, J3) maintains a value of zero.

3.8 MODAL - CALCULATION OF THE BLADE RESPONSE TO THE LOADS ON THE BLADE DURING A TIME STEP

3.8.1 Input variables

- a) NM - Number of modes to be used
- b) NSTAT - see 3.4.1(k)
- c) NN - Total number of nodes describing the blade
- d) I8 - see 3.1.13
- e) FV - see 3.1.12
- f) T - Time step size

3.8.2 Discussion

The methodology used in determining the displacement, velocity, and stress response at the nodes of the blade is described in Section 2.3. The coefficients in equations 2.3.1(p) are first calculated

using the time step length T . The generalized displacement and velocity coordinates, QI and QDI , are now calculated and their values set to Q and QD respectively. Q and QD will be used in the next time step as initial conditions for the calculation of QI and QDI .

The displacement, velocity, and stress components for each node JB , relative to their values at time zero, are now calculated, based on equations 2.3.1 (q) and (r), as follows:

in-plane displacement at node JB	$DEF(1,JB) = \sum_{\substack{\# \text{ of} \\ \text{modes}}} [PH2(1,JB,I6)][QI(I6)]$
out of plane displacement at node JB	$DEF(2,JB) = \sum_{\substack{\# \text{ of} \\ \text{modes}}} [PH2(2,JB,I6)][QI(I6)]$
in-plane velocity at node JB	$VEL(1,JB) = \sum_{\substack{\# \text{ of} \\ \text{modes}}} [PH2(1,JB,I6)][QDI(I6)]$
out of plane velocity at node JB	$VEL(2,JB) = \sum_{\substack{\# \text{ of} \\ \text{modes}}} [PH2(2,JB,I6)][QDI(I6)]$
chordwise stress at node JB	$STRSS(1,JB) = \sum_{\substack{\# \text{ of} \\ \text{modes}}} [SH2(1,JB,I6)][QI(I6)]$
radial stress at node JB	$STRSS(2,JB) = \sum_{\substack{\# \text{ of} \\ \text{modes}}} [SH2(2,JB,I6)][QI(I6)]$
shear stress at node JB	$STRSS(3,JB) = \sum_{\substack{\# \text{ of} \\ \text{modes}}} [SH2(3,JB,I6)][QI(I6)]$

The index $I6$ corresponds to mode number.

3.9 PRINTP - PRESSURE DISTRIBUTION PRINTOUT

3.9.1 Input variables

- a) I - Time step increment
- b) TIME - Absolute time at which these pressures are recorded.
- c) NR - Number of radial stations

3.9.2 Discussion

In order to minimize the amount of printout, this subroutine determines the number of radial stations that contain nodes which lie within the pressure distribution during a particular time step. Only the radial stations lying within the upper and lower radial bounds of the pressure distribution will have the pressures at their corresponding nodes printed. In addition, for time steps during which the pressure on the blade is zero, the routine instructs the computer to print a message to the user accordingly.

3.10 PRINTV - DISPLACEMENT AND STRESS OUTPUT DATA ARRANGEMENT AND STORAGE

3.10.1 Input variables

- a) I - Time step increment
- b) TIME - Absolute time
- c) IPDEL - see 3.1.1(k)
- d) ITPRNT - see 3.1.2(f)

- e) NR - Number of radial stations
- f) I7 - Index of the impact radial station
- g) DEF, VEL, STRSS - see 3.8.2
- h) XNØDE, YNØDE - see 3.4.1(a)
- i) MAX - see 3.7.1(q)

3.10.2 Discussion

At the user's request the MMBI program will print the nodal displacements and stresses for every IPDEL time step. The variable ITPRNT is updated each time this routine is entered by incrementing it with the value assigned to IPDEL as described in Section 3.1.2(f). Two formats of data printout are arranged by the routine. First, the in-plane and out-of-plane displacements and the radial stress at the leading edge, trailing edge and node NJ3(I3) (see 3.1.1(s)) for each radial station I3, are arranged in order to print them according to their radial location. Second, in order to obtain information about the variation of stress and displacement at the impact radius of the blade, the stresses and displacements at the chordwise nodes of the impact radial station and those of the nearest radial stations below and above the impact centerline are arranged for their printout vs. the planform chordwise coordinates of the nodes along the impact radial station. The information for output printout set IJPRNT is stored in arrays:

DEFBI (IJPRNT, I3) - In-plane displacement at node NJ3 (I3)
 DEEBØ (IJPRNT, I3) - Out-of-plane displacement at node NJ3 (I3)
 SIGMB1 (IJPRNT, I3, 1) - Radial stress at leading edge node
 SIGMB1 (IJPRNT, I3, 2) - Radial stress at node NJ3 (I3)
 SIGMB1 (IJPRNT, I3, 3) - Radial stress at trailing edge node
 CØDI (IJPRNT, J3) - In-plane displacement at node J3 of impact radial station
 CØDØ (IJPRNT, J3) - Out-of-plane displacement at node J3 of impact radial station

SIGMA1 (IJPRNT, I4, J3)
SIGMA2 (IJPRNT, I4, J3)
SIGMB2 (IJPRNT, J3 I4)

Three components of stress at node J3 of radial station:

I4 = 1 radial station below impact radius
I4 = 2 Impact radial station
I4 = 3 radial station above impact radius

3.11 PRINTR - DISPLACEMENT AND STRESS PRINTOUT

3.11.1 Input variables

- a) I7 - see 3.10.1(f)
- b) NSTAT - see 3.4.1(k)
- c) NR - see 3.8.1(a)
- d) IJPRNT - Total number of sets of displacement and stress printouts
- e) XNØDE, YNØDE - see 3.4.1(a)
- f) MAX - see 3.7.1(q)
- g) DEFBI, DEFBØ, CØDI, CØDØ, SIGMA1, SIGMA2, SIGMB1, SIGMB2 - see Section 3.10.1

3.11.2 Discussion

This subroutine is called by the main program (Section 3.1.14) after all time steps are completed. The routine will printout the data stored by subroutine PRINTV in the arrays listed in 3.11.1(g).

3.12 PINIT - INITIAL IMPACT FORCE

3.12.1 Input variables

- a) NVA - Number of sections describing the missile (see 3.1.1(j))
- b) BETA - see equation 3.1.2A(c)
- c) I8 - see Section 3.1.13
- d) NSTAF - Number of blade segments at the impact radial station
- e) PPII - Numerical value of $\pi = 3.141592654$
- f) DEN - Missile density

- g) I - Time step index
- h) V - Initial impact velocity of missile
- i) I7 - Impact radial station index
- j) DT - Time step size
- k) RIMP - Radial coordinate of impact station in planform system
- l) NSTAT - see 3.4.1(k)
- m) RM, XI, YI, IHIT, RL, X, Y, WM - Missile parameters (see Sections 3.1.1 and 3.1.6)
- n) XO, YO, THETA, XM - see Sections 3.1.26, 3.1.2E and 3.1.5
- o) VEL - See Section 3.8.2

3.12.2 Formation of Impacting Missile Portion

As noted in Section 3.1.9 each missile section that will impact the blade during a particular time step has associated with it an array element II(L) that is set equal to 1. Subroutine PINIT initially sums the thicknesses of these missile sections, contained in the elements of RM, and assigns the value to variable RM1. In addition, the number of missile sections making up RM1 is stored in variable NA. The width of the missile section associated with the greatest value WM is used as the width of this missile portion and the value is assigned to variable WM1. Thus, similar to the missile sections described in Section 2.1.3, the impacting missile portion is described with a thickness equal to RM1 and a width equal to WM1. The missile portion consists of a 2-D portion of width WM1-RM1 and a 3-D portion of radius RM1/2.

3.12.3 Impact location, relative velocity and relative incident angle

Analogous to the methodology described in Sections 3.1.7 and 3.1.9, associated with the impacting missile portion are the parameters:

XI1, YI1 - In-plane and out-of-plane impact coordinates

XNERL1 - Nearest chordwise node to the impact point.
 DLTAL1 - Distance between node located at XNERL1 and the impact point.
 GMAL1 - Planform x coordinate of impact point
 DFBL1 - Distance between the impact point and the centerline of the
 missile portion.
 VRL1 - Relative impact velocity
 ALPL1 - Relative impact angle
 VDTL1 - Impact length of missile portion

3.12.4 Coefficients Associated with the Fluid Jet Model

As described in Sections 2.2.1 and 2.2.2, the parameters defining the shape of the impacting fluid jet are calculated. The location of the stagnation point is assigned to variable SPP and the parameter λ_1' is calculated using equations 2.2.1(g) and 2.2.2(c). The routine now calls subroutine LAMBDA to calculate the value for λ_2' which is assigned to variable LAMD1.

3.12.5 Impact Force and Equivalent Pressure

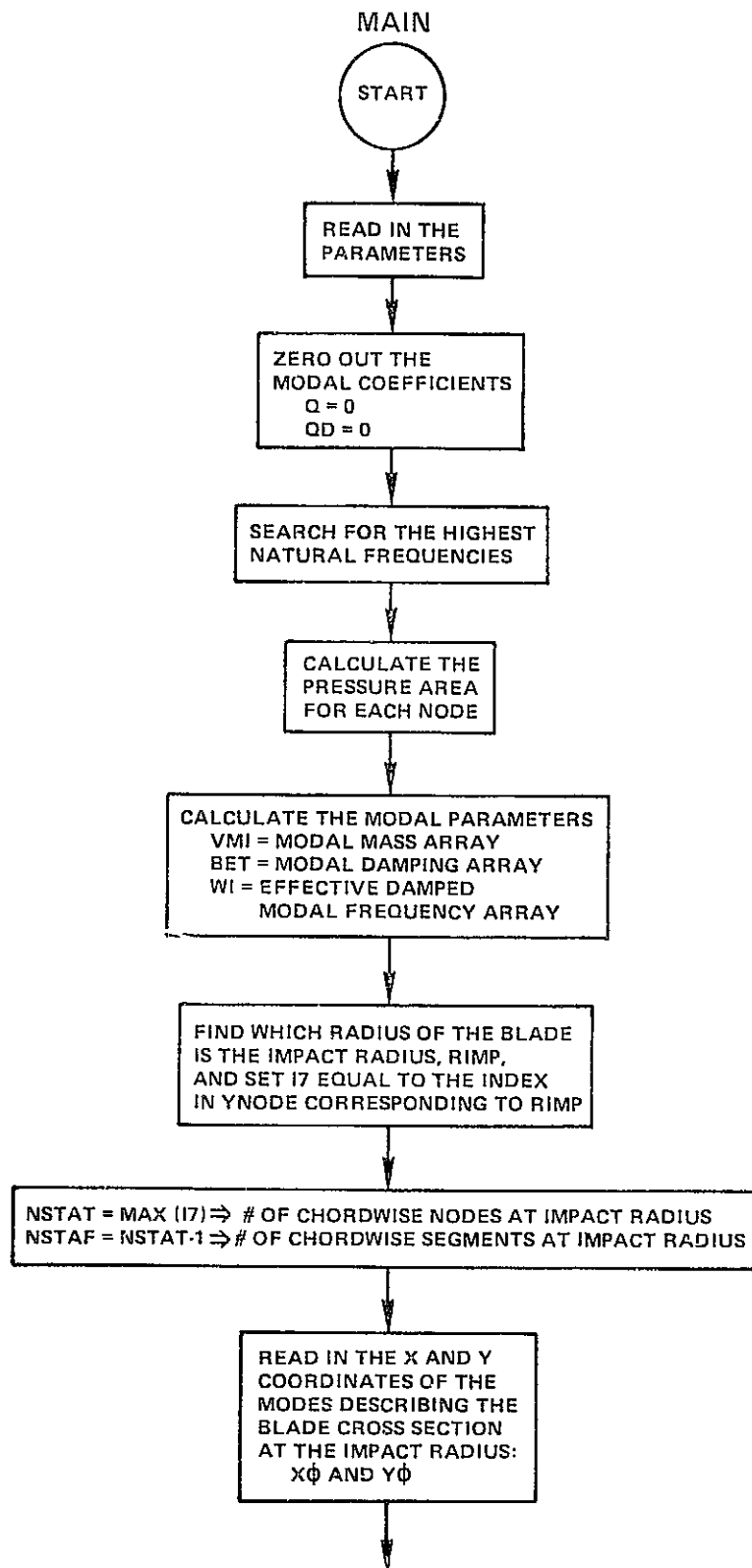
The initial impact force due to the 2-D portion of the pressure distribution is calculated and assigned to variable FIMP2D. For the impact force due the 3-D portion of the jet the routine calls subroutine P3D and assigns the value to variable FIMP3D. The total impact force is thus

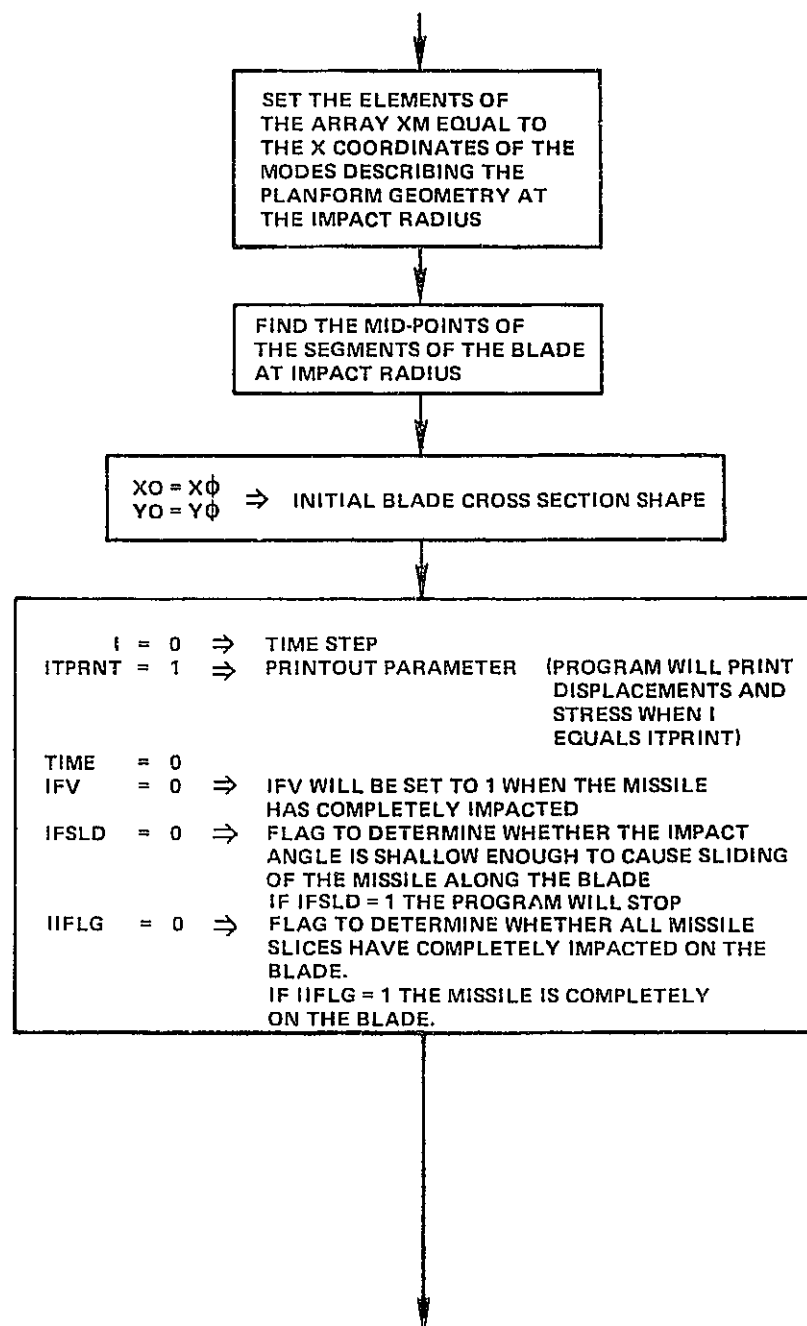
$$FIMP = FIMP2D + FIMP3D$$

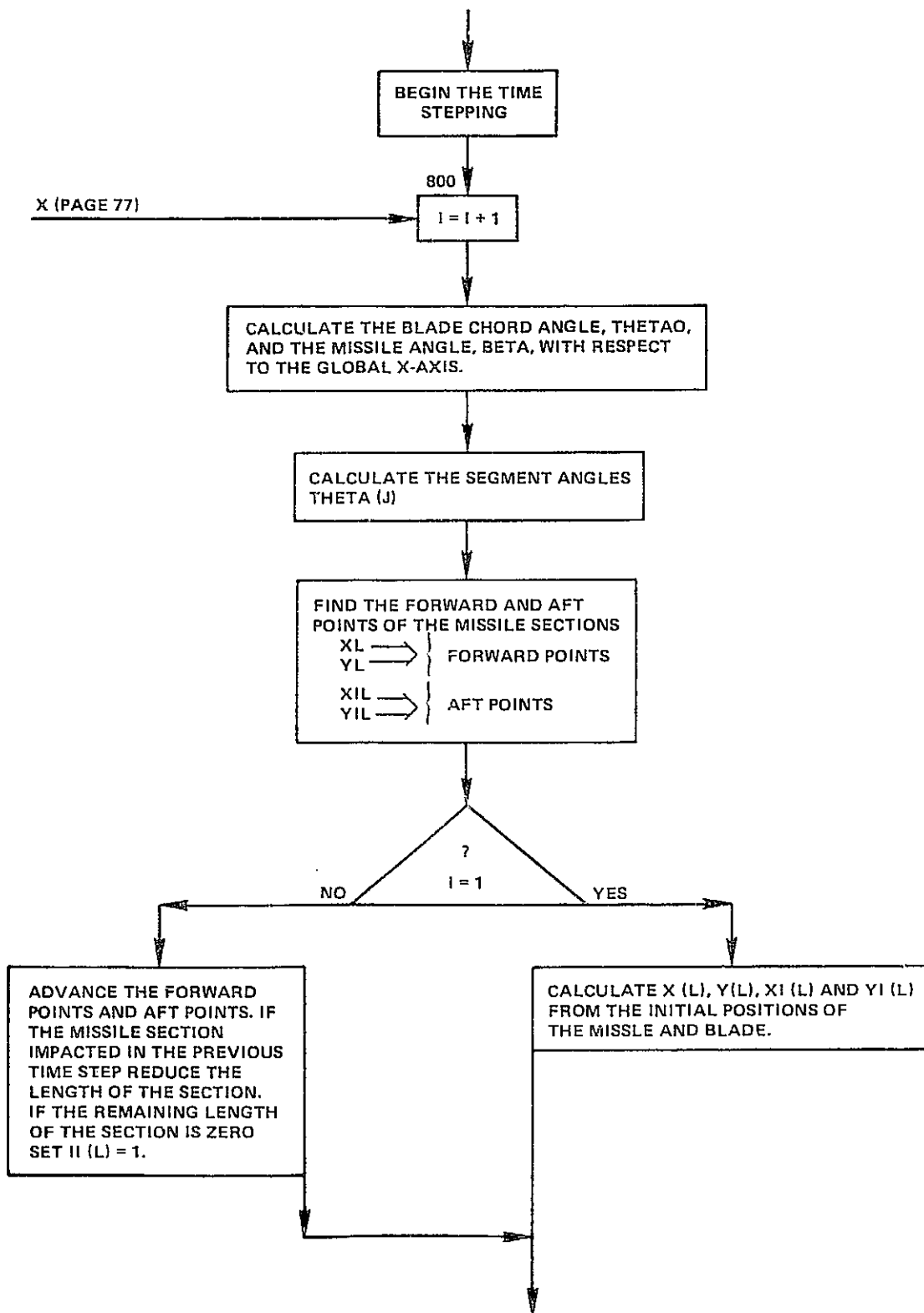
As a final step the routine distributes the total impact force as equivalent pressures located over the two closest nodes bounding the blade segment upon which the center of force is located.

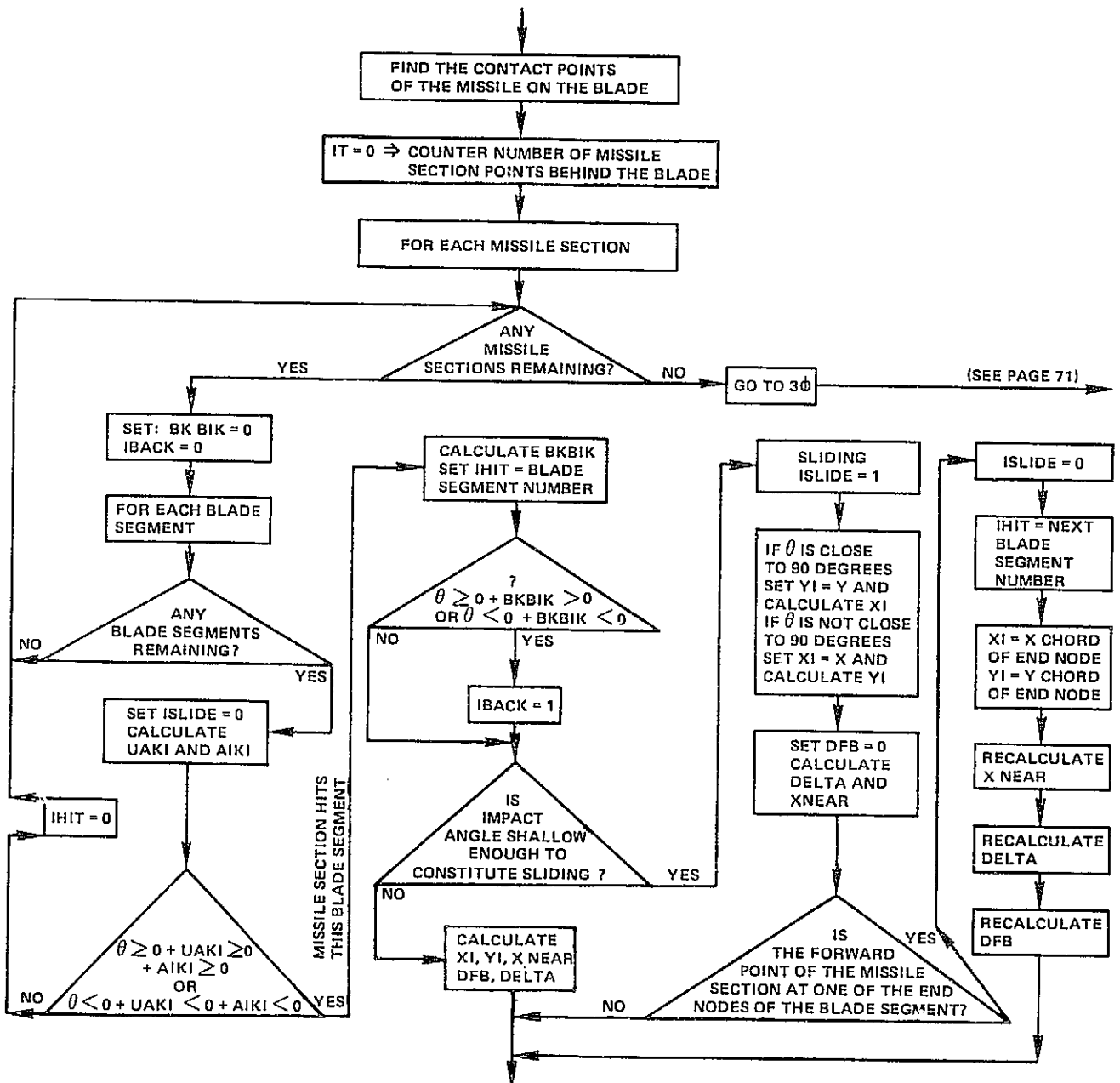
3.13 DETAILED FLOW DIAGRAMS

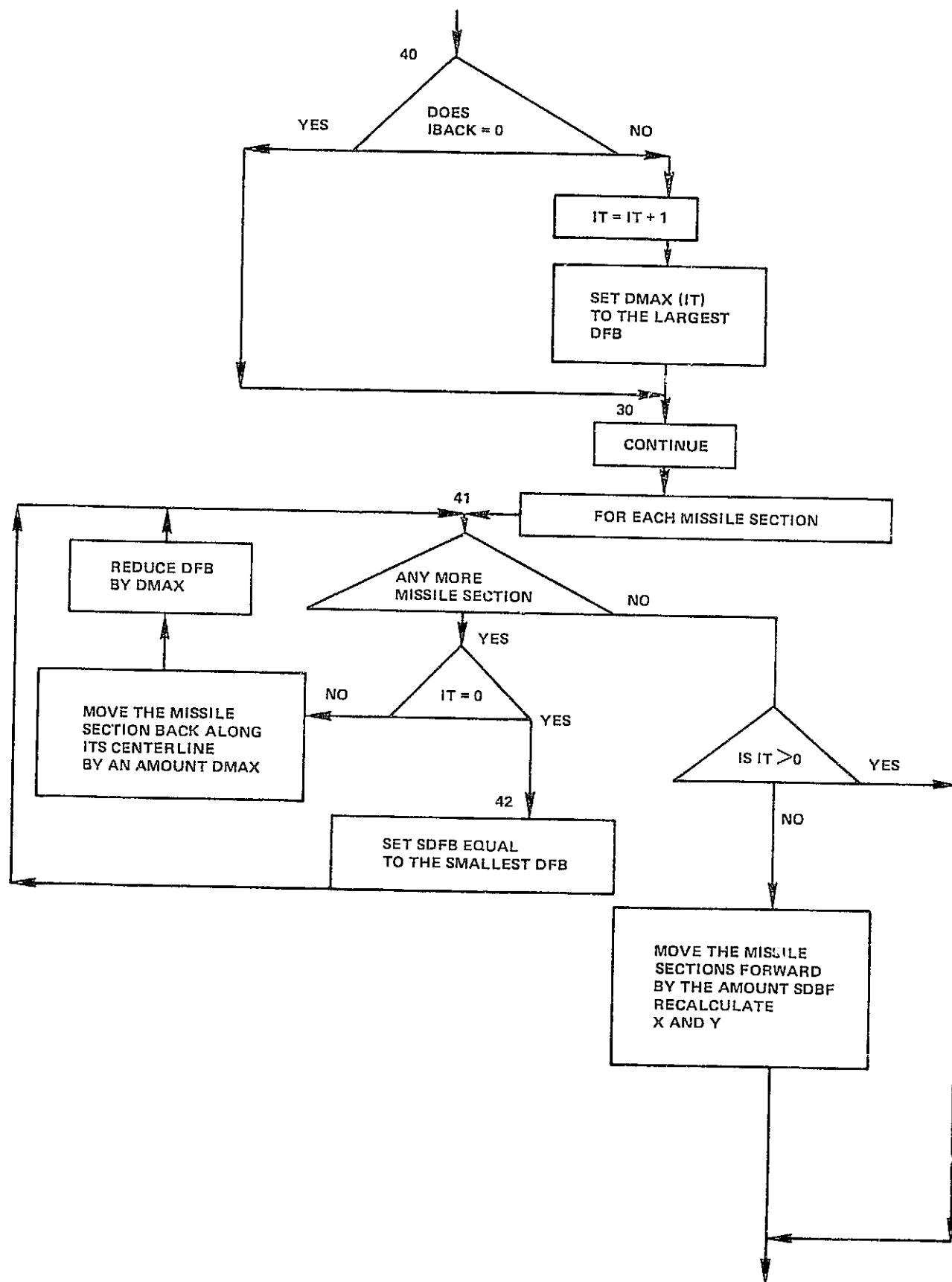
<u>ROUTINE</u>	<u>DISCUSSED IN SECTION</u>	<u>PAGE</u>
1. MAIN	3.1	67
2. P3D	3.2	78
3. LAMBDA	3.3	81
4. CAMBER	3.4	82
5. REGION	3.5	83
6. INCURV	3.6	84
7. PRESUR	3.7	85
8. MODAL	3.8	86
9. PINIT	3.12	87

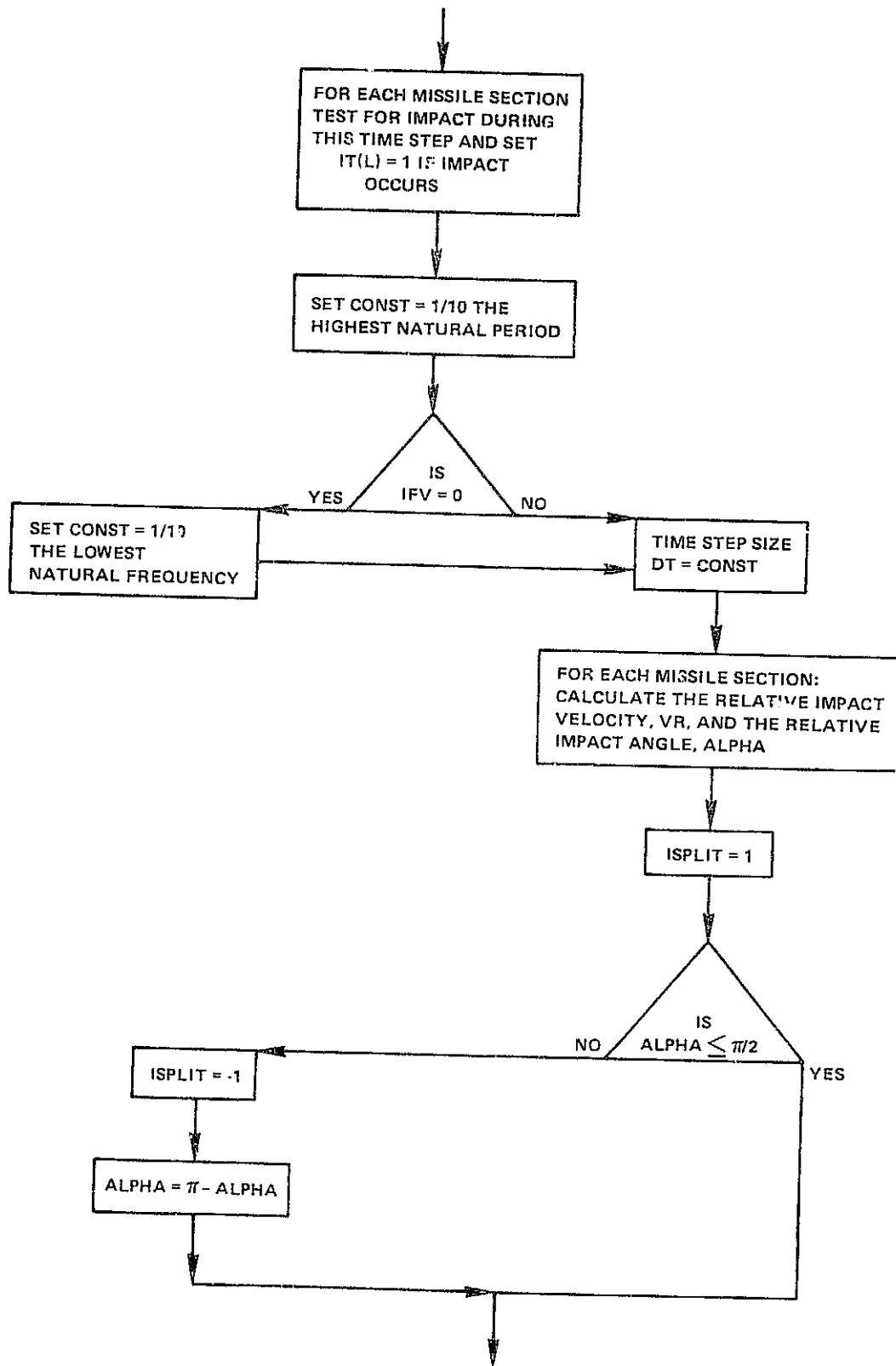


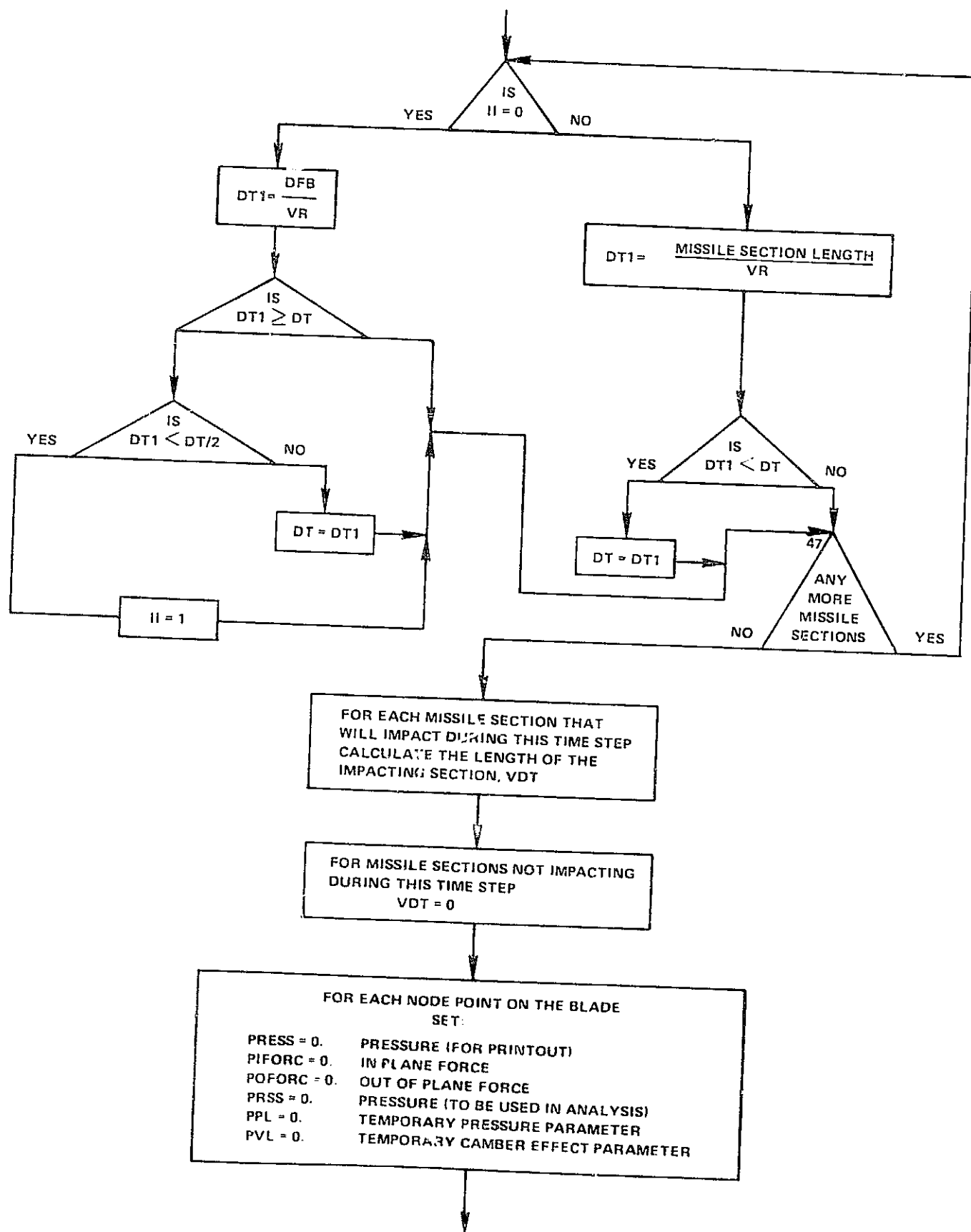


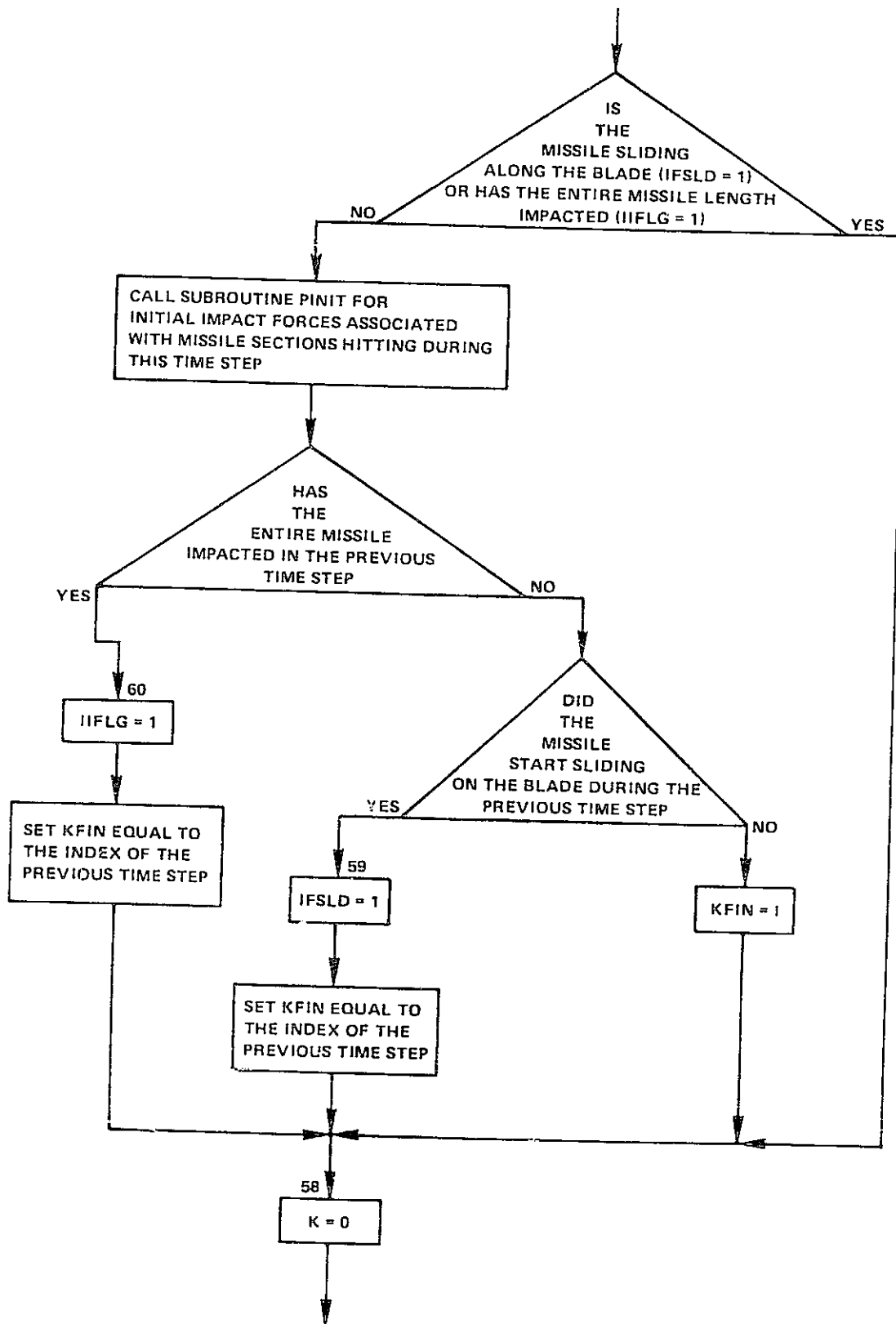


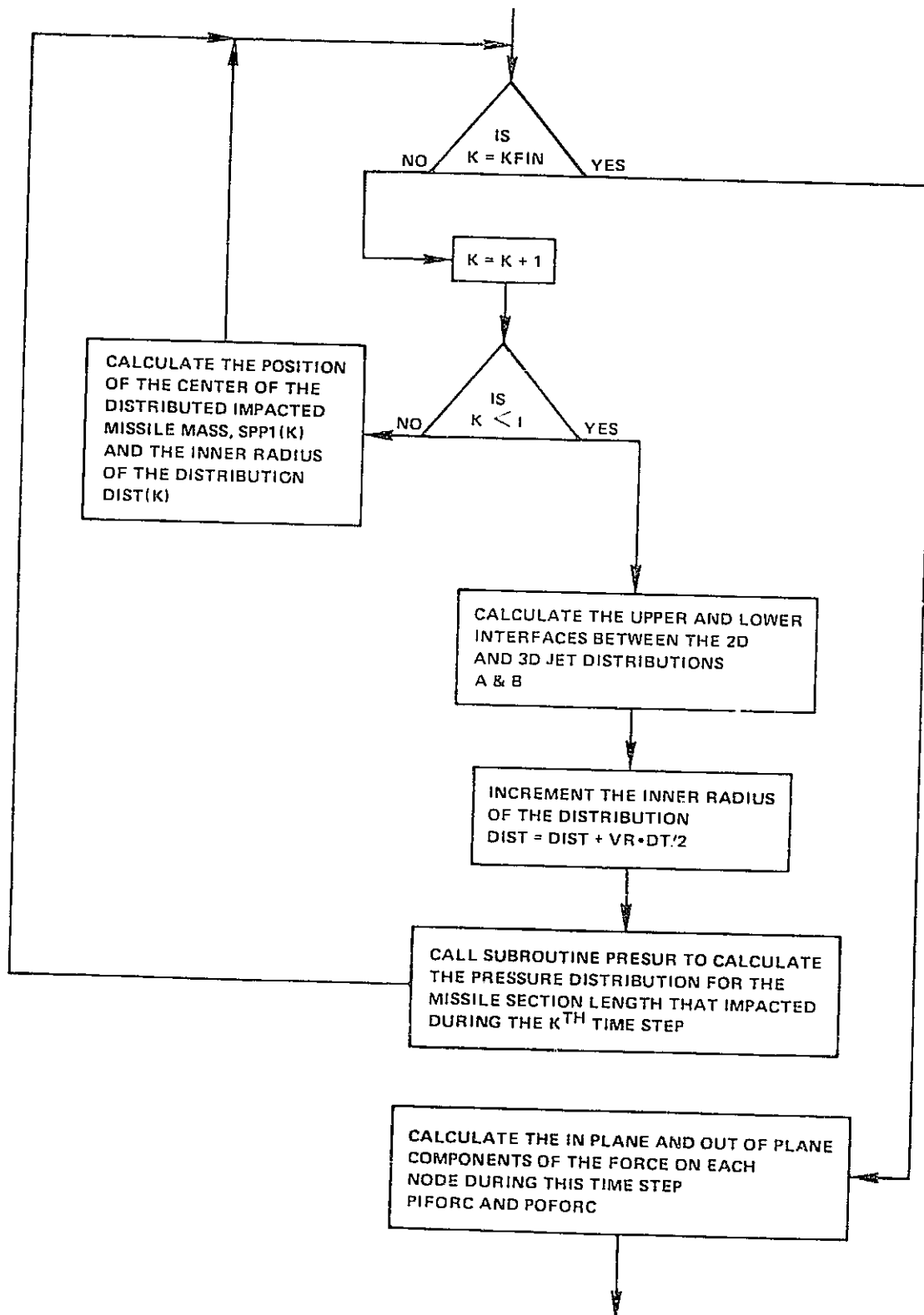


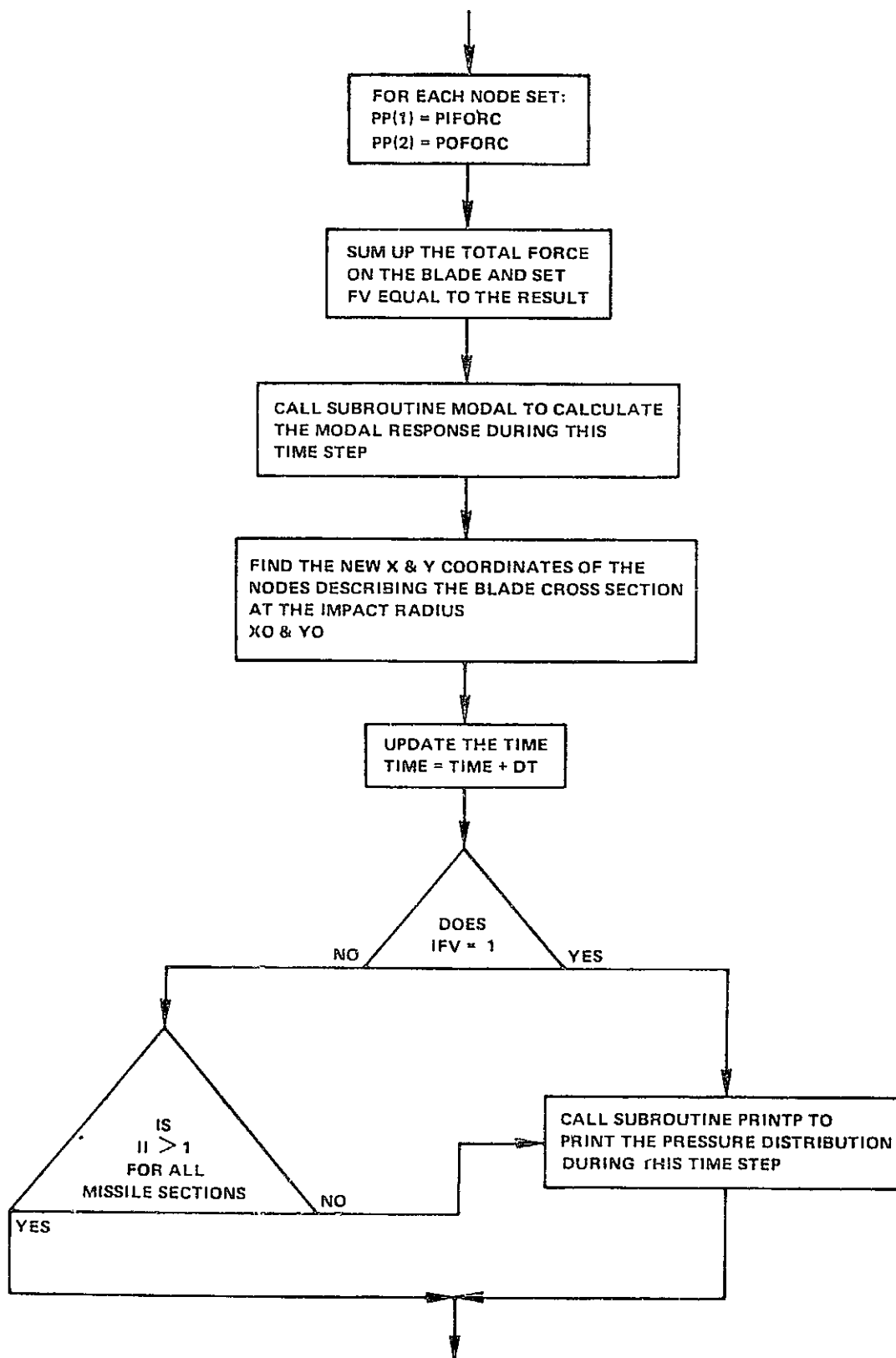


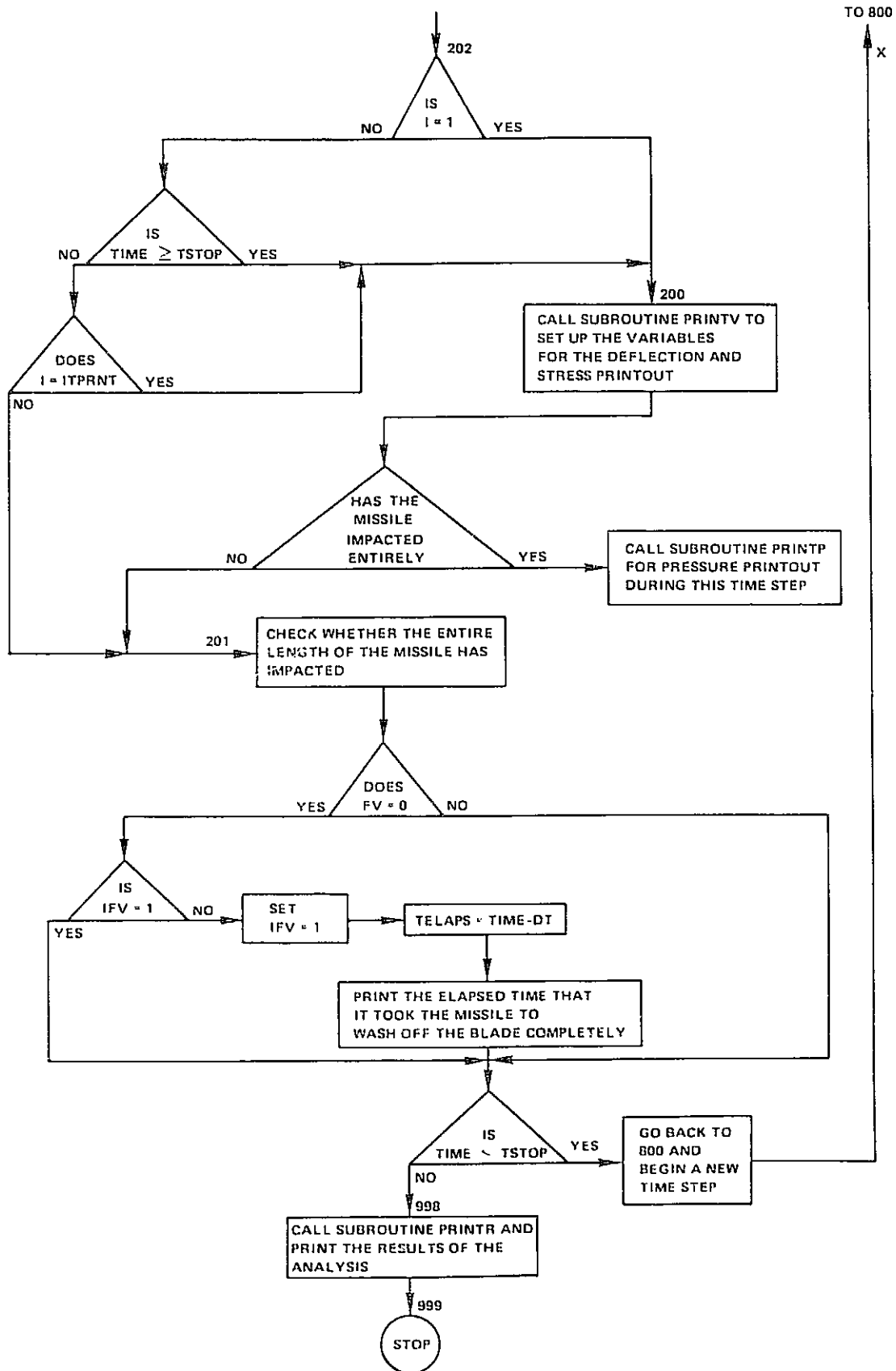


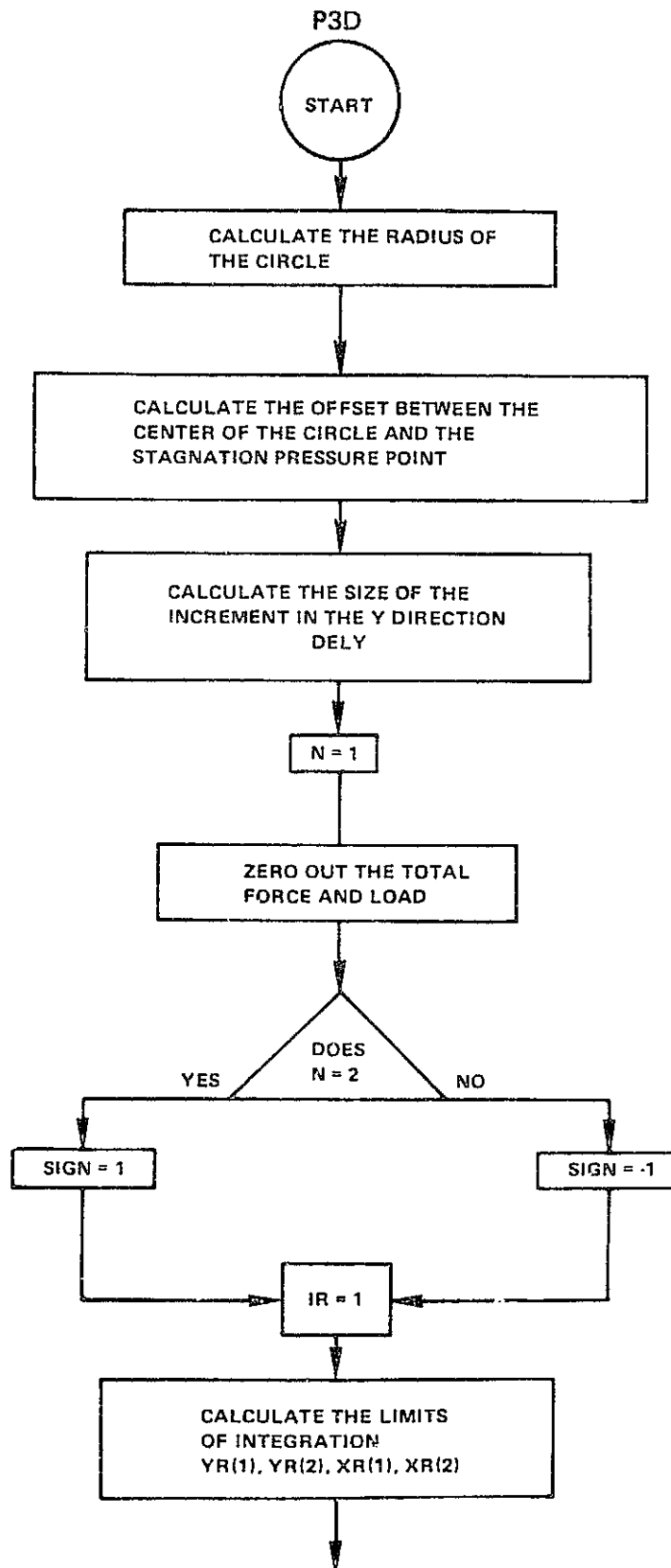


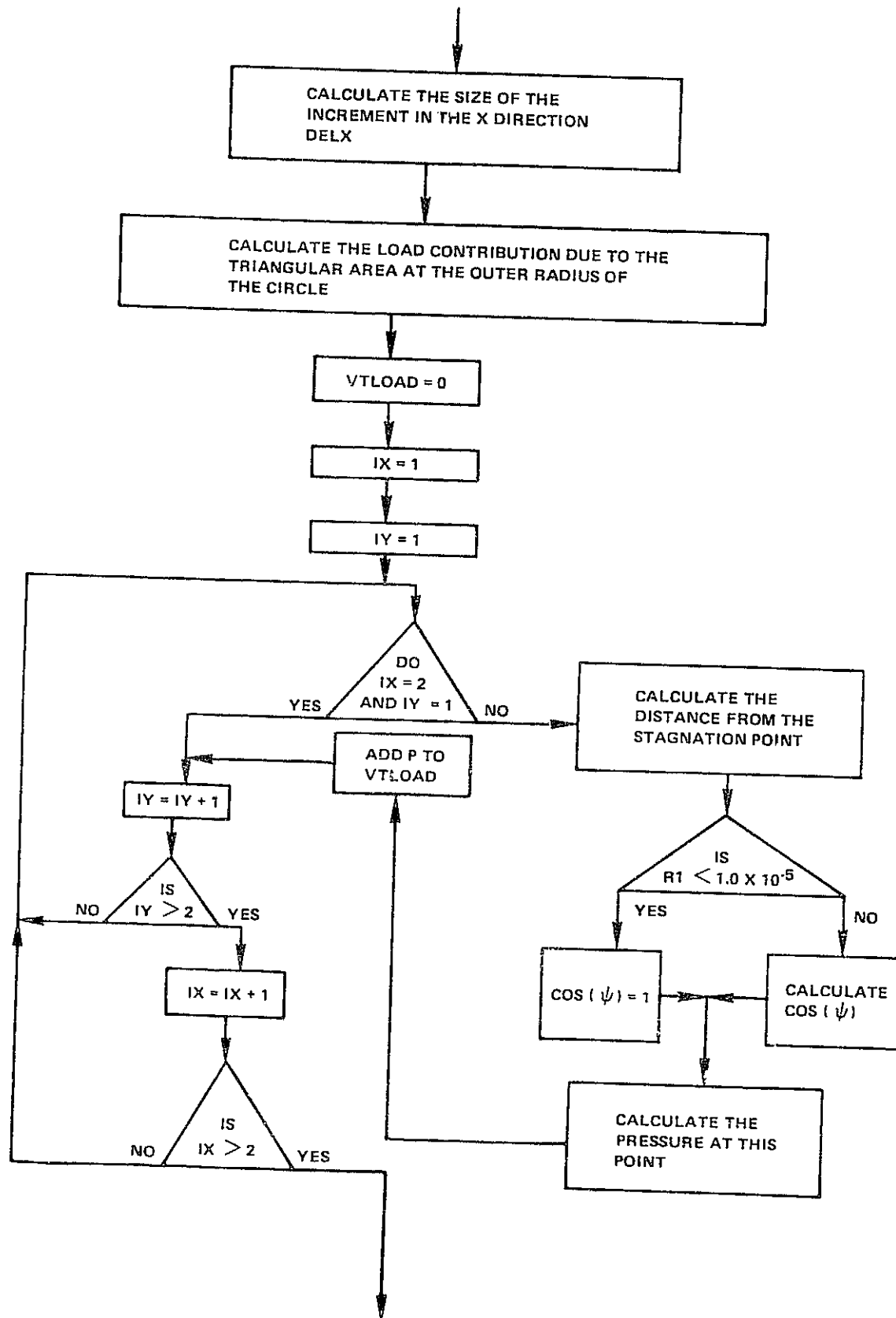


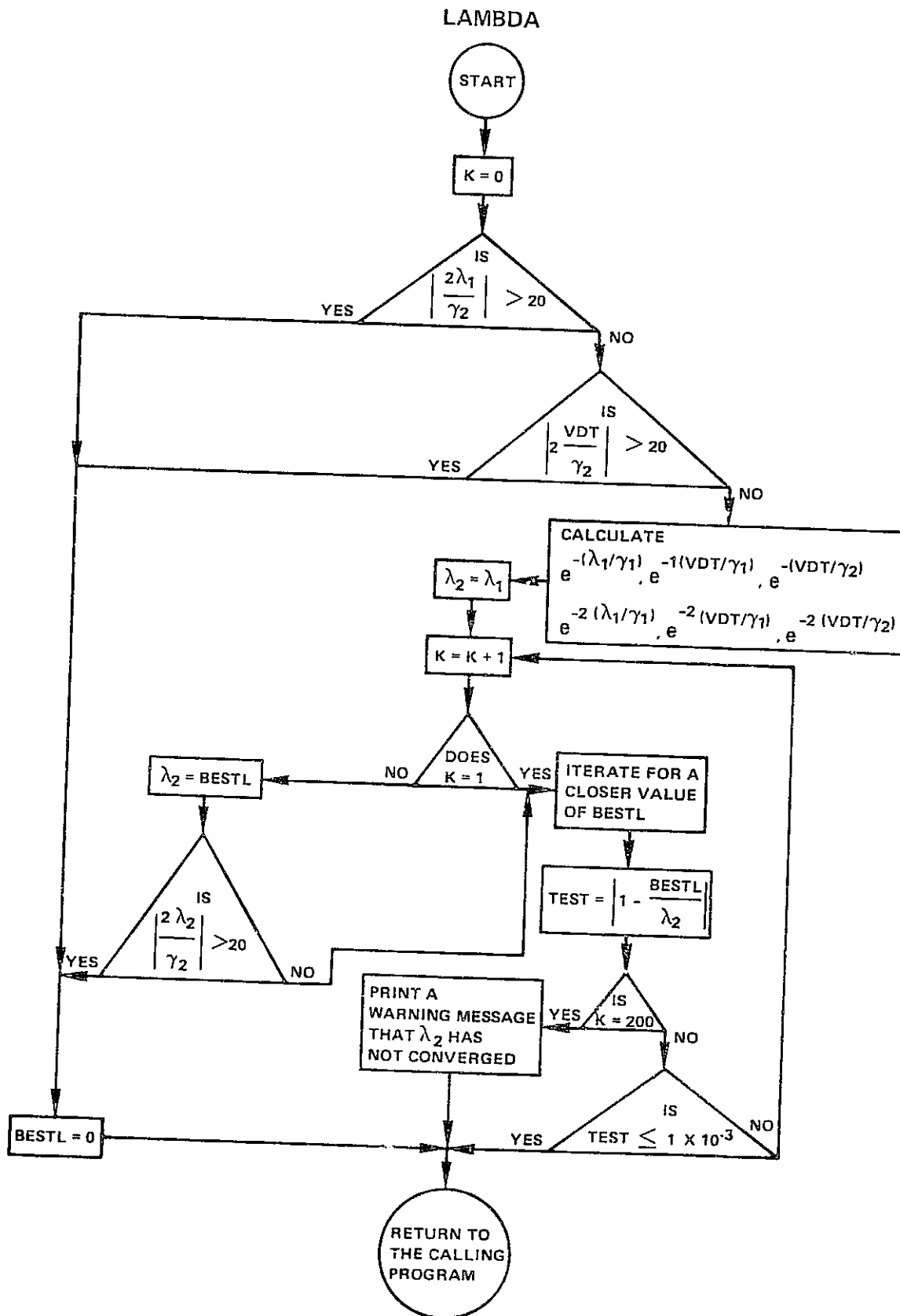


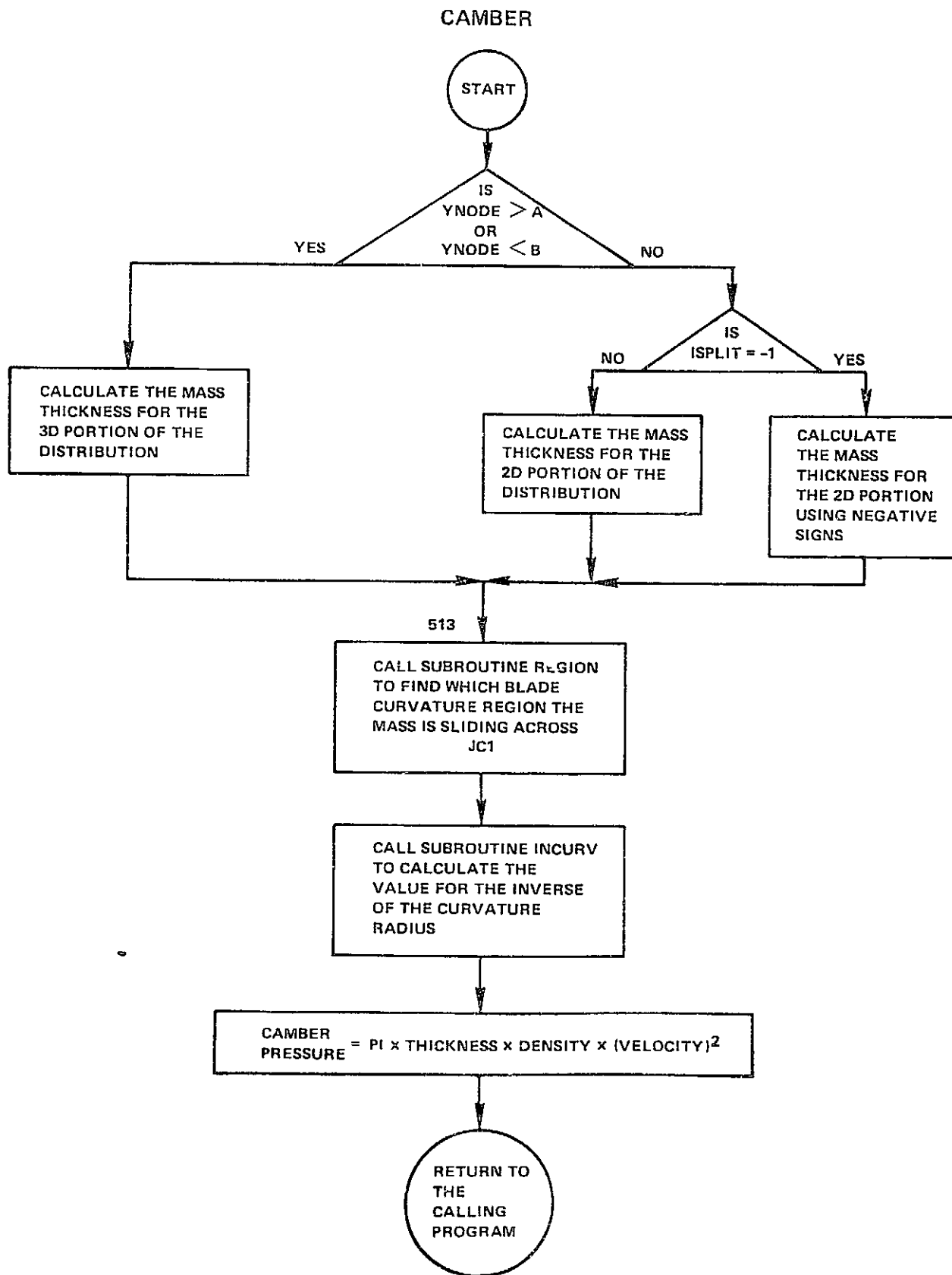


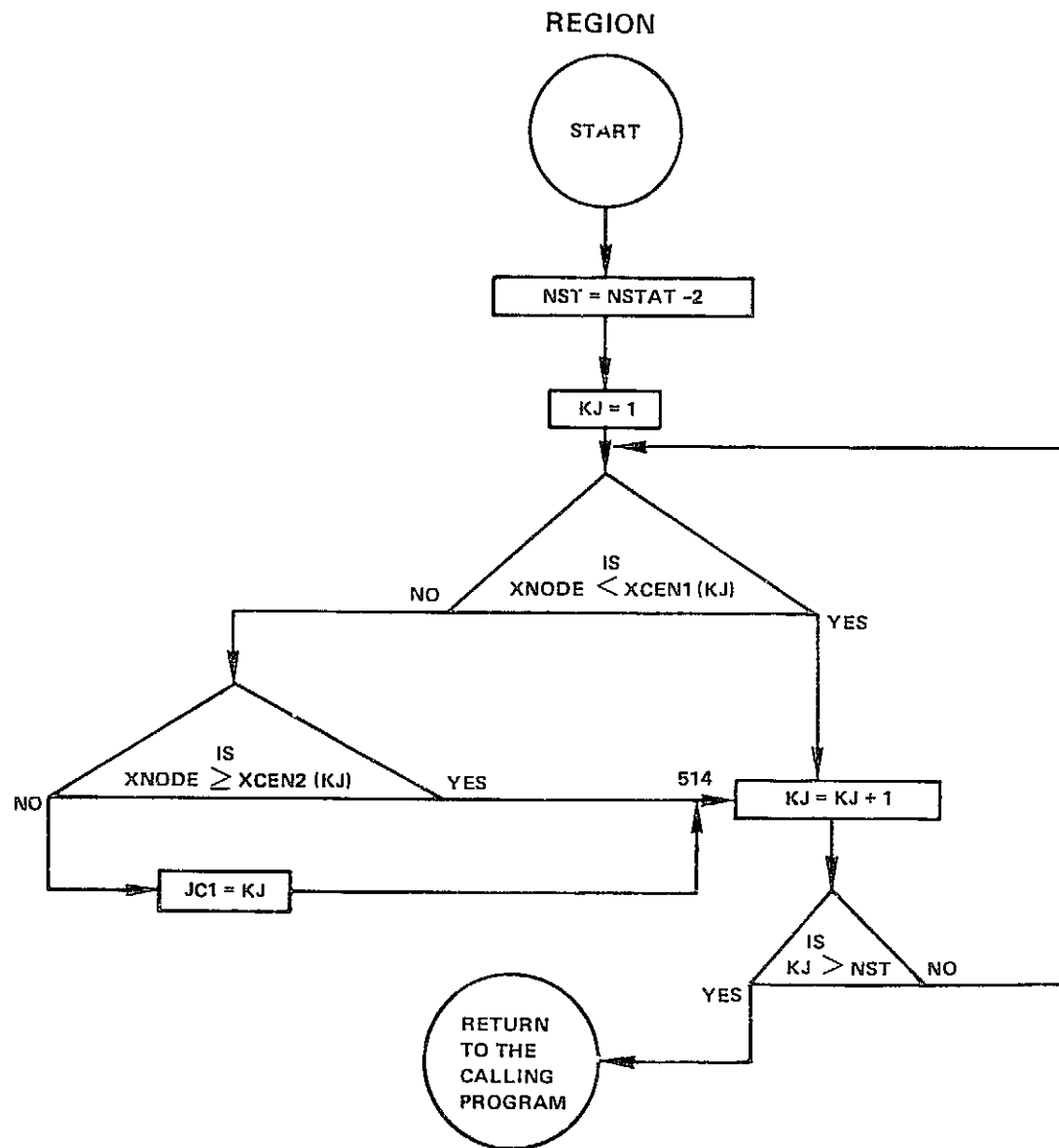


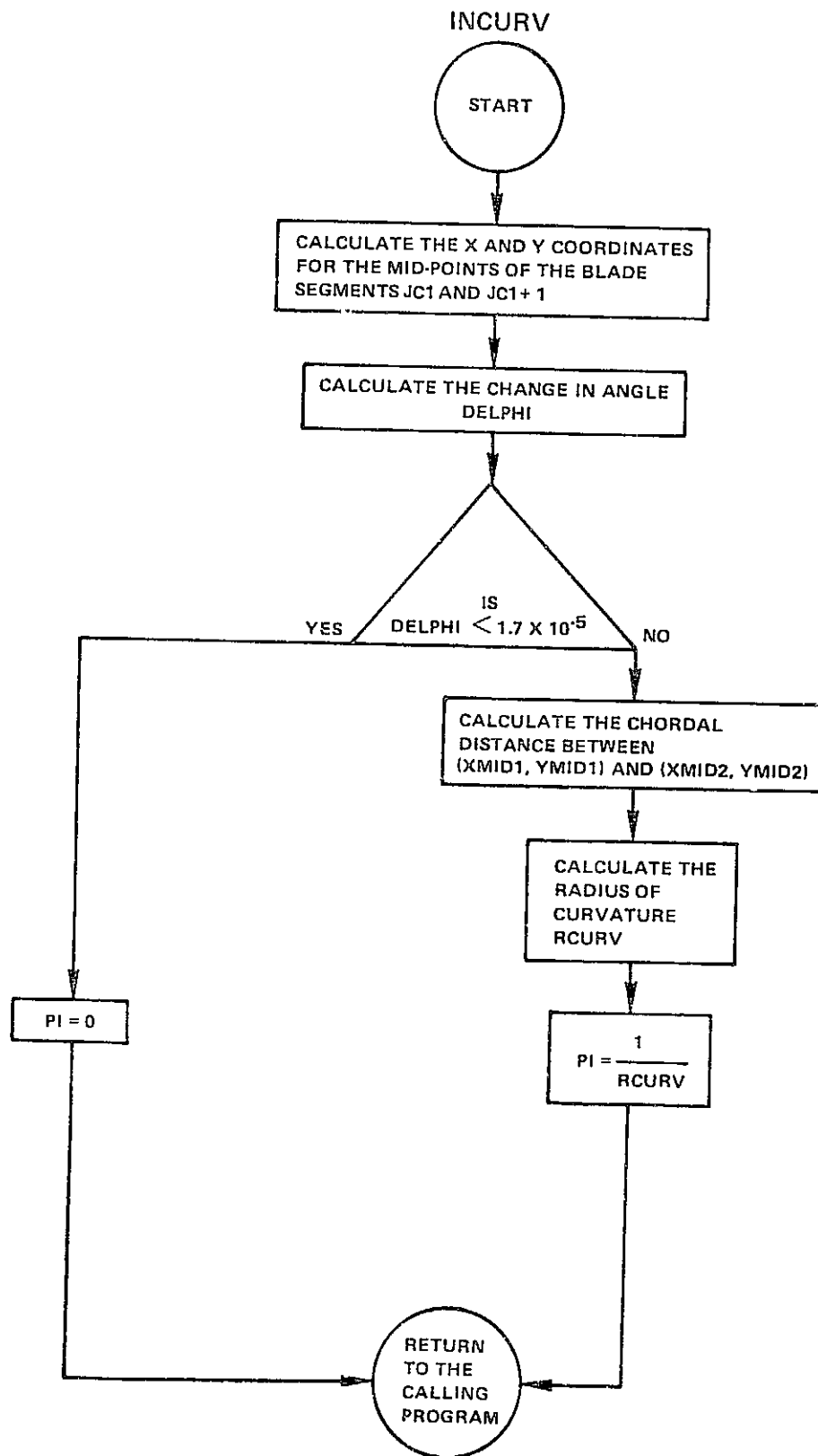


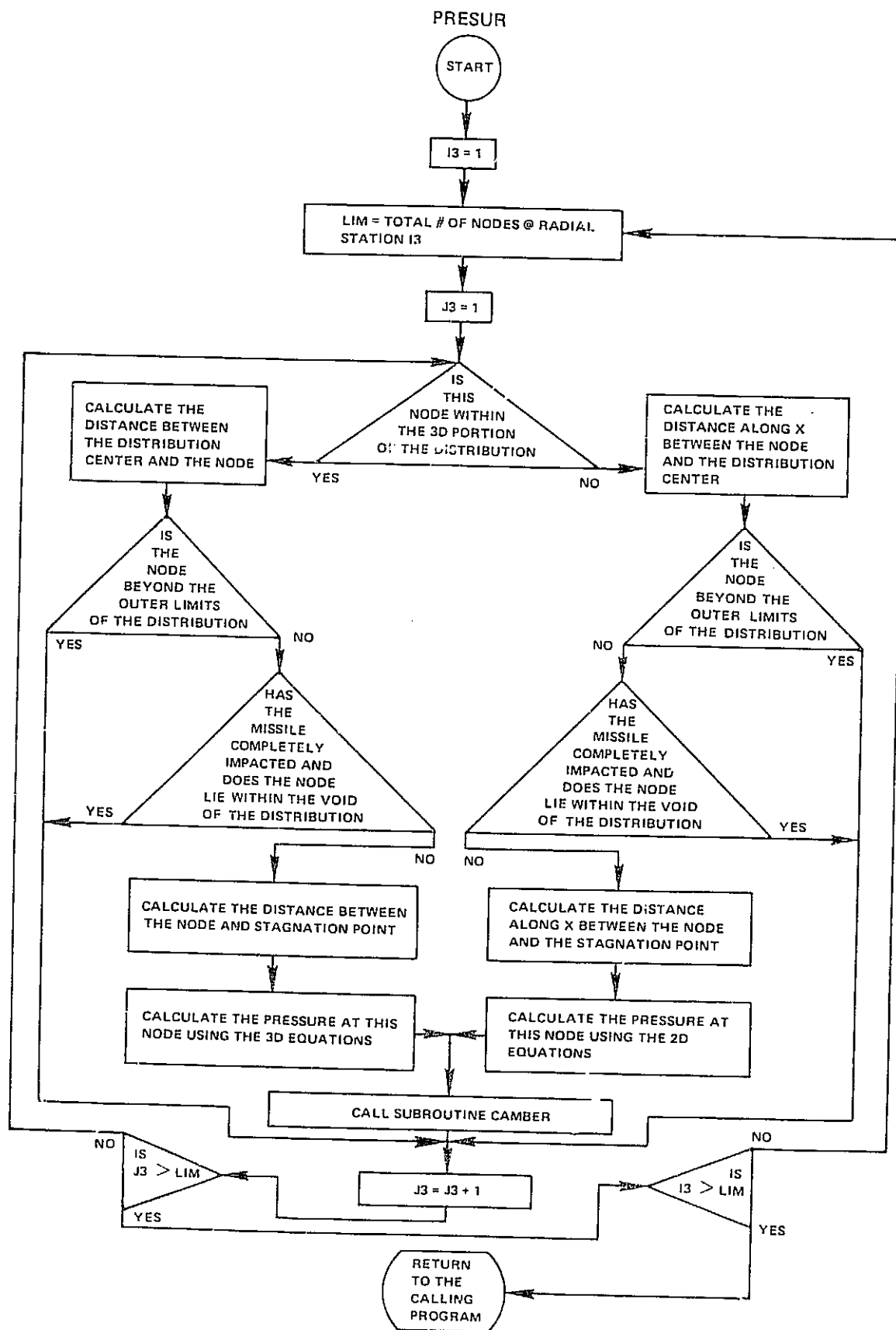


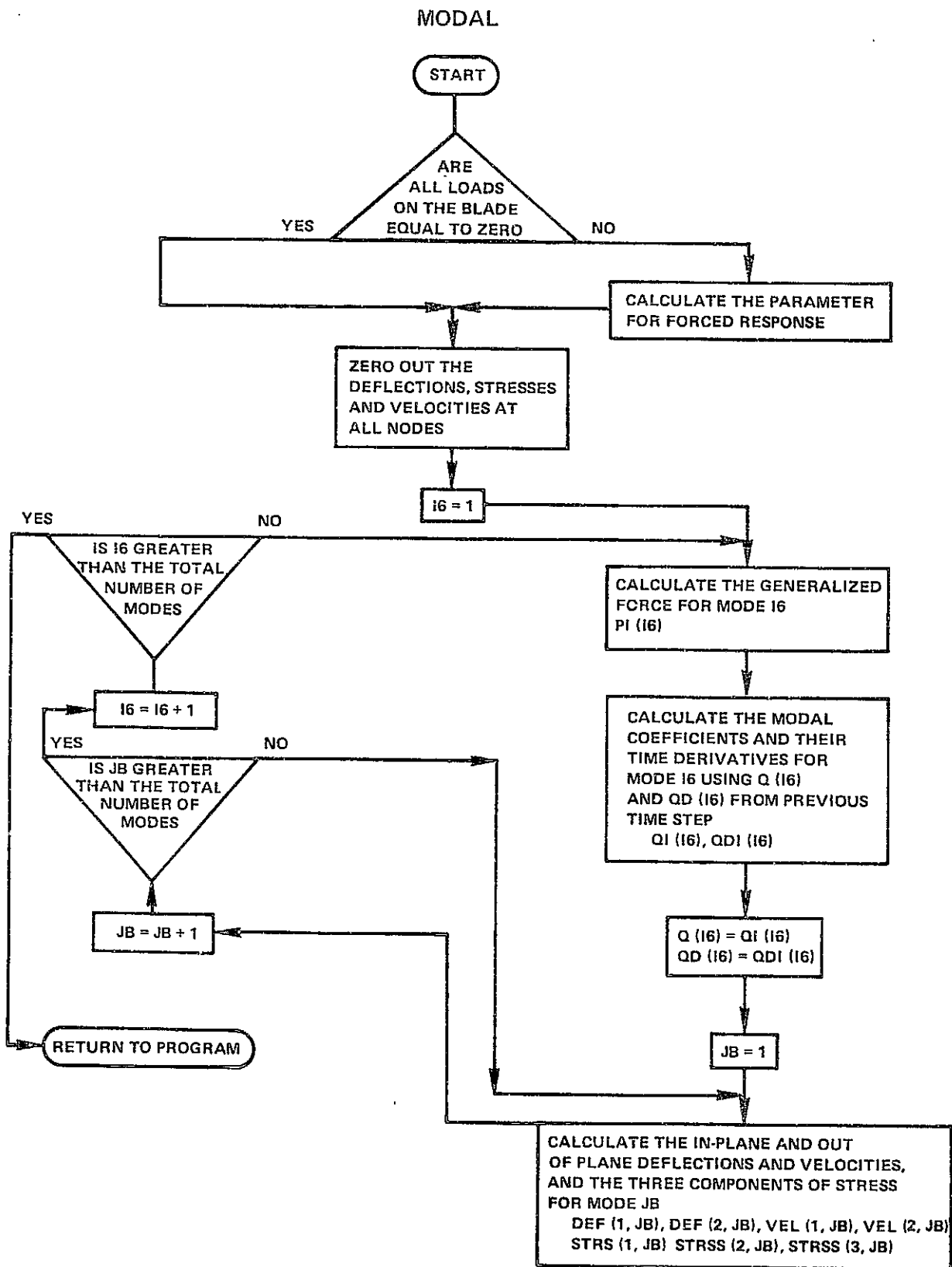


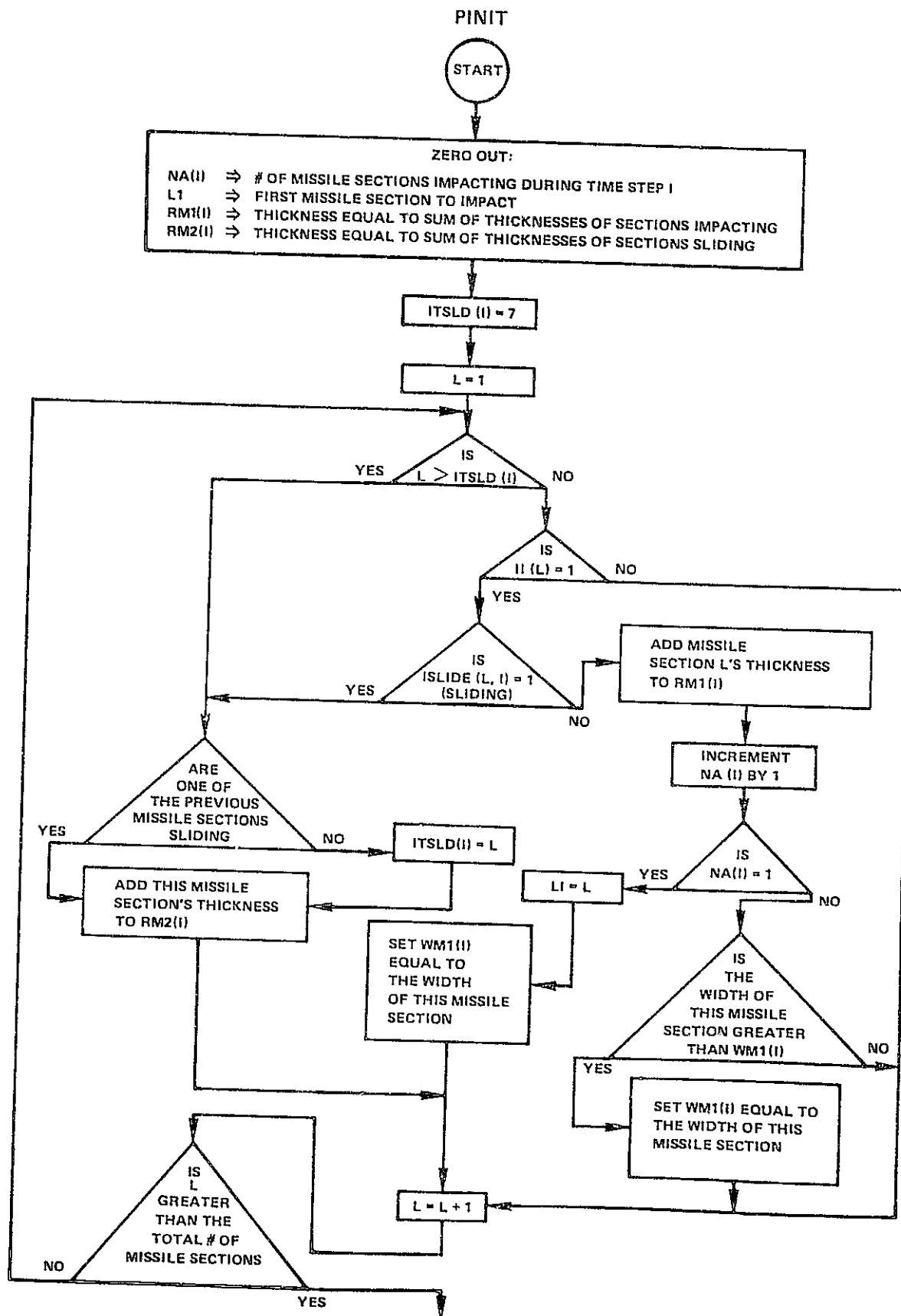


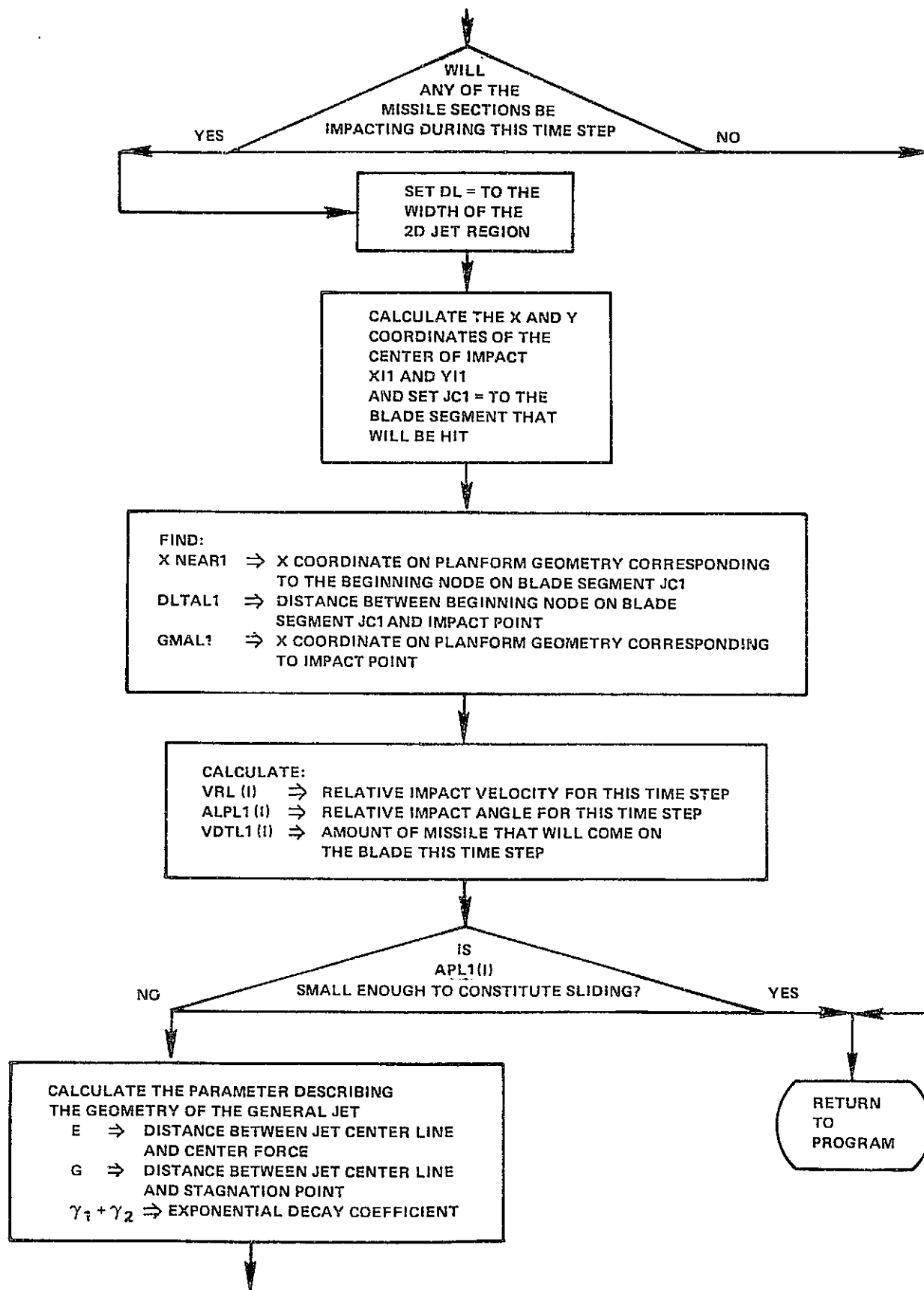


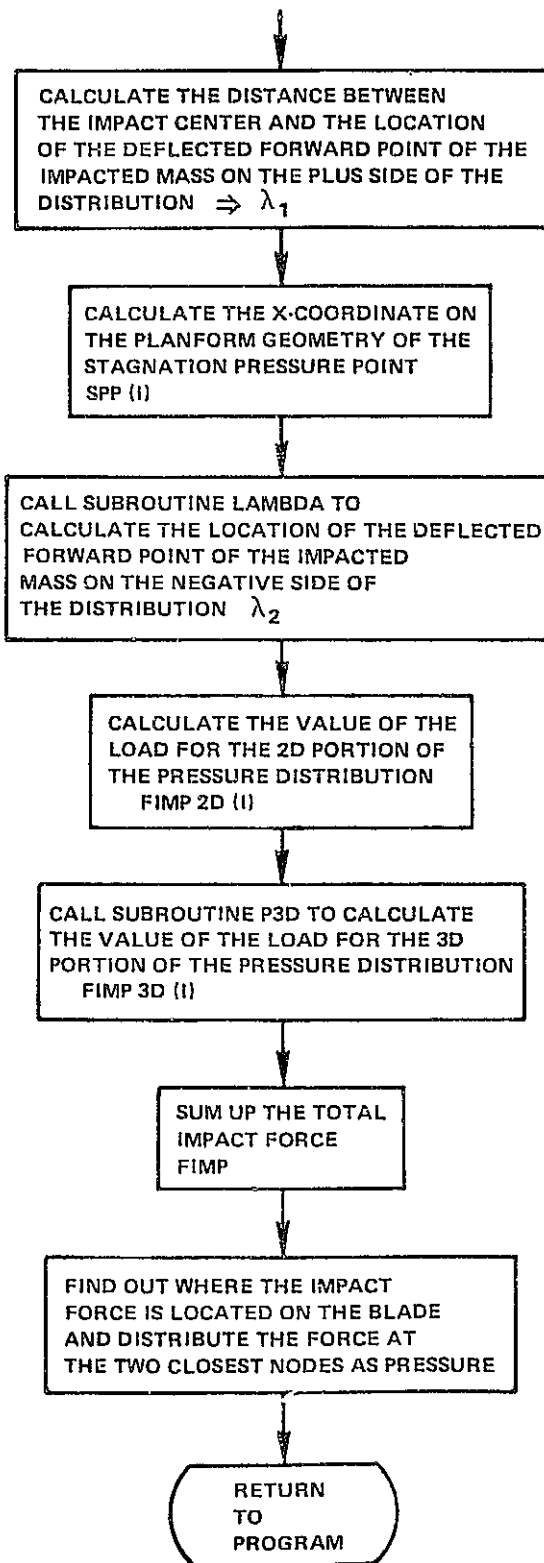












SECTION IV

INSTRUCTIONS ON THE USE OF THE PROGRAM

The MMBI program uses an unformatted method of data input. Individual items of data need only to be separated by a comma or blank. However, it is recommended that sets of data be grouped together in a manner that allows the user to keep track of the number of data points being input per set since a missing data item or a misplaced comma (or blank) may result in gross errors in the analysis. The inputs to the FOD Impact program are grouped into four categories:

- 1) Problem definition
- 2) Missile description
- 3) Modal data
- 4) Blade description

4.1 PROBLEM DEFINITION

V,RIMP,TSTØP,ALPHAO,XOCL,YOCL,NR,NN,NM,NVA,IPDEL,DEN,ISYM

- 1) V - Initial missile impact velocity (in/sec) [REAL]
- 2) RIMP - Impact radius (in.) [REAL]
- 3) TSTØP- Total length of time representing the duration of the analysis. It is recommended that on the first trial run, the user input a time length equal to the blade cord width times the inverse of the cosine of the impact angle, divided by the initial impact velocity. If this run is successful the time length for subsequent runs should be of a duration sufficient to include the impact stage of the problem and the length of time necessary to pass through one complete cycle of vibration at the lowest mode of the blade. (sec.) [REAL]
- 4) ALPHAO - Initial impact angle. Fig. 6 illustrates the sign convention for angles. This angle must be input with a value between 0 and $\frac{\pi}{2}$ radians such

that the blade chord angle, determined with a vector drawn from the leading edge to the trailing edge, must lie between 0 and $\frac{\pi}{2}$ radians (see Section 2.1.3).
(radians) [REAL]

- 5) XOCL, YOCL - In-plane, out-of-plane coordinates for the intersection of the missile centerline and the blade (see Section 2.1.3). (in.) [REAL]
- 6) NR - Total number of radial stations defining the blade. [INTEGER]
- 7) NN - Total number of nodes describing the blade. [INTEGER]
- 8) NM - Total number of nodes to be used in the problem. [INTEGER]
- 9) NVA - Total number of lengthwise sections defining the missile. [INTEGER]
- 10) IPDEL - Number of time steps between each printout of displacements and stresses. [INTEGER]
- 11) DEN - Missile density. Note that the value input for this item must be such that the mass of the missile will be consistent. Thus, if a one-pound spherical missile is being modeled the density must be such that when it is multiplied by the volume of the modeled missile it will yield one pound.

$$\frac{\text{LBS-SEC}^2}{\text{in}^4} \quad [\text{REAL}]$$

- 12) ISYM - Flag indicating whether items input in section 4.2 describe a symmetric (ISYM=0) or unsymmetric (ISYM=1) missile. If ISYM=0 NVA (see 4.1.9) must be equal to 6. [INTEGER]

4.2 MISSILE DESCRIPTION (Fig. 5)

RL(1),RL(2),RL(3),RL(4),RL(5),RL(6)

RM(1),RM(2),RM(3),RM(4),RM(5),RM(6)

CL(1),CL(2),CL(3),CL(4),CL(5),CL(6)

DETL(1),DETL(2),DETL(3),DETL(4),DETL(5),DETL(6)

WM(1),WM(2),WM(3),WM(4),WM(5),WM(6)

- 1) RL(1), RL(2), RL(3), [RL(4), RL(5), RL(6)]*** - Radial distance from missile centerline to centerline of corresponding missile section. Note the sense of positive values of radius. (*The number of input items must be equal to NVA and the numbering order must be from right to left as per Fig. 5.) (in.)
[REAL]
(** If ISYM=0 there must be three entries input for this variable.)
- 2) [RM(1), RM(2), RM(3), RM(4), RM(5), RM(6)]*** - Thickness of missile sections. (in.)
[REAL] (see starred note 4.2.1)
- 3) CL(1), CL(2), CL(3), [CL(4), CL(5), CL(6)]*** - Length of missile sections - (in.) [REAL] (see starred notes 4.2.1)
- 4) [DETL(1), DETL(2), DETL(3), DETL(4), DETL(5), DETL(6)]*** - Offset of each missile section towards aft end from missile center at forward end. (in.)
[REAL] (see starred note 4.2.1)
- 5) WM(1), WM(2), WM(3), WM(4), WM(5), WM(6) - Width of missile sections including both the 2-D and 3-D portions. (see section 2.2.3) (in.) [REAL] (see starred notes 4.2.1)

*** Needed only if ISYM=1 and NVA>3.

4.3 MODAL DATA

MAX(1), MAX(2), MAX(3), MAX(4), -----MAX(NR)

NJ3(1), NJ3(2), NJ3(3), NJ3(4), -----NJ3(NR)

VMI(1), VMI(2), VMI(3), VMI(4), -----VMI(NM)

DR(1), DR(2), DR(3), DR(4), DR(5), -----DR(NM)

WØ(1), WØ(2), WØ(3), WØ(4), -----WØ(NM)

PH2(1,1,1), PH2(1,2,1), PH2(1,3,1), -----, PH2(1,NN,1),

PH2(2,1,1), PH2(2,2,1), PH2(2,3,1), -----, PH2(2,NN,1),

PH2(1,1,2), PH2(1,2,2), PH2(1,3,2), -----, PH2(1,NN,2),

PH2(2,1,2), PH2(2,2,2), -----PH2(2,NN,2)

PH2(1,1,3), PH2(1,2,3), -----PH2(1,NN,3), -----PH2(2,NN,3), -----

PH2(1,1,NM), -----PH2(1,NN,NM), -----PH2(2,NN,NM)

SH2(1,1,1), -----SH2(1,NN,1), -----SH2(2,NN,1), -----SH2(3,NN,1),

SH2(1,1,2), -----SH2(1,NN,2), -----SH2(2,NN,2), -----SH2(3,NN,2), -----

SH2(1,1,NM), -----SH2(1,NN,NM), -----SH2(2,NN,NM), -----SH2(3,NN,NM)

- 1) MAX(1), MAX(2), ---MAX(NR) - Number of nodes at each radial station of the blade. [INTEGER]

MAX ≤ 25

- 2) NJ3(1), NJ3(2), ---NJ3(NR) - Index corresponding to the chordwise node at each radial station for which the user wishes to obtain displacement and

stress output results. (e.g. if radial station 6 of the blade has its center of twist located at node 7 from the leading edge, the user may wish to input NJ3(6) = 7). [INTEGER]

- 3) VMI(1), VMI(2), ---VMI(NM) - Modal mass corresponding to the first, second --- NM modes of the blade. ($1 \leq NM \leq 10$) [REAL]
- 4) DR(1), DR(2), --- DR(NM) - Critical damping ratio associated with each mode. ($1 \leq NM \leq 10$) [REAL]
- 5) W ϕ (1), W ϕ (2), --- W ϕ (NM) - Modal frequency associated with each mode. ($1 \leq NM \leq 10$) (Radians/sec) [REAL]
- 6) PH2(1, 1, 1), PH2(1, 2, 1), PH2(1, 3, 1) --- PH2(1, NN, 1) - In-plane displacement components for the first mode at each node of the blade.
(*The numbering of nodes is row by row from the leading edge node to the trailing edge node. Thus the data will be composed of displacements corresponding to the nodes of the lowest radial station, then the nodes of the next radial station, etc.) [REAL]
- 7) PH2 (2, 1, 1), PH2 (2, 2, 1), PH2 (2, 3, 1) --- PH2 (2, NN, 1) - Out-of-plane displacement components for the first mode at each node of the blade. [REAL]
(see starred note 4.3.6)
- 8) PH2(1, 1,2), PH2(1, 2,2), PH2(1, 3, 2) --- PH2(1, NN, 2) - In-plane displacement components for the second mode at each node of the blade. [REAL] (see starred note 4.3.6)
- 9) PH2(2, 1, 2), PH2(2, 2, 2), PH2(2, 3, 2) --- PH2(2, NN, 2) - Out-of-plane displacement components for the second mode at each node of the blade. [REAL]
(see starred note 4.3.6).
- 10) PH2(1, 1, 3) --- PH2(1, NN, 3), PH2(2, 1, 3), --- PH2(2, NN, 3), ---,
PH2(1, 1, NM), PH2(1, 2, NM), ---, PH2(1, NN, NM), PH2(2, 1, NM), PH2(2, 2, NM),
--- PH2(2, NN, NM) - In-plane and out-of-plane displacement components corresponding to each mode at the nodes of the blade. The order of

input follows the same as in 4.3.6 thru 4.3.9, i.e. first the in-plane components at each node, then the out-of-plane components at each node, etc., etc. for each mode. [REAL] (see starred note 4.3.6).

- 11) SH2(1, 1, 1), SH2(1, 2, 1), --- SH2(1, NN, 1), SH2(2, 1, 1), --- SH2(2, NN, 1), SH2(3, 1, 1), SH2(3, 2, 1), --- SH2(3, NN, 1), SH2(1, 1, 2), SH2(1, 2, 2), --- SH2(1, NN, 2), SH2(2, 1, 2), SH2(2, 2, 2), --- SH2(2, NN, 2), SH2(3, 1, 2), SH2(3, 2, 2), --- SH2(3, NN, 2), ---SH2(1, 1, NM), SH2(1, 2, NM), ---SH2(1, NN, NM), SH2(2, 1, NM), SH2(2, 2, NM), --- SH2(2, NN, NM), SH2(3, 1, NM), SH2(3, 2, NM) --- SH2(3, NN, NM) - Three components of stress at each node, for each mode. The order of input consists of first inputting the first component (usually chordwise) at each node, then the second component (usually radial) at each node, then the third component (usually shear) at each node, then repeating for the next mode until all modes have been input. [REAL] (see starred note 4.3.6).

4.4 BLADE DESCRIPTION (Figs 1 and 2)

```

YNØDE(1)

XNØDE(1,1),XNØDE(1,2),XNØDE(1,3),-----XNØDE(1,MAX(1)),

YNØDE(2)

XNØDE(2,1),XNØDE(2,2),XNØDE(2,3),-----XNØDE(2,MAX(2)),
| | | | | | | | | | | | | | | | | |
YNØDE(NR)

XNØDE(NR,1),XNØDE(NR,2),XNØDE(NR,3),-----XNØDE(NR,MAX(NR))

XØ(1), XØ(2), XØ(3), ---- XØ(MAX(impact radial station))

YØ(1), YØ(2), YØ(3), ---- YØ(MAX(impact radial station))

```

- 1) YNØDE(1) - Radius of the first radial station. (in.) [REAL]
- 2) XNØDE(1, 1), XNØDE(1, 2), ---XNØDE(1,MAX(1)) - Chordwise coordinates of the nodes lying on radial station 1. (* Input order is from the leading edge to the trailing edge.) (in.) [REAL]
- 3) YNØDE(2) - Radius of the second radial station. (in.) [REAL]
- 4) XNODE(2, 1), XNODE(2, 2), --- XNODE(2, MAX(2)) - Chordwise coordinates of the nodes lying on the second radial station. (in.) [REAL] (See starred note 4.4.2)
- 5) YNØDE(3), XNØDE(3, 1), --- XNØDE(3, MAX(3)), YNØDE(4), XNØDE(4, 1), --- XNØDE(4, MAX(4)), --- YNØDE(NR), XNØDE(NR, 1), --- XNØDE(NR, MAX(NR)) - Radial coordinate of radial stations and chordwise coordinate of nodes corresponding to each radial station. Order of inputs is as shown. NR≤25.
- 6) XØ(1), XØ(2), XØ(3), --- XØ(MAX(impact radial station)) - In-plane coordinates of nodes segmenting the blade chord at the impact radial station. (see starred note below). Input order is from the leading edge to trailing edge. (in.) [REAL]

7) $Y\phi(1), Y\phi(2), Y\phi(3), \dots, Y\phi(\text{MAX}(\text{impact radial station}))$ - Out-of-plane coordinates of nodes segmenting the blade chord at the impact radial station. Input order is from the leading edge to the trailing edge. (in.)
[REAL]

*NOTE: The coordinates $X\phi(J), Y\phi(J)$ must be such that

$$0 \leq \cos^{-1} \frac{X\phi(J+1) - X\phi(J)}{\sqrt{[X\phi(J+1) - X\phi(J)]^2 + [Y\phi(J+1) - Y\phi(J)]^2}} \leq \frac{\pi}{2}$$

4.5 OUTPUT

4.5.1 Pressure Distribution

During the time in which there remains a portion of unimpacted missile length the MMBI program prints out the pressure distribution for each time step. When the entire length of missile has impacted the blade, pressure printout is performed for every IPDEL time step until the final TSTOP is reached. In addition, when the pressures on the blade have reduced to a negligible amount, the program prints out a message to the user indicating the time elapsed to complete the impact phase of the problem. If the value of TSTOP is reached before the pressures on the blade have reduced to negligible values, the program prints out a message informing the user that the length of time allotted to solve the problem is too short.

4.5.2 Poor Convergence in Subroutine LAMBDA

As mentioned in Section 3.3.2, the program is instructed to print a warning message informing the user that it was unable to converge to a one percent accuracy

for the definition of the impacted missile mass shape. The best accuracy achieved is printed and the program will continue with the analysis. Generally, accuracies within 5 percent are acceptable, and accuracies greater than 5 percent are indicative of an error in the inputs with respect to missile shape (see 4.2).

4.5.3 Displacement and Stress

In addition to printing out the displacement and stress output for each IPDEL time step, the program will print the displacements and stresses for the first and last time steps of the problem. Displacement and stress output is printed in two configurations. The in-plane and out-of-plane displacements at the node NJ3 (see 4.3.2) of each radial station are printed out vs. the radial coordinate of the radial station. In addition, the stresses in the radial direction at the leading edge node, node NJ3, and trailing edge node of each radial station are printed out vs. the corresponding radial coordinates. Note that in order for this printout to be successful the user must input the proper component of stress as mentioned in 4.3.11. The second configuration of displacement and stress printout consists of tabulating this data with respect to the chordwise distance relative to the leading edge at the impact radial station. The in-plane and out-of-plane displacements at the nodes lying on the impact radial station are printed out versus their chordwise distance from the leading edge. The program then prints out the chordwise (STRESS-X), radial (STRESS-Y), and shear (SHEAR-XY) stress components at the nearest radial station below the impact radius, the impact radial station, and the nearest radial station above the impact radius, for chordwise distances relative to the leading edge.

SECTION V

DEMONSTRATION PROBLEMS

As noted in the introduction to Section II, the MMBI program solves the problem of missile impacts on blades in three separate phases. The demonstration problems presented in this section illustrate the program's ability to handle the missile and blade geometry and its analysis of the pressure distribution associated with the impacting missile. Presented in Section 5.2 is a complete modal response analysis of a soft body impact on a blade.

5.1 Impacts on Rigid Plates

The impacting missile used in these analyses is a 600 gram, cylindrically shaped mass with a 2 to 1 length to diameter ratio, impacting the target at a velocity of 7800 in/sec. Specifically, the length of the missile is 5.8 in., making the density $8.89 \times 10^{-5} \frac{\text{lb-sec}^2}{\text{in}^4}$. Fig. 28 illustrates the parameters used in modeling the missile for the program.

Since the target is rigid, the modal displacements are set to zero. In addition, only one mode need be used, with a frequency chosen such that the time step sizes calculated by the program will be sufficient to illustrate the variation of the pressure distribution with respect to time and target surface. Since the length of the missile is 5.8 in., the frequency is chosen as 8449.8 rad/sec. The program will calculate a time step from

$$\Delta t = \frac{2\pi}{10 \times 8449.8} = 7.4359 \times 10^{-4} \text{ sec}$$

(see Section 3.1.8)

The length of missile that will impact during each time step will then be

$$\Delta L = 7800 \times 7.4359 \times 10^{-4} = .58 \text{ in.}$$

It will therefore take 10 time steps for the missile to impact the blade at an impact angle of 90 degrees.

The program was run using impact angles of 25° , 45° and 90° . The results were then compared to experimental data reported in Ref. 20 on similar impacts. Table III summarizes the results which are plotted in Figs. 29, 30 and 31. Generally, the data points are shifted toward the stagnation pressure point by .75 inches. The general shape of the distributions for both the calculated and observed results are similar. In the case of the 25 degree impact the correlation is poor for points near the center of impact lying along the minor axis. However, the relative values for the data points located at the center of impact and at a radius of .46 inches in this case from the center to the outer point. This result is contrary to both theory and to the results for the 45 and 90-degree cases, indicating that the test data for pressure ratios along the minor axis in the 25-degree case is questionable.

5.2 30-DEGREE IMPACT OF A 1 LB. SPHERE ON A FLAT PLATE SIMULATED Q-FAN BLADE

Fig. 32 depicts the model used in performing this analysis. The blade consists of rigid steel plate bolted on a titanium spar between the 26-inch and 33.75-inch radial stations. The plate measures 10 inches between the leading edge and trailing edge, is flat on the impact face, and tapers on the rear (or spar) face from a nominal thickness of .31 inches at the center of twist to a thickness of .14 inches at the leading edge and .080 inches at the trailing edge. The leading edge is located a distance of 4.6 inches from the center of twist and is parallel to the spar's twist axis.

The missile is a 3.75-inch diameter sphere weighing 1 lb. and impacting the plate with a velocity of 600 ft/sec. at a 30° angle to the plane of the plate. Figs. 33 and 34 show the dimensions of the model depicting the missile.

The modal data used in the problem includes the first five modes of the blade. Since the plate is relatively rigid it was felt that these lower modes (i.e. the first three bending and the first two twisting modes) would be sufficient to obtain the data necessary for comparison with test results. Due to the lack of a good finite element model for the blade, consisting of a dimensional plate element, the modal data was obtained from a beam analysis eigenvalue solution. The results of this normal modes analysis was then used to determine the displacements of the plate nodes relative to the point of the plate located at the impact radius and the center of twist. Since the plate is relatively rigid this approximation should not impose any gross errors. In addition, the loads calculated by the program are maximum along the impact centerline and decay rapidly with distance from the impact centerline, thus reducing the effects of errors in the mode shapes with respect to the blade response. Below is a summary of the modal data.

MODE	SHAPE	FREQ. (HZ)	*DISPLACEMENTS		TWIST	
			IP	OOP	IMPACT STATION	BLADE TIP
1	1st BENDING	69	.383	.310	-.0407	-.108
2	2nd BENDING	139	-.205	-.116	-.0169	-.231
3	3rd BENDING	231	.375	-.515	.0237	-.191
4	1st TWIST	244	.0131	.129	.297	.0861
5	2nd TWIST	360	-.269	-.624	.217	.514

*At the impact radial station and center of twist

The impact station is at the 30-in. radius and the center of the missile impact is .6 inches off the center of twist towards the leading edge. A listing of the input data is presented in Table IV and the output results of the program are presented in Appendix G. Presented in Fig. 35 is a plot of the calculated flatwise displacement response at the blade tip and the corresponding test data. The test data indicates the presence of higher mode contributions to the displacement response of the blade, however, these contributions are minimal. With respect to the duration of the response and the general shape of the curve, the correlation between calculated and test results is very good. The peak displacement predicted by the MMBI program is within 6.7% of the test results.

Fig. 36 shows the calculated response of the blade in twist at the impact radius and the test data for twist response of the blade at the blade tip. Although the two sets of data cannot be directly compared, several encouraging conclusions can be drawn from their relative shapes. First, note that for the initial rise of the response and for the fall off after the peak, there is good correlation. This is consistent with the fact that the blade response during these time intervals is mostly due to the lower twist modes. The break away of test results from the calculated curve indicates, as with the displacement response, the presence of higher modes. Furthermore, noting that the modal data input to the program is based upon a rigid body transformation of the plate with respect to a point at the impact radius, and considering the summarized modal data, it can be seen that there is a sharp transition in the twist mode shapes between the impact radius and the tip radius. The MMBI program predicted

that the missile mass washes off the blade 1 millisecond after the initiation of impact. It would therefore be expected that the blade twist response will include the higher modes after this time as is illustrated by the test data.

It should be noted that the effects of blade camber on pressures are not present in this analysis since the plate motion is virtually rigid. However, the significance of this demonstration problem lies in the ability of the MMBI program to couple the effects of a variable sized and shaped missile with the modal characteristics of the impacted blade. The program was able to predict within acceptable accuracy, the response of the blade subjected to a nonlinear load.

5.3 RECOMMENDATIONS

In its present form, the MMBI Impact program combines the effects of coupled modal response with a time variable missile model. Although the demonstration problems presented in Sections 5.1 and 5.2 provide an insight to the capabilities of the program, it must be pointed out that a thorough evaluation of the program is still warranted.

As a first step, it is recommended that the results from available test data on missile impacts of real fan blades be compared to corresponding analyses performed with the program, e.g. missile impacts of the 3A Q-Fan Demo Blade performed for NASA Lewis by Hamilton Standard under Contract No. NAS3-17837.

Second, since successful design techniques require the analyst to conduct parametric studies on proposed designs, the evaluation of the program with respect to parametric applications is of importance.

As an outgrowth of these studies, improvements on the present modelling could be accomplished, such as:

- 1) The development of a technique for integrating the pressure distribution over the surface of the blade. Such a method has already been partially developed.
- 2) The inclusion of Hugoniot pressure for the initial shock force developed prior to steady flow.
- 3) The inclusion of an internal preprocessor for extracting the eigenvalues and eigenvectors associated with the blade. The procedure for inputting the modal data into the program is a cumbersome task due to the large volume of data that is associated with most blades. Errors in transmitting the data from an external modal preprocessor to the MMBI program can be incurred if extreme caution by the user is not exercised.

It is to be noted that the present version of the program does not account for the non-linear behavior of blades subjected to impacts. The expansion of the program to include the effects of large deformation, non-linear elastic-plastic material behavior, and as a final step, inhomogeneity, would be a significant improvement. The methodology used to determine the variation of impact load with respect to time and blade surface would be analogous to that used by the present version of the program. However, rather than purely time stepping through the problem with a single solution set for the modal

response, a time step integration technique can be developed such that the generalized coordinates corresponding to the modes of the system are solved for during each time step. This releases the constraints that the transient forcing function on the system, and that the material and stiffness properties of the system, be relatively smooth functions with time. A similar method is presented in Ref. 21.

An additional area of interest, in which the FOD Impact program could be a useful tool, concerns the subject of failure analysis. The development of the program's capability to handle delamination and fracture damage could be implemented using the methodology described above. These developments would necessitate further efforts in the improvement of the missile model. Since fracture damage constitutes discontinuities in the surface of the blade, the improved missile model would be required to respond to these discontinuities. Such a model can be developed by using a non-linear, semi-solid, theoretical substance such as Mooney-Rivlin material.

The improvements mentioned above cover a very broad and general scope of developmental work. Certainly, the area of program evaluation is a task which should be afforded immediate attention. The remainder of the recommendations constitute multiple task efforts that can be expended as longer range developments.

REFERENCES

1. Cornell, R. W., SA# 636, "Elementary Three Dimensional Flexible Blade Impact Analysis," Hamilton Standard Memorandum, November 12, 1974.
2. Cornell, R. W., "Elementary Three-Dimensional Interactive Rotor Blade Impact Analysis," Journal of Engineering for Power; Vol. 98; No. 4, October 1976; pp. 480-486.
3. Houtz, N. E., SA# 664, "Multiple Mode, Incremental Blade Impact Analysis and Computer Program," Hamilton Standard Memorandum, August 25, 1975.
4. R. L. Peterson & J. P. Barber, "Bird Impact Forces in Aircraft Windshield Design", Air Force Flight Dynamics Lab. Report AFFDL-TR-75-150; March 1956.
5. Von W. Schach, "Umlenkung eines freien Flüssigkeitsstrahles an einer ebenen Platte," Ingenieur-Archiv; V. Band, 4 Heft; 1934; pp. 245-265.
6. T. Strand, "Inviscid-Incompressible-Flow Theory of Normal and Slightly Oblique Impingement of a Static Round Jet on the Ground"; Report No. 351 Air Vehicle Corporation; also J. Aircraft, vol. 4, No. 5 Sept.-Oct. 1967, pp. 466-472.
7. Von W. Schach, "Umlenkung eines kreisförmigen Flüssigkeitsstrahles an einer ebenen Platte senkrecht zur Stromungsrichtung," Ingenieur-Archiv; VI Band, 1935; pp. 51-59.
8. Yen C. Huang, F. G. Hammitt, & W. J. Yang, "Hydrodynamic Phenomena During High-Speed Collision Between Liquid Droplet and Rigid Plane," Journal of Fluid Engineering; June 1973.
9. J. B. G. Hwang, F. G. Hammitt, "High-Speed Impact Between Curved Liquid Surface and Rigid Flat Surface", ASME Publication - Presented at Winter Annual Meeting, New York, N. Y. Dec. 5, 1976.
10. Irving Michelson, "A Solution of the Three-Dimensional Oblique-Incidence Liquid Jet Problem"; Revue Roumaine de Mathematiques Pures et Appliquees, Vol. XV, 1970.
11. G. Taylor, "Formulation of Thin Flat Sheets of Water," Proc. of the Royal Society, Vol. 259 A, Nov. 1960, pp. 1-17.
12. A. Leclerc, "Deviation d'un jet liquide par une plaque normale a son axe," La Houille Blanche; Nov.-Dec. 1950.
13. J. Foss & S. J. Kleis, "Mean Flow Characteristics for the Oblique Impingement of an Axisymmetric Jet," AIAA Journal, Vol. 14, No. 6, June 1976, pp. 705 & 706.
14. J. Foss & S. J. Kleis, "The Oblique Impingement of an Axisymmetric Jet," Univ. of Michigan, Feb. 1976.

REFERENCES (Cont'd)

15. J. Foss & S. J. Kleis, "Research of Free and Impinging Jets for the Development of STOL Aircraft," Univ. of Michigan, Jan. 1974.
16. T. Strand, "On the Theory of Normal Ground Impingement of Axisymmetric Jets in Inviscid Incompressible Flow," AIAA Paper No. 64-424, 1964.
17. S. T. K. Chan, C. H. Lee & M. R. Brashears, "Three-Dimensional Finite Element Analysis for High Velocity Impact," NASA Lewis Research Center Interim Report CR 134933, Contract NAS8-18903, August 1975.
18. G. K. Batchelor, "Introduction to Fluid Dynamics," Cambridge University Press, 1967, pp. 392-395.
19. J. P. Barber and J. S. Wilbeck, "Bird Impact Loading," Air Force Flight Dynamics Lab, presentation at NASA/AFFDL FOD Workshop; March 16, & 17, 1977.
20. J. P. Barber, J. S. Wilbeck & H. R. Taylor, "Bird Impact Forces and Pressures on Rigid and Compliant Targets," University of Dayton Research Institute Final Contract Report UDRI-TR-77-17, Contract F33615-76-C-3103, March 1977.
21. S. Levy and J. P. Wilkinson, "The Component Element Method in Dynamics," McGraw Hill, 1976.

BIBLIOGRAPHY

1. G. R. Johnson, "High Velocity Impact Calculations In Three Dimensions," Journal of Applied Mechanics, March 1977, pp. 95-100.
2. K. H. Sayers, "Design and Analysis Methods for Soft Body Impact on Laminated Composite Material and Metal Jet Engine Fan Blades," Fibre Science and Technology, 1975; pp. 173-206.
3. J. N. Reddy, "A Finite Element Formulation of High-Velocity Impact," University of Oklahoma, pp.313-323.
4. W. Johnson, "Impact Strength of Materials," Edward Arnold Ltd., 1972.
5. W. Goldsmith, "Impact," Edward Arnold Ltd., London, 1959.
6. J. H. Brunton, "The Physics of Impact and Deformation: Single Impact," University of Cambridge, pp. 79-85.
7. Barber, Taylor, and Wilbeck, "Characterization of Bird Impacts on a Rigid Plate - Part 1," AFFDL-TR-75-5; January 1975.
8. Garrett Birkhoff, Duncan P. MacDougall, Emerson M. Pugh, & Sir Geoffrey Taylor, "Explosives with Lined Cavities," Journal of Applied Physics; June 1948.
9. J. M. Walsh, R. G. Shreffler, & F. J. Willig, "Limiting Conditions for Jet Formation in High Velocity Collisions," Los Alamos Scientific Lab., Los Alamos, New Mexico; Journal of Applied Physics; March, 1953.
10. Hancox and Brunton, "The Physics of Impact and Deformation: Multiple Impact," Phil. Trans. Royal Society of London; pp. 121-152; 1966.
11. K. H. Sayers, "Design and Analysis Methods for Soft Body Impact on Laminated Composite Material and Metal Jet Engine Fan Blades," Fiber Science and Technology, (8), 1975.
12. G. W. Vickers, "Water Jet Impact Damage at Convex, Concave, and Flat Inclined Surfaces," Journal of Applied Mechanics, December 1974.
13. "Proceedings of the Army Symposium on Solid Mechanics in 1972 - The Role of Mechanics in Design - Ballistic Problems," Army Materials and Mechanics Research Center, Watertown, Mass.
14. J. Hwang, "The Impact Between a Liquid Drop and an Elastic Half-Space," University Microfilms International, Ann Arbor, Michigan, U.S.A., London, England; 1975.
15. Y. Huang, "Numerical Studies of Unsteady, Two-Dimensional Liquid Impact Phenomena," University Microfilms International, Ann Arbor, Michigan, U.S.A., London, England; 1971.
16. Michael A. Saad & Gene J. Antonides, "Flow Pattern at Two Impinging Circular Jets," University of Santa Clara, Santa Clara, Calif.; AIAA Journal; July, 1972.

BIBLIOGRAPHY (Cont'd)

17. Y. C. Shen, "Theoretical Analysis of Jet-Ground Plane Interaction," Institute of Aerospace Science Paper 62-144.
18. Andre Leclerc, "Deflection of a Liquid Jet by a Perpendicular," Thesis for M. S. in Mechanics & Hydraulics; Graduate College of the State Univ. of Iowa; August, 1948.
19. Olive G. Engel, "Waterdrop Collisions with Solid Surfaces," Journal of Research of the National Bureau of Standards; May, 1955.
20. Ray Kinslow, Dallas G. Smith, & Vireshwar Sahai, "High-Velocity Liquid Impact Damage," Tennessee Technological University Dept. of Engineering Science, Cookeville, Tennessee 38501; Prepared for: U.S. Army Missile Command, Redstone Arsenal, Alabama, Contract #DAAH01-72-C-0375; January 1974.
21. A. J. Tudor, "Experimental Techniques in Bird Ingestion Research," Proceedings of The World Conference on Bird Hazards to Aircraft, Kingston, Ontario; September, 1969.
22. G. S. Springer, "Erosion by Liquid Impact," John Wiley, 1976.
23. J. H. Brunton, "High Speed Liquid Impact," Royal Society Phil. Trans. 760A, 76-78, 1966.
24. J. H. Brunton & J. J. Camiss, "The Flow of a Liquid Drop During Impact," Third Rain Erosion Conf., pp. 327-357, 1970.
25. O. G. Engel, "Waterdrop Collision with Solid Surfaces," US NBS Journal of Research 54, pp. 281-298, 1955.
26. O. G. Engel, "Impact of Liquid Drops - Erosion & Cavitation," ASTM STP 307, ASTM 3-16, 1962.
27. F. J. Heymann, "High Speed Impact Between a Liquid Drop and a Solid Surface," Journal of Applied Physics, pp. 5113-5122, 1969.
28. M. C. Rochester & J. H. Brunton, "High Speed Impact of Liquid Jets on Solids," Proc. First Inter. Symposium on Jet Cutting Tech., pp. A1.1-A1.24, 1972.
29. O. G. Engel, "Mechanism of High Speed Waterdrop Erosion of Methyl Methacrylate Plastic," NBS Journal of Research No. 54, 1955.
30. O. G. Engel, "Erosion Damage of Solids Caused by High-Speed Collision with Rain," NBS Journal of Research No. 61, 1958.
31. G. Berkhoff, "Hydrodynamics," Princeton U. Press for U. of Cincinnati, 1950, AMR 3 Rev. 2692.

TABLE I. EXPERIMENTAL IMPACT DATA

AUTHORS	MEDIUM	DESCRIPTION	IMPACT ANGLES, α°
W. SCHACH REFERENCES 5 & 7	LIQUID	2D AND 3D OBLIQUE JETS IMPINGING PLANE	30, 45, 60, 75, 90
J.F. FOSS & S.J. KLEIS REFERENCES 13, 14, 15	AIR	3D OBLIQUE JETS IMPINGING PLANE	3, 6, 9, 12, 15, 30, 45, 60
A. LECLERC REFERENCE 12	LIQUID	3D NORMAL JET IMPINGING PLANE	90
G. TAYLOR REFERENCE 11	LIQUID	3D COLLIDING OBLIQUE JETS	30, 45, 60
T. STRAND REFERENCES 5, 16	LIQUID	3D NEAR NORMAL JETS IMPINGING PLANE	80 & 90
R.L. PETERSON & J.P. BARBER REFERENCE 4	BIRD	BIRDS OBLIQUELY IMPINGING PLANE	25, 45, 90
J.P. BARBER & J.S. WILBECK REFERENCE 19	BIRD	BIRDS OBLIQUELY IMPINGING PLANE	25, 45

TABLE II

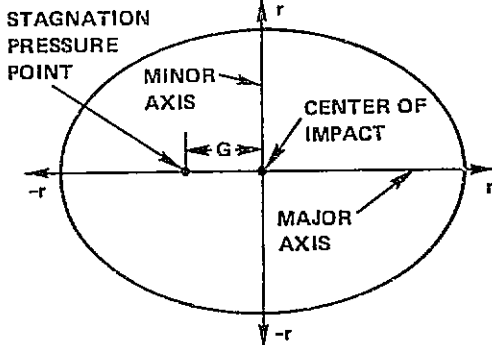
RELATIONSHIPS FOR 2D, 3D, AND GENERAL SYMMETRICAL MISSILE MODELS

1. FORWARD FLOW AREA	$A^F_2 = \frac{wa}{2} (1 + \cos \alpha)$	$A^F_3 = \frac{\pi a^2}{4} \left(1 - \frac{a}{\pi} + \frac{\sin 2\alpha}{2\pi}\right)$	$\bar{A}^F = A^F_2 + A^F_3$
2. PRESSURE DISTRIBUTION $P_o = \frac{1}{2} \rho V_o^2$	$(P/P_o)_2 = e^{-(x/\lambda)} [2 - e^{-(x/\lambda)}]$	$(P/P_o)_3 = e^{-(x/\lambda)^2} [2 - e^{-(x/\lambda)^2}]$	$\bar{P}/P_o = r_3 (P/P_o)_3 + r_2 (P/P_o)_2^*$
3. DECAY COEFFICIENTS	$\lambda_1/a = \frac{1}{3} \left(1 - \frac{a}{\pi}\right) \sin \alpha$ $\lambda_2/a = \frac{a}{3\pi} \sin \alpha$	$(\lambda/a)^2 = \frac{4}{3} \frac{\sin^3 \alpha}{(1 - \cos \psi \cos \alpha)^2} \sqrt{1 - (\cos \psi \cos \alpha)^2}$	
4. DEFLECTED THICKNESS	$(\delta/a)_2 = \frac{1}{2} (1 \pm \cos \alpha)$	$(\delta/a)_3 = \frac{a}{2\pi} \left(\frac{\sin \alpha}{1 - \cos \psi \cos \alpha} \right)^2 \sin \alpha$	$(\bar{\delta}/a) = \mu_3 (\delta/a)_3 + \mu_2 (\delta/a)_2^+$
5. FORCE FROM JET ζ_L	$(e/a)_2 = \frac{1}{2} \cot \alpha$	$(e/a)_3 = \frac{4 \cot \alpha}{3\pi (1 + \sqrt{\sin \alpha})}$	$(\bar{e}/a) = \frac{A_2 (e/a)_2 + A_3 (e/a)_3}{A_2 + A_3}$
6. STAG. PRESSURE FROM FORCE	$(f/a)_2 = \frac{14}{9} \left(1 - \frac{2\alpha}{\pi}\right) \sin \alpha$	$(f/a)_3 = \frac{2.3}{2} \left(1 - \frac{2\alpha}{\pi}\right) \left[1 - \left(1 - \frac{2\alpha}{\pi}\right)^{27}\right] + \frac{0.1 \sin 2\alpha}{2}$	
7. STAG. PRESSURE FROM JET ζ_L	$(g/a)_2 = \frac{1}{2} \left[\cot \alpha + \frac{28}{9} \left(1 - \frac{2\alpha}{\pi}\right) \sin \alpha \right]$	$(g/a)_3 = (e/a)_3 + (f/a)_3$	$(\bar{g}/a) = \frac{(g/a)_3 A_3 + (g/a)_2 A_2}{A_3 + A_2}$
$^* r_2 = \frac{1 + [wP_2/(dL/dX)]_3}{(P_2/P_3) + [wP_3/(dL/dX)]_3} ; r_3 = \frac{1 + [(dL/dX)_3/wP_2]}{(P_3/P_2) + [(dL/dX)_3/wP_2]}$			
$^+ \mu_2 = \frac{1 + A_2/A_3}{[(\bar{\delta}/a)_2/(\bar{\delta}/a)_3] + A_2/A_3} ; \mu_3 = \frac{1 + A_3/A_2}{[(\bar{\delta}/a)_3/(\bar{\delta}/a)_2] + A_3/A_2}$			

NOTE: \bar{P}_3 & $\bar{\delta}_3$ ARE VALUES FOR $\psi = 0$

$$(dL/dX)_3 \approx 2 \int_0^{\pi/2} x P_3 d\psi$$

TABLE III. PRESSURE RATIOS FOR 25, 45 AND 90 DEGREE IMPACTS
OF CYLINDRICAL MISSILES ON RIGID PLATES

	25° IMPACT G = 4.12 IN.				45° IMPACT G = 2.48 IN.				90° IMPACT G = 0.00 IN.			
	r	P/P ₀		Δ^*	r	P/P ₀		Δ^*	r	P/P ₀		Δ^*
		TEST**	THEORY			TEST**	THEORY			TEST**	THEORY	
MAJOR AXIS	-0.804	0.50	0.56	0.20	-1.19	0.93	0.96	0.25	0.0	0.924	1.0	0.95
	0.0	0.140	0.34	1.05	-0.60	0.76	0.87	0.45	0.47	0.847	0.99	0.70
	0.24	0.130	0.29	0.90	0.00	0.54	0.72	0.55	1.45	0.42	0.72	0.55
	0.64	0.093	0.21	0.85	0.38	0.38	0.60	0.70	1.92	0.15	0.46	0.62
	1.07	0.060	0.14	0.75	0.59	0.30	0.53	0.78				
					1.05	0.12	0.38	1.5				
	AVG. SHIFT OF STAG. PT. = 0.76				AVG. SHIFT OF STAG. PT. = 0.71				AVG. SHIFT OF STAG. PT. = 0.75			
MINOR AXIS	0.0	0.13	0.34	1.05	0.0	0.53	0.72	1.02				
	0.46	0.16	0.29	0.5	0.47	0.42	0.67	0.87				
	1.45	0.13	0.05	-0.2	1.44	0.22	0.36	0.37				
	1.91	0.05	0.01	-0.45								
	2.43	0.02	0.	-0.75								
	AVG. SHIFT OF STAG. PT. = 0.03				AVG. SHIFT OF STAG. PT. = 0.75							

* Δ IS THE SHIFT ALONG THE AXIS
FROM THE OBSERVED VALUE TO THE
EQUIVALENT P/P₀ ON THE CURVE.

**FROM REF. 2.

TABLE IV
INPUT DATA TO MMBI PROGRAM FOR ANALYSIS OF A 30 DEGREE IMPACT
OF A 1 LB. SPHERICAL MISSILE

```

**** TSO FOREGROUND HARDCOPY ****
DSNAME=TSOG02I.DEMO7.DATA
V |RIMP|TSTOP|ALPHA0|XDCL|YDCL|NR|NN|NM|NVA|IPDEL|DEN
7260.0,30.0,.0500,.5236,4.5460,3.7705,8,120,5,6,2,9.888-5,1
RL 1.5625,.95,.325,-.325,-.95,-1.5625,
RM .625,.60,.65,.65,.60,.625
CL 2.10,3.26,3.75,3.75,3.26,2.10,
DELT .825,.245,0.0,0.0,.245,.825,
WM 2.10,3.26,3.75,3.75,3.26,2.10
MAX 8*15
NJ3 8*9
VMI .0098558,.0042763,.009889,.0102230,.02334
DR .035,.035,.035,.035,.035
W 433.500,873.3900,1445.0,1533.100,2262.0

```

		IP DISPLACEMENT							OOP DISPLACEMENT						
		1	2	3	4	5			1	2	3	4	5		
	1	0.470906E-01	0.603713E-01	0.771465E-01	0.939220E-01	0.110697E+00			0.526383E-01	0.383952E-01	0.204040E-01	0.241280E-02	-1.55785E-01		
	2	0.127473E+00	0.144248E+00	0.161024E+00	0.177799E+00	0.194575E+00			-1.335697E-01	-1.515609E-01	-1.695521E-01	-1.875432E-01	-1.105534E+00		
	3	0.218340E+00	0.246299E+00	0.274258E+00	0.302217E+00	0.326681E+00			-1.131022E+00	-1.161007E+00	-1.190993E+00	-1.220978E+00	-1.247215E+00		
	4	0.122718E+00	0.135999E+00	0.152774E+00	0.169550E+00	0.186325E+00			-1.167010E-01	-1.329440E-01	-1.509353E-01	-1.689265E-01	-1.869179E-01		
	5	0.203100E+00	0.219876E+00	0.236651E+00	0.253427E+00	0.270202E+00			-1.104909E+00	-1.122700E+00	-1.140891E+00	-1.158883E+00	-1.176874E+00		
	6	0.293967E+00	0.321926E+00	0.349886E+00	0.377845E+00	0.402308E+00			-1.202361E+00	-1.232346E+00	-1.262332E+00	-1.292317E+00	-1.318554E+00		
	7	0.198346E+00	0.211627E+00	0.228402E+00	0.245177E+00	0.261953E+00			-1.900402E-01	-1.104283E+00	-1.122275E+00	-1.140266E+00	-1.158257E+00		
	8	0.278728E+00	0.295503E+00	0.312279E+00	0.329054E+00	0.345830E+00			-1.176248E+00	-1.194239E+00	-1.212231E+00	-1.230222E+00	-1.248213E+00		
	9	0.369595E+00	0.397554E+00	0.425513E+00	0.453472E+00	0.477936E+00			-1.271700E+00	-1.303686E+00	-1.333671E+00	-1.363656E+00	-1.389894E+00		
	10	0.273174E+00	0.287254E+00	0.304030E+00	0.320805E+00	0.337580E+00			-1.161380E+00	-1.175623E+00	-1.193614E+00	-1.211605E+00	-1.229596E+00		
	11	0.354356E+00	0.371131E+00	0.387907E+00	0.404682E+00	0.421457E+00			-1.247587E+00	-1.265579E+00	-1.283570E+00	-1.301561E+00	-1.319552E+00		
	12	0.445223E+00	0.473182E+00	0.501141E+00	0.529100E+00	0.553564E+00			-1.345040E+00	-1.375025E+00	-1.405011E+00	-1.434996E+00	-1.461233E+00		
	13	0.330694E+00	0.343975E+00	0.360750E+00	0.377526E+00	0.394301E+00			-1.214894E+00	-1.229127E+00	-1.247118E+00	-1.265109E+00	-1.283101E+00		
	14	0.411077E+00	0.427852E+00	0.444627E+00	0.461403E+00	0.478178E+00			-1.301092E+00	-1.319083E+00	-1.337074E+00	-1.355066E+00	-1.373057E+00		
	15	0.501943E+00	0.529903E+00	0.557862E+00	0.585821E+00	0.610285E+00			-1.398544E+00	-1.428530E+00	-1.458515E+00	-1.488500E+00	-1.514738E+00		
	16	0.406322E+00	0.417603E+00	0.436378E+00	0.453153E+00	0.469929E+00			-1.286223E+00	-1.300466E+00	-1.318458E+00	-1.336449E+00	-1.354440E+00		
	17	0.486704E+00	0.503479E+00	0.520255E+00	0.537030E+00	0.553806E+00			-1.372431E+00	-1.390422E+00	-1.408414E+00	-1.426405E+00	-1.444396E+00		
	18	0.577571E+00	0.605530E+00	0.633489E+00	0.661448E+00	0.685913E+00			-1.469804E+00	-1.499869E+00	-1.529854E+00	-1.559840E+00	-1.586077E+00		
	19	0.481949E+00	0.495230E+00	0.512005E+00	0.528781E+00	0.545556E+00			-1.357563E+00	-1.371806E+00	-1.389797E+00	-1.407788E+00	-1.425779E+00		
	20	0.562332E+00	0.579107E+00	0.595883E+00	0.612658E+00	0.629433E+00			-1.443770E+00	-1.461762E+00	-1.479753E+00	-1.497744E+00	-1.515735E+00		
	21	0.653199E+00	0.681258E+00	0.709117E+00	0.737076E+00	0.761540E+00			-1.541223E+00	-1.571208E+00	-1.601194E+00	-1.631179E+00	-1.657416E+00		
	22	0.557577E+00	0.570858E+00	0.587633E+00	0.604409E+00	0.621184E+00									
	23	0.637959E+00	0.654735E+00	0.671510E+00	0.688286E+00	0.705061E+00									
	24	0.728826E+00	0.756785E+00	0.784745E+00	0.812704E+00	0.837168E+00									

MODE #1

ORIGINAL PAGE IS
OF POOR QUALITY

TABLE IV (CONT'D)						MODE # 1 (CONT)
IP DISPLACEMENT	8	- .428902E+00	- .443145E+00	- .461136E+00	- .479127E+00	- .497119E+00
		- .515110E+00	- .533101E+00	- .551092E+00	- .569083E+00	- .587075E+00
		- .612562E+00	- .642547E+00	- .672533E+00	- .702518E+00	- .728755E+00
	1	- .213493E+00	- .208445E+00	- .202068E+00	- .195692E+00	- .189315E+00
		- .182938E+00	- .176562E+00	- .170185E+00	- .163808E+00	- .157432E+00
		- .148398E+00	- .137770E+00	- .127142E+00	- .116515E+00	- .107215E+00
	2	- .224593E+00	- .219545E+00	- .213168E+00	- .206791E+00	- .200415E+00
		- .194038E+00	- .187661E+00	- .181285E+00	- .174908E+00	- .168531E+00
		- .159498E+00	- .148870E+00	- .138242E+00	- .127614E+00	- .118315E+00
	3	- .235693E+00	- .230645E+00	- .224268E+00	- .217891E+00	- .211515E+00
		- .205138E+00	- .198761E+00	- .192384E+00	- .186008E+00	- .179631E+00
		- .170598E+00	- .159970E+00	- .149342E+00	- .138714E+00	- .129415E+00
4	- .246793E+00	- .241744E+00	- .235368E+00	- .228991E+00	- .222614E+00	
	- .216238E+00	- .209861E+00	- .203484E+00	- .197108E+00	- .190731E+00	
	- .181697E+00	- .171069E+00	- .160442E+00	- .149814E+00	- .140515E+00	
5	- .255117E+00	- .250069E+00	- .243692E+00	- .237316E+00	- .230939E+00	
	- .224562E+00	- .218186E+00	- .211809E+00	- .205432E+00	- .199056E+00	
	- .190022E+00	- .179394E+00	- .168766E+00	- .158139E+00	- .148839E+00	
6	- .266217E+00	- .261169E+00	- .254792E+00	- .248416E+00	- .242039E+00	
	- .235662E+00	- .229286E+00	- .222909E+00	- .216532E+00	- .210155E+00	
	- .201122E+00	- .190494E+00	- .179866E+00	- .169239E+00	- .159939E+00	
7	- .277317E+00	- .272269E+00	- .265892E+00	- .259515E+00	- .253139E+00	
	- .246762E+00	- .240335E+00	- .234009E+00	- .227632E+00	- .221255E+00	
	- .212222E+00	- .201594E+00	- .190966E+00	- .180338E+00	- .171039E+00	
8	- .288417E+00	- .283368E+00	- .276992E+00	- .270615E+00	- .264238E+00	
	- .257862E+00	- .251485E+00	- .245108E+00	- .238732E+00	- .232355E+00	
	- .223321E+00	- .212694E+00	- .202066E+00	- .191438E+00	- .182139E+00	
OOP DISPLACEMENT	1	0.187633E+00	0.181313E+00	0.173329E+00	0.165346E+00	0.157363E+00
		0.149379E+00	0.141396E+00	0.133413E+00	0.125429E+00	0.117446E+00
		0.106136E+00	0.928308E-01	0.795253E-01	0.662197E-01	0.545774E-01
	2	0.185583E+00	0.179263E+00	0.171279E+00	0.163296E+00	0.155313E+00
		0.147329E+00	0.139346E+00	0.131363E+00	0.123379E+00	0.115396E+00
		0.104086E+00	0.907609E-01	0.774753E-01	0.641698E-01	0.525275E-01
	3	0.183533E+00	0.177213E+00	0.169229E+00	0.161246E+00	0.153263E+00
		0.145279E+00	0.137296E+00	0.129313E+00	0.121329E+00	0.113346E+00
		0.102036E+00	0.887309E-01	0.754253E-01	0.621198E-01	0.504774E-01
	4	0.181483E+00	0.175163E+00	0.167179E+00	0.159196E+00	0.151213E+00
		0.143229E+00	0.135246E+00	0.127263E+00	0.119279E+00	0.111296E+00
		0.99864E-01	0.866808E-01	0.733753E-01	0.600698E-01	0.484275E-01
	5	0.179945E+00	0.173625E+00	0.165642E+00	0.157658E+00	0.149675E+00
		0.141692E+00	0.133709E+00	0.125725E+00	0.117742E+00	0.109759E+00
		0.984489E-01	0.851433E-01	0.718378E-01	0.585323E-01	0.468900E-01
	6	0.177895E+00	0.171575E+00	0.163592E+00	0.155608E+00	0.147625E+00
		0.139642E+00	0.131658E+00	0.123675E+00	0.115692E+00	0.107709E+00
		0.963989E-01	0.830933E-01	0.697878E-01	0.564823E-01	0.448400E-01
	7	0.175845E+00	0.169525E+00	0.161542E+00	0.153558E+00	0.145575E+00
		0.137592E+00	0.129609E+00	0.121625E+00	0.113642E+00	0.105659E+00
		0.943489E-01	0.810434E-01	0.677378E-01	0.544323E-01	0.427900E-01
	8	0.173795E+00	0.167475E+00	0.159492E+00	0.151508E+00	0.143525E+00
		0.135542E+00	0.127559E+00	0.119575E+00	0.111592E+00	0.103609E+00
		0.922989E-01	0.789934E-01	0.656878E-01	0.523823E-01	0.407400E-01
MODE # 3	1	- .479193E+00	- .471817E+00	- .462501E+00	- .453184E+00	- .443867E+00
		- .434550E+00	- .425233E+00	- .415917E+00	- .406600E+00	- .397283E+00
		- .384084E+00	- .368556E+00	- .353028E+00	- .337500E+00	- .323913E+00
	2	- .464694E+00	- .457318E+00	- .448001E+00	- .438684E+00	- .429368E+00
		- .420051E+00	- .410734E+00	- .401417E+00	- .392100E+00	- .382784E+00
		- .369585E+00	- .354057E+00	- .338529E+00	- .323001E+00	- .309414E+00
	3	- .450194E+00	- .442818E+00	- .433502E+00	- .424185E+00	- .414868E+00
		- .405551E+00	- .396235E+00	- .386918E+00	- .377601E+00	- .368284E+00
		- .355085E+00	- .339557E+00	- .324029E+00	- .308501E+00	- .294914E+00

TABLE IV (CONTINUED)

IP DISPLACEMENT		MODE # 3 (CONTINUED)				
4	5	- .435695E+00	- .428319E+00	- .419002E+00	- .409685E+00	- .400369E+00
		- .391052E+00	- .381735E+00	- .372418E+00	- .363101E+00	- .353785E+00
		- .340586E+00	- .325058E+00	- .309530E+00	- .294002E+00	- .280415E+00
		- .424820E+00	- .417444E+00	- .408128E+00	- .398811E+00	- .389494E+00
5	6	- .380177E+00	- .370860E+00	- .361544E+00	- .352227E+00	- .342910E+00
		- .329711E+00	- .314183E+00	- .298655E+00	- .283127E+00	- .269540E+00
		- .410321E+00	- .402945E+00	- .393628E+00	- .384311E+00	- .374995E+00
		- .365678E+00	- .356361E+00	- .347044E+00	- .337727E+00	- .328411E+00
6	7	- .315212E+00	- .299684E+00	- .284156E+00	- .268628E+00	- .255041E+00
		- .395821E+00	- .388445E+00	- .379129E+00	- .369812E+00	- .360495E+00
		- .351178E+00	- .341861E+00	- .332545E+00	- .323228E+00	- .313911E+00
		- .300712E+00	- .285184E+00	- .269656E+00	- .254128E+00	- .240541E+00
7	8	- .381322E+00	- .373946E+00	- .364629E+00	- .355312E+00	- .345996E+00
		- .336679E+00	- .327362E+00	- .318045E+00	- .308728E+00	- .299412E+00
		- .286213E+00	- .270685E+00	- .255157E+00	- .239629E+00	- .226042E+00
		- .547007E-01	- .614263E-01	- .699217E-01	- .784175E-01	- .869129E-01
8	1	- .954084E-01	- .103904E+00	- .112399E+00	- .120895E+00	- .129390E+00
		- .141425E+00	- .155584E+00	- .169743E+00	- .183902E+00	- .196292E+00
		- .183343E+00	- .190069E+00	- .198564E+00	- .207060E+00	- .215555E+00
		- .224051E+00	- .232546E+00	- .241042E+00	- .249537E+00	- .258033E+00
1	2	- .270068E+00	- .284227E+00	- .298386E+00	- .312545E+00	- .324934E+00
		- .311985E+00	- .318711E+00	- .327207E+00	- .335702E+00	- .344198E+00
		- .352693E+00	- .361189E+00	- .369684E+00	- .378179E+00	- .386675E+00
		- .398710E+00	- .412869E+00	- .427028E+00	- .441187E+00	- .455376E+00
2	3	- .440628E+00	- .447353E+00	- .455849E+00	- .464344E+00	- .472840E+00
		- .481335E+00	- .489831E+00	- .498326E+00	- .506822E+00	- .515317E+00
		- .527352E+00	- .541511E+00	- .555671E+00	- .569830E+00	- .582219E+00
		- .537109E+00	- .543835E+00	- .552330E+00	- .560826E+00	- .569321E+00
3	4	- .577817E+00	- .586312E+00	- .594808E+00	- .603303E+00	- .611799E+00
		- .623834E+00	- .637993E+00	- .652152E+00	- .666312E+00	- .673701E+00
		- .665752E+00	- .672477E+00	- .680973E+00	- .689468E+00	- .697964E+00
		- .706459E+00	- .714955E+00	- .723450E+00	- .731945E+00	- .740441E+00
4	5	- .752477E+00	- .766635E+00	- .780795E+00	- .794954E+00	- .807343E+00
		- .794324E+00	- .801120E+00	- .809615E+00	- .818110E+00	- .826606E+00
		- .835101E+00	- .843597E+00	- .852092E+00	- .860588E+00	- .869083E+00
		- .881119E+00	- .895278E+00	- .909437E+00	- .923596E+00	- .935986E+00
5	6	- .923036E+00	- .929762E+00	- .938257E+00	- .946753E+00	- .955248E+00
		- .963744E+00	- .972239E+00	- .980735E+00	- .989230E+00	- .997726E+00
		- .100976E+01	- .102392E+01	- .103808E+01	- .105224E+01	- .106640E+01
		- .779122E+00	- .711728E+00	- .626601E+00	- .541472E+00	- .456345E+00
6	7	- .371216E+00	- .286088E+00	- .200960E+00	- .115832E+00	- .030703E-01
		- .898941E-01	- .231775E+00	- .373655E+00	- .515536E+00	- .639682E+00
		- .690937E+00	- .623543E+00	- .538415E+00	- .453287E+00	- .368159E+00
		- .283031E+00	- .197903E+00	- .112775E+00	- .276468E-01	- .574816E-01
7	8	- .178079E+00	- .319961E+00	- .461841E+00	- .603721E+00	- .727866E+00
		- .602752E+00	- .535358E+00	- .450230E+00	- .365102E+00	- .279974E+00
		- .194846E+00	- .109718E+00	- .245897E-01	- .605383E-01	- .145667E+00
		- .266264E+00	- .408146E+00	- .550026E+00	- .691907E+00	- .816052E+00
8	1	- .514566E+00	- .447172E+00	- .362045E+00	- .276917E+00	- .191789E+00
		- .106661E+00	- .215327E-01	- .635955E-01	- .148724E+00	- .233852E+00
		- .354450E+00	- .496331E+00	- .638211E+00	- .780092E+00	- .904237E+00
		- .448427E+00	- .381033E+00	- .295906E+00	- .210778E+00	- .125650E+00
1	2	- .405217E-01	- .446062E-01	- .129734E+00	- .214863E+00	- .299991E+00
		- .420589E+00	- .562470E+00	- .704350E+00	- .846231E+00	- .970376E+00
		- .360242E+00	- .292848E+00	- .207721E+00	- .122593E+00	- .037464E-01
		- .476634E-01	- .132791E+00	- .217920E+00	- .303048E+00	- .388176E+00
2	3	- .508774E+00	- .650655E+00	- .792535E+00	- .934416E+00	- .105856E+01
		- .272057E+00	- .204663E+00	- .119536E+00	- .034407E-01	- .507202E-01
		- .135848E+00	- .220976E+00	- .306105E+00	- .391233E+00	- .476361E+00
		- .596959E+00	- .738841E+00	- .880721E+00	- .102260E+01	- .114675E+01

TABLE IV (CONTINUED)

OOP DISPLACEMENT							MODE # 4 (CONTINUED)
1	8	0.183872E+00	0.116478E+00	0.313503E-01	- .537779E-01	- .138905E+00	
		- .224034E+00	- .309162E+00	- .394290E+00	- .479418E+00	- .564547E+00	
		- .685144E+00	- .827026E+00	- .968906E+00	- .111079E+01	- .123493E+01	
		- .162351E+01	- .150096E+01	- .134617E+01	- .119138E+01	- .103658E+01	
	1	- .881787E+00	- .726993E+00	- .572199E+00	- .417404E+00	- .262610E+00	
		- .433183E-01	0.214672E+00	0.472663E+00	0.730653E+00	0.956395E+00	
		- .153742E+01	- .141467E+01	- .126008E+01	- .110528E+01	- .950488E+00	
	2	- .795694E+00	- .640900E+00	- .486105E+00	- .331311E+00	- .176517E+00	
2		0.427747E-01	0.300765E+00	0.558756E+00	0.816747E+00	0.104249E+01	
		- .145132E+01	- .132878E+01	- .117398E+01	- .101919E+01	- .864395E+00	
	3	- .709601E+00	- .554806E+00	- .400012E+00	- .245218E+00	- .904236E-01	
		0.128868E+00	0.386858E+00	0.644849E+00	0.902839E+00	0.112856E+01	
		- .136523E+01	- .124268E+01	- .108789E+01	- .933096E+00	- .778302E+00	
	4	- .623507E+00	- .468713E+00	- .313919E+00	- .159125E+00	- .433034E-02	
		0.214961E+00	0.472952E+00	0.730943E+00	0.988932E+00	0.121467E+01	
		- .130066E+01	- .117811E+01	- .102332E+01	- .868526E+00	- .713732E+00	
3	5	- .558937E+00	- .404143E+00	- .249349E+00	- .945548E-01	0.602396E-01	
		0.279531E+00	0.537522E+00	0.795513E+00	0.105350E+01	0.127924E+01	
		- .121457E+01	- .109202E+01	- .937228E+00	- .782433E+00	- .627639E+00	
	6	- .472845E+00	- .318050E+00	- .163256E+00	- .846177E-02	0.146333E+00	
		0.365624E+00	0.623615E+00	0.881606E+00	0.113960E+01	0.136534E+01	
		- .112847E+01	- .100593E+01	- .851134E+00	- .696340E+00	- .541546E+00	
	7	- .386751E+00	- .231957E+00	- .771627E-01	0.776315E-01	0.232426E+00	
		0.451718E+00	0.709708E+00	0.967699E+00	0.122569E+01	0.145143E+01	
4	8	- .104238E+01	- .919835E+00	- .765041E+00	- .610247E+00	- .455452E+00	
		- .300658E+00	- .145864E+00	0.893062E-02	0.163725E+00	0.318519E+00	
		0.537811E+00	0.795801E+00	0.105379E+01	0.131178E+01	0.153752E+01	
		- .851468E+00	- .890776E+00	- .940402E+00	- .990028E+00	- .103965E+01	
	1	- .108920E+01	- .113891E+01	- .118853E+01	- .123816E+01	- .128778E+01	
		- .135809E+01	- .144080E+01	- .152351E+01	- .160622E+01	- .167859E+01	
		- .570332E+00	- .609620E+00	- .659244E+00	- .708871E+00	- .758497E+00	
	2	- .808123E+00	- .857750E+00	- .907376E+00	- .957002E+00	- .100663E+01	
5		- .107693E+01	- .115964E+01	- .124235E+01	- .132506E+01	- .139744E+01	
		- .289174E+00	- .328462E+00	- .378088E+00	- .427714E+00	- .477340E+00	
	3	- .526966E+00	- .576592E+00	- .626219E+00	- .675845E+00	- .725471E+00	
		- .795775E+00	- .878486E+00	- .961196E+00	- .104391E+01	- .111628E+01	
		- .801569E-02	- .473041E-01	- .969300E-01	- .146556E+00	- .196182E+00	
	4	- .135809E+01	- .295435E+00	- .345061E+00	- .394668E+00	- .444314E+00	
		- .514618E+00	- .597326E+00	- .680039E+00	- .762749E+00	- .835120E+00	
		0.202853E+00	0.163564E+00	0.113938E+00	0.643118E-01	0.146857E-01	
6	5	- .349408E-01	- .845674E-01	- .134194E+00	- .183820E+00	- .233446E+00	
		- .303750E+00	- .386460E+00	- .469171E+00	- .551881E+00	- .624253E+00	
		0.484010E+00	0.444721E+00	0.395095E+00	0.345409E+00	0.295843E+00	
	6	0.246216E+00	0.196590E+00	0.146964E+00	0.973374E-01	0.477108E-01	
		- .225926E-01	- .105304E+00	- .188014E+00	- .270725E+00	- .343095E+00	
		0.765165E+00	0.725878E+00	0.676252E+00	0.626626E+00	0.577000E+00	
	7	0.527373E+00	0.477747E+00	0.428121E+00	0.378494E+00	0.328668E+00	
		0.258565E+00	0.175853E+00	0.931430E-01	0.104324E-01	- .619392E-01	
7	8	0.104632E+01	0.100703E+01	0.957409E+00	0.907783E+00	0.858157E+00	
		0.808531E+00	0.758905E+00	0.709278E+00	0.659652E+00	0.610025E+00	
		0.539722E+00	0.457011E+00	0.374300E+00	0.291590E+00	0.219218E+00	
		0.473928E+00	0.573437E+00	0.699132E+00	0.824827E+00	0.950522E+00	
	1	0.107622E+01	0.120191E+01	0.132761E+01	0.145330E+01	0.157900E+01	
		0.175706E+01	0.196656E+01	0.217605E+01	0.238554E+01	0.256885E+01	
		0.194690E+00	0.294199E+00	0.419894E+00	0.545590E+00	0.671284E+00	
	2	0.796980E+00	0.922675E+00	0.104837E+01	0.117406E+01	0.129976E+01	
8		0.147783E+01	0.168732E+01	0.189631E+01	0.210630E+01	0.228961E+01	
		- .845468E-01	0.149618E-01	0.140656E+00	0.266352E+00	0.392047E+00	
	3	0.517742E+00	0.643437E+00	0.769133E+00	0.894828E+00	0.102052E+01	
		0.119859E+01	0.140808E+01	0.161757E+01	0.182707E+01	0.201037E+01	

ORIGINAL PAGE IS
OF POOR QUALITY

TABLE IV (CONTINUED)

		OOP DISPLACEMENT					MODE # 5 (CONTINUED)
		4	5	6	7	8	
		- .363784E+00	- .264275E+00	- .138581E+00	- .128852E-01	0.112810E+00	
		0.239505E+00	0.364200E+00	0.489895E+00	0.615590E+00	0.741286E+00	
		0.919353E+00	0.112885E+01	0.133834E+01	0.154783E+01	0.173113E+01	
		- .573212E+00	- .473703E+00	- .348009E+00	- .222313E+00	- .966182E-01	
		0.290771E-01	0.154772E+00	0.280467E+00	0.406163E+00	0.531857E+00	
		0.709925E+00	0.919418E+00	0.112891E+01	0.133840E+01	0.152170E+01	
		- .852450E+00	- .752940E+00	- .627246E+00	- .501550E+00	- .375855E+00	
		- .250160E+00	- .124465E+00	0.123000E-02	0.126925E+00	0.252621E+00	
		0.430688E+00	0.640180E+00	0.849671E+00	0.105916E+01	0.124247E+01	
		- .113169E+01	- .103218E+01	- .906463E+00	- .780788E+00	- .655092E+00	
		- .529397E+00	- .403702E+00	- .278007E+00	- .152312E+00	- .266171E-01	
		0.151451E+00	0.360942E+00	0.570434E+00	0.779926E+00	0.963231E+00	
		- .141092E+01	- .131141E+01	- .118572E+01	- .106002E+01	- .934330E+00	
		- .808635E+00	- .682940E+00	- .557244E+00	- .431549E+00	- .305855E+00	
		- .127786E+00	0.817063E-01	0.291196E+00	0.500688E+00	0.683995E+00	
		STRESS X					MODE # 1
		1	2	3	4	5	
		15*1.880+4	15*1.662+4	15*1.515+4	15*1.422+4	15*1.352+4	
		15*1.134+4	15*1.134+4	15*1.134+4	15*1.134+4	15*1.134+4	
		15*9.170+3	15*9.170+3	15*9.170+3	15*9.170+3	15*9.170+3	
		15*7.024+3	15*7.024+3	15*7.024+3	15*7.024+3	15*7.024+3	
		STRESS Y					MODE # 1
		1	2	3	4	5	
		15*-2.335+4	15*-2.066+4	15*-1.885+4	15*-1.771+4	15*-1.664+4	
		15*-1.664+4	15*-1.664+4	15*-1.664+4	15*-1.664+4	15*-1.664+4	
		15*-1.416+4	15*-1.416+4	15*-1.416+4	15*-1.416+4	15*-1.416+4	
		15*-1.149+4	15*-1.149+4	15*-1.149+4	15*-1.149+4	15*-1.149+4	
		15*-8.852+3	15*-8.852+3	15*-8.852+3	15*-8.852+3	15*-8.852+3	
		SHEAR XY					MODE # 1
		1	2	3	4	5	
		15*-6.650+2	15*-6.650+2	15*-6.649+2	15*-6.649+2	15*-6.649+2	
		15*-6.649+2	15*-6.649+2	15*-6.649+2	15*-6.649+2	15*-6.649+2	
		15*-6.642+2	15*-6.642+2	15*-6.642+2	15*-6.642+2	15*-6.642+2	
		15*-6.626+2	15*-6.626+2	15*-6.626+2	15*-6.626+2	15*-6.626+2	
		15*-6.597+2	15*-6.597+2	15*-6.597+2	15*-6.597+2	15*-6.597+2	
		STRESS X					MODE # 2
		1	2	3	4	5	
		15*-4.283+3	15*-3.280+3	15*-2.603+3	15*-2.177+3	15*-1.852+3	
		15*-8.522+2	15*-8.522+2	15*-8.522+2	15*-8.522+2	15*-8.522+2	
		15*1.290+2	15*1.290+2	15*1.290+2	15*1.290+2	15*1.290+2	
		15*1.051+3	15*1.051+3	15*1.051+3	15*1.051+3	15*1.051+3	
		STRESS Y					MODE # 2
		1	2	3	4	5	
		15*3.062+4	15*2.661+4	15*2.390+4	15*2.220+4	15*2.089+4	
		15*1.689+4	15*1.689+4	15*1.689+4	15*1.689+4	15*1.689+4	
		15*1.294+4	15*1.294+4	15*1.294+4	15*1.294+4	15*1.294+4	
		15*9.094+3	15*9.094+3	15*9.094+3	15*9.094+3	15*9.094+3	
		SHEAR XY					MODE # 2
		1	2	3	4	5	
		15*-3.072+3	15*-3.072+3	15*-3.071+3	15*-3.071+3	15*-3.071+3	
		15*-3.071+3	15*-3.071+3	15*-3.071+3	15*-3.071+3	15*-3.071+3	

ORIGINAL PAGE IS
TABLE IV (CONTINUED)
OF POOR QUALITY

			MODE #2 (CONT)
		6 15*-3.072+3 7 15*-3.074+3 8 15*-3.077+3	
	STRESS X	1 15*-3.134+5 2 15*-2.767+5 3 15*-2.520+5 4 15*-2.365+5 5 15*-2.247+5 6 15*-1.884+5 7 15*-1.525+5 8 15*-1.172+5	
	STRESS Y	1 15*-2.594+5 2 15*-2.277+5 3 15*-2.064+5 4 15*-1.930+5 5 15*-1.828+5 6 15*-1.514+5 7 15*-1.207+5 8 15*-9.099+4	MODE #3
	SHEAR XY	1 15*-3.610+3 2 15*-3.609+3 3 15*-3.608+3 4 15*-3.608+3 5 15*-3.607+3 6 15*-3.592+3 7 15*-3.564+3 8 15*-3.527+3	
	STRESS X	1 15*1.378+5 2 15*1.194+5 3 15*1.070+5 4 15*9.921+4 5 15*9.329+4 6 15*7.520+4 7 15*5.754+4 8 15*4.084+4	
	STRESS Y	1 15*2.036+3 2 15*5.077+2 3 15*2.225+3 4 15*3.304+3 5 15*4.128+3 6 15*6.655+3 7 15*9.017+3 8 15*1.064+4	MODE #4
	SHEAR XY	1 15*5.286+4 2 15*5.284+4 3 15*5.261+4 4 15*5.280+4 5 15*5.279+4 6 15*5.272+4 7 15*5.256+4 8 15*5.225+4	
	STRESS X	1 15*-4.971+5 2 15*-4.174+5 3 15*-3.637+5 4 15*-3.301+5 5 15*-3.045+5 6 15*-2.263+5 7 15*-1.508+5 8 15*-8.069+4	MODE #5
		1 15*-1.718+3	

TABLE IV (CONTINUED)

STRESS Y		SHEAR XY	
2	15*-2.115+4	1	15*9.835+4
3	15*-3.426+4	2	15*9.828+4
4	15*-4.251+4	3	15*9.821+4
5	15*-4.882+4	4	15*9.817+4
6	15*-6.822+4	5	15*9.814+4
7	15*-8.642+4	6	15*9.780+4
8	15*-1.009+5	7	15*9.704+4
		8	15*9.570+4

YNODE(1) 27.0
 XNODE { 11.0,11.6,12.2,12.8,13.4,14.0,14.6,15.2,15.8,16.4,17.25,
 18.25,19.25,20.25,21.00
 YNODE(2) 28.0
 XNODE { 11.0,11.6,12.2,12.8,13.4,14.0,14.6,15.2,15.8,16.4,17.25,
 18.25,19.25,20.25,21.00
 YNODE(3) 29.0
 XNODE { 11.0,11.6,12.2,12.8,13.4,14.0,14.6,15.2,15.8,16.4,17.25,
 18.25,19.25,20.25,21.00
 YNODE(4) 30.0
 XNODE { 11.0,11.6,12.2,12.8,13.4,14.0,14.6,15.2,15.8,16.4,17.25,
 18.25,19.25,20.25,21.00
 YNODE(5) 30.75
 XNODE { 11.0,11.6,12.2,12.8,13.4,14.0,14.6,15.2,15.8,16.4,17.25,
 18.25,19.25,20.25,21.00
 YNODE(6) 31.75
 XNODE { 11.0,11.6,12.2,12.8,13.4,14.0,14.6,15.2,15.8,16.4,17.25,
 18.25,19.25,20.25,21.00
 YNODE(7) 32.75
 XNODE { 11.0,11.6,12.2,12.8,13.4,14.0,14.6,15.2,15.8,16.4,17.25,
 18.25,19.25,20.25,21.00
 YNODE(8) 33.75
 XNODE { 11.0,11.6,12.2,12.8,13.4,14.0,14.6,15.2,15.8,16.4,17.25,
 18.25,19.25,20.25,21.00
 X ϕ { 1.0,1.473,1.946,2.418,2.891,3.364,3.837,4.310,4.782,5.255,5.925,6.713,
 7.501,8.289,8.860
 Y ϕ { 1.0,1.369,1.739,2.108,2.478,2.847,3.216,3.586,3.955,4.325,4.848,5.463,
 6.079,6.695,7.141

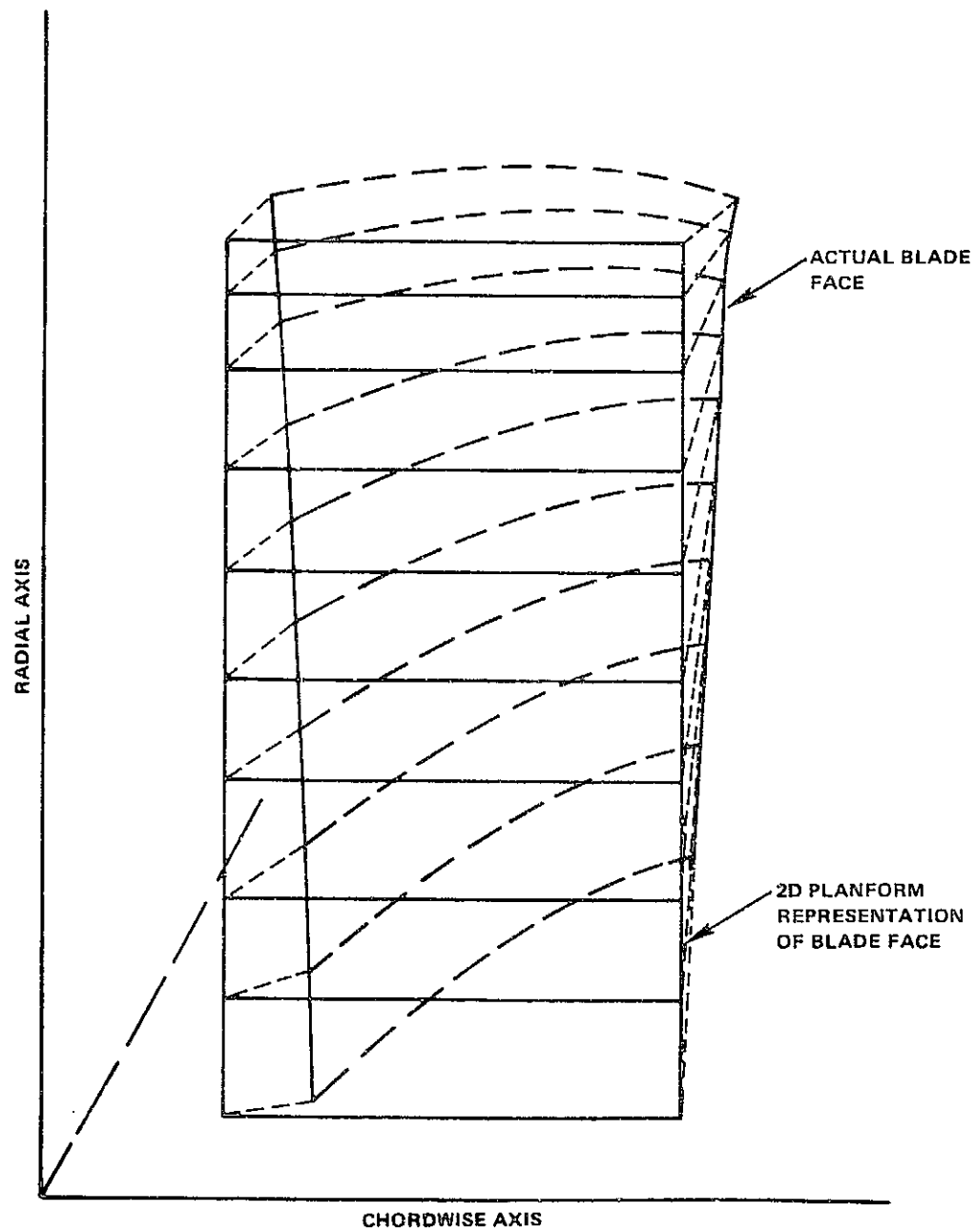


FIGURE 1. BLADE FACE MAPPED OUT ON PLANFORM PLANE

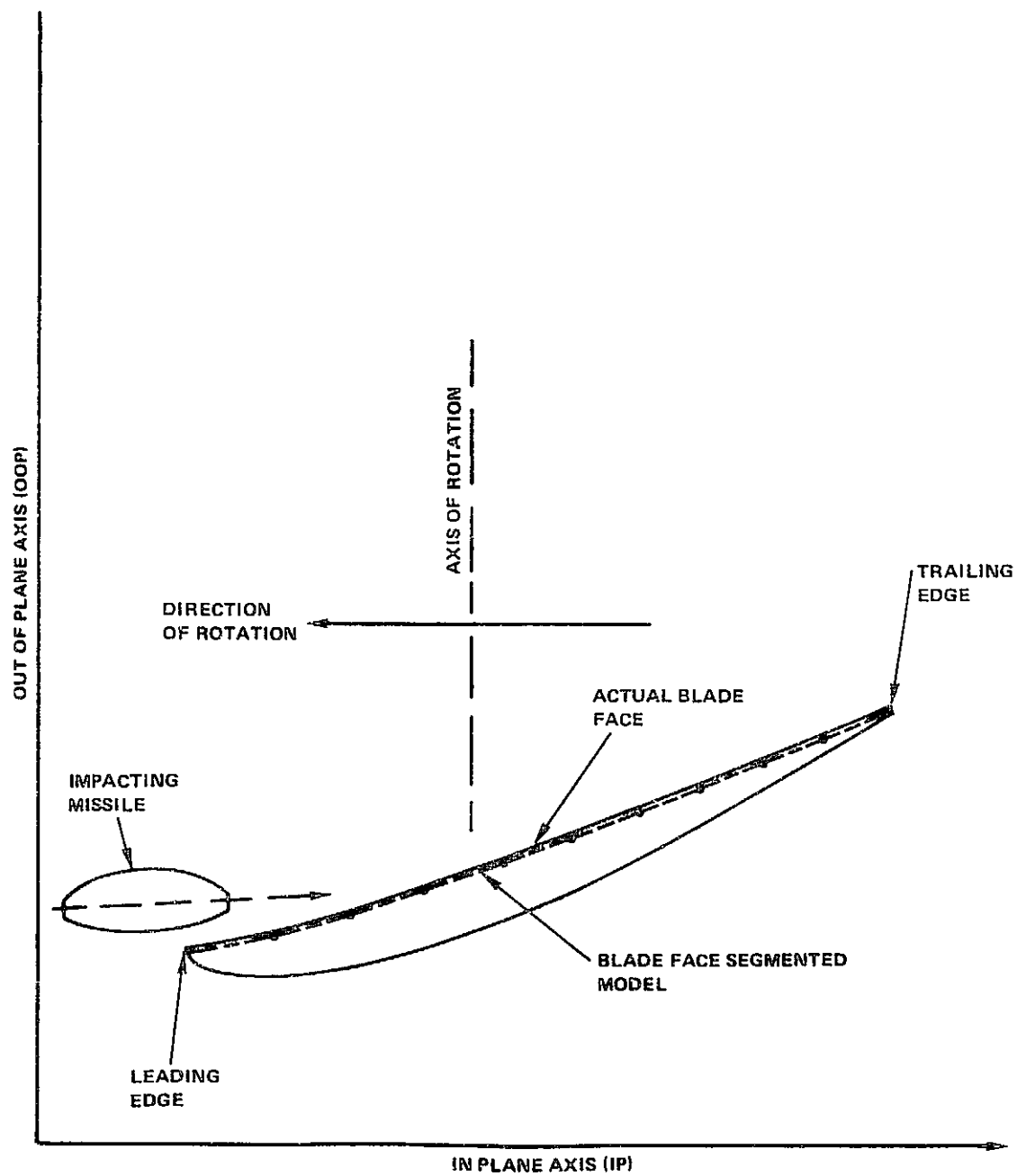


FIGURE 2. BLADE CROSS SECTION IN IP-OOP FRAME

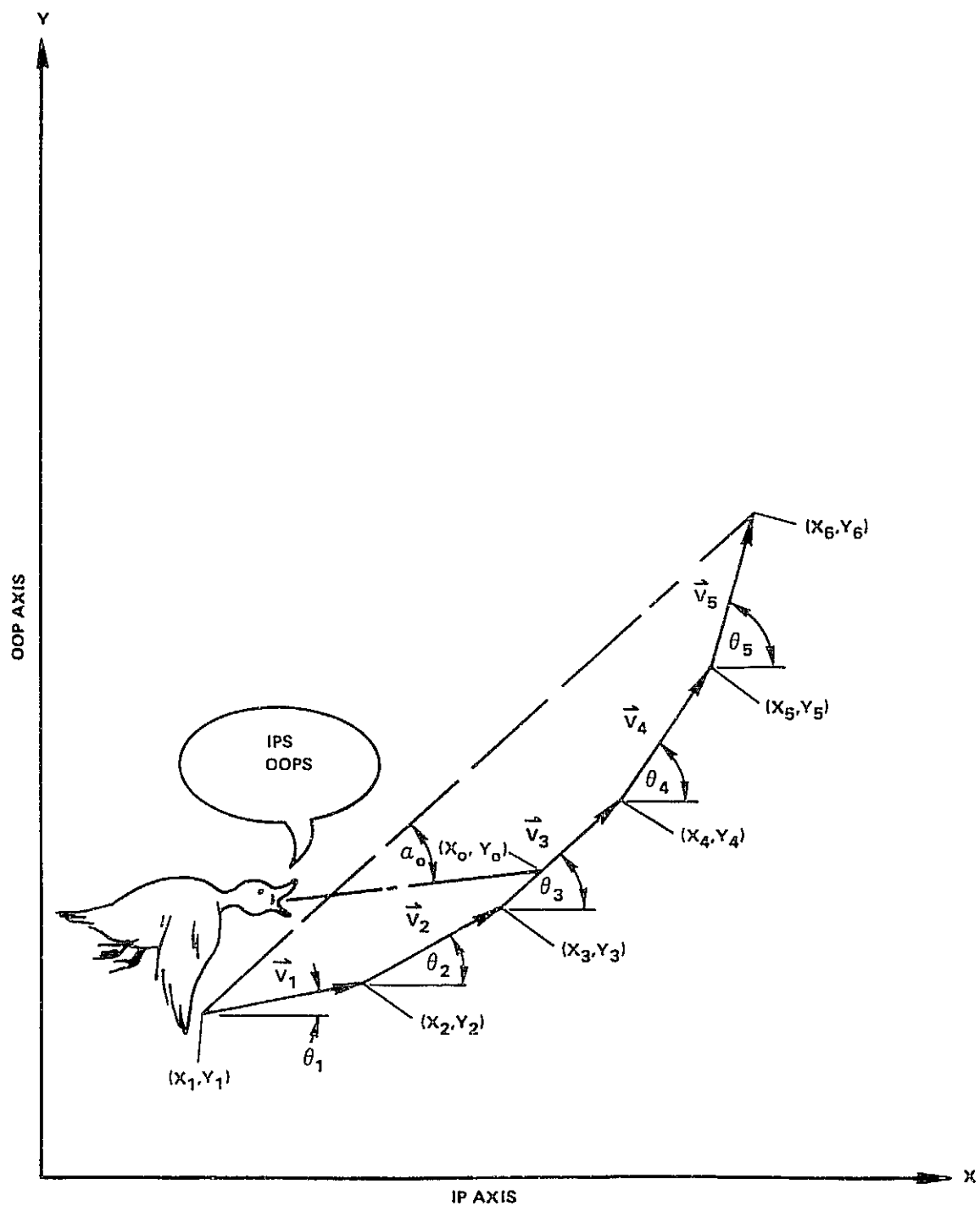


FIGURE 3. BLADE SEGMENTS IN IP-OOP FRAME

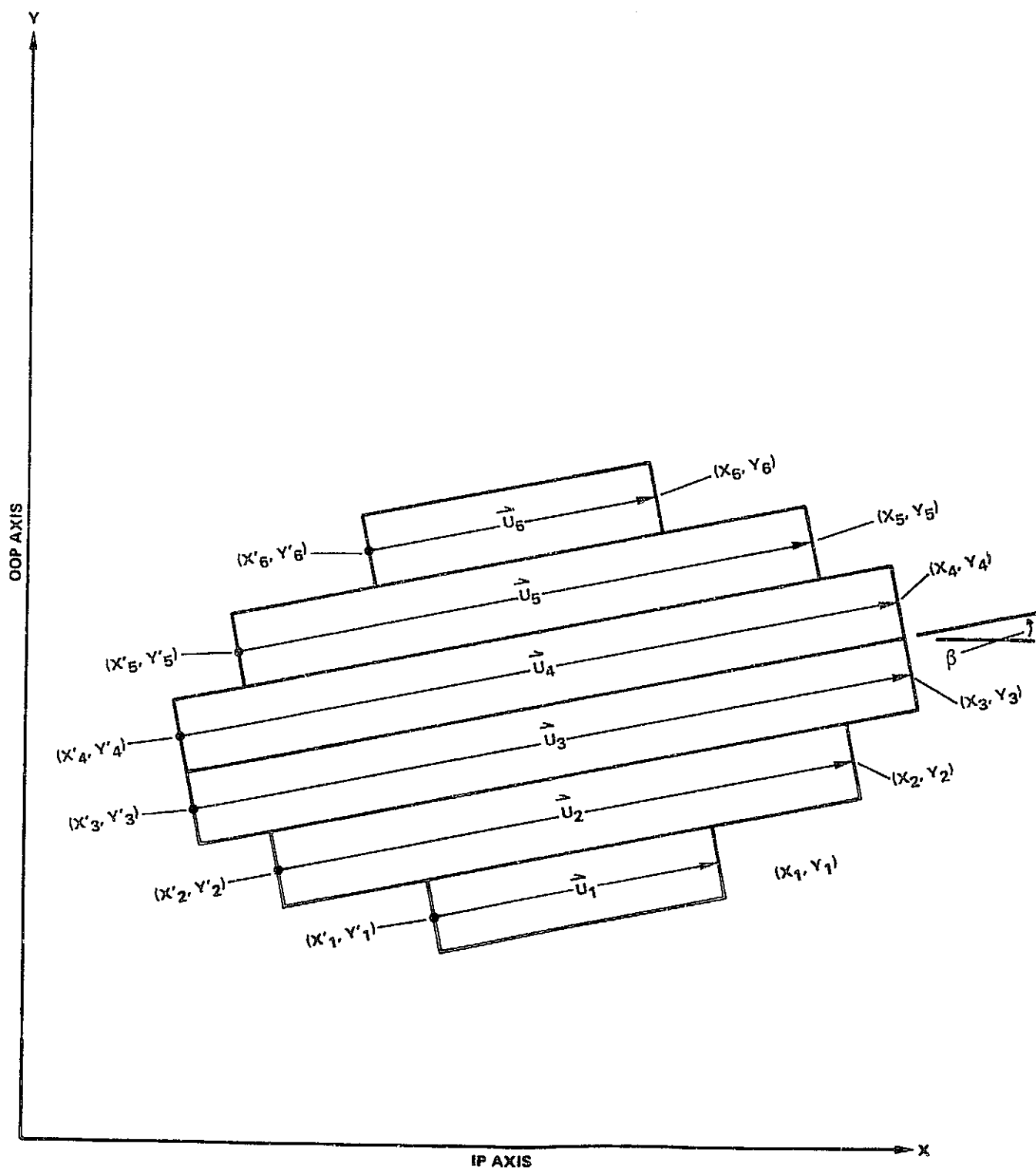


FIGURE 4. MISSILE SECTIONS IN IP-OOP FRAME

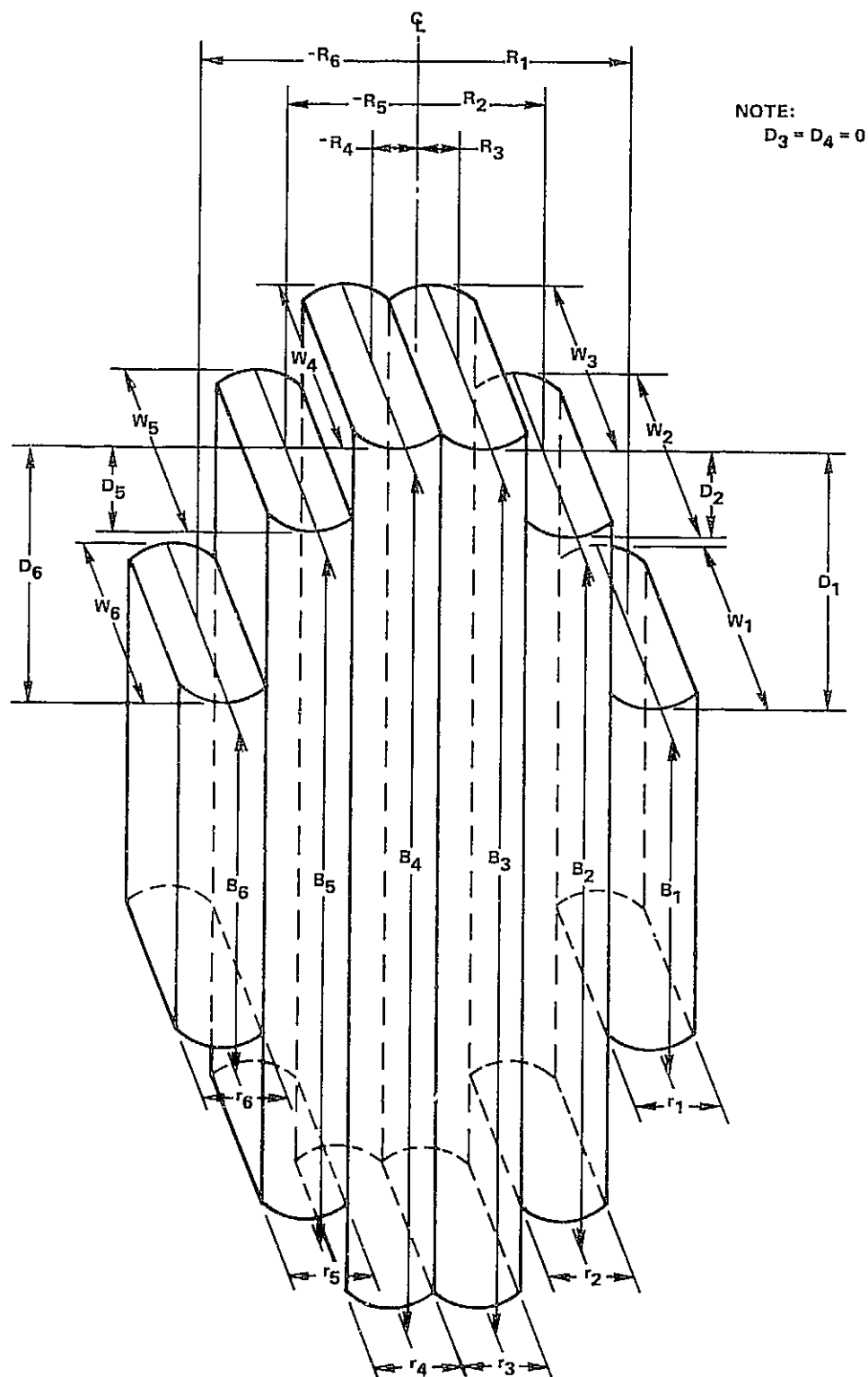


FIGURE 5. MISSILE DEFINITION

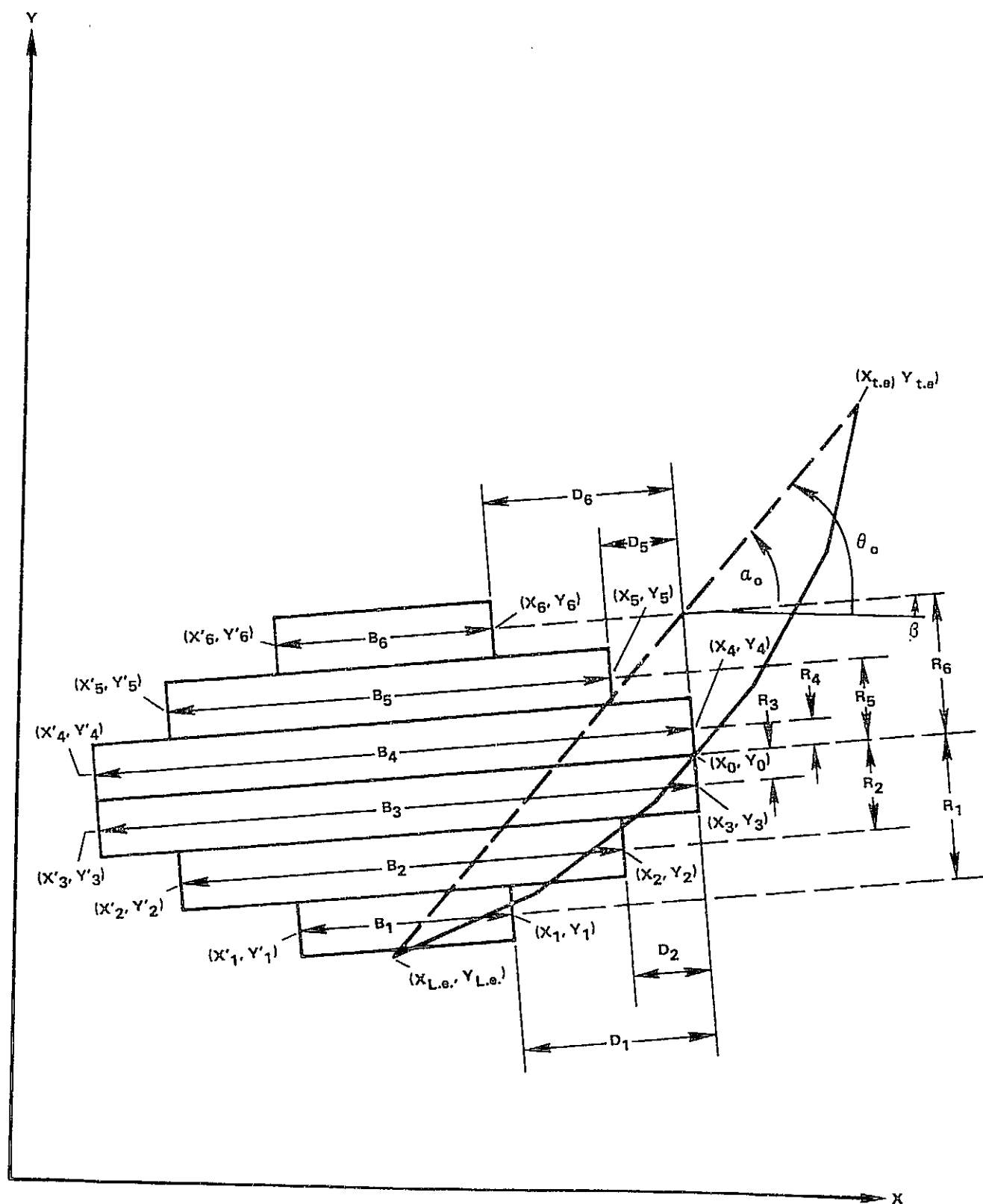


FIGURE 6. INITIAL MISSILE AND BLADE GEOMETRY

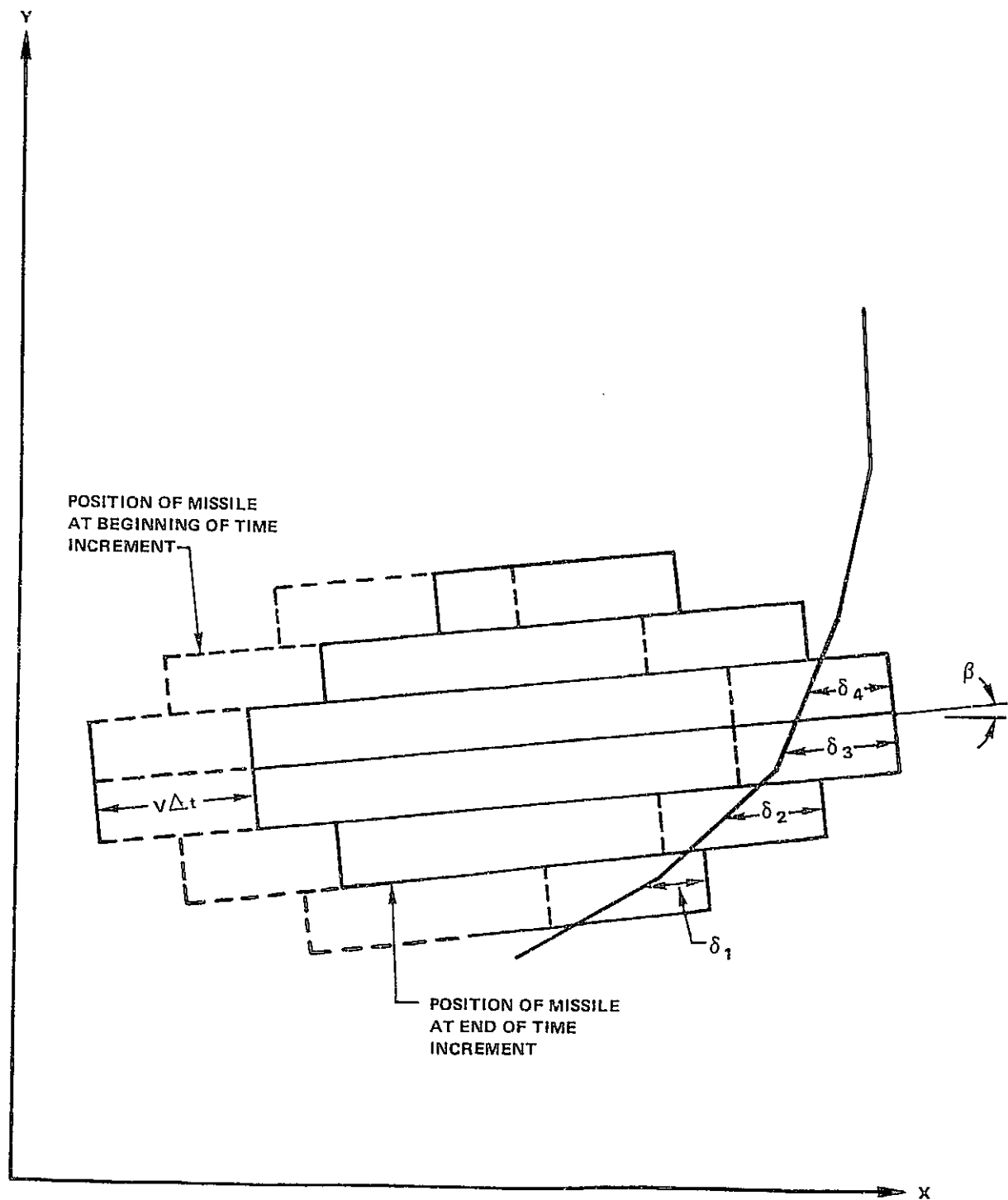


FIGURE 7. MISSILE AND BLADE GEOMETRY DURING TIMES OF IMPACT

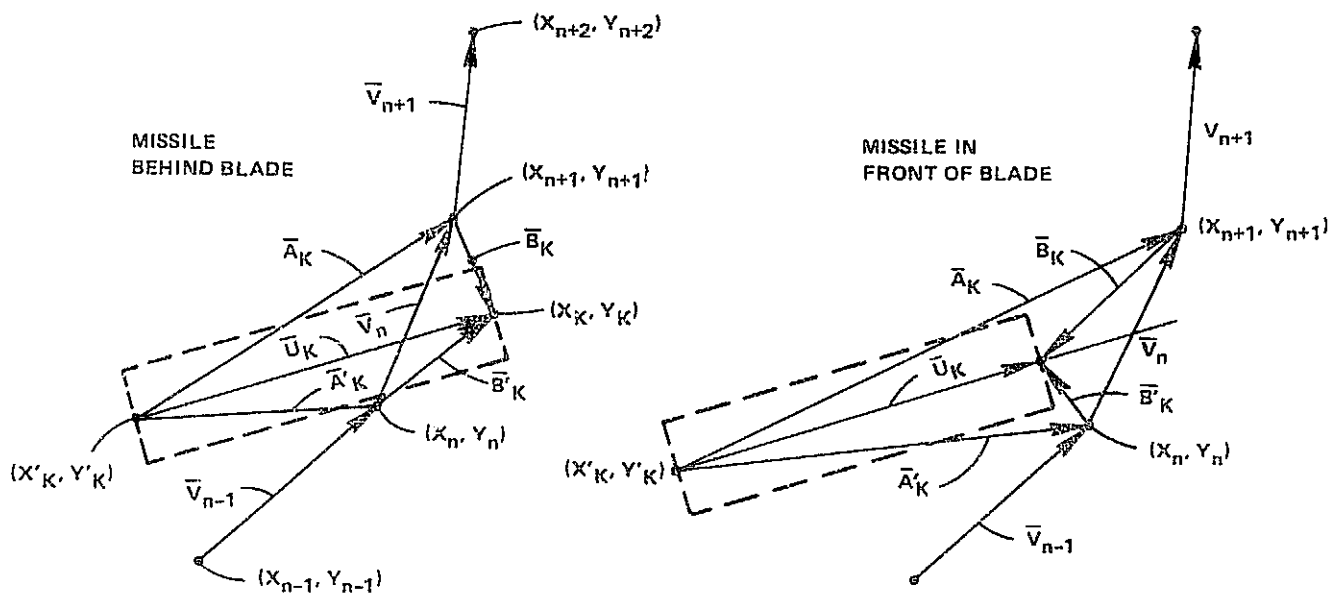
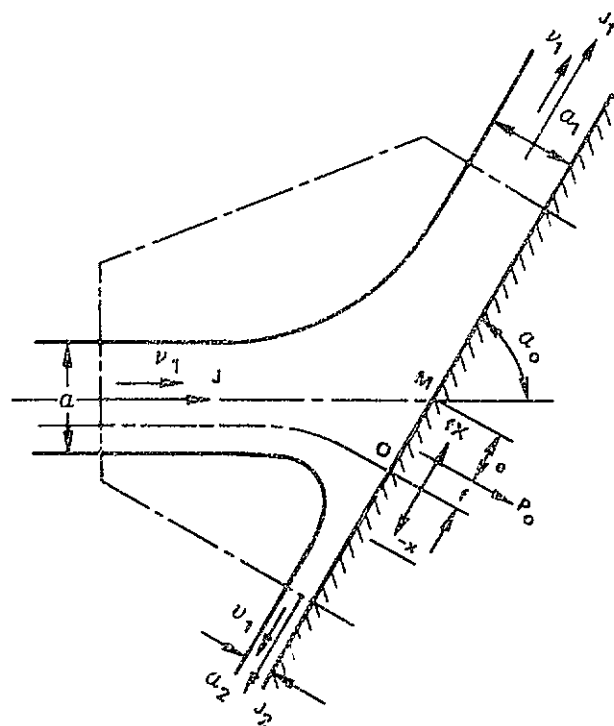


FIGURE 8. DETERMINATION OF BLADE SEGMENT TO BE HIT



$$a_1/a = \cos^2 \alpha_0/2 ; a_2/a = \sin^2 \alpha_0/2$$

$$b/a = 1/2 \cot \alpha_0$$

$$f/a = \frac{1}{\pi} \left[\cos \alpha_0 \ln (2 \sin \alpha_0) + \ln \cot \frac{\alpha_0}{2} + \left(\frac{\pi}{2} - \alpha_0 \right) \sin \alpha_0 \right]$$

$$P_0 = \rho v_1^2 \sin \alpha_0$$

$$x/b = \frac{1}{\pi} \left[\cos \alpha_0 \ln \left\{ \left(\frac{1}{1-r^2} \right) \left(\frac{\sin \alpha_0}{\sin \gamma} \right)^2 \right\} + \ln \left(\frac{1+r}{1-r} \right) + 2 (\pi - \alpha_0 - \gamma) \sin \alpha_0 \right]$$

$$P = P_0 (1-r^2)$$

$$r = v/v_1 ; \tan \gamma = \frac{1 \text{ OR } 2}{r - \cos \alpha_0} ; P_0 = 1/2 \rho v_1^2$$

FIGURE 9. TWO DIMENSIONAL JET MISSILE - SCHACH

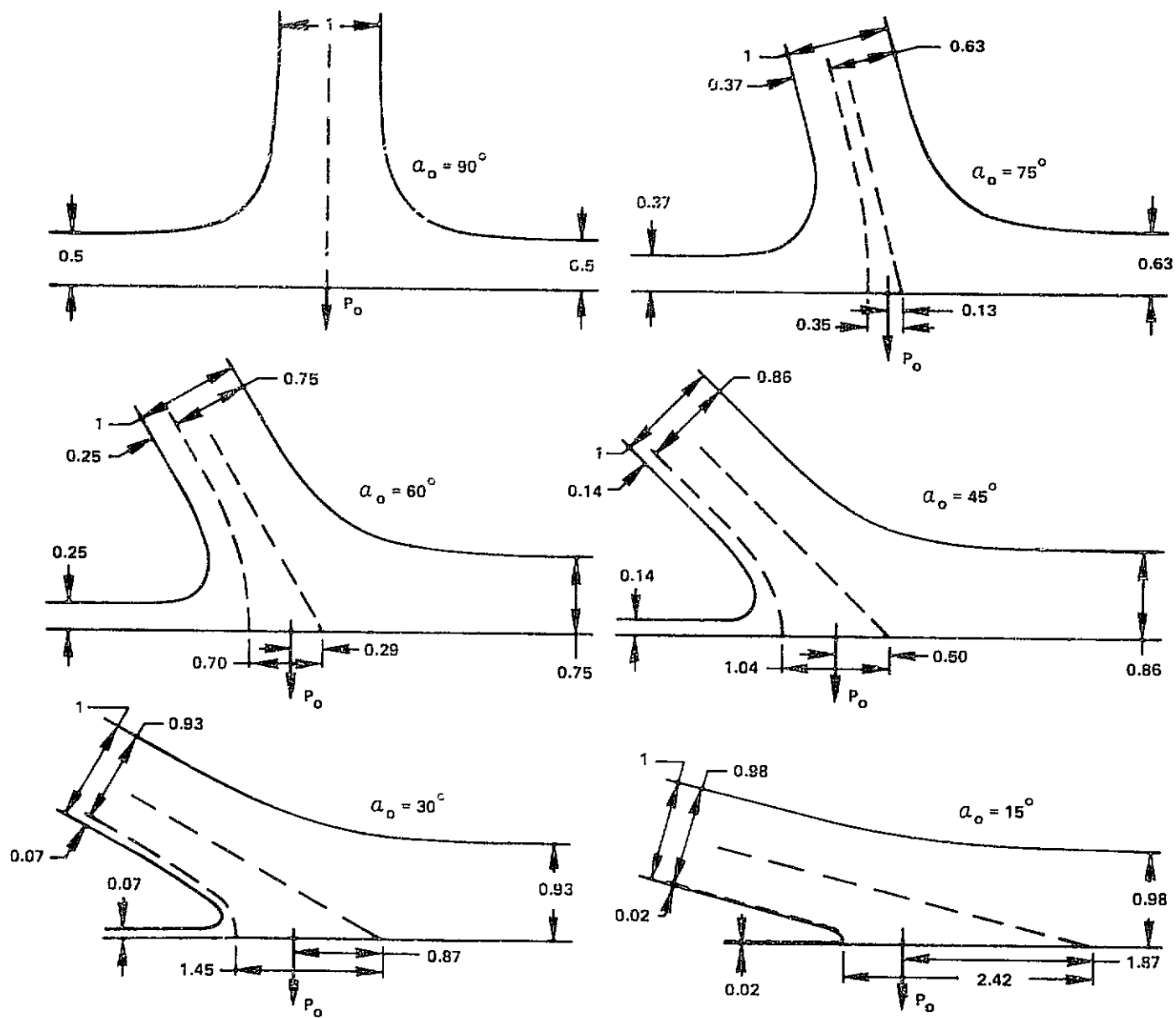


FIGURE 10. STREAMFORM FOR 2D JET - SCHACH

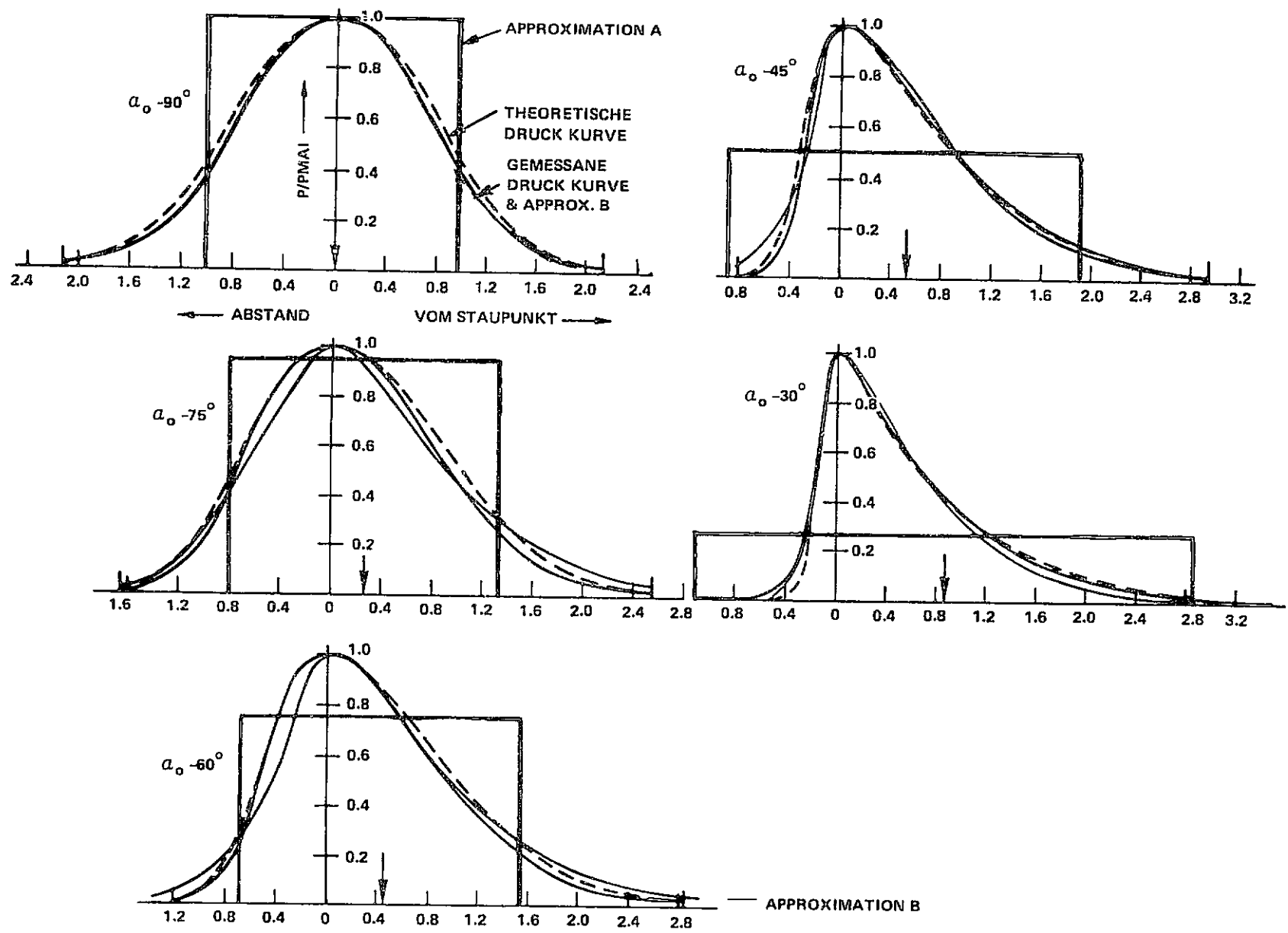


FIGURE 11. PRESSURE DISTRIBUTIONS FOR 2D JET MEASURED, SCHACH & APPROXIMATIONS

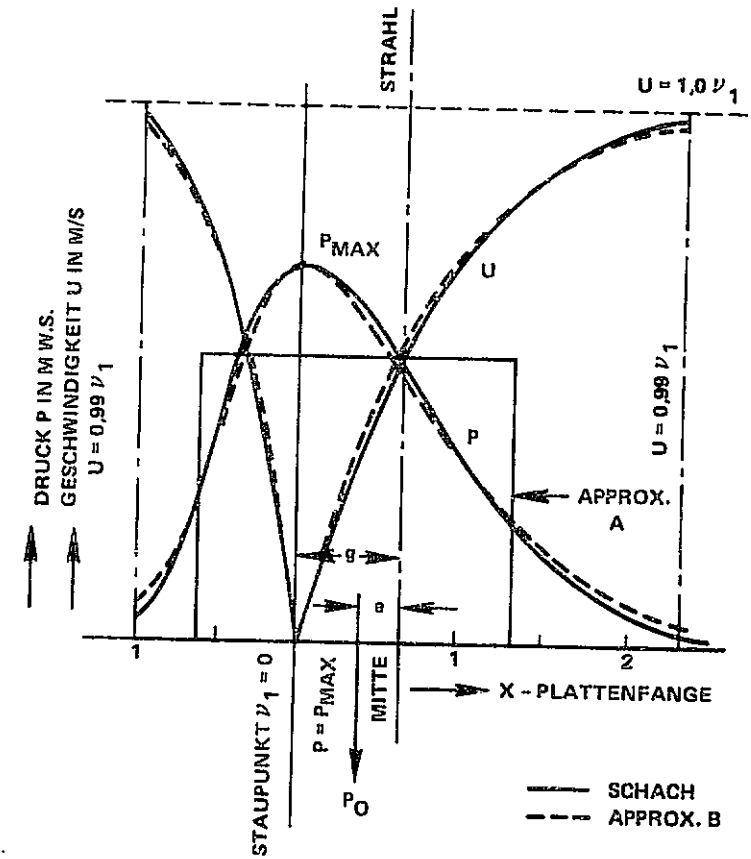
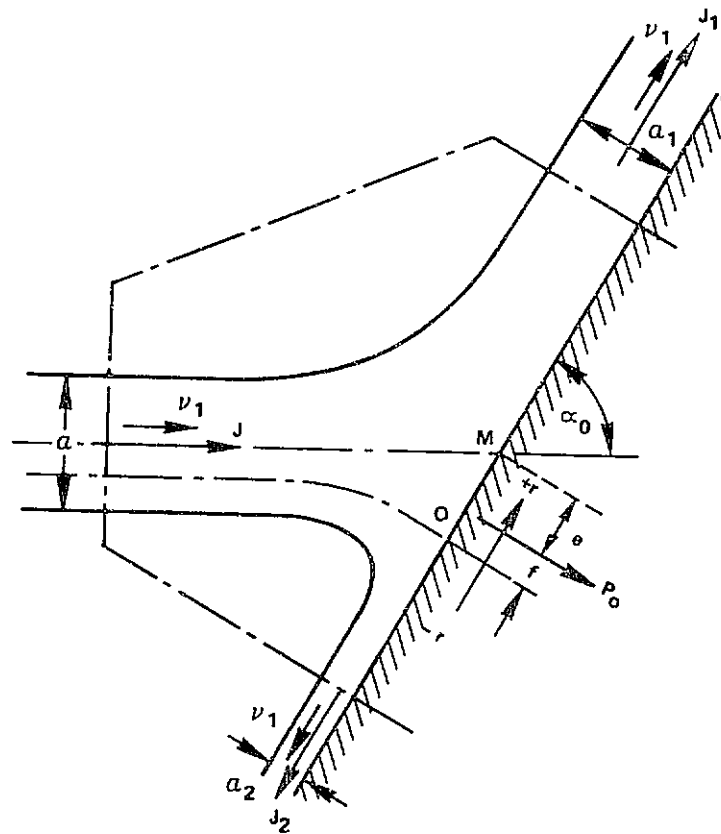


FIGURE 12. PRESSURE & VELOCITY DISTRIBUTIONS FOR 60° IMPINGEMENT OF 2D JET SCHACH & APPROXIMATIONS

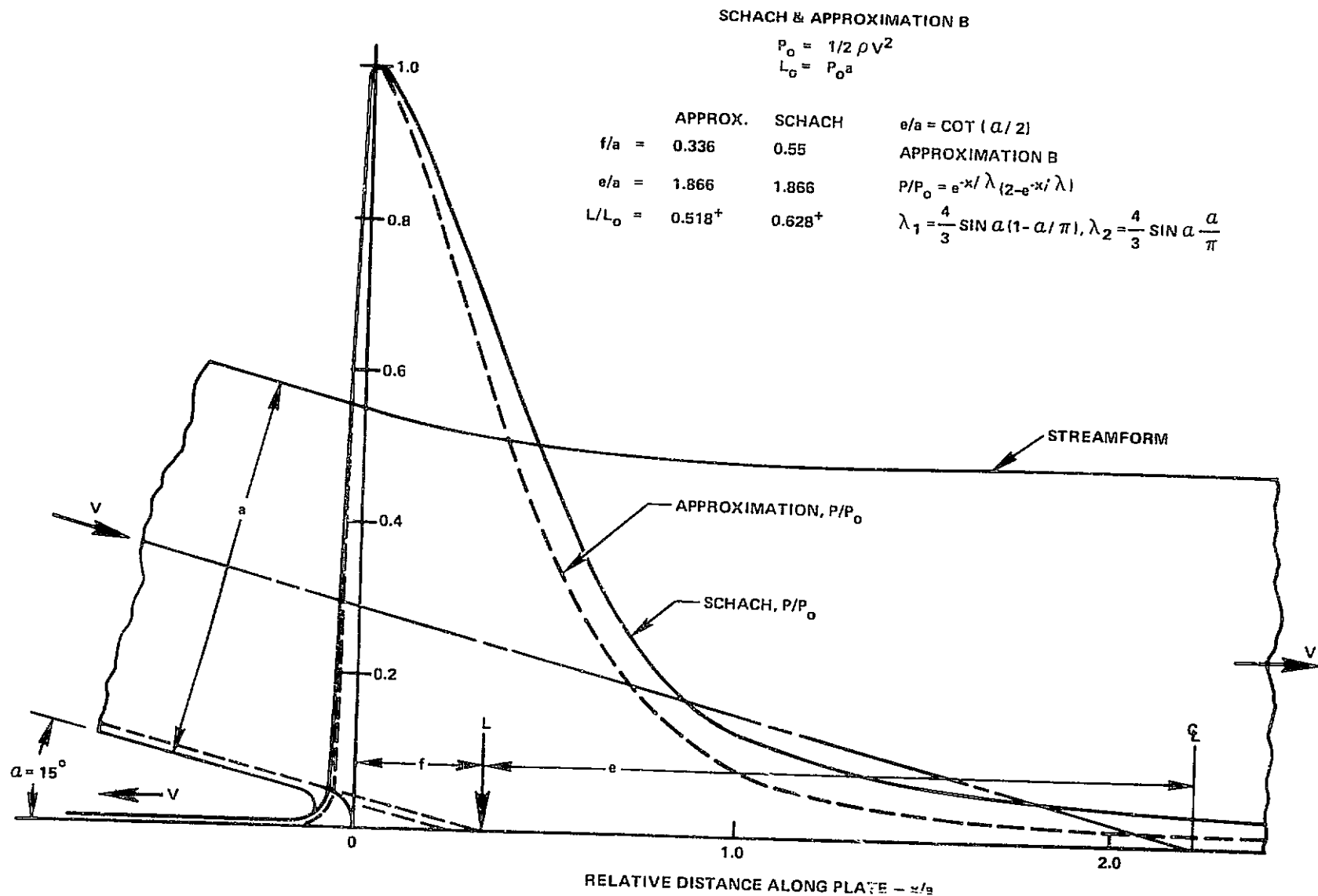


FIGURE 13. PRESSURE DISTRIBUTIONS FOR 15° 2D JET

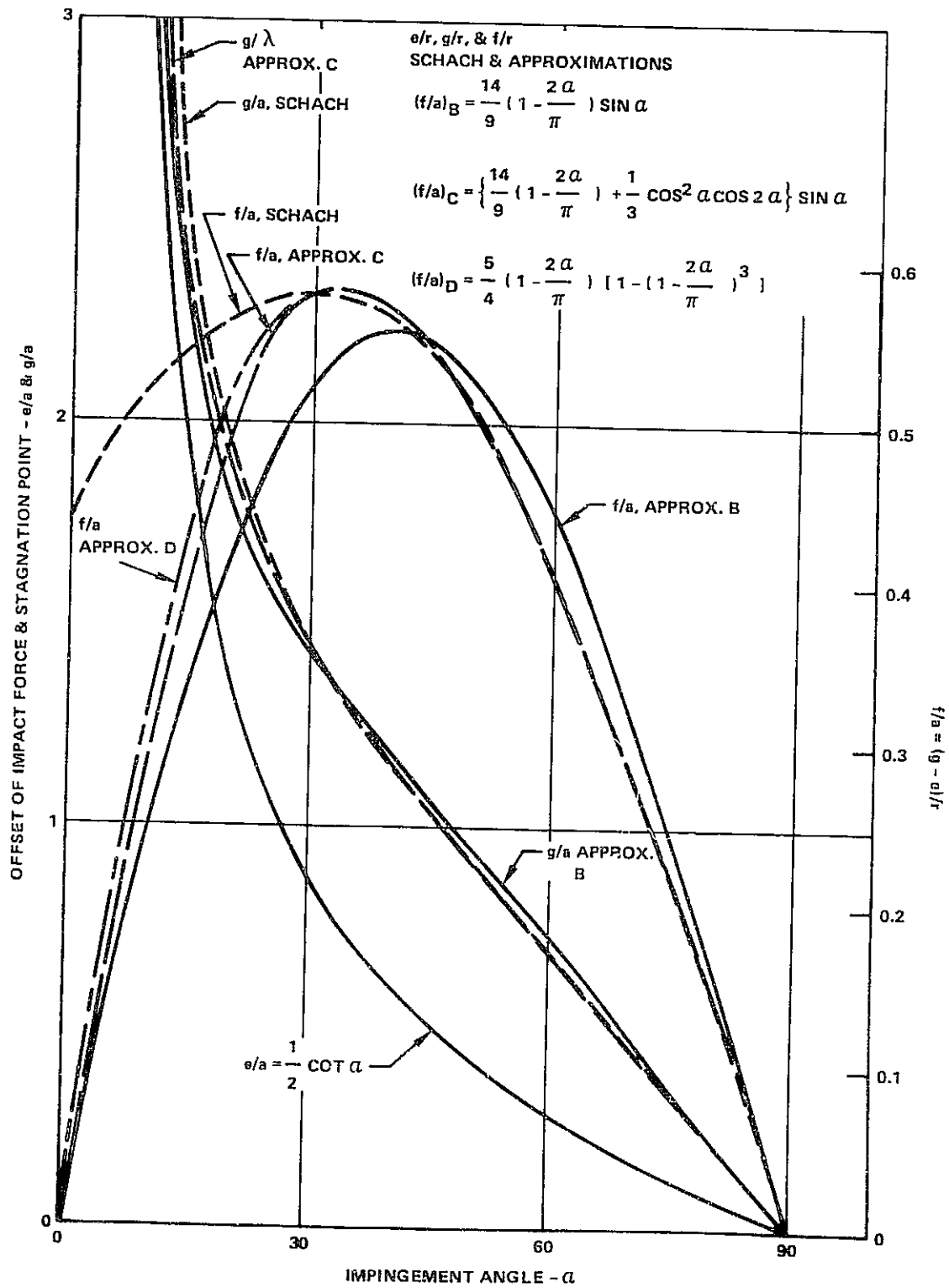


FIGURE 14. LOCATIONS FOR 2D JET OF IMPACT FORCE & STAGNATION POINT

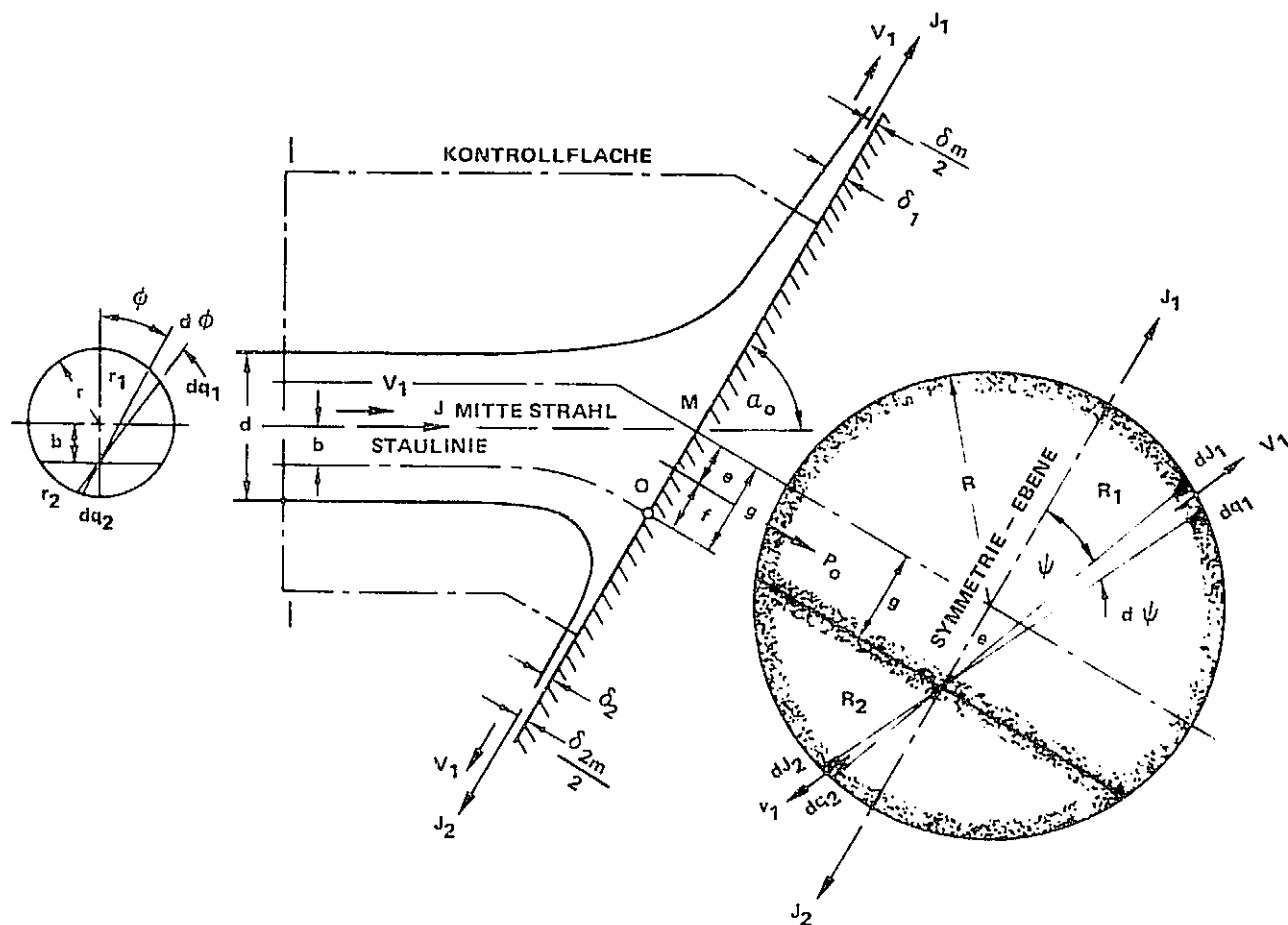


FIGURE 15. 3D JET MISSILE MODEL PER SCHACH

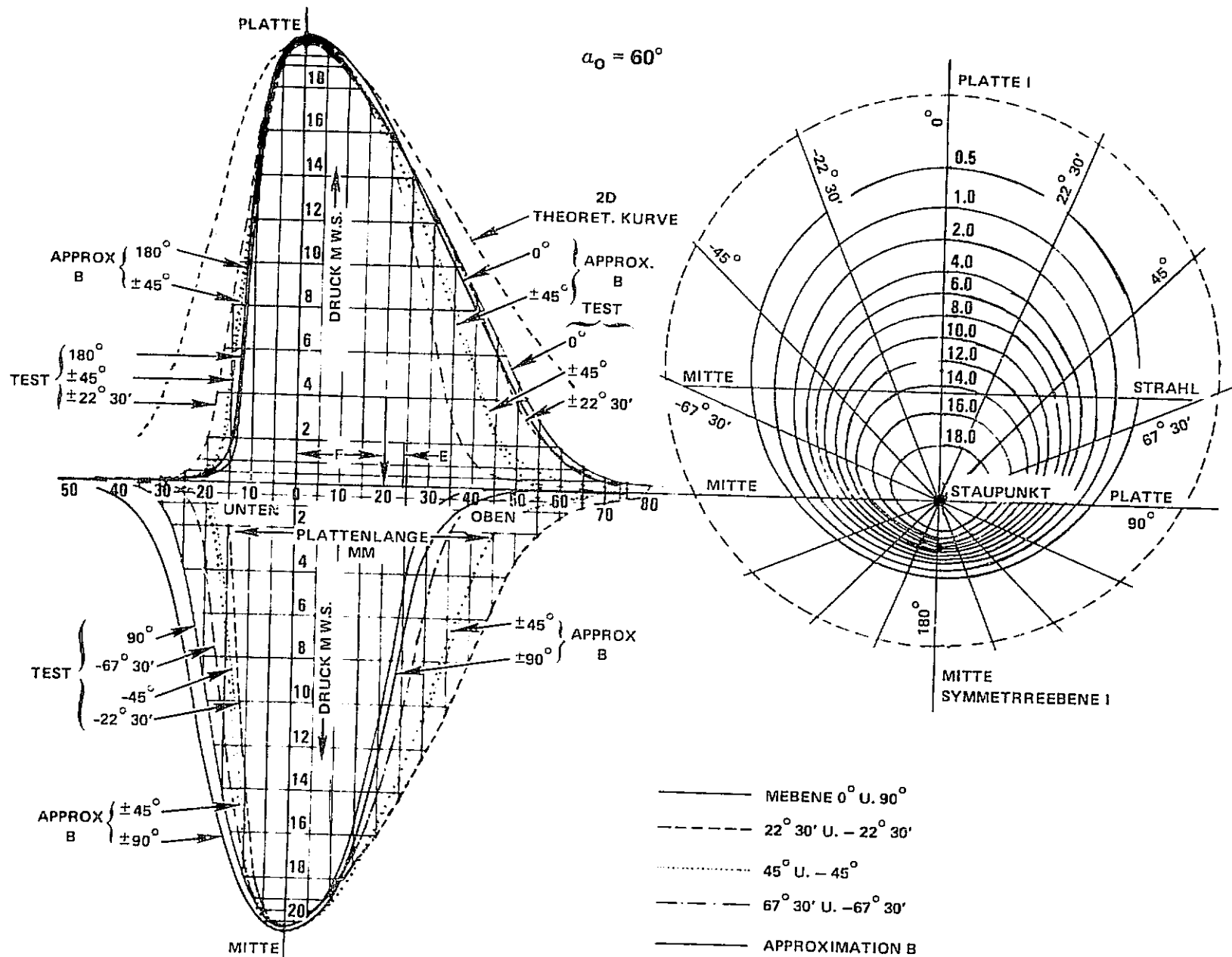


FIGURE 16. PRESSURE DISTRIBUTION FOR 3D JET MEASURED & SCHACH'S THEORY

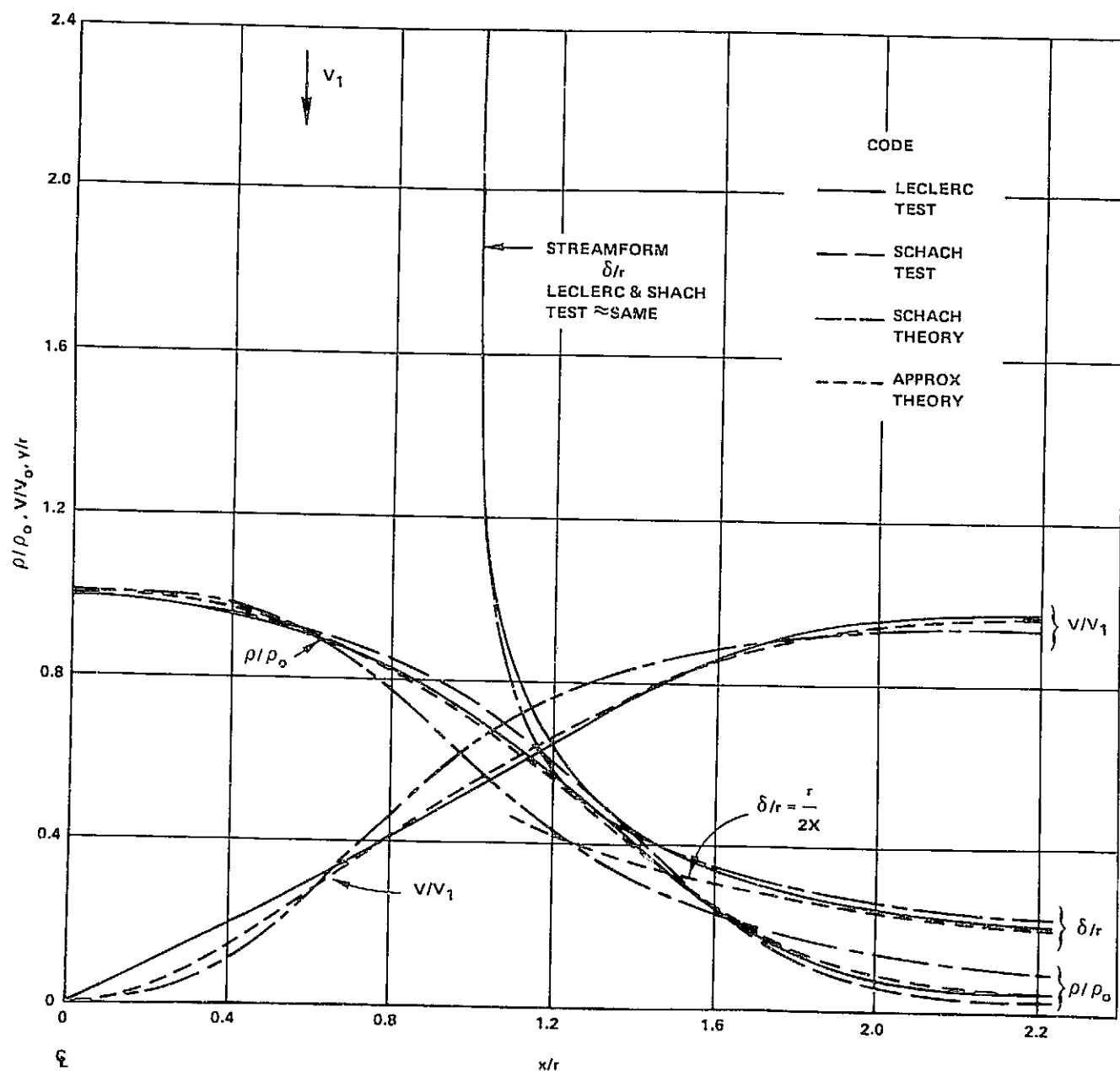


FIGURE 17. NORMAL IMPINGEMENT OF 3D JET PRESSURE, STREAMFORM & VELOCITY DISTRIBUTIONS - THEORY & TEST

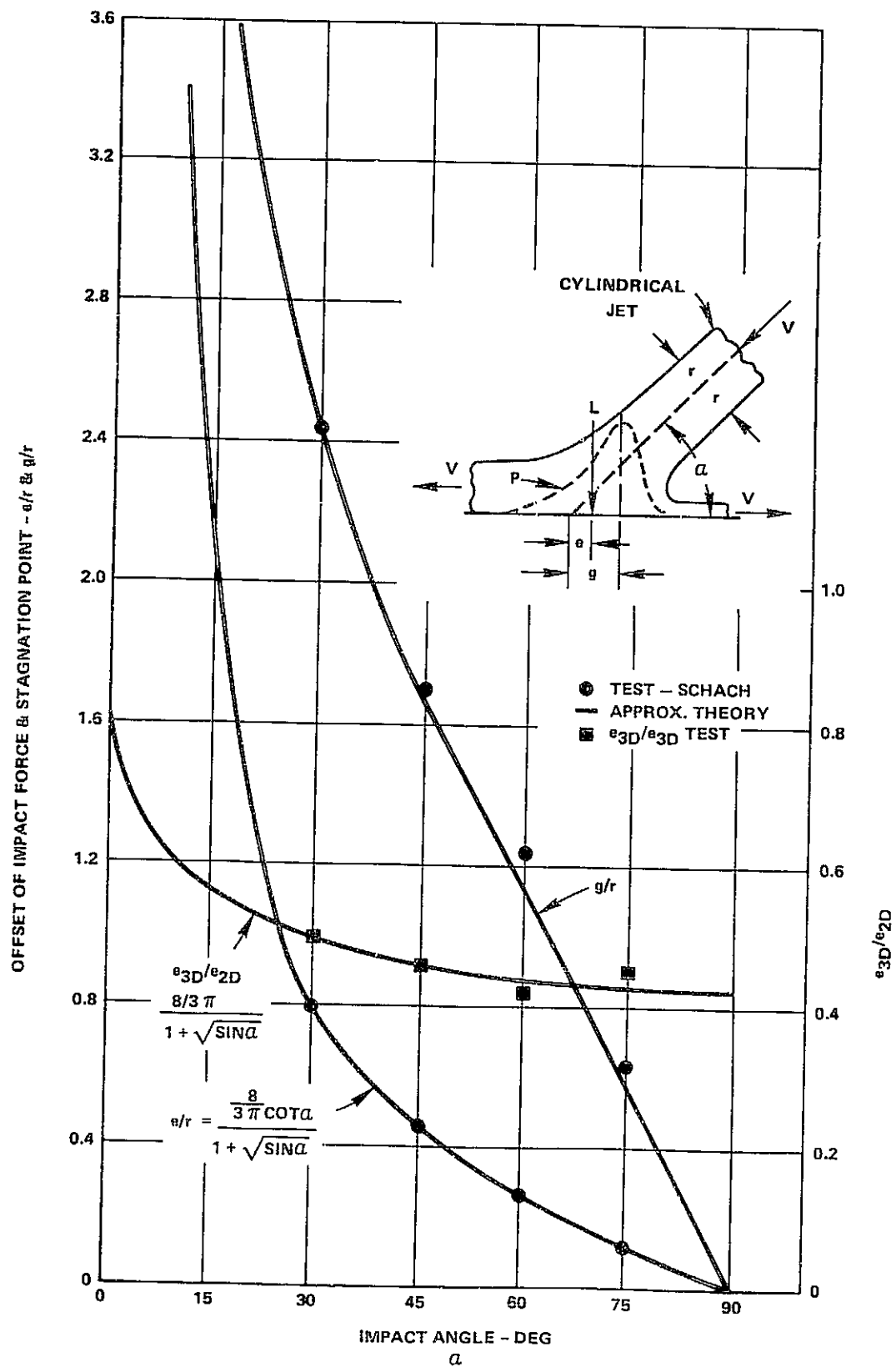


FIGURE 18. 3D JET LOCATIONS OF IMPACT FORCE & STAGNATION POINT e/r & g/r

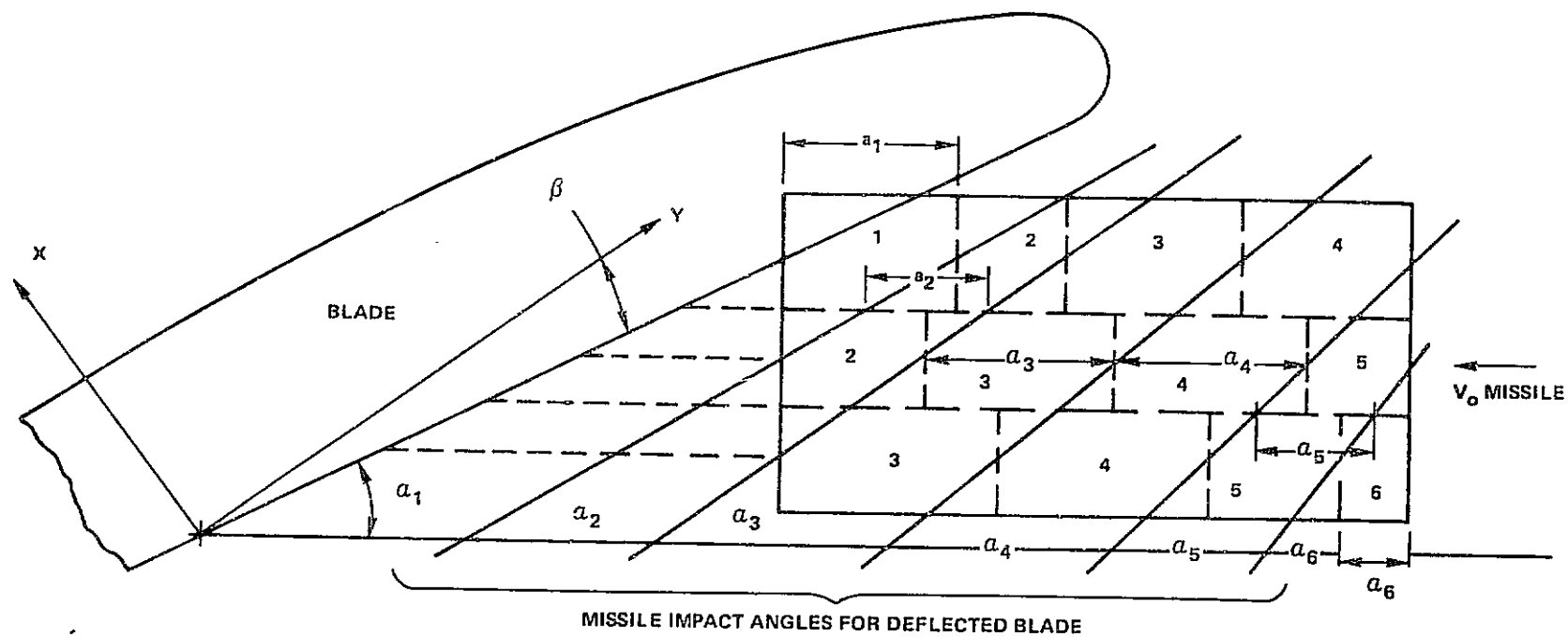
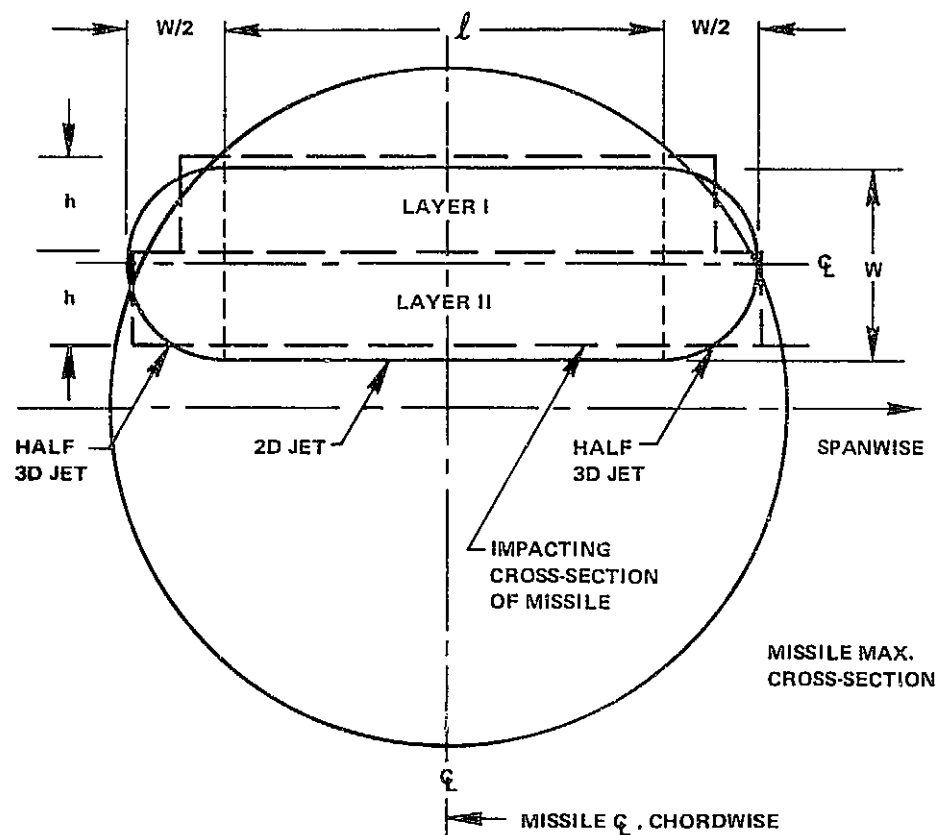


FIGURE 19. VARYING MULTI-SEGMENT MISSILE



$$W = 2h \text{ OR } mh_m$$

$$A_{\text{sect}} = A_3 + A_2 = \sum_{\text{Impact}} A_{\text{Layers}}$$

$$A_3 = \frac{\pi}{4} W^2$$

$$A_2 = l W$$

m = NUMBER OF RECTANGULAR
LAYERS h THICK
SIMULATING MISSILE

FIGURE 20. APPROXIMATION OF GENERAL SHAPED MISSILE FROM 2D AND 3D JETS

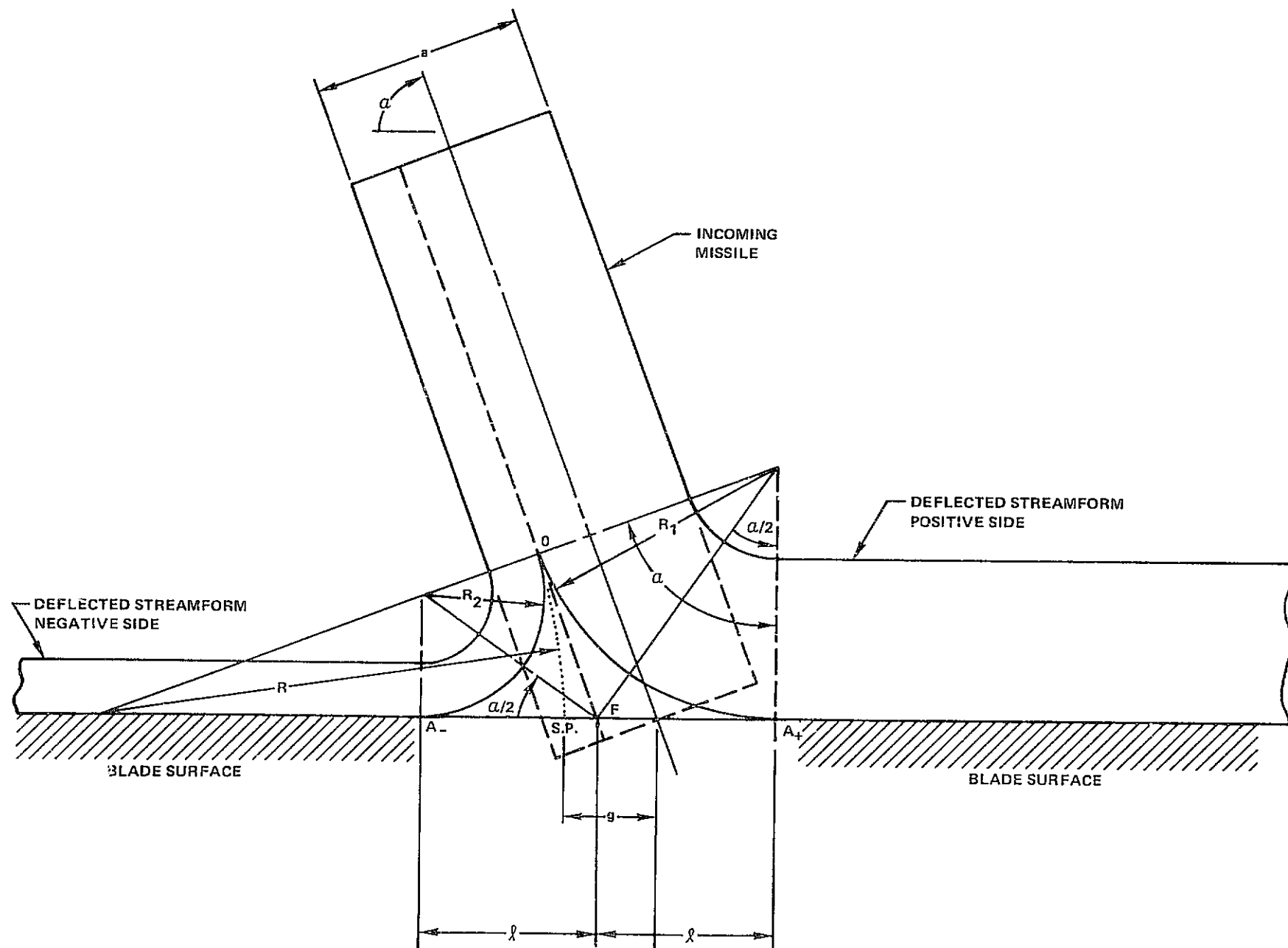


FIGURE 21. APPROXIMATED STREAMFORM PARAMETERS

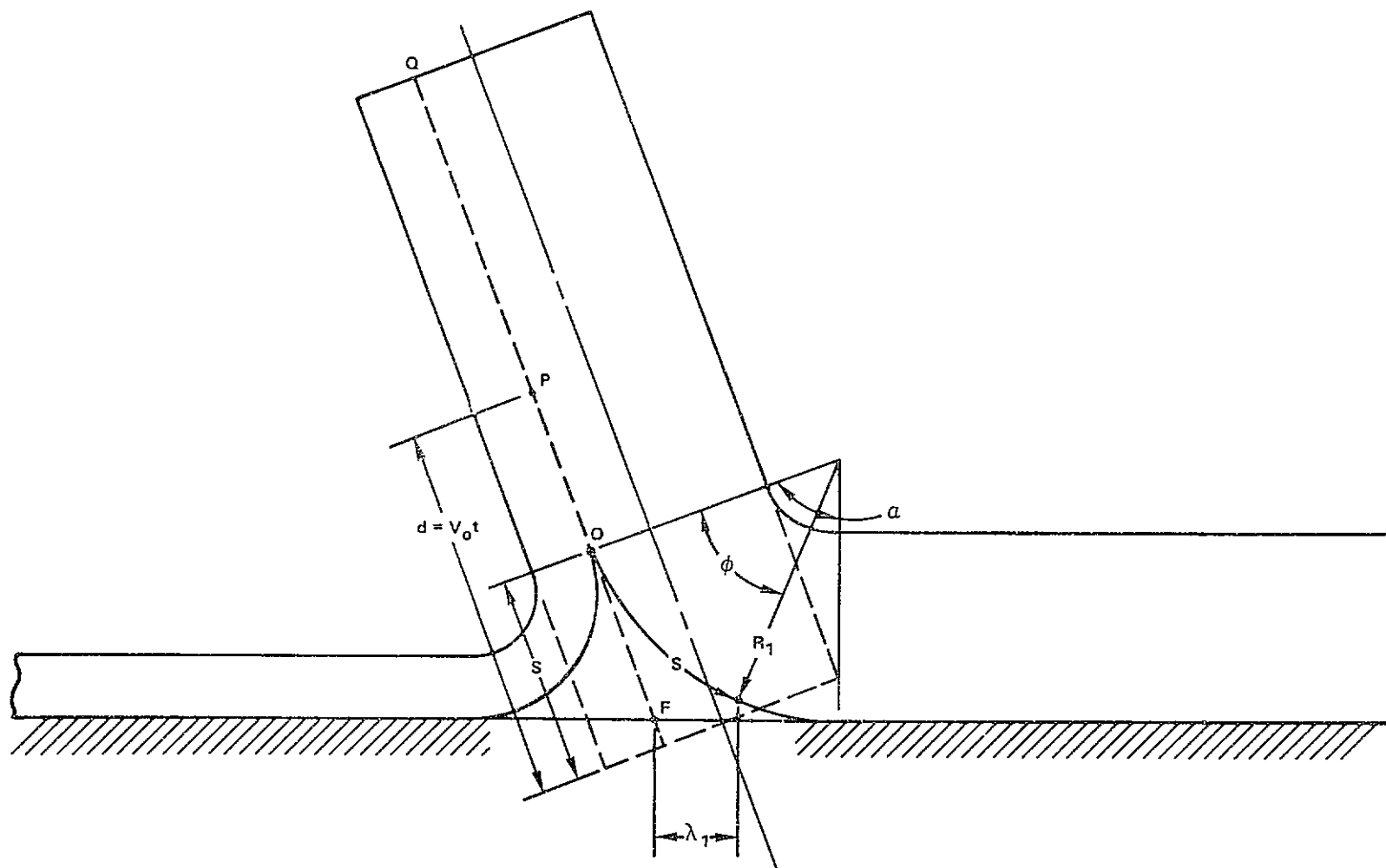


FIGURE 22. PATH AND LOCATION OF AN ELEMENTAL VOLUME OF FLUID

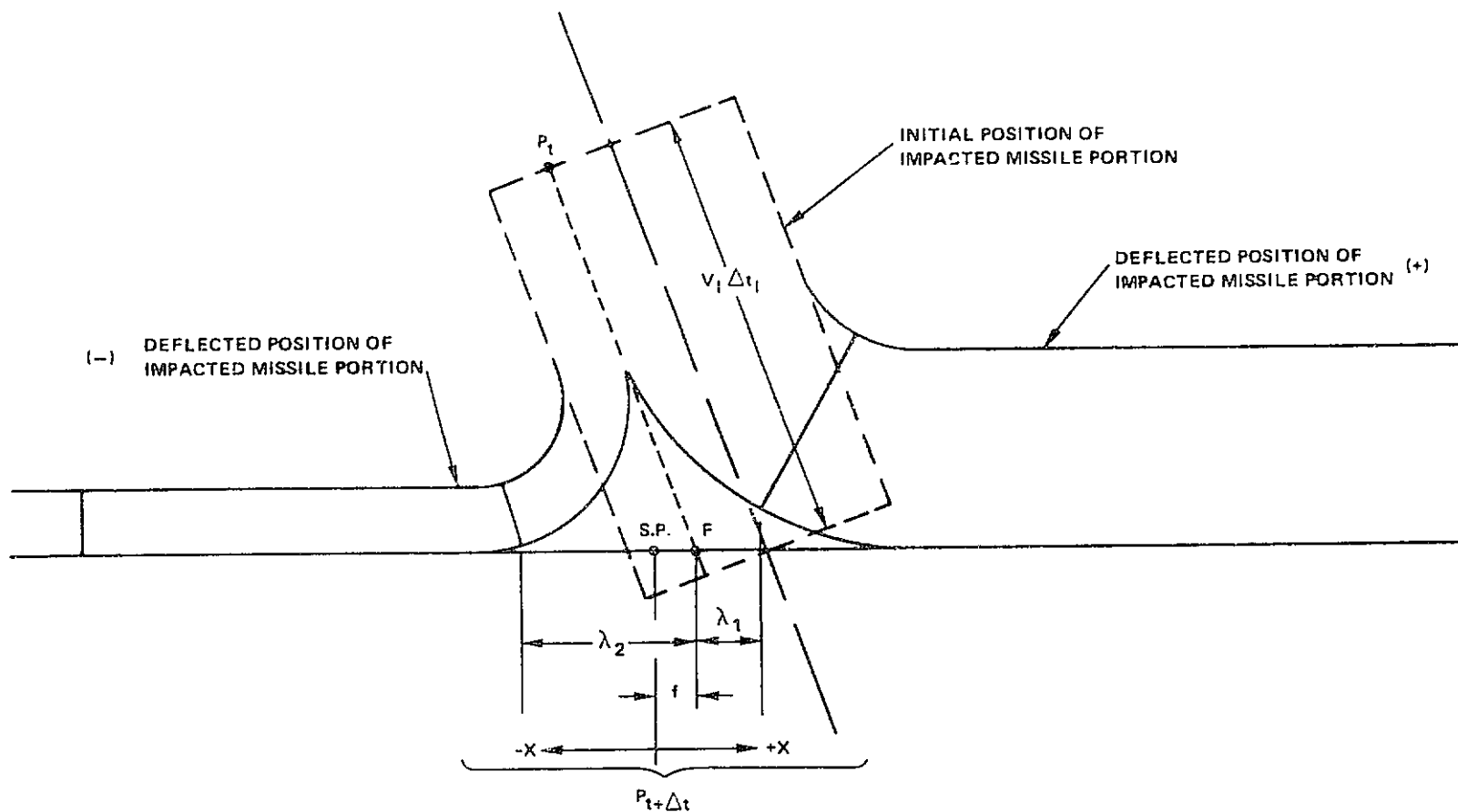


FIGURE 23. INITIAL AND FINAL FORM OF AN IMPACTING MISSILE PORTION

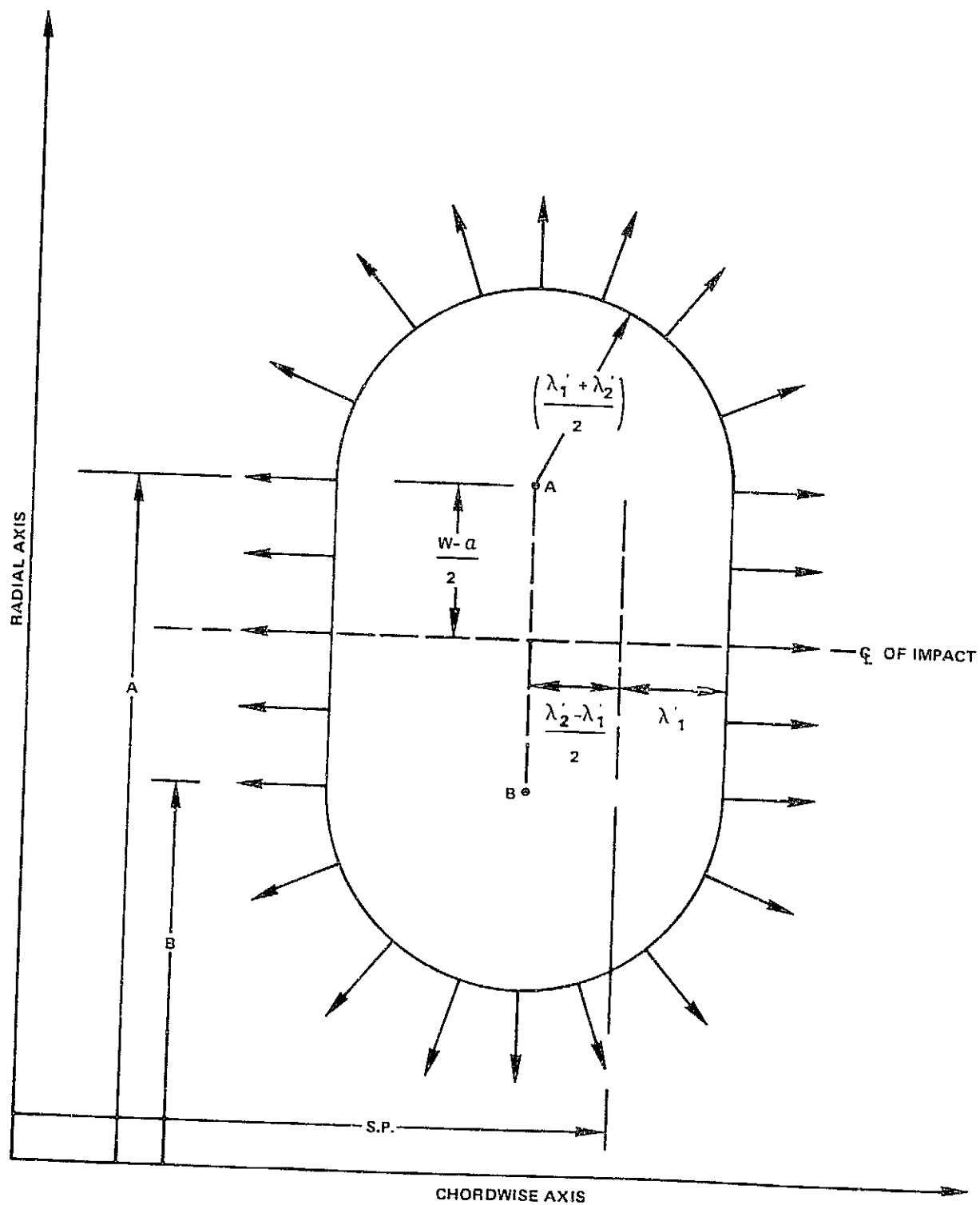


FIGURE 24. GENERAL IMPACTED MISSILE MASS DISTRIBUTION

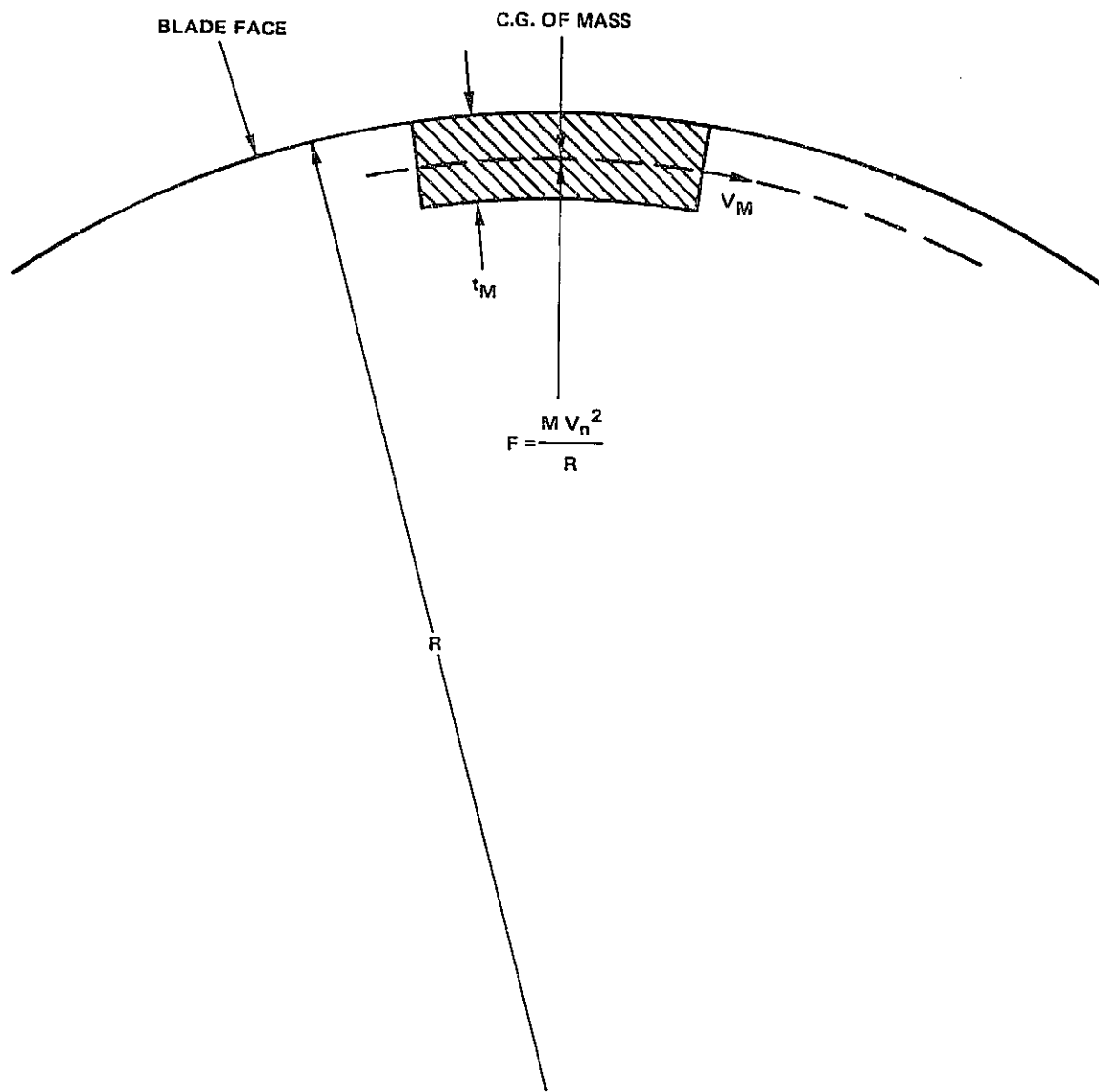


FIGURE 26. ELEMENTAL MASS VOLUME TRAVERSING A CURVED SURFACE

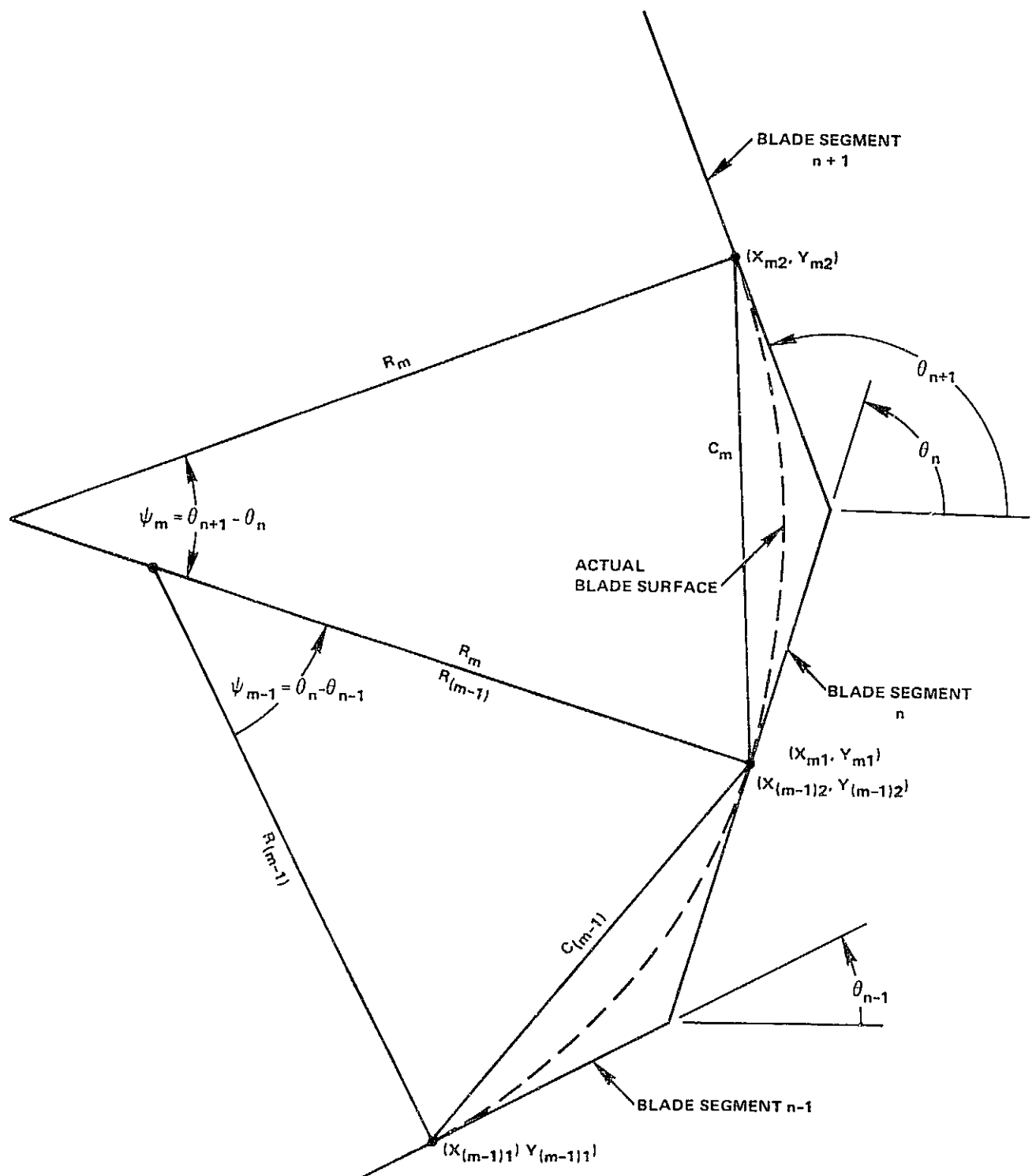


FIGURE 27. BLADE CAMBER CURVATURE GEOMETRY

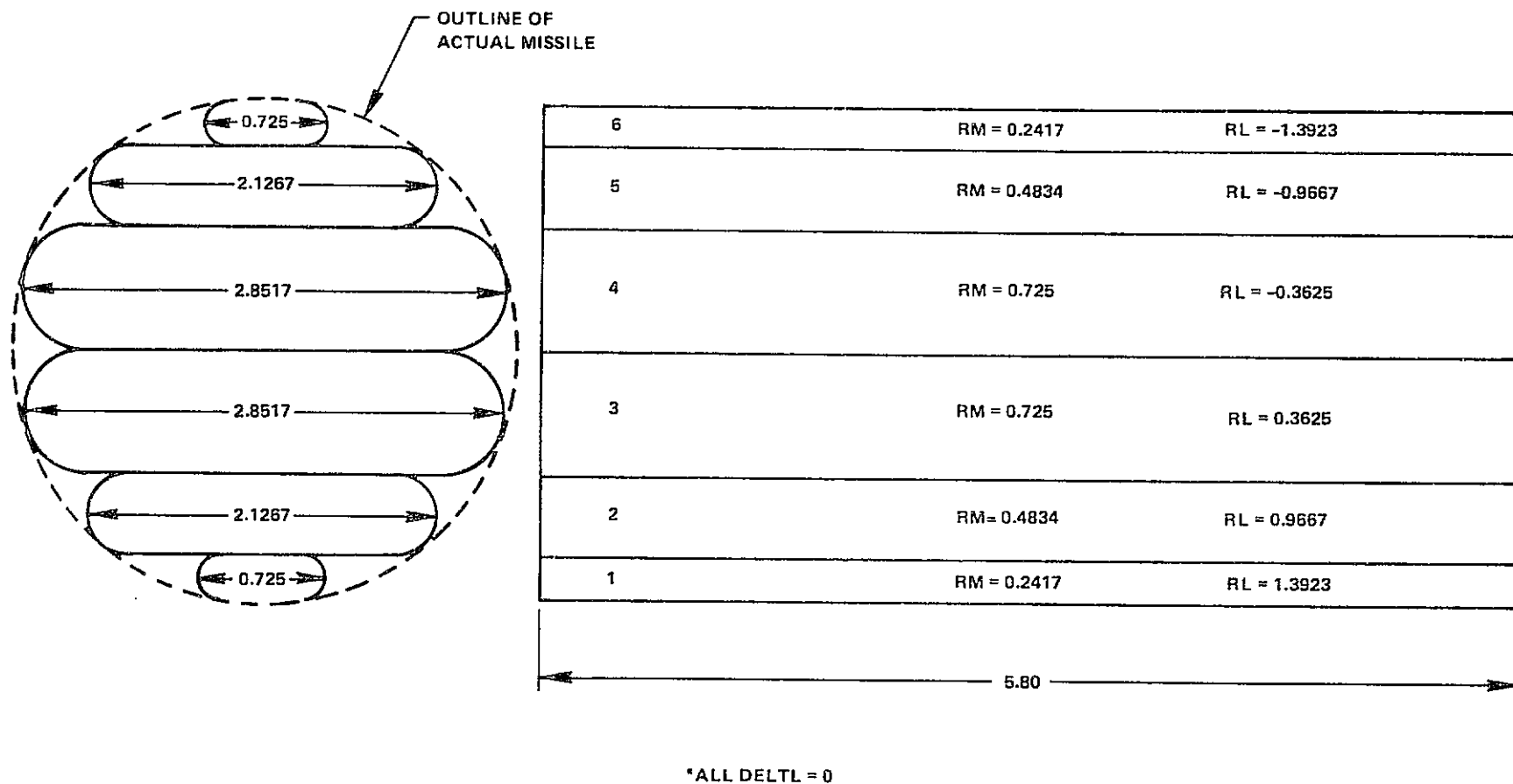


FIGURE 28. MISSILE MODEL USED FOR IMPACTS ON RIGID TARGETS

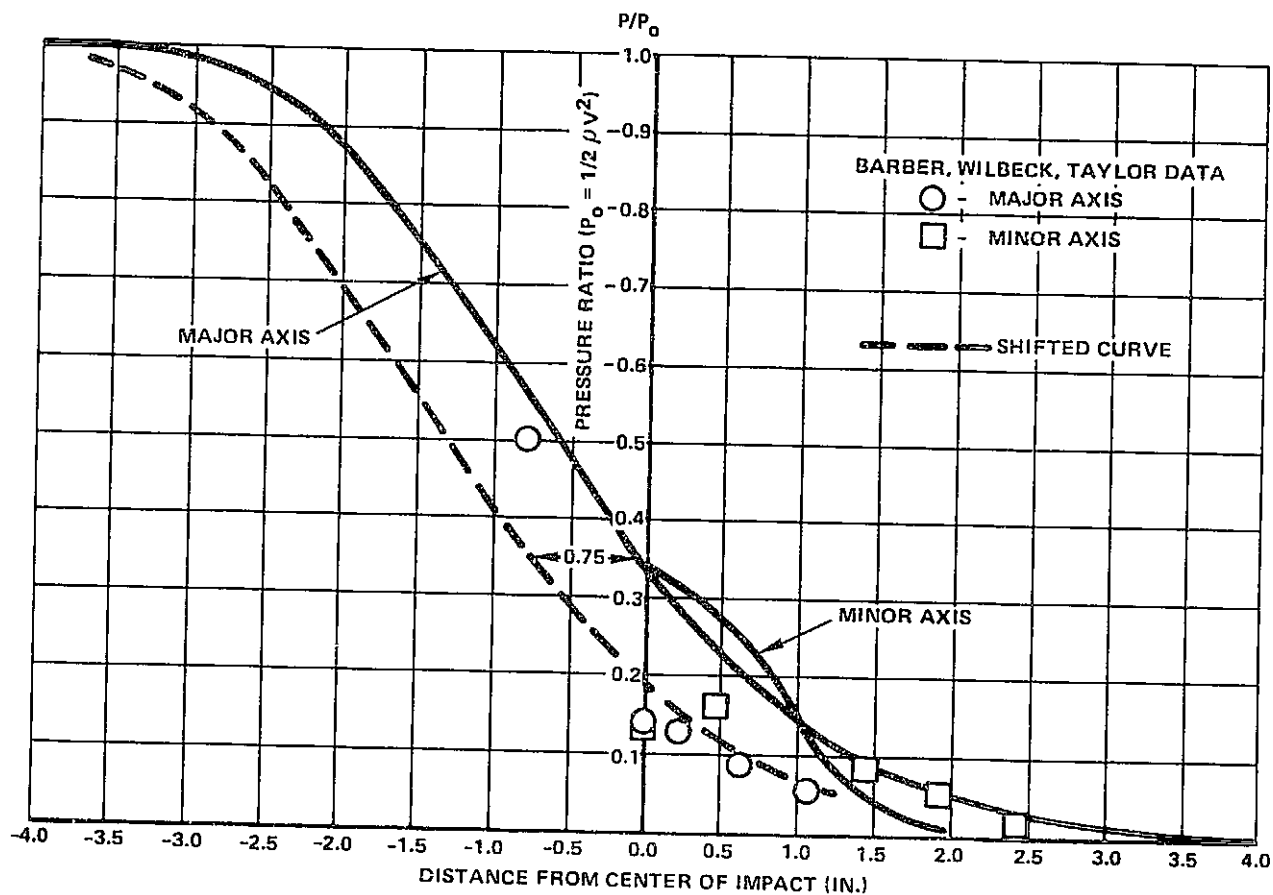


FIGURE 29. 25° IMPACT ON RIGID PLATE

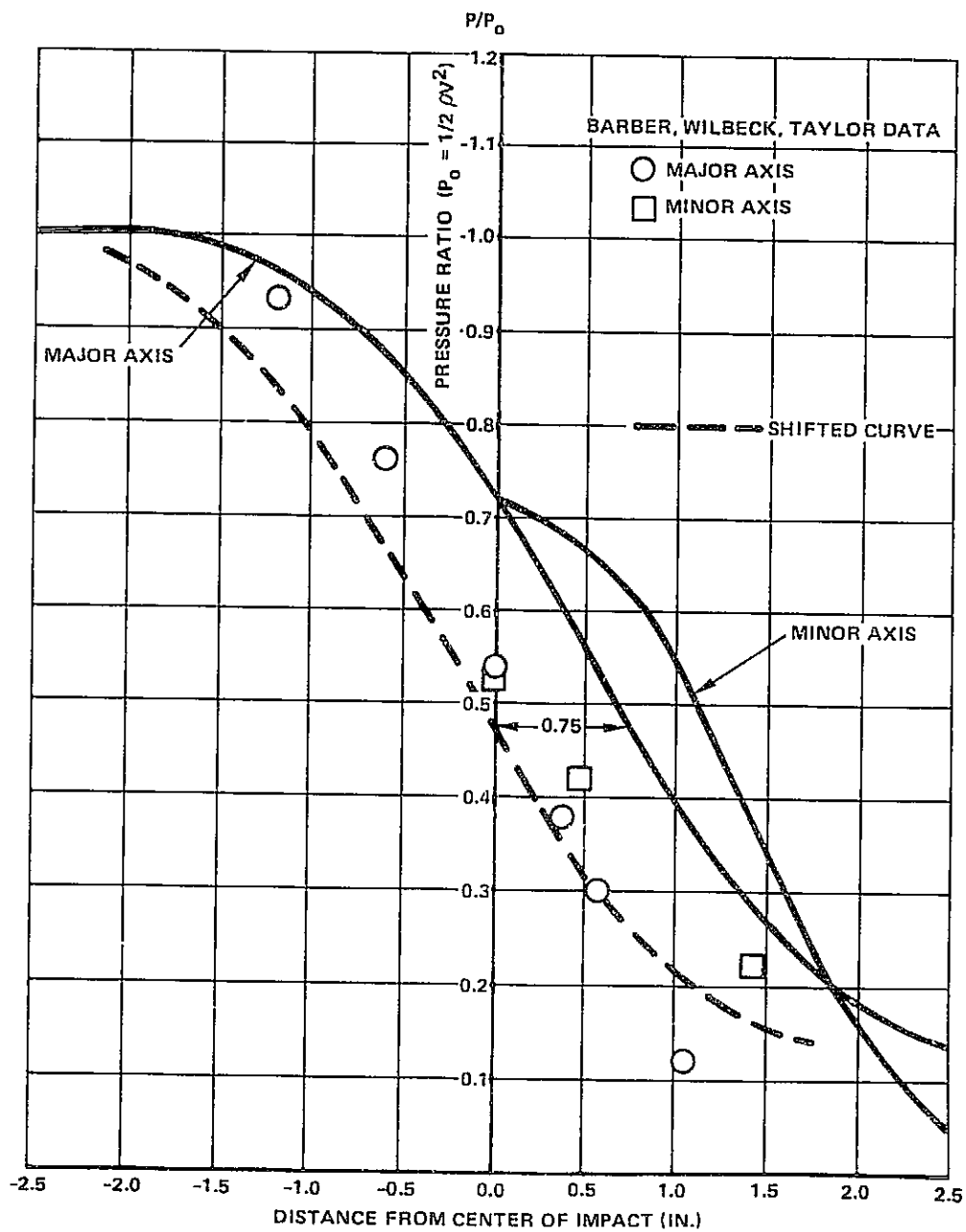


FIGURE 30. 45° IMPACT ON RIGID PLATE

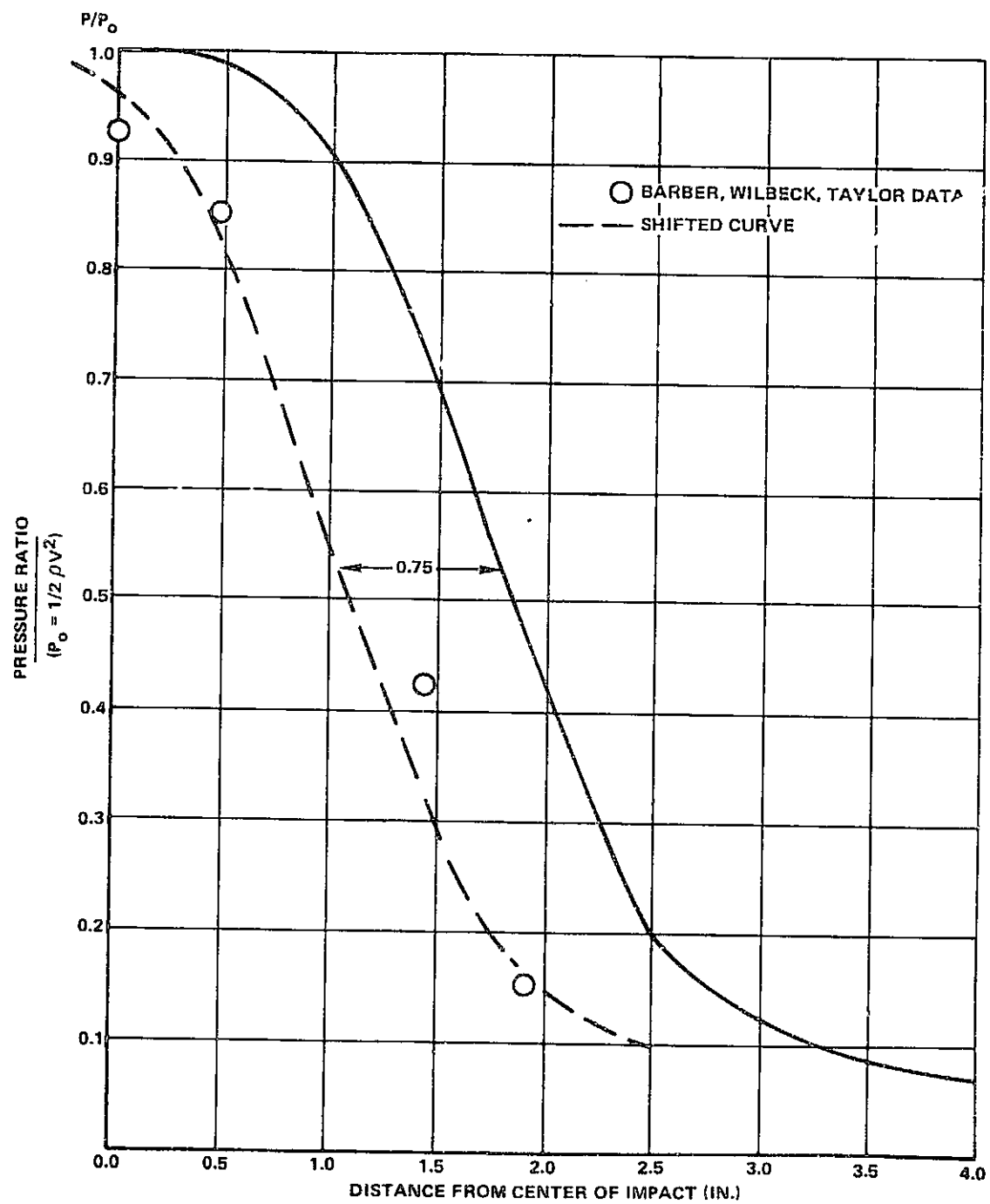


FIGURE 31. 90° IMPACT ON RIGID PLATE

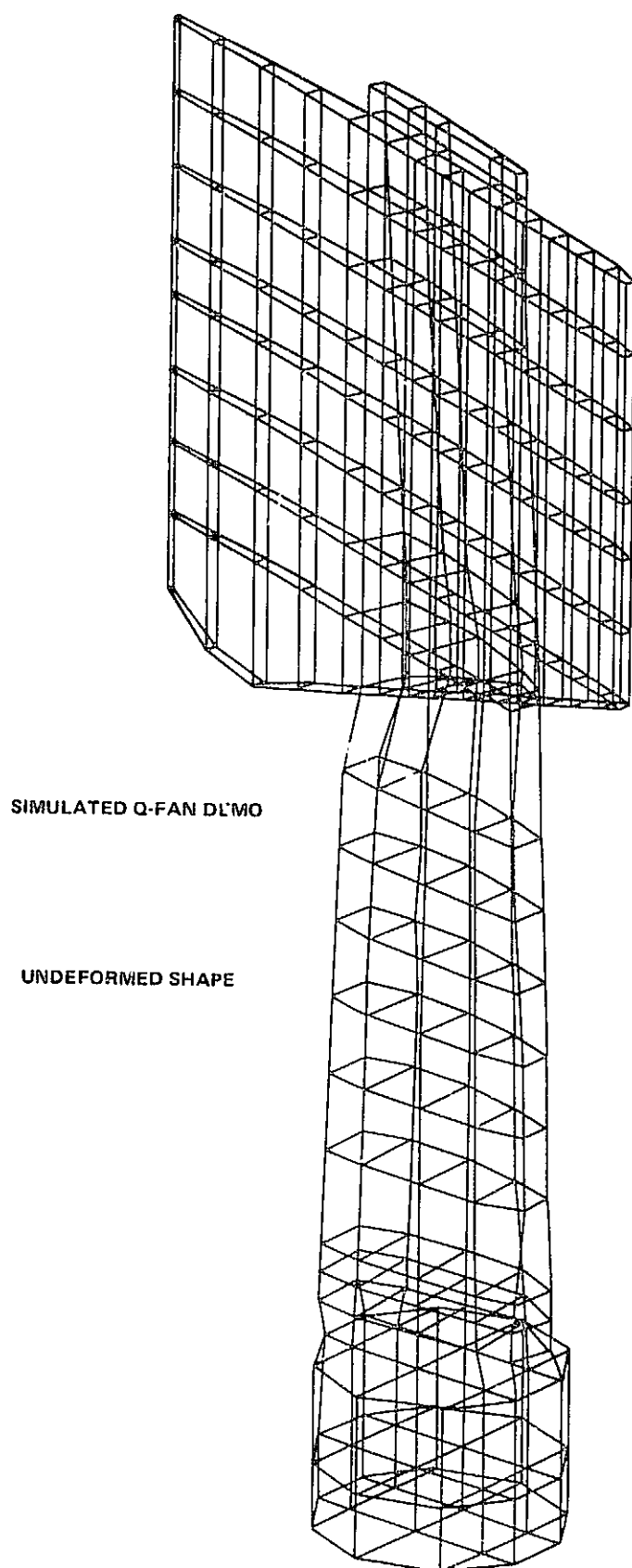


FIGURE 32. FLAT PLATE SIMULATED Q-FAN BLADE MODEL

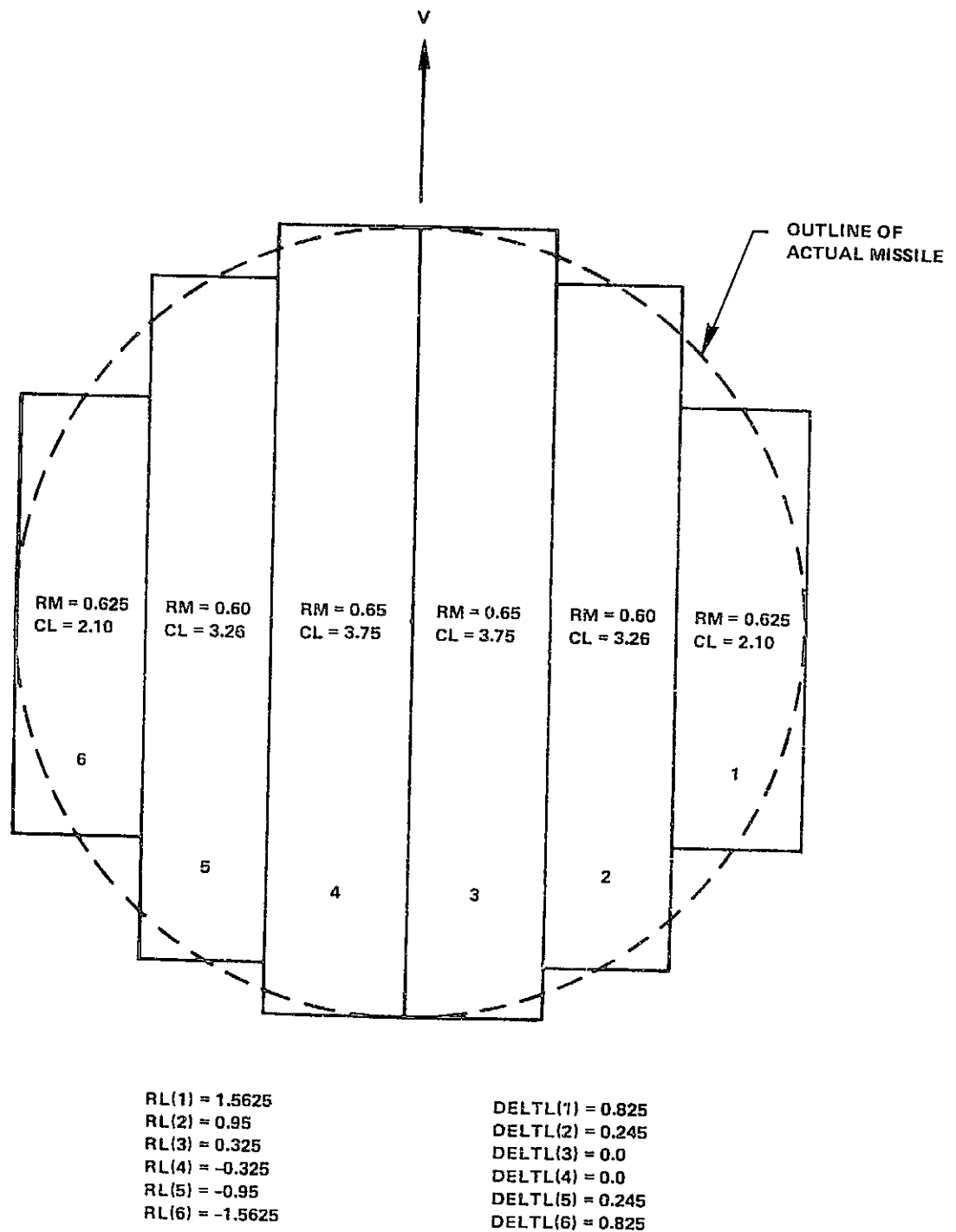


FIGURE 33. SIDE VIEW OF SPHERICAL MISSILE MODEL

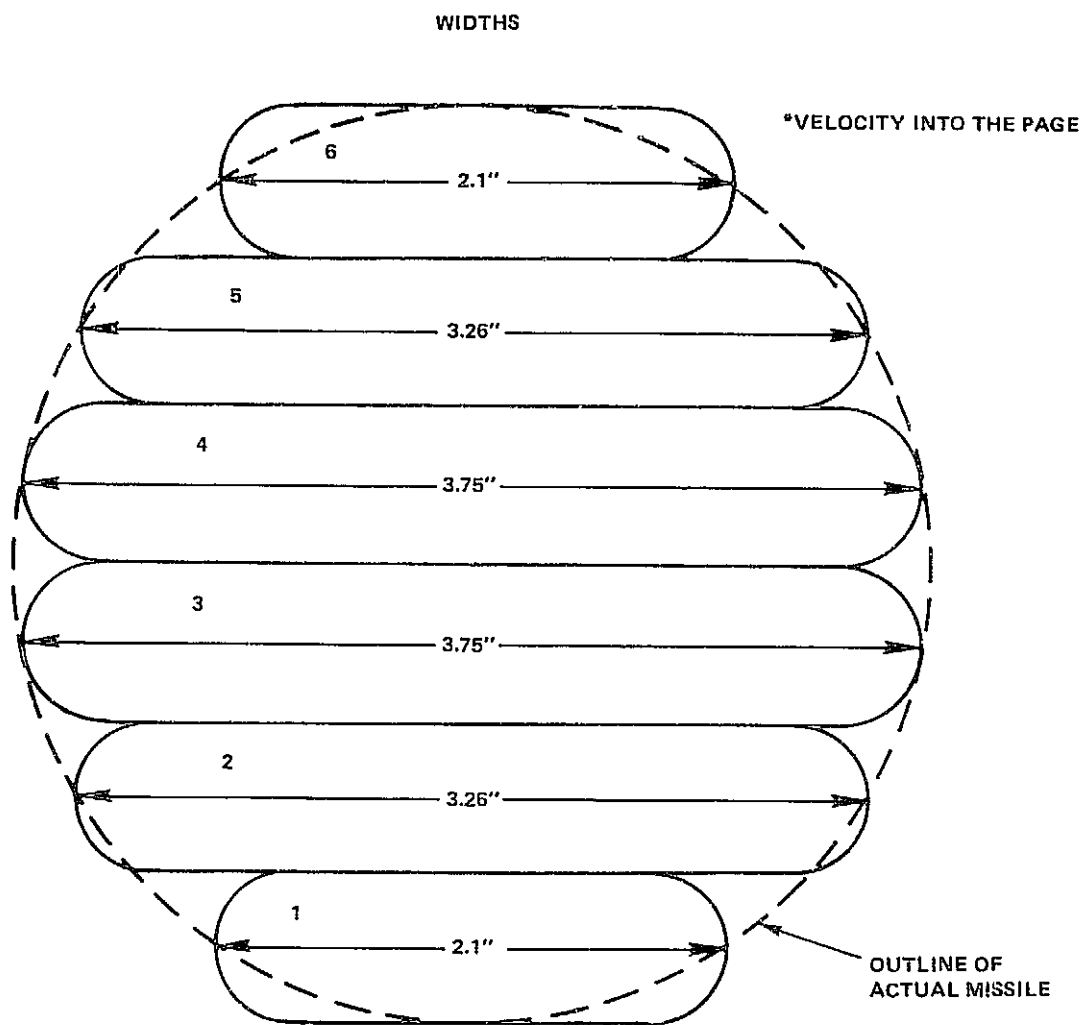


FIGURE 34. CROSS SECTION OF SPHERICAL MISSILE MODEL

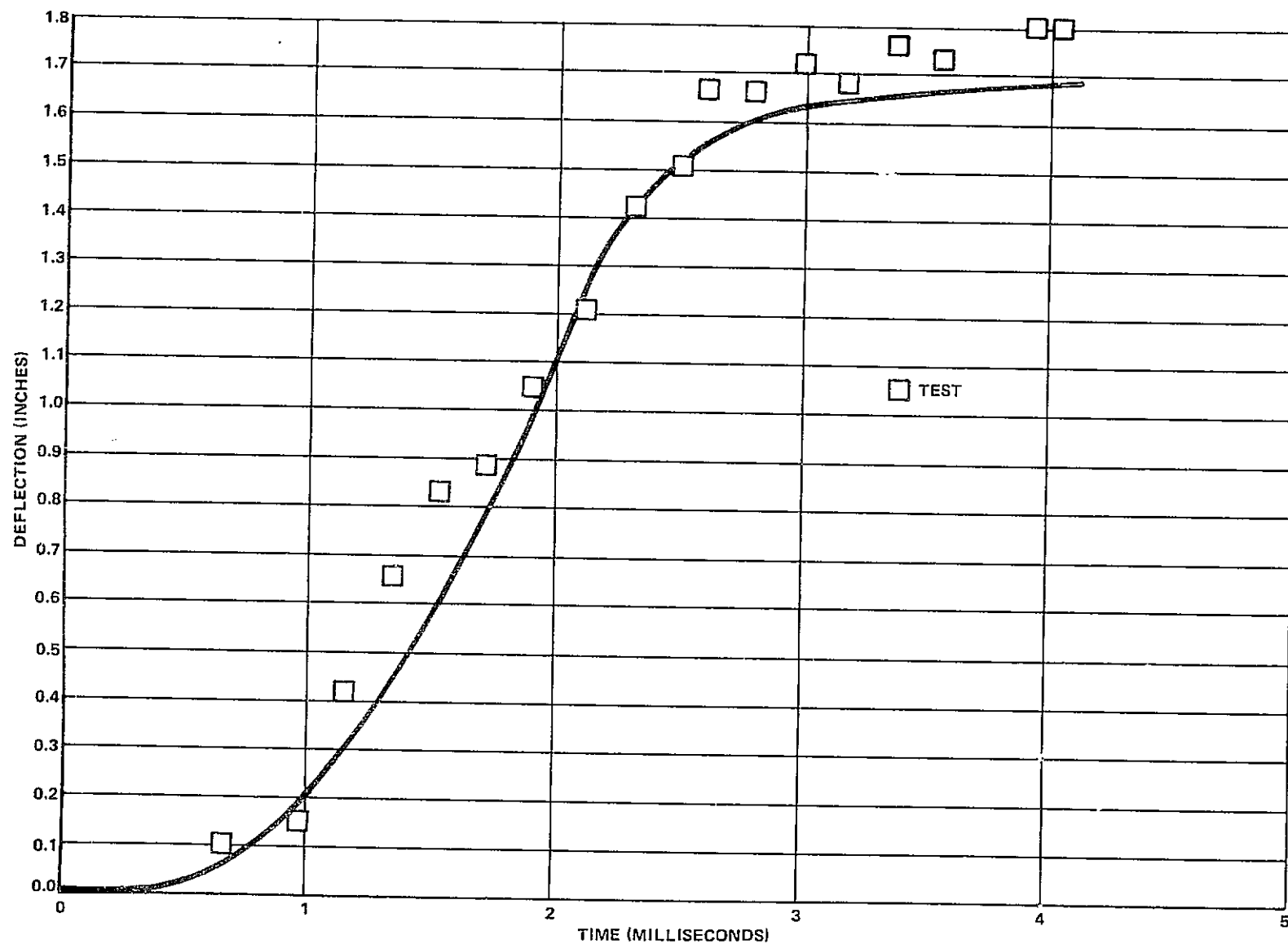


FIGURE 35. FLATWISE DISPLACEMENT RESPONSE OF SIMULATED Q-FAN BLADE SUBJECTED TO A 30° IMPACT OF A 1 LB. SPHERE AT 600 FT/SEC.

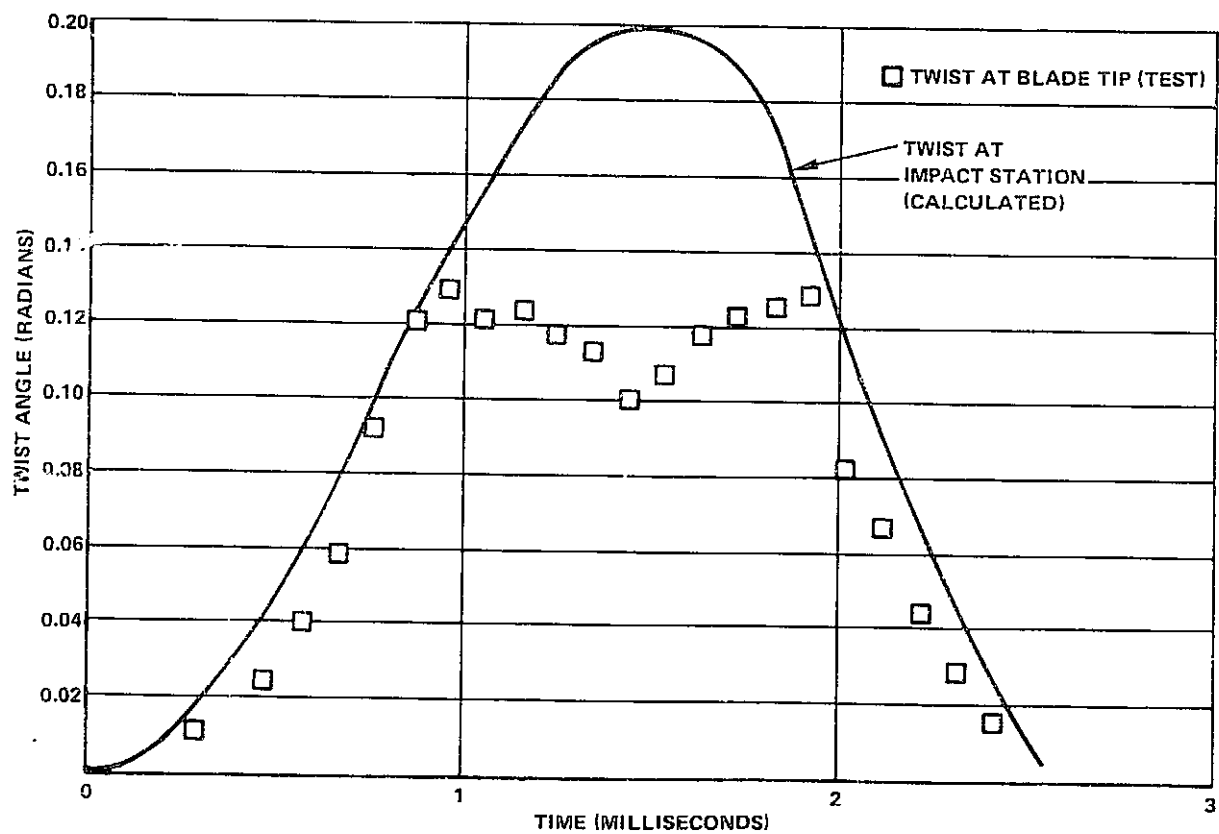


FIGURE 36. TWIST RESPONSE OF SIMULATED Q-FAN BLADE SUBJECTED TO A 30° IMPACT OF A 1 LB. SPHERE AT 600 FT/SEC.

APPENDIX A

SPRING-MASS ELEMENTAL MISSILE MODEL

Approach

This spring-mass elemental analysis approach is analogous to a finite element analysis but simpler in execution. In this analysis the missile is analyzed as a finite slug of fluid impacting an inclined surface and includes all the six requirements defined by the contract and listed in the Introduction. In this approach the fluid slug is divided into a finite number of mass blocks as shown in Fig. 1A. The mass of each block is concentrated at the center of the block and these masses are connected to the neighboring masses sharing a common surface. The volume enclosing the mass of each fluid slug can be calculated by summing the triple vector products of the relative position by computing the appropriate cross-products. Once the volume of the block is known the density can be calculated from

$$\rho_i = m_i/V_i \quad (1A)$$

where:

m_i is the mass of block i ,

V_i is the volume of block i , and

ρ_i is the density of block i .

The pressure at the center of block i can be found from a constitutive relation. In the present analysis the pressure, P , is computed as

$$P = \frac{\rho_o C_o^2}{\gamma + 1} \left[\frac{\rho}{\rho_o} \quad \gamma + 1 \quad -1 \right] + P_a \quad (2A)$$

when $P \geq -P_T$

and as

$$P = -P_T \quad (3A)$$

if

$$P < -P_T \quad (4A)$$

where:

ρ_o is the nominal density,

C_o is the speed of sound at $P = P_o$,

γ is a material parameter,

P_a is the ambient pressure, and

P_T is the tensile pressure failure load.

These constitutive relations are similar to those used in Ref. 8. The interface pressures can be computed as the average of the pressures at two connected masses. The forces on the masses can then be evaluated by using the calculated interface areas. The position of the particles at the end of the time increment can now be found from Newton's second law of motion. Presently the integration in time is done using the Runge-Kutta method.

Status & Results

Using the scheme just described, the two-dimensional model in Fig. 1A was examined at various angles of attack. As the angle of attack is increased, the analysis showed that backflow (i.e., reverse flow up the plane in Fig. 1A) was initiated at the angle of attack for which it was expected. This angle depends upon whether the flow is two- or three-dimensional and the fineness of the grid.

Table IA presents the peak pressure that occurred for the model in Fig. 2A and the elapsed time when the peak pressure was reached. Cases 1 and 2 in Table IA are for arbitrary material properties, while Case 3 uses the material properties of water given in Ref. 8. The results for Case 3 are comparable to the results in Ref. 8 where the normal impact of water droplets was examined.

Figure 2A presents the average pressure over the blocks intersecting the surface as a function of time for Case 1 of Table IA. Note that there is a high initial peak response followed by a relatively steady portion. As shown in Fig. 2A this steady portion actually has a great deal of noise resulting from numerical instabilities.

The time domain integration algorithm and the finite grid are contributing to the numerical instabilities. In addition to this the model does not include any cushioning for the leading masses, which could also be contributing to the numerical instability.

Improvements

Without adding to the complexity, an improved representation of the missile could be obtained by: (1) adding zero masses to the outside surface which will allow the program to track the surface of the missile in order to obtain the cushioning effect, and (2) moving the pressure calculation points to the element interfaces instead of placing them at the lumped masses. The numerical stability in the time domain could be improved by: (1) using an implicit integration scheme in time or (2) evaluating the stability criteria, and if necessary, (3) updating the grid periodically. Concurrently with this effort it might be advantageous to undertake to obtain, test, and evaluate the COMCAM program, the code used in Ref. 8. For the angles of attack of interest ($\alpha \lesssim 30$ deg), the total impact force and center of pressure would be presented as a function of time. In addition, the force distribution for each time increment required by the Multi-Mode Blade Impact Program would be evaluated. These improvements to the present model should result in an improved, but relatively simple, technique to predict the pressure loading due to foreign object impacts.

TABLE 1A
PEAK PRESSURE AND ELAPSED TIME AT PEAK PRESSURE

NOTE 1. PARAMETER DEFINITIONS:

H = 10 CM
D = 4 CM
 $V_o = 20 \times 10^3$ CM/SEC
 $\alpha = 30$ DEG
 $\theta = 0$
 $P_o = 0$
 $P_t = 0$

NOTE 2. CASE 3 IS FOR WATER

CASE NO.	ρ_o (G/CM ³)	C_o (CM/SEC)	γ	$\rho_o C_o V_o$ (DYNES/CM ²)	$\frac{P_{MAX}}{\rho_o C_o V_o}$	t^* (μ SEC)	$C_o t^*$ D
1	1.0	250×10^3	-0.78	0.5×10^9	2.58	250	1.56
2	1.0	150×10^3	-0.78	3.0×10^9	1.23	16.7	0.626
3	1.0	150×10^3	6.15	3.0×10^9	1.98	13.3	0.499

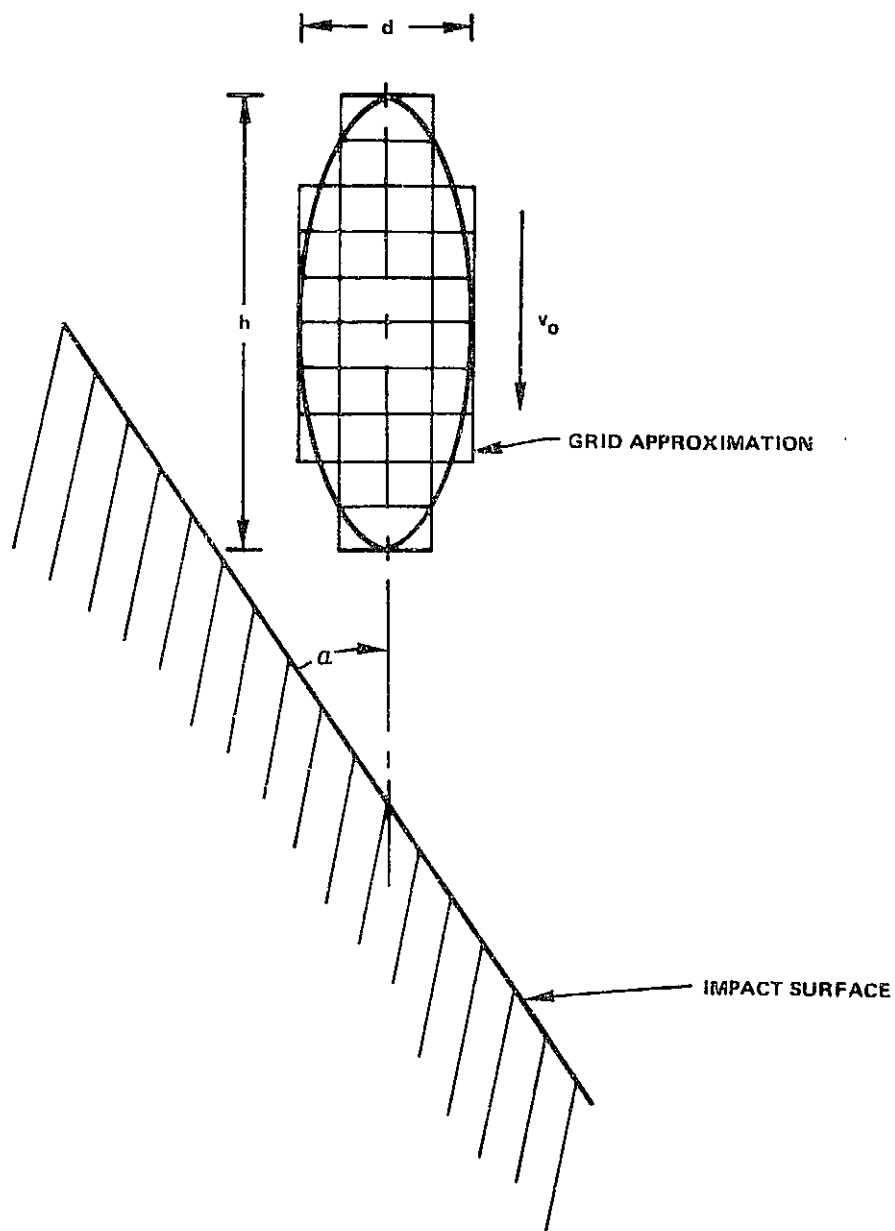


FIGURE 1A. MODEL DESCRETIZATION FOR A TWO DIMENSIONAL ELLIPTICAL FLUID MISSILE INTERSECTING A RIGID FLAT SURFACE

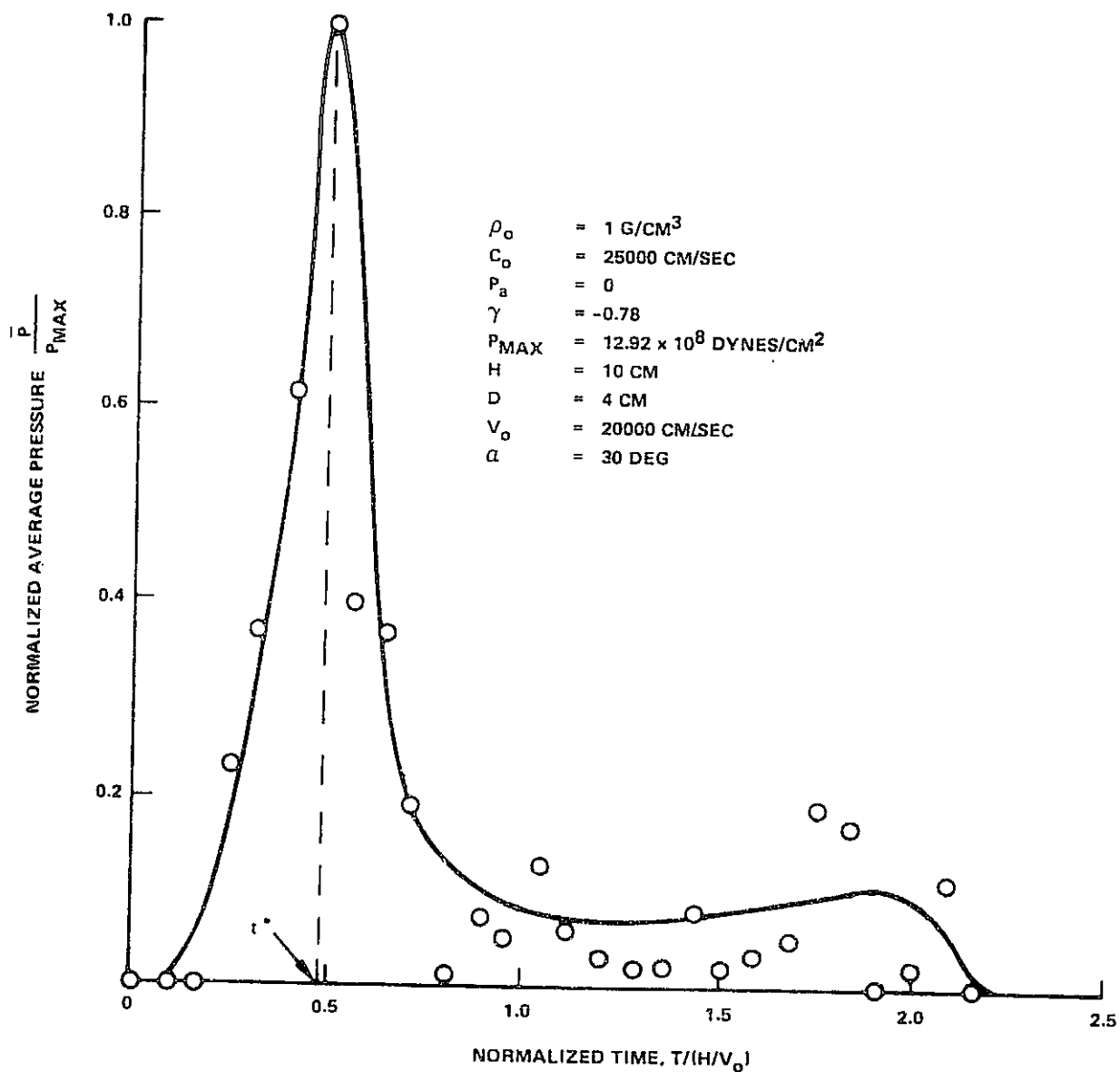


FIGURE 2A. AVERAGE IMPACT PRESSURE OVER THE IMPACTED SURFACE VS TIME FOR CASE 1 OF TABLE I

APPENDIX B

UNIFORM PRESSURE, 2D & 3D OBLIQUE IMPACTING JET MISSILES

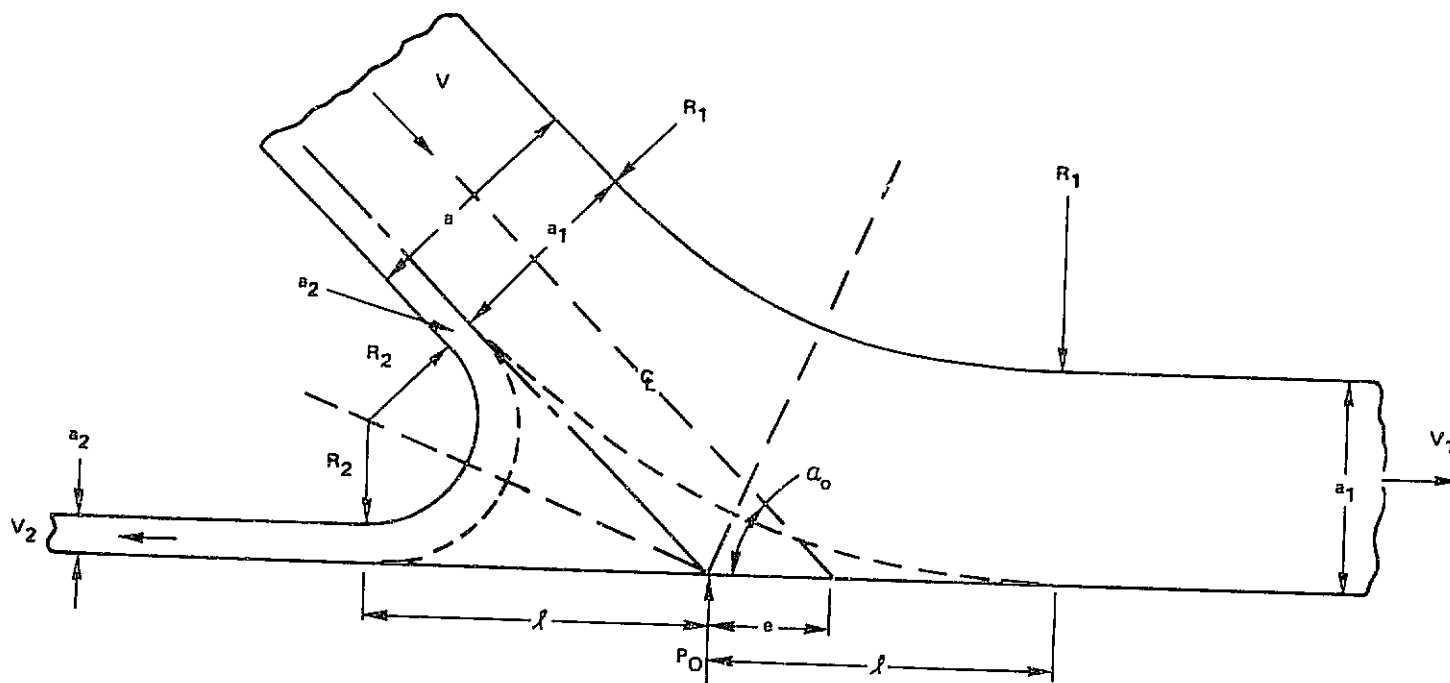
Reference 4 presents test results which show that birds behave as a fluid during impact at high speeds and that the maximum steady impact pressure for low impact angles is proportional to $p_0(\sin \alpha)^2$, where p_0 is the stagnation pressure and α the impact angle. The test results also show that there is a critical impingement angle between 25° and 45° below which a relatively uniform impact pressure of this magnitude occurs over the impacted area. The approximate analyses developed below were based on this test information. More recently it was learned by Reference 19 that the test results were not fully evaluated and, therefore, in error. Because of this and the acquisition of References 5 and 7, which permitted the development of a better missile model, the simplistic, uniform pressure missile developed herein was abandoned in favor of the missiles developed in Appendices C, D, and E.

2D Oblique Impacting Jet Missile

Numerous texts and articles give the solution for the splitting of the 2D jet and the magnitude and position of the impulse load on the plate; see for example Reference 18. These quantities plus the fact that the magnitude of the fluid velocity is maintained can be derived using the theories of continuity, momentum, and energy; see Figure 1B. However, there is no simple way of arriving at the pressure loading distribution on the plate. Because originally no known solution was found in the literature (later Reference 5 was found), an approximate analysis was developed based on the uniform pressure test finding reported in Reference 4. In this analysis the deflected streamform is assumed to be given by circular arcs which result in a core of uniform pressure over a length, l , either side of the impulse load point; see Figure 1B.

3D Oblique Impacting Jet Missile

The same uniform pressure and constant radius streamform assumptions were used for the approximate 3D analysis as for the above 2D analysis. However, in this case the jet is split into radial sectors in which the fluid is assumed to flow. Thus, the radius of the streamform is a continuous function of the azimuthal angle and is symmetrical about the line of impingement of the jet. The derivation of the approximate 3D jet analysis assuming a uniform pressure is given in Figure 2B. Note that centerline of the split is the same as that for the two dimensional jet - i.e., $b = r \cos \alpha$ and $\Delta = r \cot \alpha$. For this analysis the resultant impulse force is located a distance $e/r \approx (.265 - .022 \cos \alpha) \cot \alpha$ aft of the impingement center of the jet, and the uniform pressure area is centered about this location. The separation line for forward and rearward flow is a distance $f/r = \sqrt{2} \cot \alpha$ aft of the load center e/r . Figure 3B presents the variation of the envelope dimensions of the uniform elliptic pressure distribution with impingement angle, and the location of the resultant impact force from the jet centerline.



CONTINUITY: $V_1 a_1 + V_2 a_2 = V_a$

MOMENTUM: $V_a \cos \alpha_o = V_1 a_1 - V_2 a_2$

$$P_o = \rho_a v^2 \sin \alpha_o$$

ENERGY: $V_1^2 a_1 + V_2^2 a_2 = V^2 a$

PRESSURE:
(UNIFORM)

$$P = \frac{a_2 V_2}{R_2 + a_2} = \frac{a_1 V_1}{R_1 + a_1}$$

$$= 1/2 \rho v^2 \sin^2 \alpha_o$$

RESULTS: $V_1 = V_2 = V$

$$a_1/a = \cos^2 \frac{\alpha_0}{2}$$

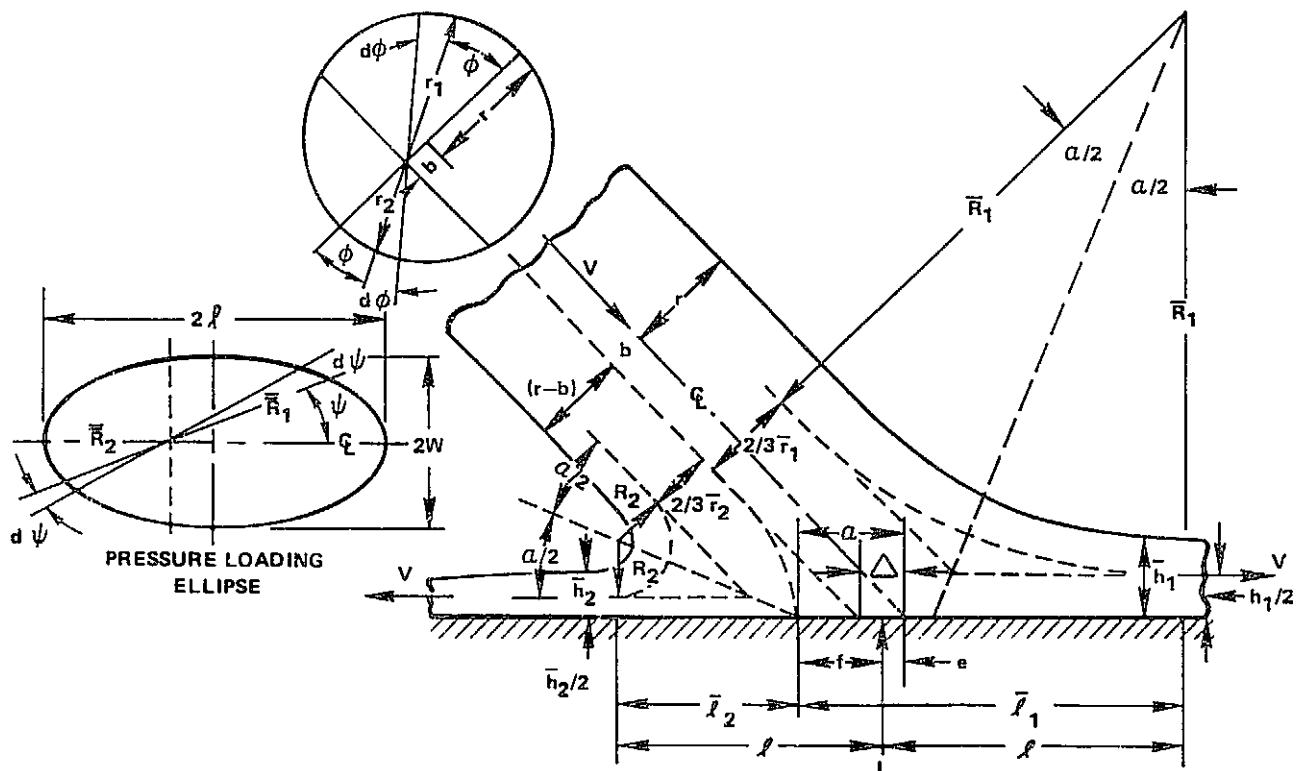
$$a_2/a = \sin^2 \frac{a_0}{2}$$

$$(a_1 + R_1)/a = 1/2 \sin^2 \alpha_0/2$$

$$(a_2 + R_2)/a = 1/2 \cos^2 \alpha_0/2$$

$$\lambda/a = 1/\sin \alpha_0$$

FIGURE 1B. APPROXIMATE 2D JET MISSILE



CONTINUITY:

$$\frac{1}{2} r_1^2 d\phi = l_1 h_1 d\psi \text{ \& \; } \frac{1}{2} r_2^2 d\phi = l_2 h_2 d\psi$$

$$\tan \psi = \tan \phi \sin \alpha$$

$$d\psi / \cos^2 \psi = d\phi \sin \alpha / \cos^2 \phi$$

MOMENTUM:

$$\begin{aligned} \text{(HORIZ)} \quad \pi r^2 \rho v^2 \cos \alpha &= 2 \rho v^2 \left[\int_0^{\pi/2} \frac{1}{2} r_1^2 \cos \psi d\phi - \int_0^{\pi/2} \frac{1}{2} r_2^2 \cos \psi d\phi \right] \\ &= \rho v^2 \int_0^{\pi/2} (r_1^2 - r_2^2) \cos \psi d\phi \end{aligned}$$

AND

$$(r_1^2 - r_2^2) = 4br \cos \phi \sqrt{1 - \frac{b^2 \sin^2 \phi}{r^2}}$$

$$\tan \psi = \tan \phi \sin \alpha \quad \text{OR} \quad \cos \psi = 1 / \sqrt{1 + \tan^2 \phi \sin^2 \alpha}$$

FIGURE 2B. APPROXIMATE 3D JET MISSILE

MOMENTUM:

$$\pi \cos \alpha = 4 \frac{b}{r} \int_0^{\pi/2} \frac{\cos \phi \sqrt{1 - b^2 \sin^2 \phi / r^2}}{\sqrt{1 + \tan^2 \phi \sin^2 \alpha}} d\phi$$

→ IF $b/r = \cos \alpha$, THIS EQUALITY EQUATION IS MET.

THUS, $\Delta/r = \cot \alpha$ AND

$$\rightarrow \bar{r}_1/r = (1 + \cos \alpha) \text{ \& } \bar{r}_2/r = (1 - \cos \alpha)$$

(VERT.) ASSUME $p = \frac{1}{2} \rho V^2 \sin^2 \alpha = \bar{p}_1 = \bar{p}_2$

$$\bar{p}_1 = \frac{1/2 \bar{r}_1^2 \rho V^2 \sin \alpha d\phi}{1/2 \bar{\ell}_1^2 d\psi} \text{ \& } \bar{p}_2 = \frac{1/2 \bar{r}_2^2 \rho V^2 \sin \alpha d\phi}{1/2 \bar{\ell}_2^2 d\psi}$$

THUS,

$$\rightarrow \bar{\ell}_1/r = \sqrt{2} / \tan \alpha/2 \text{ \& } \bar{\ell}_2/r = \sqrt{2} \tan \alpha/2$$

AND

$$\rightarrow \bar{h}_1/r = (1 + \cos \alpha) / 2\sqrt{2} \text{ \& } \bar{h}_2/r = (1 - \cos \alpha) / 2\sqrt{2}$$

$$\rightarrow \ell/r = 1/2 \left(\frac{\bar{\ell}_1 + \bar{\ell}_2}{r} \right) = \sqrt{2} / \sin \alpha$$

$$\rightarrow f/r = \left(\frac{\bar{\ell}_1 - \bar{\ell}_2}{r} \right) = \sqrt{2} \cot \alpha \text{ (FLOW DIVISION LINE)}$$

EQUILIBRIUM:

$$L = \rho \pi r^2 V^2 \sin \alpha = \pi r^2 \left(\frac{\ell}{r} \right) \left(\frac{w}{r} \right) p$$

$$\rightarrow w/r = 2/(\ell/r) \sin \alpha = \sqrt{2}$$

$$\begin{aligned} \rightarrow e/r &= \frac{\sqrt{2} \cot \alpha}{4\pi} \int_0^{\pi/2} [3 + \cos^2 \alpha - 4 \sin^2 \phi \cos^2 \alpha] [1 - \sin^2 \phi \cos^2 \alpha]^{1/4} \cos^2 \phi d\phi \\ &\approx (0.265 - 0.022 \cos \alpha) \cot \alpha \end{aligned}$$

FIGURE 2B. APPROXIMATE 3D JET MISSILE (CONTINUED)

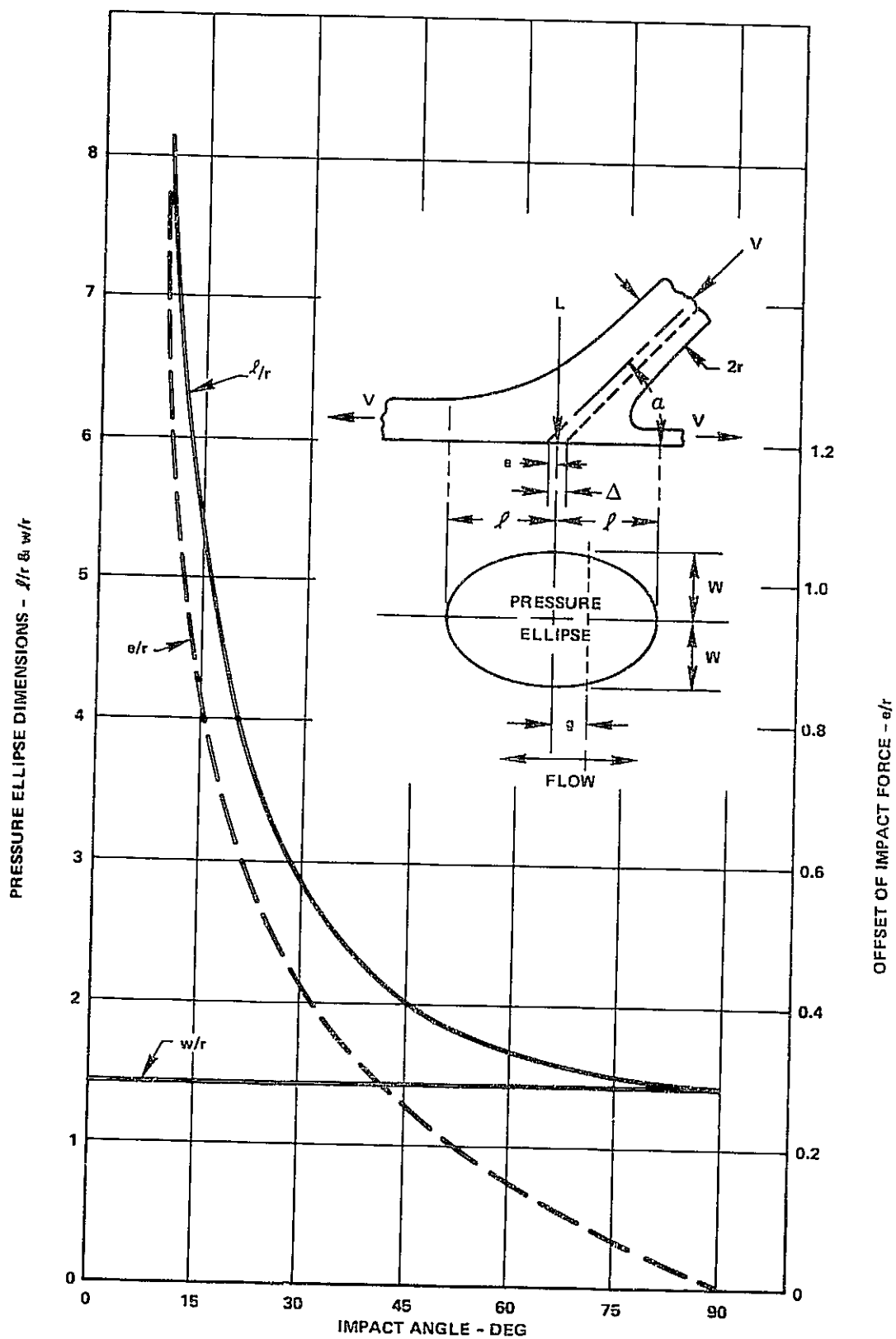


FIGURE 3B. PRESSURE ELLIPSE DIMENSIONS AND OFFSET OF IMPACT FORCE FOR APPROXIMATE 3D JET IMPACT $\Delta/r = \cot \alpha$

APPENDIX C

APPROXIMATION FOR 2D OBLIQUE IMPACTING JET MISSILE

The conformal transformation solution for the steady state, oblique, impingement of a 2D jet on a flat plate given in Reference 5 and recent test results given in Reference 19 show that the pressure distribution on the plate is not uniform for low impingement angles as originally reported in Reference 4 and assumed in Appendix B. Therefore, a new representation of a 2D jet missile was developed. To facilitate computations and to alleviate some anomalies in the solution given in Reference 5 for low impingement angles, an approximate analysis was developed based on the analysis and test results given by Schach in Reference 5. The approximate analysis is based on the assumption that the velocity distribution along the plate can be represented by the expression $V/V_0 = (1 - e^{-x/\lambda})$. Because the pressure on the plate surface is equal to $P_0 = 1 - (V/V_0)^2$, the resulting pressure distribution will have the form $P/P_0 = e^{-x/\lambda} (2 - e^{-x/\lambda})$. Figure 4 shows that such expressions for V/V_0 and P/P_0 fit the experimental and Schach's results very well. Thus, the only requirement is to determine the decay parameters λ_1 and λ_2 for each side.

The results given in Figure 1B for the splitting of the jet is still valid, being based on momentum, energy, and continuity, i.e.,

$$\begin{aligned} V_1 &= V_2 = V_0 \\ a_1/a &= \cos^2 \alpha/2 \\ a_2/a &= \sin^2 \alpha/2 \end{aligned}$$

and $e/a = 1/2 \cot \alpha$. The decay parameters must be such as to satisfy the force and its position on the plate recognizing the pressure distributions are based on the stagnation point. Thus

$$\text{Force} \quad \int_0^{\infty} P_1/P_0 \, dx_1 + \int_0^{\infty} P_2/P_0 \, dx_2 = 2a \sin \alpha$$

$$\text{or} \quad \lambda_1 + \lambda_2 = \frac{4}{3} a \sin \alpha$$

(1C)

and

$$\text{Position} \quad \int_0^{\infty} P_1/P_0 \, x_1 \, dx_1 - \int_0^{\infty} P_2/P_0 \, x_2 \, dx_2 = 2 f a \sin \alpha$$

$$\text{or} \quad \lambda_1^2 - \lambda_2^2 = \frac{8}{7} f a \sin \alpha$$

(2C)

Solving Equations (1C) and (2C) we find that

$$\begin{aligned}\lambda_1 &= \frac{2}{3} a \sin \alpha + \frac{3}{7} f \\ \lambda_2 &= \frac{2}{3} a \sin \alpha - \frac{3}{7} f\end{aligned}\tag{3C}$$

Now evaluation of test and analysis results, see Reference 5, show that f can be approximated to varying degrees of accuracy by the following expressions:

$$f_1/a = \frac{14}{9} \left(1 - \frac{2\alpha}{\pi}\right) \sin \alpha\tag{4C}$$

$$f_2/a = \left[\frac{14}{9} \left(1 - \frac{2\alpha}{\pi}\right) + \frac{1}{3} \cos^2 \alpha \cos 2\alpha \right] \sin \alpha\tag{5C}$$

$$f_4/a = 1.25 \left(1 - \frac{2\alpha}{\pi}\right)^3\tag{6C}$$

$$f_3/a = \frac{\ln 4}{\pi} \cos \alpha (1 + \sin \alpha)\tag{7C}$$

Although Equation (7C) matches the load position given by Schach's solution, the rearward decay constant, λ_2 , becomes negative for impingement angles less than 22° , which is impossible. This is the result of the anomaly in Schach's solution which has the stagnation center outside of the jet for small impingement angles. Although Equation (5C) and (6C) fit the test and analysis results slightly better than Equation (4C), the extra complication did not seem warranted; see Figure 6. Thus, substituting Equation (4C) into (3C) we find

$$\begin{aligned}\lambda_1 &= \frac{4}{3} \left(1 - \frac{\alpha}{\pi}\right) \sin \alpha \\ \lambda_2 &= \frac{4}{3} \left(\frac{\alpha}{\pi}\right) \sin \alpha\end{aligned}\tag{7C}$$

APPENDIX D

APPROXIMATE 3D OBLIQUE IMPACTING JET MISSILE

The assumption of a constant pressure distribution over the impingement area used in the development of the 3D missile model in Appendix B was found to be unrealistic, even for shallow angles; see References 5 and 19. Therefore a new representation of a 3D jet missile was developed based on the concepts and test information given in Reference 5. This new, approximate analysis assumes the fluid in the impacting jet is split into and remains in radial sectors after being deflected by the plate. This assumption is the same as used in Appendix B. Thus, the derivation of the splitting of the jet presented in Figure 2B applies to this analysis, i.e. $b/r = \cos \alpha$; see Figure 15. This split of the jet was found to correlate very well with test results; see Reference 5.

The approximate 3D Jet Missile analysis is based on the assumption that the velocity distribution along the plate can be represented by the expression $V/V_0 = (1 - e^{-(x/\lambda)^2})$, where x is the radial distance from the stagnation point and λ is a decay parameter that is a function of $\cos \psi$; see Figure 15. The resulting pressure distribution is given by the expression

$$P/P_0 = 1 - (V/V_0)^2 = e^{-(x/\lambda)^2} [2 - e^{-(x/\lambda)^2}] \quad (1D)$$

It was found that these expressions for V/V_0 and P/P_0 fitted the experimental data quite well; see Figures 16 and 17.

The expression for the decay parameter, λ , is derived so that the pressure distribution gives the proper normal impulse force and its location. The development of the differential loading for each sector requires considerable trigonometric manipulations as given below:

$$dL/P_0 = \frac{1}{2} \cdot 2 \bar{r}^2 \sin \bar{\alpha} d\theta = 2 \delta x \sin \bar{\alpha} d\psi \quad (2D)$$

Now

$$\begin{aligned} \bar{r}/r &= \cos \phi \cos \alpha + \sqrt{1 - \sin^2 \phi \cos^2 \alpha} \\ \tan \psi &= \tan \phi \sin \alpha \\ \sin \phi &= \sin \psi / \sqrt{1 - \cos^2 \psi \cos^2 \alpha} \\ \cos \phi &= \sin \alpha \cos \psi / \sqrt{1 - \cos^2 \psi \cos^2 \alpha} \\ d\phi/d\psi &= \sin \alpha / (1 - \cos^2 \psi \cos^2 \alpha) \\ \cos \bar{\alpha} &= \cos \phi \cos \alpha \\ \sin \bar{\alpha} &= \sin \alpha / \sqrt{1 - \sin^2 \phi \cos^2 \alpha} = \sqrt{1 - \cos^2 \psi \cos^2 \alpha} \end{aligned}$$

so that

$$(\bar{r}/r)^2 = \sin^2 \alpha \left(\frac{1 + \cos \alpha \cos \psi}{1 - \cos \alpha \cos \psi} \right) \quad (3D)$$

Thus,

$$\begin{aligned} dL/P_0 &= r^2 \sin^3 \alpha \left(\frac{1 + \cos \alpha \cos \psi}{1 - \cos \alpha \cos \psi} \right) \frac{d\psi}{\sqrt{1 - \cos^2 \psi \cos^2 \alpha}} \\ \text{or} \quad dL/P_0 &= r^2 \sin^3 \alpha \left(\frac{1 + \cos \alpha \cos \psi}{(1 - \cos \alpha \cos \psi)^3} \right) d\psi \end{aligned} \quad (4D)$$

Assuming $P/P_0 = 2e^{-\left(\frac{x}{\lambda}\right)^2} - e^{-2\left(\frac{x}{\lambda}\right)^2}$, we find that

$$dL/P_0 = \int_0^{\infty} P/P_0 x dx d\psi = \frac{3}{4} \lambda^2 d\psi \quad (5D)$$

The decay parameter is obtained by equating Equations (4D) and (5D) giving

$$\lambda^2 = \frac{4}{3} r^2 \sin^3 \alpha \sqrt{\frac{(1 + \cos \psi \cos \alpha)}{(1 - \cos \psi \cos \alpha)}} \quad (6D)$$

The location of the resultant load from the stagnation point, f , can be obtained by including the moment arm when integrating over the pressure area, i.e.

$$\begin{aligned} fL/P_0 &= 2 \int_0^{\pi} \int_0^{\infty} \left(2x^2 \cos \psi e^{-\left(\frac{x}{\lambda}\right)^2} - x^2 \cos \psi e^{-2\left(\frac{x}{\lambda}\right)^2} \right) dx d\psi \\ &= \pi \left(1 - \frac{1}{4\sqrt{2}} \right) \int_0^{\pi} \lambda^3 \cos \psi d\psi \end{aligned} \quad (7D)$$

Now, $L/P_0 = 2\pi r^2 \sin^3 \alpha$, and λ is given by Equation 6D, so that

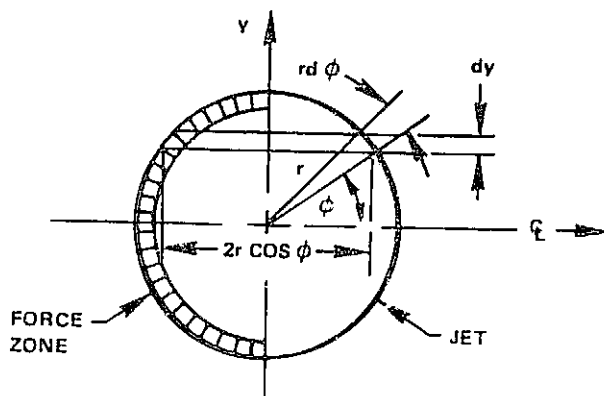
$$\begin{aligned} f/r &= \frac{4}{3} \sqrt{\frac{1}{6\pi}} \left(\sqrt{2} - \frac{1}{4} \right) \sin^{\frac{7}{2}} \alpha \int_0^{\pi} \left[\frac{1 + \cos \psi \cos \alpha}{(1 - \cos \psi \cos \alpha)} \right]^{3/4} \cos \psi d\psi \\ &= .35754 \sin^{\frac{7}{2}} \alpha \int_0^{\pi} \frac{(1 - \cos^2 \psi \cos^2 \alpha)^{3/4}}{(1 - \cos \psi \cos \alpha)^3} \cos \psi d\psi \end{aligned} \quad (8D)$$

There appears to be no closed form solution of the integral in Equation (8D). However, integrating it graphically results in the following values of f/r (See Figure 1D):

α	0	7.5°	15°	30°	45°	60°	75°	90°
f/r	0	1.94	1.98	1.62	1.23	.87	.44	0
e/r	α	4.71	2.09	.80	.44	.25	.11	0
g/r	∞	6.65	4.07	2.42	1.67	1.12	.55	0

Reference 5 points out that there is no corresponding simple way to determine the location of the resulting load from the center of the 3D jet as there was for a 2D jet. Thus, one must resort to using the test results given in Reference 5. These results are plotted in Figure 18 and show that for high impingement angles the load position from the jet centerline is about .43 of that found for the 2D jet. Although the test results indicate this value increases as the impingement angle decreases, the question arises as to what value it goes to as $\alpha \rightarrow 0$.

The limiting value of the coefficient was obtained by assuming that as $\alpha \rightarrow 0$, the 3D jet acts like a series of parallel, 2D jets as depicted below. The analysis in Appendix C for the 2D jet shows that the resultant load ends at



$$dL = 2r \cos \phi dy \rho V^2 \sin \alpha$$

$$dM = r \cos \phi \cot \alpha d\psi \rho V^2 \quad (9D)$$

$$dM/P_0 = 4r^3 \cos^3 \phi \cot \alpha \sin \alpha d\phi \quad (\text{SMALL } \alpha)$$

the edge of the jet as the impingement angle approaches zero. The magnitude of the resultant load is proportional to its deflected area. Based on the above relationships, Equations (9D), we find for small impingement angles, i.e. $\alpha \rightarrow 0$,

$$M/P_0 = 8r^3 \cot \alpha \sin \alpha \int_0^{\pi/2} \cos^3 \phi d\phi = \frac{16}{3} r^3 \sin \alpha \cot \alpha \quad (10D)$$

Dividing Equation (10D) by $L/P_0 = 2\pi r^2 \sin \alpha$ we find

$$g/r = \frac{M}{Lr} = \frac{8}{3\pi} \cot \alpha \quad (11D)$$

Using this value for $\alpha \rightarrow 0$ and the test value of about $4/3\pi$ for the large impingement angles, we find that the following expression for the normal load position from the jet centerline e/r fits the test data very well; see Figure 18:

$$e/r = \frac{8 \cot \alpha / 3\pi}{1 + \sqrt{\sin \alpha}} \quad (12D)$$

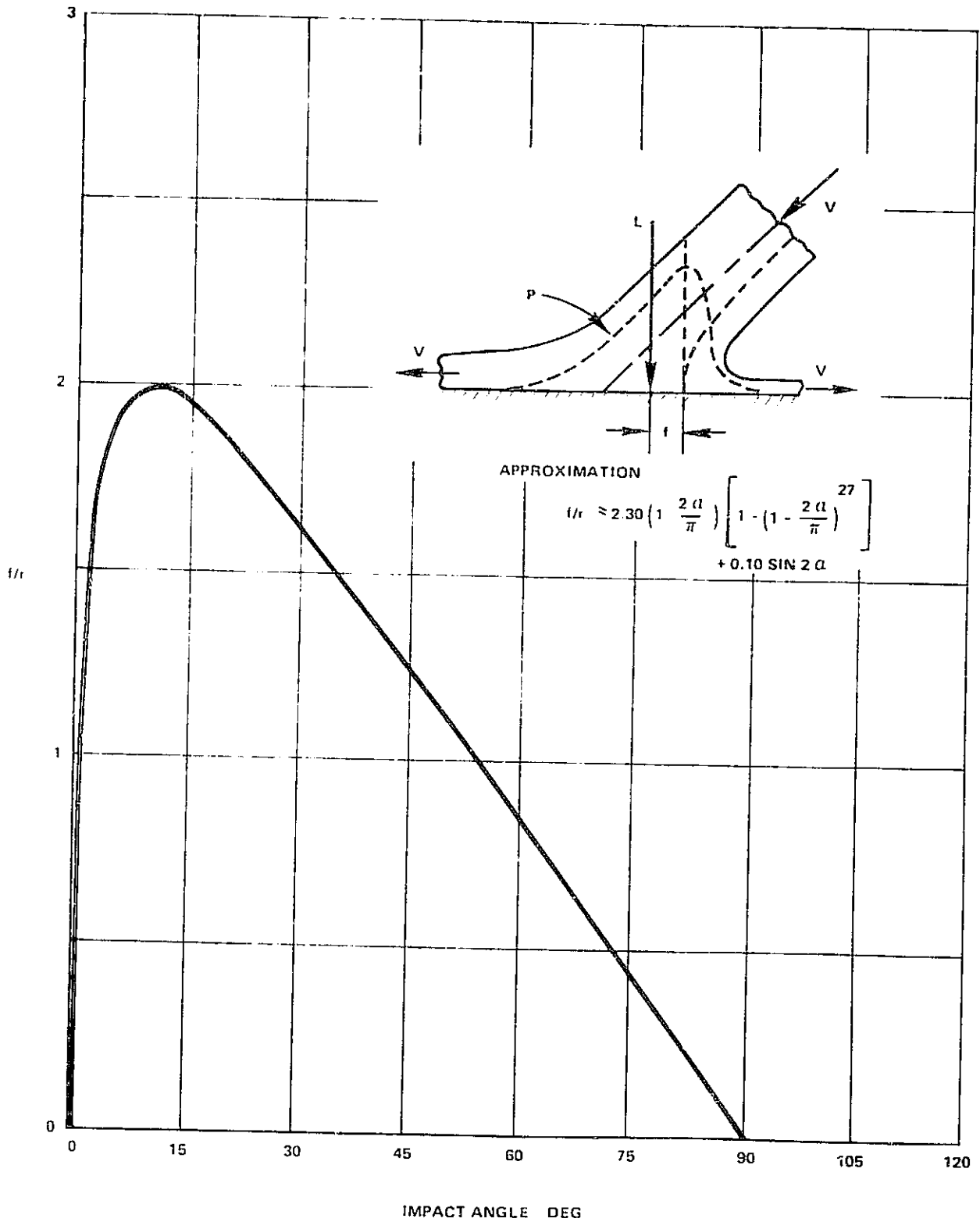


FIGURE 1D. DISTANCE OF RESULTANT LOAD FROM STAGNATION POINT
FOR 3D OBLIQUE IMPACTING JET MISSILE

APPENDIX E

GENERAL, SYMMETRICAL 3D, OBLIQUE IMPINGING JET MISSILE

To model a general, symmetrical shaped missile using oblique impinging jet theory, the 2D and 3D jet models, developed in Appendices C and D, are combined as shown in Figure 20. The resulting model has the center section depicted by the 2D jet and the two sides are depicted by halves of a 3D jet. As such an oblong jet becomes a square or round jet, the equivalent model degenerates into an equivalent pure, round jet. Such a model composed of 2D and 3D jets appears appropriate because the dividing lines for forward and rearward flow for oblique impinging 2D and 3D jets are the same, i.e. $\Delta/r = \cot \alpha$. The assumptions and relationships needed for simulating a general, symmetrical 3D jet missile by a combination of 2D and 3D jets are given below.

The impacting missile is assumed to be symmetrical about the blade chord-wise impact centerline; see Figure 20. It is also assumed that the missile impacting cross-section is depicted by a number of rectangular sections parallel to the velocity axis of the missile. First, the n rectangular impinging layers h thick are approximated by a combination of 2D and 3D jets as shown in Figure 20. Naturally the total cross-sectioned areas must be the same. For simplicity the width, W , of the approximate model is made the same as the original, rectangular layered missile, i.e. $W = nh$. Although this assumption for W introduces a slight error in approximating the layered missile, an evaluation of the error for typical missiles showed it to be small.

The centerline position of the approximate missile is such that its center of gravity is consistent with the original, layered missile. The position of the centerline of the approximate missile relative to the centerline of the first rectangular layer of the original missile is given by the expression

$$\Delta_{1-AM} = \sum_{j=2}^n A_j (n-1)h / \sum_{j=1}^n A_j \quad (1E)$$

where

$$A_{AM} = A_2 + A_3 = (1 + \frac{\pi}{4} W)W = \sum_{j=1}^n A_j \quad (2E)$$

Although the dividing lines for forward and rearward flow for the 2D and 3D jets are the same, the positions of their resultant forces are not. Because of the sideward spreading action of the 3D jet its resultant force is not displaced as far aft of the jet centerline as that for the 2D jet; see Figures 14 & 18. Since their impingement forces are proportional to their respective areas, A_3 and A_2 , the effective resultant position is represented by the weighted average based on area, i.e. -

$$\bar{e}/r = \frac{A_2(e/r)_2 + A_3(e/r)_3}{A_2 + A_3} \quad (3E)$$

where $r = W/2$.

The resulting pressure distribution decay and spreading action of the 2D and 3D jets are different, which result in discontinuities at their common boundaries. To prevent these discontinuities from occurring, correction factors are applied to the 2D and 3D results such that the total incremental load and flow area at a given radius from the pressure stagnation point and flow dividing line, respectively, are maintained. For the flow area this poses no problem because the flow dividing lines for the 2D and 3D jets are the same; see Figure 1E. In general, for shallow impingement angles, α , almost all of the fluid is deflected forward, for

$$\begin{aligned} A_3^{\text{Fwd}} &= \pi r^2 \left(1 - \frac{\alpha}{\pi} + \frac{\sin 2\alpha}{2\pi} \right) \approx \pi r^2, \text{ if } \alpha < 45^\circ \text{ (<9\% error)} \\ A_2^{\text{Fwd}} &= 2r (1 + \cos \alpha) \approx 2r, \text{ if } \alpha < 45^\circ \text{ (<15\% error)} \end{aligned} \quad (4E)$$

Thus, for simplicity the rearward flow can be neglected and the correction factors μ_3 and μ_2 for the 3D and 2D spreading thicknesses are approximated as follows:

$$(\delta/r)_3^c = \mu_3 (\delta/r)_3 \text{ \& } (\delta/r)_2^c = \mu_2 (\delta/r)_2 \text{ (c = corrected)} \quad (5E)$$

$$\mu_3 A_3^{\text{Fwd}} + \mu_2 A_2^{\text{Fwd}} = A_3^{\text{Fwd}} + A_2^{\text{Fwd}}$$

or
approx. $\mu_3 A_3 + \mu_2 A_2 = A_3 + A_2 \quad (6E)$

$$(\bar{\delta}/r)_3 \mu_3 = (\delta/r)_2 \mu_2 \text{ (Junction)} \left[\bar{\delta}_3 = \delta_2 (\sim \text{Junction}) \right] \quad (7E)$$

Thus,

$$\mu_3 = \left[\frac{1 + A_3/A_2}{(\bar{\delta}/r)_3 + \frac{A_3}{A_2}} \right] \text{ \& } \mu_2 = \left[\frac{1 + A_2/A_3}{(\bar{\delta}/r)_2 + \frac{A_2}{A_3}} \right] \quad (8E)$$

For the uniform thickness region the spreading thickness is given by combining Equations (5E) and (8E) or

$$(\delta/r)_2^c = (\bar{\delta}/r)_3^c = \left[\frac{A_2 + A_3}{\frac{A_3}{(\delta/r)_3} + \frac{A_2}{(\delta/r)_2}} \right] \quad (9E)$$

A more sophisticated approximation can be made if both the forward and rearward discontinuities are to be prevented. This can be done by using a linearly changing correction factor for the 3D side jet results and front and rear correction factors for the 2D center jet. Considering the other approximations in the analysis, such additional complexity did not appear justified initially.

The location of the stagnation pressure points for the 2D and 3D jets from the missile centerline differ slightly. Also, their respective decay rates differ. The simplest way to tie the two pressure distributions together without any discontinuities is to assume they both have a common pressure stagnation point relative to the missile centerline. Because the pressure loadings of the 2D and 3D jets are proportional to their respective areas, the weighted average position of the stagnation point from the missile centerline can be expressed as follows:

$$\bar{g}/r = \frac{(g/r)_3 A_3 + (g/r)_2 A_2}{A_3 + A_2} \quad (10E)$$

Even though the pressure distributions for the 2D and 3D jets are made to start at a common stagnation point given by Equation (10E), pressure discontinuities will occur at their junctions because of their different pressure decay expressions. To rectify this situation the magnitudes of the pressures can be modified by factors γ_3 and γ_2 so as to satisfy equilibrium and alleviate the pressure discontinuity at the junctions. These pressure correction factors are obtained in a manner similar to that done for the flow spreading correction factors. As for the flow case, the pressure load due to the rearward flow is assumed small and neglected for simplicity. Then, referring to Figure 1E, vertical equilibrium incremental loading gives

$$\left. \begin{aligned} (dL/dx)_3 &\approx 2 \int_0^{\pi/2} \times P_3 d\psi \quad \text{where } P_3 = f(\psi) \\ (dL/dx)_2 &\approx \mathbb{P}_2 \end{aligned} \right\} \quad (11E)$$

so that

$$\gamma_3 (dL/dx)_3 + \gamma_2 (dL/dx)_2 = (dL/dx)_3 + (dL/dx)_2 \quad (12E)$$

and

$$\gamma_3 \bar{P}_3 = \gamma_2 P_2 \quad (\text{Junction}) \quad \left[\bar{P}_3 - P_3 \text{ @ Junction} \right] \quad (13E)$$

Thus,

$$\gamma_3 = \left[\frac{1 + (dL/dx)_3 / \mathbb{P}_2}{\bar{P}_3 / P_2 + (dL/dx)_3 / \mathbb{P}_2} \right]$$

and

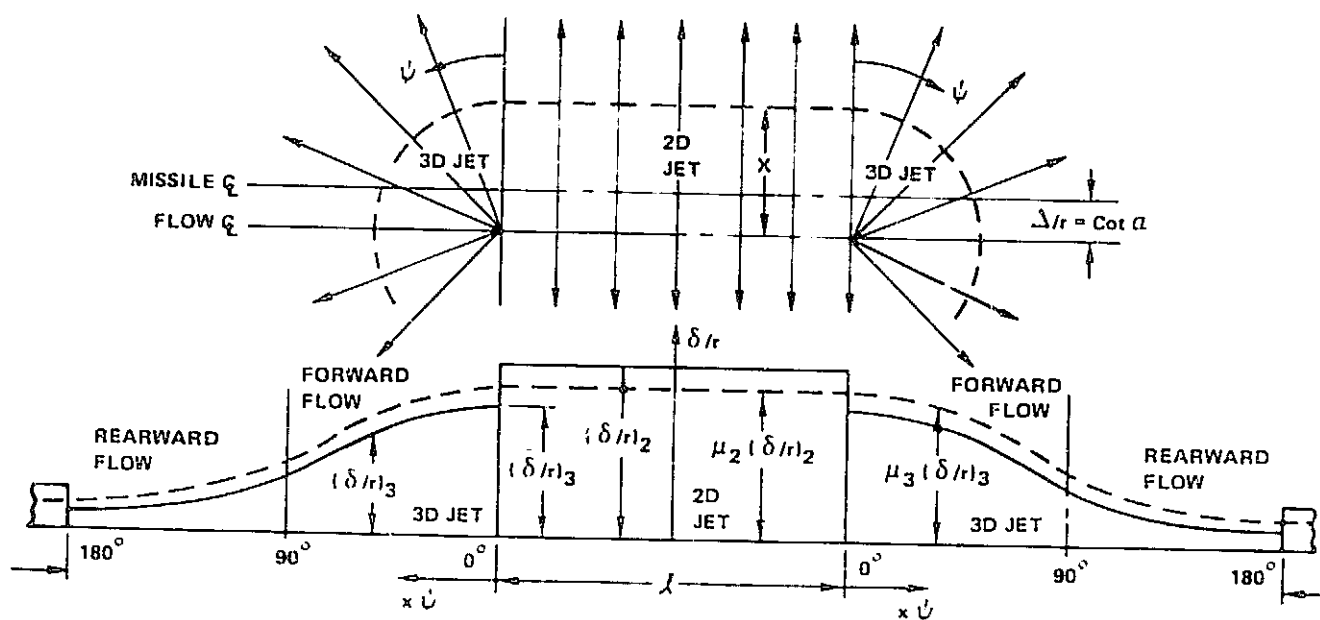
$$\gamma_2 = \left[\frac{1 + \mathbb{P}_2 / (dL/dx)_3}{P_2 / \bar{P}_3 + \mathbb{P}_2 / (dL/dx)_3} \right] \quad (14E)$$

where P_3/P_0 is given by Equations (1D) and (6D). For the uniform pressure region the pressure is given by combining Equations (13E) and (14E) or

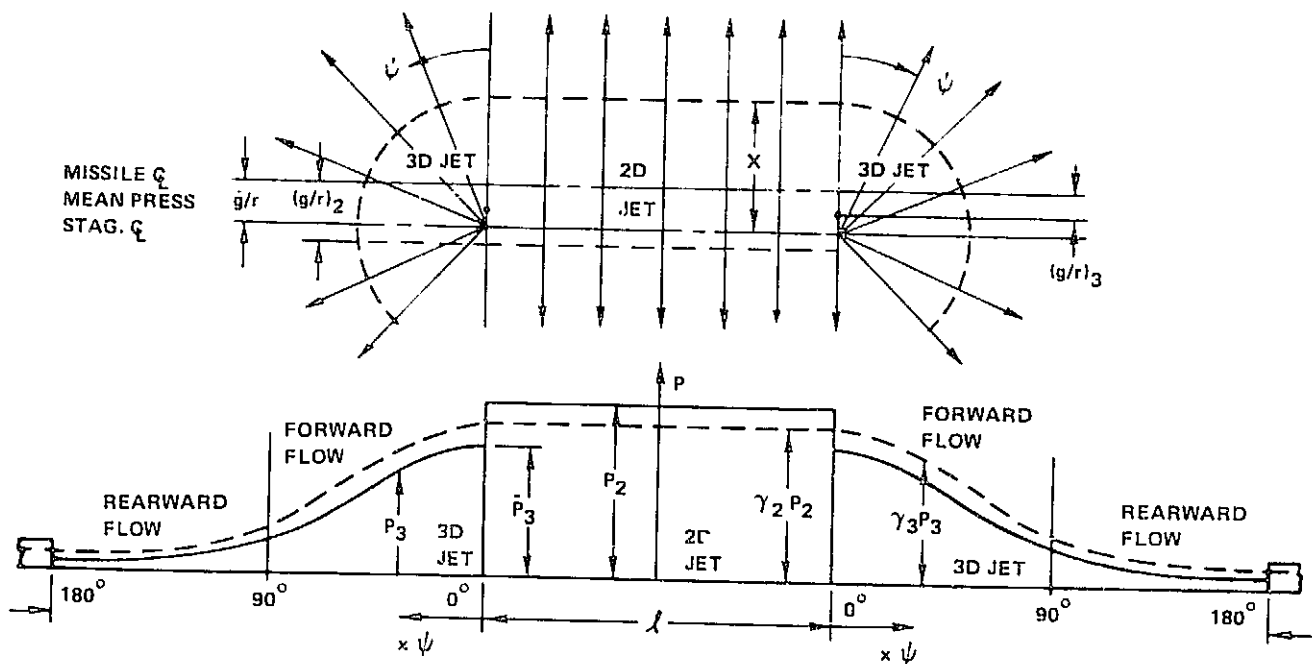
$$P_3^c = P_2^c = \left[\frac{P_2 + (dL/dx)_3}{1 + \frac{(dL/dx)_3}{\bar{P}_3}} \right] \quad (15E)$$

Just as for the spreading thickness case, a more exact but more sophisticated approach could be used to smooth out the pressure distribution of the 2D and 3D jets, but it did not appear warranted initially.

Table II summarizes the pertinent equations for modeling and analyzing a general, symmetrical 3D oblique impinging jet missile. Appendix F gives a procedure for modifying the 2D and 3D jet pressure and thickness distribution results for the entire jet, not just for the forward deflected portion. To do this requires three correction factors, rather than two, so that no discontinuity occurs between the junction of the 3D side jet and the 2D rearward jet as well as between the 2D forward jet.



SPREADING CORRECTION FACTORS



PRESSURE LOADING CORRECTION FACTORS

FIGURE 1E. CORRECTION FACTORS FOR SPREADING & PRESSURE LOADING FOR GENERAL, SYMMETRICAL JET MISSILE

APPENDIX F

SUPPLEMENTARY RELATIONSHIPS FOR GENERAL MISSILE MODEL

Appendix E gives relationships for defining the general missile model assuming most of the flow is diverted towards the direction of impact, thus simplifying the corrections necessary to tie together the 2D and 3D jet models that make up the general missile. Because of the desire to have the computer program plot pressure contour lines, a more elaborate correction is necessary to prevent any discontinuities in pressure in the rearward flow. This is also true of the squashing or thickness expressions. This Appendix presents a more exact modifying procedure, so that there will be no discontinuities in the pressure or squashing contour distributions in any direction.

Appendix E suggests that all the pressure discontinuities could be eliminated by using a linearly changing correction factor for the 3D jets; i.e. $\gamma_3 = \bar{\gamma}_3 + \bar{\gamma}_3 \psi / \pi$. However, such a correction function is inconsistent with the 3D pressure distribution, so that, although the junction discontinuities are eliminated, a distorted unrealistic pressure distribution can result between $\psi=0$ and 180° . In order to circumvent this problem and still eliminate the discontinuities between the 2D and 3D jets, it is proposed to perturbate the 3D pressure distribution using the following relationship:

$$\bar{P}_3 = P_3 + \left(\frac{P_3 - P_3^{180}}{P_3^\sigma - P_3^{180}} \right) \gamma_3^1 + \left(\frac{P_3^\sigma - P_3}{P_3^\sigma - P_3^{180}} \right) \gamma_3^2 \quad (1F)$$

A similar perturbation expression can be used for smoothing of the spreading/thickness of the jet; i.e.

$$\bar{\delta}_3 = \delta_3 + \left(\frac{\delta_3 - \delta_3^{180}}{\delta_3^\sigma - \delta_3^{180}} \right) \mu_3^1 + \left(\frac{\delta_3^\sigma - \delta_3}{\delta_3^\sigma - \delta_3^{180}} \right) \mu_3^2 \quad (2F)$$

In order to satisfy the force equilibrium or continuity, moment equilibrium or flow split, and avoid discontinuities in the pressure or thickness for both rearward and forward flows of the 2D jet and 3D jet, four correction factors are needed. Two of these correction factors are in the perturbation of the pressure or thickness for the side 3D jets, whereas the other two correction factors apply to the front and rear 2D jets. The expressions for the necessary four correction factors for both the pressure and thickness distributions are derived below:

Pressure Distribution: Expressions for P_2 and P_3 are given in Table II. The location of the pressures is based on the stagnation point defined by g ; see Table II.

Load Equilibrium: (Correction Factors $\gamma_2^1, \gamma_2^2, \gamma_3^1, \text{ \& } \gamma_3^2$)

$$(P_2^1 + P_2^2) \ell + 2X \int_0^\pi P_3 d\psi = (\gamma_2^1 P_2^1 + \gamma_2^2 P_2^2) \ell + 2X \int_0^\pi \bar{P}_3 d\psi \quad (3F)$$

Moment Equilibrium:

$$(P_2^1 + P_2^2) \ell X + 2X^2 \int_0^\pi P_3 \cos \psi d\psi = (\gamma_2^1 P_2^1 + \gamma_2^2 P_2^2) \ell X + 2X^2 \int_0^\pi \bar{P}_3 \cos \psi d\psi \quad (4F)$$

Boundary Conditions:

$$\bar{P}_3^{\circ} = \gamma_2^1 P_2^1 \text{ and } \bar{P}_3^{180^\circ} = \gamma_2^2 P_2^2 \quad (5F)$$

Substituting Equations (1F) and (5F) into Equations (3F) and (4F) we find

$$(P_2^1 + P_2^2) \ell = (\bar{P}_3^{\circ} + P_3^{180^\circ}) \ell + 2X \left[\gamma_3^1 \int_0^\pi \left(\frac{P_3 - P_3^{180^\circ}}{P_3^{\circ} - P_3^{180^\circ}} \right) d\psi + \gamma_3^2 \int_0^\pi \left(\frac{P_3^{\circ} - P_3}{P_3^{\circ} - P_3^{180^\circ}} \right) d\psi \right]$$

or

$$\left[P_2^1 + P_2^2 - (\bar{P}_3^{\circ} + P_3^{180^\circ}) \right] \ell = \left[\gamma_3^1 + \gamma_3^2 \right] \ell + 2X \left[\gamma_3^1 \int_0^\pi \left(\frac{P_3 - P_3^{180^\circ}}{P_3^{\circ} - P_3^{180^\circ}} \right) d\psi + \gamma_3^2 \int_0^\pi \left(\frac{P_3^{\circ} - P_3}{P_3^{\circ} - P_3^{180^\circ}} \right) d\psi \right] \quad (6F)$$

and

$$\left[P_2^1 - P_2^2 \right] \ell = (\bar{P}_3^{\circ} - P_3^{180^\circ}) \ell + 2X \int_0^\pi \left[\left(\frac{P_3 - P_3^{180^\circ}}{P_3^{\circ} - P_3^{180^\circ}} \right) \gamma_3^1 + \left(\frac{P_3^{\circ} - P_3}{P_3^{\circ} - P_3^{180^\circ}} \right) \gamma_3^2 \right] \cos \psi d\psi \quad (7F)$$

or

$$\left[(P_2^1 - P_2^2) - (\bar{P}_3^{\circ} - P_3^{180^\circ}) \right] \ell = \left[\gamma_3^1 - \gamma_3^2 \right] \ell + 2X \int_0^\pi \left[\left(\frac{P_3 - P_3^{180^\circ}}{P_3^{\circ} - P_3^{180^\circ}} \right) \gamma_3^1 + \left(\frac{P_3^{\circ} - P_3}{P_3^{\circ} - P_3^{180^\circ}} \right) \gamma_3^2 \right] \cos \psi d\psi$$

After integrating the integral quantities in Equations (6F) and (7F) one obtains two equations in two unknowns, γ_3^1 and γ_3^2 . Once γ_3^1 and γ_3^2 are determined from Equations (6F) and (7F), γ_2^1 and γ_2^2 can be solved for using Equations (5F). Knowing all four correction factors, the pressure distribution is then defined everywhere for that particular value of X.

Thickness Distribution: Expressions for δ_2 and δ_3 are given in Table II. The location of the thicknesses is based on the stagnation point defined by g; see Table II. The thickness distribution is only valid for $X/r \gg 1/\sin \alpha$.

Flow Continuity: (Correction Factors μ_2^1 , μ_2^2 , μ_3^1 , & μ_3^2)

$$\mu_2^1 A_2^1 + \mu_2^2 A_2^2 + 2X \int_0^\pi \bar{\delta}_3 d\psi = A_2^1 + A_2^2 + A_3 = A_T$$

or

(8F)

$$\ell (\mu_2^1 \delta_2^1 + \mu_2^2 \delta_2^2) + 2X \int_0^\pi \bar{\delta}_3 d\psi = (2 \ell r + \pi r^2) = A_T$$

Flow Split:

$$\mu_2^1 A_2^1 + 2X \int_0^{\pi/2} \bar{\delta}_3 d\psi = A_2^1 + 2X \int_0^{\pi/2} \delta_3 d\psi$$

or

(9F)

$$\mu_2^1 \delta_2^1 \ell + 2X \int_0^{\pi/2} \bar{\delta}_3 d\psi = \ell \delta_2^1 + 2X \int_0^{\pi/2} \delta_3 d\psi$$

Boundary Conditions:

$$\mu_2^1 \delta_2^1 = \bar{\delta}_3^0 \text{ and } \mu_2^2 \delta_2^2 = \bar{\delta}_3^{180^\circ}$$

(10F)

Substituting Equations (2F) and (10F) into Equations (8F) and (9F) we find

$$\ell (\bar{\delta}_3^0 + \bar{\delta}_3^{180^\circ}) + 2X \int_0^\pi \bar{\delta}_3 d\psi = (2 \ell r + \pi r^2) = A_T$$

or

$$\ell (\mu_3^1 + \mu_3^2 + \bar{\delta}_3^0 + \bar{\delta}_3^{180^\circ}) + 2X \left[\mu_3^1 \int_0^\pi \left(\frac{\delta_3 - \bar{\delta}_3^{180^\circ}}{\delta_3^0 - \bar{\delta}_3^{180^\circ}} \right) d\psi + \mu_3^2 \int_0^\pi \left(\frac{\delta_3^0 - \delta_3}{\delta_3^0 - \bar{\delta}_3^{180^\circ}} \right) d\psi \right] = 2 \ell r \quad (11F)$$

and

$$\ell (\mu_3^1 + \bar{\delta}_3^0) + 2X \left[\mu_3^1 \int_0^{\pi/2} \left(\frac{\delta_3 - \bar{\delta}_3^{180^\circ}}{\delta_3^0 - \bar{\delta}_3^{180^\circ}} \right) d\psi + \mu_3^2 \int_0^{\pi/2} \left(\frac{\delta_3^0 - \delta_3}{\delta_3^0 - \bar{\delta}_3^{180^\circ}} \right) d\psi \right] = \ell \delta_2^1 \quad (12F)$$

After integrating the integral quantities in Equations (11F) and (12F) one obtains two equations in two unknowns, μ_3^1 and μ_3^2 . Once μ_3^1 and μ_3^2 are determined from Equations (11F) and (12F), μ_2^1 and μ_2^2 can be solved for using Equations (10F). Knowing all four correction factors, the thickness distribution is then defined everywhere for that particular value of X .

Because of the form of the expression for δ_3 , the bracketed quantities under the integral signs in Equations (11F) and (12F) are the same for all values of X/r . Thus, the respective values of the integrals remain the same for all X 's for a given impact configuration. Specifically, the first and second integral take the form, see Table II,

$$\int \left(\frac{\delta_3^{\circ} - \delta_3}{\delta_3^{\circ} - \delta_3^{180^{\circ}}} \right) d\psi = \left[\frac{1}{\left(\frac{1 + \cos \alpha}{1 - \cos \alpha} \right)^2 - 1} \right] \int \left[\left(\frac{1 + \cos \alpha}{1 - \cos \alpha \cos \psi} \right)^2 - 1 \right] d\psi$$

and

$$\int \left(\frac{\delta_3^{\circ} - \delta_3}{\delta_3^{\circ} - \delta_3^{180^{\circ}}} \right) d\psi = \left[\frac{1}{\left(\frac{1 + \cos \alpha}{1 - \cos \alpha} \right)^2 - 1} \right] \int \left[\left(\frac{1 + \cos \alpha}{1 - \cos \alpha} \right)^2 - \left(\frac{1 + \cos \alpha}{1 - \cos \alpha \cos \psi} \right)^2 \right] d\psi$$

Thus, only the integral $\int \left[(1 + \cos \alpha)^2 / (1 - \cos \alpha \cos \psi)^2 \right] d\psi$ needs to be evaluated numerically once for all the thickness distributions for the particular impact configuration.

APPENDIX G

LISTING OF COMPUTER OUTPUT RESULTS FOR DEMONSTRATION PROBLEM 5.2

(PAGES 180-251)

V,RIMP,TSTOP,ALPHA0,XOCL,YOCL,NR,MN,NM,NVA,IPDEL,DEN,ISYM

0.726000E+04,0.300000E+02,0.500000E-01,0.523600E+00,0.454600E+01,0.377050E+01, 8,120, 5, 6, 2,0.988800E-04, 1

RL 1, 2, 3, 4, 5, 6,

0.156250E+01,0.950000E+00,0.325000E+00,-.325000E+00,-.950000E+00,-.156250E+01,

RM 1, 2, 3, 4, 5, 6,

0.625000E+00,0.600000E+00,0.650000E+00,0.650000E+00,0.600000E+00,0.625000E+00,

CL 1, 2, 3, 4, 5, 6,

0.210000E+01,0.326000E+01,0.375000E+01,0.375000E+01,0.326000E+01,0.210000E+01,

DETL 1, 2, 3, 4, 5, 6,

0.825000E+00,0.245000E+00,0.0 ,0.0 ,0.245000E+00,0.825000E+00,

WM 1, 2, 3, 4, 5, 6,

0.210000E+01,0.326000E+01,0.375000E+01,0.375000E+01,0.326000E+01,0.210000E+01,

MAX 1, 2, 3, 4, 5, 6, 7, 8,

15, 15, 15, 15, 15, 15, 15, 15,

NJ3 1, 2, 3, 4, 5, 6, 7, 8,

9, 9, 9, 9, 9, 9, 9, 9,

VMI 1, 2, 3, 4, 5,

0.98558E-02,0.42763E-02,0.98890E-02,0.10223E-01,0.23340E-01,

DR 1, 2, 3, 4, 5,

0.35000E-01,0.35000E-01,0.35000E-01,0.35000E-01,0.35000E-01,

WD 1, 2, 3, 4, 5,

0.43350E+03,0.87339E+03,0.14450E+04,0.15331E+04,0.22620E+04,

PH2(1,1, 1) THRU PH2(1,120, 1)

0.47091E-01,0.60371E-01,0.77146E-01,0.93922E-01,0.11070E+00,0.12747E+00,0.14425E+00,0.16102E+00,0.17780E+00,0.19458E+00,
0.21834E+00,0.24630E+00,0.27426E+00,0.30222E+00,0.32668E+00,0.12272E+00,0.13600E+00,0.15277E+00,0.16955E+00,0.18633E+00,
0.20310E+00,0.21988E+00,0.23665E+00,0.25343E+00,0.27020E+00,0.29397E+00,0.32193E+00,0.34989E+00,0.37784E+00,0.40231E+00,
0.19835E+00,0.21163E+00,0.22640E+00,0.24518E+00,0.26195E+00,0.27873E+00,0.29550E+00,0.31228E+00,0.32905E+00,0.34583E+00,
0.36959E+00,0.39755E+00,0.42551E+00,0.45347E+00,0.47794E+00,0.27397E+00,0.28725E+00,0.30403E+00,0.32081E+00,0.33758E+00,
0.35436E+00,0.37113E+00,0.38791E+00,0.40468E+00,0.42146E+00,0.44522E+00,0.47318E+00,0.50114E+00,0.52910E+00,0.55356E+00,
0.33069E+00,0.34398E+00,0.36075E+00,0.37753E+00,0.39430E+00,0.41106E+00,0.42785E+00,0.44463E+00,0.46140E+00,0.47818E+00,
0.50194E+00,0.52990E+00,0.55786E+00,0.58582E+00,0.61028E+00,0.40632E+00,0.41960E+00,0.43638E+00,0.45315E+00,0.46993E+00,
0.48670E+00,0.50348E+00,0.52026E+00,0.53703E+00,0.55381E+00,0.57757E+00,0.60553E+00,0.63349E+00,0.66145E+00,0.68591E+00,
0.48195E+00,0.49523E+00,0.51200E+00,0.52878E+00,0.54556E+00,0.56233E+00,0.57911E+00,0.59589E+00,0.61266E+00,0.62943E+00,
0.65320E+00,0.68116E+00,0.70912E+00,0.73708E+00,0.76154E+00,0.55758E+00,0.57086E+00,0.58763E+00,0.60441E+00,0.62118E+00,
0.63796E+00,0.65474E+00,0.67151E+00,0.68829E+00,0.70506E+00,0.72883E+00,0.75678E+00,0.78474E+00,0.81270E+00,0.83717E+00,

PH2(2,1, 1) THRU PH2(2,120, 1)

0.52638E-01,0.38395E-01,0.20404E-01,0.24128E-02,-.15579E-01,-.33570E-01,-.51561E-01,-.69552E-01,-.87543E-01,-.10553E+00,
-.13102E+00,-.16101E+00,-.19099E+00,-.22098E+00,-.24721E+00,-.19701E-01,-.32944E-01,-.50935E-01,-.68927E-01,-.86918E-01,
-.10491E+00,-.12290E+00,-.14089E+00,-.15888E+00,-.17687E+00,-.20236E+00,-.23235E+00,-.26233E+00,-.29232E+00,-.31855E+00,
-.90040E-01,-.10428E+00,-.12227E+00,-.14027E+00,-.15826E+00,-.17625E+00,-.19424E+00,-.21223E+00,-.23022E+00,-.24821E+00,
-.27370E+00,-.30369E+00,-.33367E+00,-.36366E+00,-.38989E+00,-.16138E+00,-.17562E+00,-.19361E+00,-.21161E+00,-.22960E+00,
-.24759E+00,-.26558E+00,-.28357E+00,-.30156E+00,-.31955E+00,-.34504E+00,-.37502E+00,-.40501E+00,-.43500E+00,-.46123E+00,
-.21488E+00,-.22913E+00,-.24712E+00,-.26511E+00,-.28310E+00,-.30109E+00,-.31908E+00,-.33707E+00,-.35507E+00,-.37306E+00,

ORIGINAL PAGE IS
OF POOR QUALITY

-.39854E+00,-.42853E+00,-.45851E+00,-.48850E+00,-.51474E+00,-.28622E+00,-.30047E+00,-.31846E+00,-.33645E+00,-.35444E+00,
-.37243E+00,-.39042E+00,-.40841E+00,-.42641E+00,-.44440E+00,-.46988E+00,-.49987E+00,-.52985E+00,-.55984E+00,-.58608E+00,
-.35756E+00,-.37181E+00,-.38980E+00,-.40779E+00,-.42578E+00,-.44377E+00,-.46176E+00,-.47975E+00,-.49774E+00,-.51573E+00,
-.54122E+00,-.57121E+00,-.60119E+00,-.63118E+00,-.65742E+00,-.42890E+00,-.44314E+00,-.46114E+00,-.47913E+00,-.49712E+00,
-.51511E+00,-.53310E+00,-.55109E+00,-.56908E+00,-.58707E+00,-.61256E+00,-.64255E+00,-.67253E+00,-.70252E+00,-.72875E+00,

PH2(1,1, 2) THRU PH2(1,120, 2)

-.21349E+00,-.20845E+00,-.20207E+00,-.19569E+00,-.18932E+00,-.18294E+00,-.17656E+00,-.17019E+00,-.16381E+00,-.15743E+00,
-.14840E+00,-.13777E+00,-.12714E+00,-.11651E+00,-.10721E+00,-.22459E+00,-.21955E+00,-.21317E+00,-.20679E+00,-.20042E+00,
-.19404E+00,-.18766E+00,-.18129E+00,-.17491E+00,-.16853E+00,-.15950E+00,-.14887E+00,-.13824E+00,-.12761E+00,-.11831E+00,
-.23569E+00,-.23065E+00,-.22427E+00,-.21789E+00,-.21152E+00,-.20514E+00,-.19876E+00,-.19238E+00,-.18601E+00,-.17963E+00,
-.17060E+00,-.15997E+00,-.14934E+00,-.13871E+00,-.12941E+00,-.24679E+00,-.24174E+00,-.23537E+00,-.22899E+00,-.22261E+00,
-.21624E+00,-.20986E+00,-.20348E+00,-.19711E+00,-.19073E+00,-.18170E+00,-.17107E+00,-.16044E+00,-.14981E+00,-.14052E+00,
-.25512E+00,-.25007E+00,-.24369E+00,-.23732E+00,-.23094E+00,-.22456E+00,-.21819E+00,-.21181E+00,-.20543E+00,-.19906E+00,
-.19002E+00,-.17939E+00,-.16877E+00,-.15814E+00,-.14884E+00,-.26622E+00,-.26117E+00,-.25479E+00,-.24842E+00,-.24204E+00,
-.23566E+00,-.22929E+00,-.22291E+00,-.21653E+00,-.21016E+00,-.20112E+00,-.19049E+00,-.17987E+00,-.16924E+00,-.15994E+00,
-.27732E+00,-.27227E+00,-.26589E+00,-.25951E+00,-.25314E+00,-.24676E+00,-.24038E+00,-.23401E+00,-.22763E+00,-.22126E+00,
-.21222E+00,-.20159E+00,-.19097E+00,-.18034E+00,-.17104E+00,-.28842E+00,-.28337E+00,-.27699E+00,-.27061E+00,-.26424E+00,
-.25786E+00,-.25148E+00,-.24511E+00,-.23873E+00,-.23235E+00,-.22332E+00,-.21269E+00,-.20207E+00,-.19144E+00,-.18214E+00,

PH2(2,1, 2) THRU PH2(2,120, 2)

0.18763E+00,0.18131E+00,0.17333E+00,0.16535E+00,0.15736E+00,0.14938E+00,0.14140E+00,0.13341E+00,0.12543E+00,0.11745E+00,
0.10614E+00,0.92831E-01,0.79525E-01,0.66220E-01,0.54577E-01,0.43558E+00,0.32926E+00,0.22926E+00,0.13330E+00,0.15531E+00,
0.14733E+00,0.13935E+00,0.13136E+00,0.12338E+00,0.11540E+00,0.10409E+00,0.90781E-01,0.77475E-01,0.64170E-01,0.52527E-01,
0.18353E+00,0.17721E+00,0.16923E+00,0.16125E+00,0.15326E+00,0.14528E+00,0.13730E+00,0.12931E+00,0.12133E+00,0.11335E+00,
0.10204E+00,0.88731E-01,0.75425E-01,0.62120E-01,0.50477E-01,0.18148E+00,0.17516E+00,0.16718E+00,0.15920E+00,0.15121E+00,
0.14323E+00,0.13525E+00,0.12726E+00,0.11928E+00,0.11130E+00,0.10332E+00,0.96399E-01,0.83093E-01,0.69788E-01,0.56482E-01,
0.17994E+00,0.17362E+00,0.16564E+00,0.15766E+00,0.14968E+00,0.14169E+00,0.13371E+00,0.12572E+00,0.11774E+00,0.10976E+00,
0.98449E-01,0.85143E-01,0.71838E-01,0.58532E-01,0.46890E-01,0.17790E+00,0.17158E+00,0.16359E+00,0.15561E+00,0.14763E+00,
0.13964E+00,0.13166E+00,0.12367E+00,0.11569E+00,0.10771E+00,0.96399E-01,0.83093E-01,0.69788E-01,0.56482E-01,0.44840E-01,
0.17585E+00,0.16953E+00,0.16154E+00,0.15356E+00,0.14557E+00,0.13759E+00,0.12961E+00,0.12163E+00,0.11364E+00,0.10566E+00,
0.94349E-01,0.81043E-01,0.67738E-01,0.54432E-01,0.42790E-01,0.17379E+00,0.16747E+00,0.15949E+00,0.15151E+00,0.14353E+00,
0.13554E+00,0.12756E+00,0.11958E+00,0.11159E+00,0.10361E+00,0.92299E-01,0.78993E-01,0.65688E-01,0.52382E-01,0.40740E-01,

PH2(1,1, 3) THRU PH2(1,120, 3)

-.47919E+00,-.47182E+00,-.46250E+00,-.45318E+00,-.44387E+00,-.43455E+00,-.42523E+00,-.41592E+00,-.40660E+00,-.39728E+00,
-.38408E+00,-.36856E+00,-.35303E+00,-.33750E+00,-.32391E+00,-.46469E+00,-.45732E+00,-.44800E+00,-.43868E+00,-.42937E+00,
-.42005E+00,-.41073E+00,-.40142E+00,-.39210E+00,-.38278E+00,-.36958E+00,-.35406E+00,-.33853E+00,-.32300E+00,-.30941E+00,
-.45019E+00,-.44282E+00,-.43350E+00,-.42418E+00,-.41487E+00,-.40555E+00,-.39623E+00,-.38692E+00,-.37760E+00,-.36828E+00,
-.35509E+00,-.33956E+00,-.32403E+00,-.30850E+00,-.29491E+00,-.43569E+00,-.42832E+00,-.41900E+00,-.40969E+00,-.40037E+00,
-.39105E+00,-.38174E+00,-.37242E+00,-.36310E+00,-.35378E+00,-.34059E+00,-.32506E+00,-.30953E+00,-.29400E+00,-.28041E+00,
-.42482E+00,-.41744E+00,-.40813E+00,-.39881E+00,-.38949E+00,-.38018E+00,-.37086E+00,-.36154E+00,-.35223E+00,-.34291E+00,
-.32971E+00,-.31418E+00,-.29865E+00,-.28313E+00,-.26954E+00,-.41032E+00,-.40294E+00,-.39363E+00,-.38431E+00,-.37499E+00,
-.36568E+00,-.35636E+00,-.34704E+00,-.33773E+00,-.32841E+00,-.31521E+00,-.29968E+00,-.28416E+00,-.26863E+00,-.25504E+00,
-.39582E+00,-.38845E+00,-.37913E+00,-.36981E+00,-.36049E+00,-.35118E+00,-.34186E+00,-.33254E+00,-.32323E+00,-.31391E+00,
-.30071E+00,-.28518E+00,-.26966E+00,-.25413E+00,-.24054E+00,-.38132E+00,-.37395E+00,-.36463E+00,-.35531E+00,-.34600E+00,
-.33668E+00,-.32736E+00,-.31805E+00,-.30873E+00,-.29941E+00,-.28621E+00,-.27069E+00,-.25516E+00,-.23963E+00,-.22604E+00,

PH2(2,1, 3) THRU PH2(2,120, 3)

C-3

-.54701E-01,-.61426E-01,-.69922E-01,-.78417E-01,-.86913E-01,-.95408E-01,-.10390E+00,-.11240E+00,-.12090E+00,-.12939E+00,
 -.14143E+00,-.15558E+00,-.16974E+00,-.18390E+00,-.19629E+00,-.18334E+00,-.19007E+00,-.19856E+00,-.20706E+00,-.21556E+00,
 -.22405E+00,-.23255E+00,-.24104E+00,-.24954E+00,-.25803E+00,-.27007E+00,-.28423E+00,-.29839E+00,-.31255E+00,-.32493E+00,
 -.31199E+00,-.31871E+00,-.32721E+00,-.33570E+00,-.34420E+00,-.35269E+00,-.36119E+00,-.36968E+00,-.37818E+00,-.38668E+00,
 -.39871E+00,-.41287E+00,-.42703E+00,-.44119E+00,-.45358E+00,-.44063E+00,-.44735E+00,-.45585E+00,-.46434E+00,-.47284E+00,
 -.48133E+00,-.48983E+00,-.49833E+00,-.50682E+00,-.51532E+00,-.52735E+00,-.54151E+00,-.55567E+00,-.56983E+00,-.58222E+00,
 -.53711E+00,-.54383E+00,-.55233E+00,-.56083E+00,-.56932E+00,-.57782E+00,-.58631E+00,-.59481E+00,-.60330E+00,-.61180E+00,
 -.62383E+00,-.63799E+00,-.65215E+00,-.66631E+00,-.67670E+00,-.66575E+00,-.67248E+00,-.68097E+00,-.68947E+00,-.69796E+00,
 -.70646E+00,-.71495E+00,-.72345E+00,-.73194E+00,-.74044E+00,-.75248E+00,-.76664E+00,-.78079E+00,-.79495E+00,-.80734E+00,
 -.79439E+00,-.80112E+00,-.80962E+00,-.81811E+00,-.82661E+00,-.83510E+00,-.84360E+00,-.85209E+00,-.86059E+00,-.86908E+00,
 -.88112E+00,-.89528E+00,-.90944E+00,-.92360E+00,-.93599E+00,-.92304E+00,-.92976E+00,-.93826E+00,-.94675E+00,-.95525E+00,
 -.96374E+00,-.97224E+00,-.98074E+00,-.98923E+00,-.99773E+00,-.10098E+01,-.10239E+01,-.10381E+01,-.10522E+01,-.10646E+01,

PH2(1,1, 4) THRU PH2(1,120, 4)

0.77912E+00,0.71173E+00,0.62660E+00,0.54147E+00,0.45635E+00,0.37122E+00,0.28609E+00,0.20096E+00,0.11583E+00,0.30703E-01,
 -.89894E-01,-.23177E+00,-.37366E+00,-.51554E+00,-.63968E+00,0.69094E+00,0.62354E+00,0.53842E+00,0.45329E+00,0.36816E+00,
 0.28303E+00,0.19790E+00,0.11278E+00,0.27647E-01,-.57482E-01,-.17808E+00,-.31996E+00,-.46184E+00,-.60372E+00,-.72787E+00,
 0.60275E+00,0.53536E+00,0.45023E+00,0.36510E+00,0.27997E+00,0.19485E+00,0.10972E+00,0.24590E-01,-.60538E-01,-.14567E+00,
 -.26626E+00,-.40815E+00,-.55003E+00,-.69191E+00,-.81605E+00,0.51457E+00,0.44717E+00,0.36204E+00,0.27692E+00,0.19179E+00,
 0.10666E+00,0.21533E-01,-.63595E-01,-.14872E+00,-.23385E+00,-.35445E+00,-.49633E+00,-.63821E+00,-.78009E+00,-.90424E+00,
 0.44843E+00,0.38103E+00,0.29591E+00,0.21078E+00,0.12565E+00,0.40522E-01,-.44606E-01,-.12973E+00,-.21486E+00,-.29999E+00,
 -.42059E+00,-.56247E+00,-.70435E+00,-.84623E+00,-.97038E+00,0.36024E+00,0.29285E+00,0.20772E+00,0.12259E+00,0.37465E-01,
 -.47663E-01,-.13279E+00,-.21792E+00,-.30305E+00,-.38818E+00,-.50877E+00,-.65065E+00,-.79254E+00,-.93442E+00,-.10586E+01,
 0.27206E+00,0.20466E+00,0.11954E+00,0.34407E-01,-.50720E-01,-.13585E+00,-.22098E+00,-.30611E+00,-.39123E+00,-.47636E+00,
 -.59696E+00,-.73884E+00,-.88072E+00,-.10226E+01,-.11466E+01,0.18387E+00,0.11648E+00,0.31350E-01,-.53778E-01,-.13690E+00,
 -.22403E+00,-.30916E+00,-.39429E+00,-.47942E+00,-.56455E+00,-.68514E+00,-.82703E+00,-.96891E+00,-.11108E+01,-.12349E+01,

PH2(2,1, 4) THRU PH2(2,120, 4)

-.16235E+01,-.15010E+01,-.13462E+01,-.11914E+01,-.10366E+01,-.88179E+00,-.72699E+00,-.57220E+00,-.41740E+00,-.26261E+00,
 -.43318E-01,0.21467E+00,0.47266E+00,0.73065E+00,0.95639E+00,-.15374E+01,-.14149E+01,-.12601E+01,-.11053E+01,-.95049E+00,
 -.79569E+00,-.64090E+00,-.48611E+00,-.33131E+00,-.17652E+00,0.42775E-01,0.30076E+00,0.55876E+00,0.81675E+00,0.10425E+01,
 -.14513E+01,-.13288E+01,-.11740E+01,-.10192E+01,-.86440E+00,-.70960E+00,-.55481E+00,-.40001E+00,-.24522E+00,-.90424E-01,
 0.12887E+00,0.38686E+00,0.64485E+00,0.90284E+00,0.11286E+01,-.13652E+01,-.12427E+01,-.10879E+01,-.93310E+00,-.77830E+00,
 -.62351E+00,-.46871E+00,-.31392E+00,-.15912E+00,-.43303E-02,0.21496E+00,0.47295E+00,0.73094E+00,0.98893E+00,0.12147E+01,
 -.13007E+01,-.11781E+01,-.10233E+01,-.86853E+00,-.71373E+00,-.55894E+00,-.40414E+00,-.24935E+00,-.94555E-01,0.60240E-01,
 0.27953E+00,0.53752E+00,0.79551E+00,0.10535E+01,0.12792E+01,-.12146E+01,-.10920E+01,-.93723E+00,-.78243E+00,-.62764E+00,
 -.47285E+00,-.31805E+00,-.16326E+00,-.84618E-02,0.14633E+00,0.36562E+00,0.62362E+00,0.88161E+00,0.11396E+01,0.13653E+01,
 -.11285E+01,-.10059E+01,-.85113E+00,-.69634E+00,-.54155E+00,-.38675E+00,-.23196E+00,-.77163E-01,0.77631E-01,0.23243E+00,
 0.45172E+00,0.70971E+00,0.96770E+00,0.12257E+01,0.14514E+01,-.10424E+01,-.91983E+00,-.76504E+00,-.61025E+00,-.45545E+00,
 -.30066E+00,-.14566E+00,0.89306E-02,0.16373E+00,0.31852E+00,0.53781E+00,0.79580E+00,0.10538E+01,0.13118E+01,0.15375E+01,

PH2(1,1, 5) THRU PH2(1,120, 5)

-.85149E+00,-.89078E+00,-.94040E+00,-.99003E+00,-.10396E+01,-.10893E+01,-.11389E+01,-.11885E+01,-.12382E+01,-.12878E+01,
 -.13581E+01,-.14408E+01,-.15235E+01,-.16062E+01,-.16786E+01,-.17033E+00,-.60962E+00,-.65924E+00,-.70887E+00,-.75850E+00,
 -.80812E+00,-.85775E+00,-.90738E+00,-.95700E+00,-.10066E+01,-.10769E+01,-.11596E+01,-.12423E+01,-.13251E+01,-.13974E+01,
 -.28917E+00,-.32845E+00,-.37809E+00,-.42771E+00,-.47734E+00,-.52697E+00,-.57659E+00,-.62622E+00,-.67585E+00,-.72547E+00,
 -.79577E+00,-.87849E+00,-.96120E+00,-.10439E+01,-.11163E+01,-.80157E-02,-.47304E-01,-.96930E-01,-.14656E+00,-.19618E+00,
 -.24581E+00,-.29544E+00,-.34506E+00,-.39469E+00,-.44431E+00,-.51462E+00,-.59733E+00,-.68004E+00,-.76275E+00,-.83512E+00,
 0.20265E+00,0.16356E+00,0.11394E+00,0.64312E-01,0.14686E-01,-.34941E-01,-.84567E-01,-.13419E+00,-.18382E+00,-.23345E+00,
 -.30375E+00,-.38646E+00,-.46917E+00,-.55188E+00,-.62425E+00,0.48401E+00,0.44472E+00,0.39509E+00,0.34547E+00,0.29584E+00,

0.24622E+00,0.19659E+00,0.14696E+00,0.97337E-01,0.47711E-01,-.22593E-01,-.10530E+00,-.18801E+00,-.27073E+00,-.34310E+00,
0.76516E+00,0.72588E+00,0.67625E+00,0.62663E+00,0.57700E+00,0.52737E+00,0.47775E+00,0.42812E+00,0.37849E+00,0.32887E+00,
0.25857E+00,0.17585E+00,0.93143E-01,0.10432E-01,-.61939E-01,0.10463E+01,0.10070E+01,0.95741E+00,0.90778E+00,0.85816E+00,
0.80853E+00,0.75890E+00,0.70928E+00,0.65965E+00,0.61002E+00,0.53972E+00,0.45701E+00,0.37430E+00,0.29159E+00,0.21922E+00,

PH2(2,1, 5) THRU PH2(2,120, 5)

0.47393E+00,0.57344E+00,0.69913E+00,0.82483E+00,0.95052E+00,0.10762E+01,0.12019E+01,0.13276E+01,0.14533E+01,0.15790E+01,
0.17571E+01,0.19666E+01,0.21761E+01,0.23855E+01,0.25688E+01,0.19469E+00,0.29420E+00,0.41989E+00,0.54559E+00,0.67128E+00,
0.79698E+00,0.92268E+00,0.10484E+01,0.11741E+01,0.12998E+01,0.14778E+01,0.16873E+01,0.18968E+01,0.21063E+01,0.22896E+01,
0.24547E+01,0.14962E-01,0.14066E+00,0.26635E+00,0.39205E+00,0.51774E+00,0.64344E+00,0.76913E+00,0.89483E+00,0.10205E+01,
0.11986E+01,0.14081E+01,0.16176E+01,0.18271E+01,0.20104E+01,-.36378E+00,-.26428E+00,-.13858E+00,-.12835E+01,0.11281E+00,
0.23851E+00,0.36420E+00,0.48989E+00,0.61559E+00,0.74129E+00,0.91935E+00,0.11288E+01,0.13383E+01,0.15478E+01,0.17311E+01,
0.19092E+00,0.21942E+00,0.24801E+00,-.22231E+00,-.96618E-01,0.29077E-01,0.15477E+00,0.28047E+00,0.40616E+00,0.53186E+00,
0.70992E+00,0.91942E+00,0.11289E+01,0.13384E+01,0.15217E+01,-.85245E+00,-.75294E+00,-.62725E+00,-.50155E+00,-.37586E+00,
0.25016E+00,-.12446E+00,0.12300E-02,0.12692E+00,0.25262E+00,0.43069E+00,0.64018E+00,0.84967E+00,0.10592E+01,0.12425E+01,
0.1317E+01,-.10322E+01,-.90648E+00,-.78079E+00,-.65509E+00,-.52940E+00,-.40370E+00,-.27801E+00,-.15231E+00,-.26617E-01,
0.15145E+00,0.36094E+00,0.57043E+00,0.77993E+00,0.96323E+00,-.14109E+01,-.13114E+01,-.11857E+01,-.10600E+01,-.93433E+00,
0.80863E+00,-.68294E+00,-.55724E+00,-.43155E+00,-.30585E+00,-.12779E+00,0.81706E-01,0.29120E+00,0.50069E+00,0.68400E+00,

SH2(1,1, 1) THRU SH2(1,120, 1)

0.18800E+05,0.18800E+05,0.18800E+05,0.18800E+05,0.18800E+05,0.18800E+05,0.18800E+05,0.18800E+05,0.18800E+05,0.18800E+05,
0.18800E+05,0.18800E+05,0.18800E+05,0.18800E+05,0.18800E+05,0.18800E+05,0.18800E+05,0.18800E+05,0.18800E+05,0.18800E+05,
0.16620E+05,0.16620E+05,0.16620E+05,0.16620E+05,0.16620E+05,0.16620E+05,0.16620E+05,0.16620E+05,0.16620E+05,0.16620E+05,
0.15150E+05,0.15150E+05,0.15150E+05,0.15150E+05,0.15150E+05,0.15150E+05,0.15150E+05,0.15150E+05,0.15150E+05,0.15150E+05,
0.15150E+05,0.15150E+05,0.15150E+05,0.15150E+05,0.15150E+05,0.15150E+05,0.15150E+05,0.15150E+05,0.15150E+05,0.15150E+05,
0.14220E+05,0.14220E+05,0.14220E+05,0.14220E+05,0.14220E+05,0.14220E+05,0.14220E+05,0.14220E+05,0.14220E+05,0.14220E+05,
0.13520E+05,0.13520E+05,0.13520E+05,0.13520E+05,0.13520E+05,0.13520E+05,0.13520E+05,0.13520E+05,0.13520E+05,0.13520E+05,
0.13520E+05,0.13520E+05,0.13520E+05,0.13520E+05,0.13520E+05,0.13520E+05,0.13520E+05,0.13520E+05,0.13520E+05,0.13520E+05,
0.11340E+05,0.11340E+05,0.11340E+05,0.11340E+05,0.11340E+05,0.11340E+05,0.11340E+05,0.11340E+05,0.11340E+05,0.11340E+05,
0.11340E+05,0.11340E+05,0.11340E+05,0.11340E+05,0.11340E+05,0.11340E+05,0.11340E+05,0.11340E+05,0.11340E+05,0.11340E+05,
0.91700E+04,0.91700E+04,0.91700E+04,0.91700E+04,0.91700E+04,0.91700E+04,0.91700E+04,0.91700E+04,0.91700E+04,0.91700E+04,
0.91700E+04,0.91700E+04,0.91700E+04,0.91700E+04,0.91700E+04,0.91700E+04,0.91700E+04,0.91700E+04,0.91700E+04,0.91700E+04,
0.70240E+04,0.70240E+04,0.70240E+04,0.70240E+04,0.70240E+04,0.70240E+04,0.70240E+04,0.70240E+04,0.70240E+04,0.70240E+04,

SH2(2,1, 1) THRU SH2(2,120, 1)

-.23350E+05,-.23350E+05,-.23350E+05,-.23350E+05,-.23350E+05,-.23350E+05,-.23350E+05,-.23350E+05,-.23350E+05,-.23350E+05,
-.23350E+05,-.23350E+05,-.23350E+05,-.23350E+05,-.23350E+05,-.23350E+05,-.23350E+05,-.23350E+05,-.23350E+05,-.23350E+05,
-.20660E+05,-.20660E+05,-.20660E+05,-.20660E+05,-.20660E+05,-.20660E+05,-.20660E+05,-.20660E+05,-.20660E+05,-.20660E+05,
-.18850E+05,-.18850E+05,-.18850E+05,-.18850E+05,-.18850E+05,-.18850E+05,-.18850E+05,-.18850E+05,-.18850E+05,-.18850E+05,
-.18850E+05,-.18850E+05,-.18850E+05,-.18850E+05,-.18850E+05,-.18850E+05,-.18850E+05,-.18850E+05,-.18850E+05,-.18850E+05,
-.17710E+05,-.17710E+05,-.17710E+05,-.17710E+05,-.17710E+05,-.17710E+05,-.17710E+05,-.17710E+05,-.17710E+05,-.17710E+05,
-.16840E+05,-.16840E+05,-.16840E+05,-.16840E+05,-.16840E+05,-.16840E+05,-.16840E+05,-.16840E+05,-.16840E+05,-.16840E+05,
-.16840E+05,-.16840E+05,-.16840E+05,-.16840E+05,-.16840E+05,-.16840E+05,-.16840E+05,-.16840E+05,-.16840E+05,-.16840E+05,
-.14160E+05,-.14160E+05,-.14160E+05,-.14160E+05,-.14160E+05,-.14160E+05,-.14160E+05,-.14160E+05,-.14160E+05,-.14160E+05,
-.14160E+05,-.14160E+05,-.14160E+05,-.14160E+05,-.14160E+05,-.14160E+05,-.14160E+05,-.14160E+05,-.14160E+05,-.14160E+05,
-.11490E+05,-.11490E+05,-.11490E+05,-.11490E+05,-.11490E+05,-.11490E+05,-.11490E+05,-.11490E+05,-.11490E+05,-.11490E+05,
-.11490E+05,-.11490E+05,-.11490E+05,-.11490E+05,-.11490E+05,-.11490E+05,-.11490E+05,-.11490E+05,-.11490E+05,-.11490E+05,
-.88520E+04,-.88520E+04,-.88520E+04,-.88520E+04,-.88520E+04,-.88520E+04,-.88520E+04,-.88520E+04,-.88520E+04,-.88520E+04,

SH2(3,1, 1) THRU SH2(3,120, 1)

SH2(1,1, 2) THRU SH2(1,120, 2)

SH2(2,1, 2) THRU SH2(2,120, 2)

SH2(3,1, 2) THRU SH2(3,120, 2)

ORIGINAL PAGE IS
OF POOR QUALITY

SH2(2,1, 4) THRU SH2(2,120, 4)

SH2(3,1, 4) THRU SH2(3,120, 4)

SH2(1,1, 5) THRU SH2(1,120, 5)

[illegible]

ORIGINAL PAGE
OF POOR QUALITY

[illegible][illegible][illegible]

PLANFORM GEOMETRY OF BLADE

Y= 27.0000

X 1	X 2	X 3	X 4	X 5	X 6	X 7	X 8	X 9	X10
11.0000	11.6000	12.2000	12.8000	13.4000	14.0000	14.6000	15.2000	15.8000	16.4000
X11	X12	X13	X14	X15	X				
17.2500	18.2500	19.2500	20.2500	21.0000					

Y= 28.0000

X 1	X 2	X 3	X 4	X 5	X 6	X 7	X 8	X 9	X10
11.0000	11.6000	12.2000	12.8000	13.4000	14.0000	14.6000	15.2000	15.8000	16.4000
X11	X12	X13	X14	X15	X				
17.2500	18.2500	19.2500	20.2500	21.0000					

Y= 29.0000

X 1	X 2	X 3	X 4	X 5	X 6	X 7	X 8	X 9	X10
11.0000	11.6000	12.2000	12.8000	13.4000	14.0000	14.6000	15.2000	15.8000	16.4000
X11	X12	X13	X14	X15	X				
17.2500	18.2500	19.2500	20.2500	21.0000					

Y= 30.0000

X 1	X 2	X 3	X 4	X 5	X 6	X 7	X 8	X 9	X10
11.0000	11.6000	12.2000	12.8000	13.4000	14.0000	14.6000	15.2000	15.8000	16.4000
X11	X12	X13	X14	X15	X				
17.2500	18.2500	19.2500	20.2500	21.0000					

Y= 30.7500

X 1	X 2	X 3	X 4	X 5	X 6	X 7	X 8	X 9	X10
11.0000	11.6000	12.2000	12.8000	13.4000	14.0000	14.6000	15.2000	15.8000	16.4000
X11	X12	X13	X14	X15	X				

17.2500 18.2500 19.2500 20.2500 21.0000

Y= 31.7500

X 1	X 2	X 3	X 4	X 5	X 6	X 7	X 8	X 9	X10
11.0000	11.6000	12.2000	12.8000	13.4000	14.0000	14.6000	15.2000	15.8000	16.4000
X11	X12	X13	X14	X15	X				
17.2500	18.2500	19.2500	20.2500	21.0000					

Y= 32.7500

X 1	X 2	X 3	X 4	X 5	X 6	X 7	X 8	X 9	X10
11.0000	11.6000	12.2000	12.8000	13.4000	14.0000	14.6000	15.2000	15.8000	16.4000
X11	X12	X13	X14	X15	X				
17.2500	18.2500	19.2500	20.2500	21.0000					

Y= 33.7500

X 1	X 2	X 3	X 4	X 5	X 6	X 7	X 8	X 9	X10
11.0000	11.6000	12.2000	12.8000	13.4000	14.0000	14.6000	15.2000	15.8000	16.4000
X11	X12	X13	X14	X15	X				
17.2500	18.2500	19.2500	20.2500	21.0000					

INITIAL BLADE CAMBER GEOMETRY AT IMPACT STATION

NODE	IN-PLANE COORDINATE	OUT OF PLANE COORDINATE
1	1.00000	1.00000
2	1.47300	1.36900
3	1.94600	1.73900
4	2.41800	2.10800
5	2.89100	2.47800
6	3.36400	2.84700
7	3.83700	3.21600
8	4.31000	3.58600
9	4.78200	3.95500
10	5.25500	4.32500
11	5.72500	4.69400
12	6.19300	5.06300
13	6.66100	5.43200
14	7.12900	5.80100
15	7.59700	6.17000

MISSILE GEOMETRY

SECTION	THICKNESS	WIDTH	LENGTH	OFFSET
1	0.625	2.100	2.100	0.825
2	0.600	3.260	3.260	0.245
3	0.650	3.750	3.750	0.0
4	0.650	3.750	3.750	0.0
5	0.600	3.260	3.260	0.245
6	0.625	2.100	2.100	0.825

MODAL DATA

MODE	FREQ(RAD/SEC)	MODAL MASS	MODAL STIFFNESS	DAMPING RATIO
1	0.433500E+03	0.985580E-02	0.185212E+04	0.350000E-01
2	0.873390E+03	0.427630E-02	0.326201E+04	0.350000E-01
3	0.144500E+04	0.988900E-02	0.206485E+05	0.350000E-01
4	0.153310E+04	0.102230E-01	0.240281E+05	0.350000E-01
5	0.226200E+04	0.233400E-01	0.119422E+06	0.350000E-01

IMPACT VELOCITY	IMPACT ANGLE	MISSILE DENSITY	CHORDWISE IMPACT COORDINATES		IMPACT RADIUS
			IN-PLANE	OUT-OF-PLANE	
0.726000E+04	0.523600E+00	0.988800E-04	0.454600E+01	0.377050E+01	0.300000E+02

ORIGINAL PAGE IS
OF POOR QUALITY

TIME STEP= 2 TIME=0.289325E-03 SEC

Y=0.27000E+02		Y=0.28000E+02		Y=0.29000E+02		Y=0.30000E+02		Y=0.30750E+02	
X	P	X	P	X	P	X	P	X	P
0.1100E+02	0.0	0.1100E+02	0.8107E-09	0.1100E+02	0.4178E+03	0.1100E+02	0.4178E+03	0.1100E+02	0.4178E+03
0.1160E+02	0.6337E-18	0.1160E+02	0.1909E+00	0.1160E+02	0.2341E+04	0.1160E+02	0.2341E+04	0.1160E+02	0.2341E+04
0.1220E+02	0.8497E-11	0.1220E+02	0.1157E+02	0.1220E+02	0.1263E+04	0.1220E+02	0.1263E+04	0.1220E+02	0.1263E+04
0.1280E+02	0.1376E-07	0.1280E+02	0.1858E+02	0.1280E+02	0.5739E+03	0.1280E+02	0.5739E+03	0.1280E+02	0.5739E+03
0.1340E+02	0.2943E-06	0.1340E+02	0.8981E+01	0.1340E+02	0.2465E+03	0.1340E+02	0.2465E+03	0.1340E+02	0.2465E+03
0.1400E+02	0.6495E-06	0.1400E+02	0.2218E+01	0.1400E+02	0.1036E+03	0.1400E+02	0.1036E+03	0.1400E+02	0.1036E+03
0.1460E+02	0.3672E-06	0.1460E+02	0.3262E+00	0.1460E+02	0.4319E+02	0.1460E+02	0.4319E+02	0.1460E+02	0.4319E+02
0.1520E+02	0.0	0.1520E+02	0.3017E-01	0.1520E+02	0.1794E+02	0.1520E+02	0.1794E+02	0.1520E+02	0.1794E+02
0.1580E+02	0.0	0.1580E+02	0.0	0.1580E+02	0.0	0.1580E+02	0.0	0.1580E+02	0.0
0.1640E+02	0.0	0.1640E+02	0.0	0.1640E+02	0.0	0.1640E+02	0.0	0.1640E+02	0.0
0.1725E+02	0.0	0.1725E+02	0.0	0.1725E+02	0.0	0.1725E+02	0.0	0.1725E+02	0.0
0.1825E+02	0.0	0.1825E+02	0.0	0.1825E+02	0.0	0.1825E+02	0.0	0.1825E+02	0.0
0.1925E+02	0.0	0.1925E+02	0.0	0.1925E+02	0.0	0.1925E+02	0.0	0.1925E+02	0.0
0.2025E+02	0.0	0.2025E+02	0.0	0.2025E+02	0.0	0.2025E+02	0.0	0.2025E+02	0.0
0.2100E+02	0.0	0.2100E+02	0.0	0.2100E+02	0.0	0.2100E+02	0.0	0.2100E+02	0.0

Y=0.31750E+02

Y=0.32750E+02

Y=0.33750E+02

Y=

X	P	X	P	X	P
0.1100E+02	0.5323E-05	0.1100E+02	0.9295E-26	0.1100E+02	0.0
0.1160E+02	0.3275E+02	0.1160E+02	0.2893E-12	0.1160E+02	0.0
0.1220E+02	0.2196E+03	0.1220E+02	0.1278E-06	0.1220E+02	0.3203E-28
0.1280E+02	0.1647E+03	0.1280E+02	0.2229E-04	0.1280E+02	0.1637E-21
0.1340E+02	0.5879E+02	0.1340E+02	0.1232E-03	0.1340E+02	0.8665E-18
0.1400E+02	0.1253E+02	0.1400E+02	0.1183E-03	0.1400E+02	0.0
0.1460E+02	0.1697E+01	0.1460E+02	0.3928E-04	0.1460E+02	0.0
0.1520E+02	0.1494E+00	0.1520E+02	0.0	0.1520E+02	0.0
0.1580E+02	0.0	0.1580E+02	0.0	0.1580E+02	0.0
0.1640E+02	0.0	0.1640E+02	0.0	0.1640E+02	0.0
0.1725E+02	0.0	0.1725E+02	0.0	0.1725E+02	0.0
0.1825E+02	0.0	0.1825E+02	0.0	0.1825E+02	0.0
0.1925E+02	0.0	0.1925E+02	0.0	0.1925E+02	0.0
0.2025E+02	0.0	0.2025E+02	0.0	0.2025E+02	0.0
0.2100E+02	0.0	0.2100E+02	0.0	0.2100E+02	0.0

ORIGINAL PAGE IS
OF POOR QUALITY

TIME STEP= 3 TIME=0.293143E-03 SEC

Y=0.27000E+02

Y=0.28000E+02

Y=0.29000E+02

Y=0.30000E+02

Y=0.30750E+02

X	P	X	P	X	P	X	P	X	P
0.1100E+02	0.0	0.1100E+02	0.1259E+00	0.1100E+02	0.9760E+03	0.1100E+02	0.1688E+04	0.1100E+02	0.1688E+04
0.1160E+02	0.3641E-05	0.1160E+02	0.6397E+02	0.1160E+02	0.2608E+04	0.1160E+02	0.2341E+04	0.1160E+02	0.2341E+04
0.1220E+02	0.1799E-02	0.1220E+02	0.2621E+03	0.1220E+02	0.2480E+04	0.1220E+02	0.1606E+04	0.1220E+02	0.1606E+04
0.1280E+02	0.3144E-01	0.1280E+02	0.3022E+03	0.1280E+02	0.2027E+04	0.1280E+02	0.9956E+03	0.1280E+02	0.9956E+03
0.1340E+02	0.1040E+00	0.1340E+02	0.2168E+03	0.1340E+02	0.1333E+04	0.1340E+02	0.5891E+03	0.1340E+02	0.5891E+03
0.1400E+02	0.1384E+00	0.1400E+02	0.1168E+03	0.1400E+02	0.6953E+03	0.1400E+02	0.3405E+03	0.1400E+02	0.3405E+03
0.1460E+02	0.1050E+00	0.1460E+02	0.5007E+02	0.1460E+02	0.2913E+03	0.1460E+02	0.1944E+03	0.1460E+02	0.1944E+03
0.1520E+02	0.0	0.1520E+02	0.1751E+02	0.1520E+02	0.9970E+02	0.1520E+02	0.1103E+03	0.1520E+02	0.1103E+03
0.1580E+02	0.0	0.1580E+02	0.0	0.1580E+02	0.2825E+02	0.1580E+02	0.6230E+02	0.1580E+02	0.6230E+02
0.1640E+02	0.0	0.1640E+02	0.0	0.1640E+02	0.0	0.1640E+02	0.0	0.1640E+02	0.0
0.1725E+02	0.0	0.1725E+02	0.0	0.1725E+02	0.0	0.1725E+02	0.0	0.1725E+02	0.0
0.1825E+02	0.0	0.1825E+02	0.0	0.1825E+02	0.0	0.1825E+02	0.0	0.1825E+02	0.0
0.1925E+02	0.0	0.1925E+02	0.0	0.1925E+02	0.0	0.1925E+02	0.0	0.1925E+02	0.0
0.2025E+02	0.0	0.2025E+02	0.0	0.2025E+02	0.0	0.2025E+02	0.0	0.2025E+02	0.0
0.2100E+02	0.0	0.2100E+02	0.0	0.2100E+02	0.0	0.2100E+02	0.0	0.2100E+02	0.0

Y=0.31750E+02

Y=0.32750E+02

Y=0.33750E+02

Y=

X	P	X	P	X	P
0.1100E+02	0.5219E+01	0.1100E+02	0.9295E-26	0.1100E+02	0.0
0.1160E+02	0.5096E+03	0.1160E+02	0.8261E-03	0.1160E+02	0.0
0.1220E+02	0.9150E+03	0.1220E+02	0.1052E+00	0.1220E+02	0.3203E-28
0.1280E+02	0.7926E+03	0.1280E+02	0.7624E+00	0.1280E+02	0.1637E-21
0.1340E+02	0.5093E+03	0.1340E+02	0.1463E+01	0.1340E+02	0.8665E-18
0.1400E+02	0.2604E+03	0.1400E+02	0.1383E+01	0.1400E+02	0.0
0.1460E+02	0.1083E+03	0.1460E+02	0.8385E+00	0.1460E+02	0.0
0.1520E+02	0.3710E+02	0.1520E+02	0.0	0.1520E+02	0.0
0.1580E+02	0.0	0.1580E+02	0.0	0.1580E+02	0.0
0.1640E+02	0.0	0.1640E+02	0.0	0.1640E+02	0.0
0.1725E+02	0.0	0.1725E+02	0.0	0.1725E+02	0.0
0.1825E+02	0.0	0.1825E+02	0.0	0.1825E+02	0.0
0.1925E+02	0.0	0.1925E+02	0.0	0.1925E+02	0.0
0.2025E+02	0.0	0.2025E+02	0.0	0.2025E+02	0.0
0.2100E+02	0.0	0.2100E+02	0.0	0.2100E+02	0.0

TIME STEP= 4 TIME=0.299168E-03 SEC

Y=0.27000E+02

Y=0.28000E+02

Y=0.29000E+02

Y=0.30000E+02

Y=0.30750E+02

X	P	X	P	X	P	X	P	X	P
0.1100E+02	0.0	0.1100E+02	0.1259E+00	0.1100E+02	0.9760E+03	0.1100E+02	0.1688E+04	0.1100E+02	0.1688E+04
0.1160E+02	0.3641E-05	0.1160E+02	0.6397E+02	0.1160E+02	0.2620E+04	0.1160E+02	0.2432E+04	0.1160E+02	0.2432E+04
0.1220E+02	0.1799E-02	0.1220E+02	0.2621E+03	0.1220E+02	0.2522E+04	0.1220E+02	0.1717E+04	0.1220E+02	0.1717E+04
0.1280E+02	0.3144E-01	0.1280E+02	0.3206E+03	0.1280E+02	0.2113E+04	0.1280E+02	0.1079E+04	0.1280E+02	0.1079E+04
0.1340E+02	0.1640E+00	0.1340E+02	0.2393E+03	0.1340E+02	0.1431E+04	0.1340E+02	0.6439E+03	0.1340E+02	0.6439E+03
0.1400E+02	0.1384E+00	0.1400E+02	0.1327E+03	0.1400E+02	0.7685E+03	0.1400E+02	0.3747E+03	0.1400E+02	0.3747E+03
0.1460E+02	0.1050E+00	0.1460E+02	0.5830E+02	0.1460E+02	0.3304E+03	0.1460E+02	0.2151E+03	0.1460E+02	0.2151E+03
0.1520E+02	0.0	0.1520E+02	0.1751E+02	0.1520E+02	0.9970E+02	0.1520E+02	0.1103E+03	0.1520E+02	0.1103E+03
0.1580E+02	0.0	0.1580E+02	0.0	0.1580E+02	0.2825E+02	0.1580E+02	0.6230E+02	0.1580E+02	0.6230E+02
0.1640E+02	0.0	0.1640E+02	0.0	0.1640E+02	0.0	0.1640E+02	0.0	0.1640E+02	0.0
0.1725E+02	0.0	0.1725E+02	0.0	0.1725E+02	0.0	0.1725E+02	0.0	0.1725E+02	0.0
0.1825E+02	0.0	0.1825E+02	0.0	0.1825E+02	0.0	0.1825E+02	0.0	0.1825E+02	0.0
0.1925E+02	0.0	0.1925E+02	0.0	0.1925E+02	0.0	0.1925E+02	0.0	0.1925E+02	0.0
0.2025E+02	0.0	0.2025E+02	0.0	0.2025E+02	0.0	0.2025E+02	0.0	0.2025E+02	0.0
0.2100E+02	0.0	0.2100E+02	0.0	0.2100E+02	0.0	0.2100E+02	0.0	0.2100E+02	0.0

Y=0.31750E+02

Y=0.32750E+02

Y=0.33750E+02

Y=

X	P	X	P	X	P
0.1100E+02	0.5219E+01	0.1100E+02	0.9295E-26	0.1100E+02	0.0
0.1160E+02	0.5096E+03	0.1160E+02	9.8261E-03	0.1160E+02	0.0
0.1220E+02	0.9271E+03	0.1220E+02	0.1052E+00	0.1220E+02	0.3203E-28
0.1280E+02	0.8424E+03	0.1280E+02	0.7730E+00	0.1280E+02	0.1637E-21
0.1340E+02	0.5582E+03	0.1340E+02	0.1624E+01	0.1340E+02	0.8665E-18
0.1400E+02	0.2930E+03	0.1400E+02	0.1383E+01	0.1400E+02	0.0
0.1460E+02	0.1248E+03	0.1460E+02	0.8385E+00	0.1460E+02	0.0
0.1520E+02	0.3710E+02	0.1520E+02	0.0	0.1520E+02	0.0
0.1580E+02	0.0	0.1580E+02	0.0	0.1580E+02	0.0
0.1640E+02	0.0	0.1640E+02	0.0	0.1640E+02	0.0
0.1725E+02	0.0	0.1725E+02	0.0	0.1725E+02	0.0
0.1825E+02	0.0	0.1825E+02	0.0	0.1825E+02	0.0
0.1925E+02	0.0	0.1925E+02	0.0	0.1925E+02	0.0
0.2025E+02	0.0	0.2025E+02	0.0	0.2025E+02	0.0
0.2100E+02	0.0	0.2100E+02	0.0	0.2100E+02	0.0

ORIGINAL PAGE
OF FOUR QUALITY

TIME STEP= 5 TIME=0.504719E-03 SEC

Y=0.27000E+02

Y=0.28000E+02

Y=0.29000E+02

Y=0.30000E+02

Y=0.30750E+02

X	P	X	P	X	P	X	P	X	P
0.1100E+02	0.8094E-11	0.1100E+02	0.1259E+00	0.1100E+02	0.9760E+03	0.1100E+02	0.1688E+04	0.1100E+02	0.1688E+04
0.1160E+02	0.3641E-05	0.1160E+02	0.6397E+02	0.1160E+02	0.2620E+04	0.1160E+02	0.2436E+04	0.1160E+02	0.2436E+04
0.1220E+02	0.1799E-02	0.1220E+02	0.2621E+03	0.1220E+02	0.2524E+04	0.1220E+02	0.1722E+04	0.1220E+02	0.1722E+04
0.1280E+02	0.3144E-01	0.1280E+02	0.3215E+03	0.1280E+02	0.2117E+04	0.1280E+02	0.1083E+04	0.1280E+02	0.1083E+04
0.1340E+02	0.1162E+00	0.1340E+02	0.2405E+03	0.1340E+02	0.1436E+04	0.1340E+02	0.6467E+03	0.1340E+02	0.6467E+03
0.1400E+02	0.1653E+00	0.1400E+02	0.1335E+03	0.1400E+02	0.7721E+03	0.1400E+02	0.3764E+03	0.1400E+02	0.3764E+03
0.1460E+02	0.1308E+00	0.1460E+02	0.5873E+02	0.1460E+02	0.3324E+03	0.1460E+02	0.2162E+03	0.1460E+02	0.2162E+03
0.1520E+02	0.5361E-01	0.1520E+02	0.2103E+02	0.1520E+02	0.1166E+03	0.1520E+02	0.1232E+03	0.1520E+02	0.1232E+03
0.1580E+02	0.2013E-01	0.1580E+02	0.5056E+01	0.1580E+02	0.3379E+02	0.1580E+02	0.6994E+02	0.1580E+02	0.6994E+02
0.1640E+02	0.0	0.1640E+02	0.1213E+01	0.1640E+02	0.6674E+01	0.1640E+02	0.3513E+02	0.1640E+02	0.3513E+02
0.1725E+02	0.0	0.1725E+02	0.0	0.1725E+02	0.0	0.1725E+02	0.0	0.1725E+02	0.0
0.1825E+02	0.0	0.1825E+02	0.0	0.1825E+02	0.0	0.1825E+02	0.0	0.1825E+02	0.0
0.1925E+02	0.0	0.1925E+02	0.0	0.1925E+02	0.0	0.1925E+02	0.0	0.1925E+02	0.0
0.2025E+02	0.0	0.2025E+02	0.0	0.2025E+02	0.0	0.2025E+02	0.0	0.2025E+02	0.0
0.2100E+02	0.0	0.2100E+02	0.0	0.2100E+02	0.0	0.2100E+02	0.0	0.2100E+02	0.0

Y=0.31750E+02

Y=0.32750E+02

Y=0.33750E+02

Y=

X	P	X	P	X	P
0.1100E+02	0.5219E+01	0.1100E+02	0.1028E-07	0.1100E+02	0.0
0.1160E+02	0.5096E+03	0.1160E+02	0.8261E-03	0.1160E+02	0.1967E-14
0.1220E+02	0.9277E+03	0.1220E+02	0.1052E+00	0.1220E+02	0.8080E-10
0.1280E+02	0.8449E+03	0.1280E+02	0.7742E+00	0.1280E+02	0.3556E-07
0.1340E+02	0.5607E+03	0.1340E+02	0.1634E+01	0.1340E+02	0.1085E-05
0.1400E+02	0.2947E+03	0.1400E+02	0.1631E+01	0.1400E+02	0.6603E-05
0.1460E+02	0.1257E+03	0.1460E+02	0.1026E+01	0.1460E+02	0.1437E-04
0.1520E+02	0.4408E+02	0.1520E+02	0.3679E+00	0.1520E+02	0.0
0.1580E+02	0.1056E+02	0.1580E+02	0.1242E+00	0.1580E+02	0.0
0.1640E+02	0.2507E+01	0.1640E+02	0.0	0.1640E+02	0.0
0.1725E+02	0.0	0.1725E+02	0.0	0.1725E+02	0.0
0.1825E+02	0.0	0.1825E+02	0.0	0.1825E+02	0.0
0.1925E+02	0.0	0.1925E+02	0.0	0.1925E+02	0.0
0.2025E+02	0.0	0.2025E+02	0.0	0.2025E+02	0.0
0.2100E+02	0.0	0.2100E+02	0.0	0.2100E+02	0.0

TIME STEP= 6 TIME=0.519678E-03 SEC

Y=0.27000E+02

Y=0.28000E+02

Y=0.29000E+02

Y=0.30000E+02

Y=0.30750E+02

X	P	X	P	X	P	X	P	X	P
0.1100E+02	0.8094E-11	0.1100E+02	0.1259E+00	0.1100E+02	0.9760E+03	0.1100E+02	0.1688E+04	0.1100E+02	0.1688E+04
0.1160E+02	0.3641E-05	0.1160E+02	0.6397E+02	0.1160E+02	0.2620E+04	0.1160E+02	0.2436E+04	0.1160E+02	0.2436E+04
0.1220E+02	0.1799E-02	0.1220E+02	0.2621E+03	0.1220E+02	0.2524E+04	0.1220E+02	0.1722E+04	0.1220E+02	0.1722E+04
0.1280E+02	0.3144E-01	0.1280E+02	0.3215E+03	0.1280E+02	0.2644E+04	0.1280E+02	0.2485E+04	0.1280E+02	0.2485E+04
0.1340E+02	0.1162E+00	0.1340E+02	0.2621E+03	0.1340E+02	0.2557E+04	0.1340E+02	0.1785E+04	0.1340E+02	0.1785E+04
0.1400E+02	0.1653E+00	0.1400E+02	0.3385E+03	0.1400E+02	0.2173E+04	0.1400E+02	0.1138E+04	0.1400E+02	0.1138E+04
0.1460E+02	0.1508E+00	0.1460E+02	0.2594E+03	0.1460E+02	0.1505E+04	0.1460E+02	0.6684E+03	0.1460E+02	0.6684E+03
0.1520E+02	0.2171E+00	0.1520E+02	0.1478E+03	0.1520E+02	0.8313E+03	0.1520E+02	0.4054E+03	0.1520E+02	0.4054E+03
0.1580E+02	0.1753E+00	0.1580E+02	0.6698E+02	0.1580E+02	0.3692E+03	0.1580E+02	0.2354E+03	0.1580E+02	0.2354E+03
0.1640E+02	0.9495E-01	0.1640E+02	0.2479E+02	0.1640E+02	0.1340E+03	0.1640E+02	0.1357E+03	0.1640E+02	0.1357E+03
0.1725E+02	0.0	0.1725E+02	0.4395E+01	0.1725E+02	0.2318E+02	0.1725E+02	0.6171E+02	0.1725E+02	0.6171E+02
0.1825E+02	0.0	0.1825E+02	0.0	0.1825E+02	0.0	0.1825E+02	0.0	0.1825E+02	0.0
0.1925E+02	0.0	0.1925E+02	0.0	0.1925E+02	0.0	0.1925E+02	0.0	0.1925E+02	0.0
0.2025E+02	0.0	0.2025E+02	0.0	0.2025E+02	0.0	0.2025E+02	0.0	0.2025E+02	0.0
0.2100E+02	0.0	0.2100E+02	0.0	0.2100E+02	0.0	0.2100E+02	0.0	0.2100E+02	0.0

Y=0.31750E+02

Y=0.32750E+02

Y=0.33750E+02

Y=

X	P	X	P	X	P
0.1100E+02	0.5219E+01	0.1100E+02	0.1028E-07	0.1100E+02	0.2379E-22
0.1160E+02	0.5096E+03	0.1160E+02	0.8261E-03	0.1160E+02	0.1967E-14
0.1220E+02	0.9277E+03	0.1220E+02	0.1052E+00	0.1220E+02	0.8080E-10
0.1280E+02	0.8449E+03	0.1280E+02	0.7742E+00	0.1280E+02	0.3556E-07
0.1340E+02	0.9385E+03	0.1340E+02	0.1634E+01	0.1340E+02	0.1085E-05
0.1400E+02	0.8758E+03	0.1400E+02	0.1631E+01	0.1400E+02	0.6603E-05
0.1460E+02	0.5945E+03	0.1460E+02	0.1978E+01	0.1460E+02	0.1437E-04
0.1520E+02	0.3208E+03	0.1520E+02	0.2013E+01	0.1520E+02	0.1553E-04
0.1580E+02	0.1409E+03	0.1580E+02	0.1298E+01	0.1580E+02	0.3368E-04
0.1640E+02	0.5111E+02	0.1640E+02	0.6040E+00	0.1640E+02	0.0
0.1725E+02	0.8888E+01	0.1725E+02	0.1317E+00	0.1725E+02	0.0
0.1825E+02	0.0	0.1825E+02	0.0	0.1825E+02	0.0
0.1925E+02	0.0	0.1925E+02	0.0	0.1925E+02	0.0
0.2025E+02	0.0	0.2025E+02	0.0	0.2025E+02	0.0
0.2100E+02	0.0	0.2100E+02	0.0	0.2100E+02	0.0

TIME STEP= 7 TIME=0.548717E-03 SEC

Y=0.27000E+02

Y=0.28000E+02

Y=0.29000E+02

Y=0.30000E+02

Y=0.30750E+02

X	P	X	P	X	P	X	P	X	P
0.1100E+02	0.8094E-11	0.1100E+02	0.1259E+00	0.1100E+02	0.9760E+03	0.1100E+02	0.1688E+04	0.1100E+02	0.1688E+04
0.1160E+02	0.3641E-05	0.1160E+02	0.6397E+02	0.1160E+02	0.2620E+04	0.1160E+02	0.2436E+04	0.1160E+02	0.2436E+04
0.1220E+02	0.1799E-02	0.1220E+02	0.2621E+03	0.1220E+02	0.2524E+04	0.1220E+02	0.1722E+04	0.1220E+02	0.1722E+04
0.1280E+02	0.3144E-01	0.1280E+02	0.3215E+03	0.1280E+02	0.2644E+04	0.1280E+02	0.2599E+04	0.1280E+02	0.2649E+04
0.1340E+02	0.1162E+00	0.1340E+02	0.2780E+03	0.1340E+02	0.2557E+04	0.1340E+02	0.2160E+04	0.1340E+02	0.2623E+04
0.1400E+02	0.1653E+00	0.1400E+02	0.4528E+03	0.1400E+02	0.2370E+04	0.1400E+02	0.1623E+04	0.1400E+02	0.2478E+04
0.1460E+02	0.2717E+01	0.1460E+02	0.4576E+03	0.1460E+02	0.2005E+04	0.1460E+02	0.1159E+04	0.1460E+02	0.2131E+04
0.1520E+02	0.4259E+01	0.1520E+02	0.3635E+03	0.1520E+02	0.1506E+04	0.1520E+02	0.8047E+03	0.1520E+02	0.1621E+04
0.1580E+02	0.1753E+00	0.1580E+02	0.2447E+03	0.1580E+02	0.9950E+03	0.1580E+02	0.5491E+03	0.1580E+02	0.1080E+04
0.1640E+02	0.9495E-01	0.1640E+02	0.1438E+03	0.1640E+02	0.5784E+03	0.1640E+02	0.3707E+03	0.1640E+02	0.6313E+03
0.1725E+02	0.2384E-01	0.1725E+02	0.4395E+01	0.1725E+02	0.2180E+03	0.1725E+02	0.2102E+03	0.1725E+02	0.2388E+03
0.1825E+02	0.0	0.1825E+02	0.0	0.1825E+02	0.0	0.1825E+02	0.0	0.1825E+02	0.0
0.1925E+02	0.0	0.1925E+02	0.0	0.1925E+02	0.0	0.1925E+02	0.0	0.1925E+02	0.0
0.2025E+02	0.0	0.2025E+02	0.0	0.2025E+02	0.0	0.2025E+02	0.0	0.2025E+02	0.0
0.2100E+02	0.0	0.2100E+02	0.0	0.2100E+02	0.0	0.2100E+02	0.0	0.2100E+02	0.0

Y=0.31750E+02

Y=0.32750E+02

Y=0.33750E+02

Y=

X	P	X	P	X	P
0.1100E+02	0.5219E+01	0.1100E+02	0.1028E-07	0.1100E+02	0.2379E-22
0.1160E+02	0.5096E+03	0.1160E+02	0.8261E-03	0.1160E+02	0.1967E-14
0.1220E+02	0.9277E+03	0.1220E+02	0.1052E+00	0.1220E+02	0.8080E-10
0.1280E+02	0.8449E+03	0.1280E+02	0.7742E+00	0.1280E+02	0.3556E-07
0.1340E+02	0.9385E+03	0.1340E+02	0.1634E+01	0.1340E+02	0.1237E-05
0.1400E+02	0.9746E+03	0.1400E+02	0.6915E+01	0.1400E+02	0.6603E-05
0.1460E+02	0.8664E+03	0.1460E+02	0.1490E+02	0.1460E+02	0.1437E-04
0.1520E+02	0.6486E+03	0.1520E+02	0.1848E+02	0.1520E+02	0.1553E-04
0.1580E+02	0.4234E+03	0.1580E+02	0.1638E+02	0.1580E+02	0.3368E-04
0.1640E+02	0.2442E+03	0.1640E+02	0.6040E+00	0.1640E+02	0.3832E-04
0.1725E+02	0.8888E+01	0.1725E+02	0.1317E+00	0.1725E+02	0.0
0.1825E+02	0.0	0.1825E+02	0.0	0.1825E+02	0.0
0.1925E+02	0.0	0.1925E+02	0.0	0.1925E+02	0.0
0.2025E+02	0.0	0.2025E+02	0.0	0.2025E+02	0.0
0.2100E+02	0.0	0.2100E+02	0.0	0.2100E+02	0.0

ORIGINAL PAGE IS
OF POOR QUALITY

TIME STEP= 8 TIME=0.713245E-03 SEC

Y=0.27000E+02		Y=0.28000E+02		Y=0.29000E+02		Y=0.30000E+02		Y=0.30750E+02	
X	P	X	P	X	P	X	P	X	P
0.1100E+02	0.8094E-11	0.1100E+02	0.1259E+00	0.1100E+02	0.9760E+03	0.1100E+02	0.1688E+04	0.1100E+02	0.1688E+04
0.1160E+02	0.3641E-05	0.1160E+02	0.6397E+02	0.1160E+02	0.2620E+04	0.1160E+02	0.2436E+04	0.1160E+02	0.2436E+04
0.1220E+02	0.1799E-02	0.1220E+02	0.2621E+03	0.1220E+02	0.2524E+04	0.1220E+02	0.1722E+04	0.1220E+02	0.1722E+04
0.1280E+02	0.3144E-01	0.1280E+02	0.3215E+03	0.1280E+02	0.2644E+04	0.1280E+02	0.2606E+04	0.1280E+02	0.2649E+04
0.1340E+02	0.1162E+00	0.1340E+02	0.2780E+03	0.1340E+02	0.2557E+04	0.1340E+02	0.2178E+04	0.1340E+02	0.2624E+04
0.1400E+02	0.8995E+00	0.1400E+02	0.4566E+03	0.1400E+02	0.2378E+04	0.1400E+02	0.1642E+04	0.1400E+02	0.2484E+04
0.1460E+02	0.2798E+01	0.1460E+02	0.4644E+03	0.1460E+02	0.2018E+04	0.1460E+02	0.1175E+04	0.1460E+02	0.2143E+04
0.1520E+02	0.4415E+01	0.1520E+02	0.3704E+03	0.1520E+02	0.1521E+04	0.1520E+02	0.8171E+03	0.1520E+02	0.1637E+04
0.1580E+02	0.4596E+01	0.1580E+02	0.2502E+03	0.1580E+02	0.1009E+04	0.1580E+02	0.5583E+03	0.1580E+02	0.1094E+04
0.1640E+02	0.3608E+01	0.1640E+02	0.1474E+03	0.1640E+02	0.5883E+03	0.1640E+02	0.3774E+03	0.1640E+02	0.6417E+03
0.1725E+02	0.2384E-01	0.1725E+02	0.5653E+02	0.1725E+02	0.2226E+03	0.1725E+02	0.2143E+03	0.1725E+02	0.2437E+03
0.1825E+02	0.0	0.1825E+02	0.3616E+00	0.1825E+02	0.1867E+01	0.1825E+02	0.2431E+02	0.1825E+02	0.2431E+02
0.1925E+02	0.0	0.1925E+02	0.0	0.1925E+02	0.0	0.1925E+02	0.0	0.1925E+02	0.0
0.2025E+02	0.0	0.2025E+02	0.0	0.2025E+02	0.0	0.2025E+02	0.0	0.2025E+02	0.0
0.2100E+02	0.0	0.2100E+02	0.0	0.2100E+02	0.0	0.2100E+02	0.0	0.2100E+02	0.0

Y=0.31750E+02

Y=0.32750E+02

Y=0.33750E+02

Y=

X	P	X	P	X	P
0.1100E+02	0.5219E+01	0.1100E+02	0.1028E-07	0.1100E+02	0.2379E-22
0.1160E+02	0.5096E+03	0.1160E+02	0.8261E-03	0.1160E+02	0.1967E-14
0.1220E+02	0.9277E+03	0.1220E+02	0.1052E+00	0.1220E+02	0.8080E-10
0.1280E+02	0.8449E+03	0.1280E+02	0.7742E+00	0.1280E+02	0.3556E-07
0.1340E+02	0.9385E+03	0.1340E+02	0.1634E+01	0.1340E+02	0.1237E-05
0.1400E+02	0.9819E+03	0.1400E+02	0.7007E+01	0.1400E+02	0.6322E-05
0.1460E+02	0.8771E+03	0.1460E+02	0.1527E+02	0.1460E+02	0.1930E-04
0.1520E+02	0.6590E+03	0.1520E+02	0.1905E+02	0.1520E+02	0.1553E-04
0.1580E+02	0.4316E+03	0.1580E+02	0.1695E+02	0.1580E+02	0.3368E-04
0.1640E+02	0.2496E+03	0.1640E+02	0.1195E+02	0.1640E+02	0.3832E-04
0.1725E+02	0.9413E+02	0.1725E+02	0.1317E+00	0.1725E+02	0.1975E-04
0.1825E+02	0.7209E+00	0.1825E+02	0.0	0.1825E+02	0.0
0.1925E+02	0.0	0.1925E+02	0.0	0.1925E+02	0.0
0.2025E+02	0.0	0.2025E+02	0.0	0.2025E+02	0.0
0.2100E+02	0.0	0.2100E+02	0.0	0.2100E+02	0.0

ORIGINAL PAGE IS
OF POOR QUALITY

TIME STEP= 9 TIME=0.719889E-03 SEC

Y=0.27000E+02

Y=0.28000E+02

Y=0.29000E+02

Y=0.30000E+02

Y=0.30750E+02

X	P	X	P	X	P	X	P	X	P
0.1100E+02	0.8094E-11	0.1100E+02	0.1259E+00	0.1100E+02	0.9760E+03	0.1100E+02	0.1688E+04	0.1100E+02	0.1688E+04
0.1160E+02	0.3641E-05	0.1160E+02	0.6397E+02	0.1160E+02	0.2620E+04	0.1160E+02	0.2436E+04	0.1160E+02	0.2436E+04
0.1220E+02	0.1799E-02	0.1220E+02	0.2621E+03	0.1220E+02	0.2524E+04	0.1220E+02	0.1722E+04	0.1220E+02	0.1722E+04
0.1280E+02	0.3144E-01	0.1280E+02	0.3215E+03	0.1280E+02	0.2644E+04	0.1280E+02	0.2605E+04	0.1280E+02	0.2649E+04
0.1340E+02	0.1162E+00	0.1340E+02	0.2780E+03	0.1340E+02	0.2557E+04	0.1340E+02	0.2178E+04	0.1340E+02	0.2624E+04
0.1400E+02	0.8995E+00	0.1400E+02	0.4566E+03	0.1400E+02	0.2656E+04	0.1400E+02	0.2626E+04	0.1400E+02	0.2626E+04
0.1460E+02	0.2798E+01	0.1460E+02	0.4644E+03	0.1460E+02	0.2613E+04	0.1460E+02	0.2051E+04	0.1460E+02	0.2143E+04
0.1520E+02	0.4415E+01	0.1520E+02	0.4386E+03	0.1520E+02	0.2324E+04	0.1520E+02	0.1375E+04	0.1520E+02	0.1637E+04
0.1580E+02	0.4596E+01	0.1580E+02	0.3552E+03	0.1580E+02	0.1703E+04	0.1580E+02	0.8634E+03	0.1580E+02	0.1094E+04
0.1640E+02	0.3608E+01	0.1640E+02	0.2110E+03	0.1640E+02	0.9930E+03	0.1640E+02	0.5251E+03	0.1640E+02	0.6417E+03
0.1725E+02	0.3743E+00	0.1725E+02	0.6796E+02	0.1725E+02	0.3151E+03	0.1725E+02	0.2525E+03	0.1725E+02	0.2525E+03
0.1825E+02	0.0	0.1825E+02	0.1072E+02	0.1825E+02	0.4857E+02	0.1825E+02	0.1047E+03	0.1825E+02	0.1047E+03
0.1925E+02	0.0	0.1925E+02	0.0	0.1925E+02	0.0	0.1925E+02	0.0	0.1925E+02	0.0
0.2025E+02	0.0	0.2025E+02	0.0	0.2025E+02	0.0	0.2025E+02	0.0	0.2025E+02	0.0
0.2100E+02	0.0	0.2100E+02	0.0	0.2100E+02	0.0	0.2100E+02	0.0	0.2100E+02	0.0

Y=0.31750E+02

Y=0.32750E+02

Y=0.33750E+02

Y=

X	P	X	P	X	P
0.1100E+02	0.5219E+01	0.1100E+02	0.1028E-07	0.1100E+02	0.2379E-22
0.1160E+02	0.5096E+03	0.1160E+02	0.6261E-03	0.1160E+02	0.1967E-14
0.1220E+02	0.9277E+03	0.1220E+02	0.1052E+00	0.1220E+02	0.8080E-10
0.1280E+02	0.8449E+03	0.1280E+02	0.7742E+00	0.1280E+02	0.3556E-07
0.1340E+02	0.9385E+03	0.1340E+02	0.1634E+01	0.1340E+02	0.1237E-05
0.1400E+02	0.9819E+03	0.1400E+02	0.7007E+01	0.1400E+02	0.8322E-05
0.1460E+02	0.1032E+04	0.1460E+02	0.1527E+02	0.1460E+02	0.2654E-02
0.1520E+02	0.1049E+04	0.1520E+02	0.1905E+02	0.1520E+02	0.1067E-01
0.1580E+02	0.7508E+03	0.1580E+02	0.1695E+02	0.1580E+02	0.3368E-04
0.1640E+02	0.4242E+03	0.1640E+02	0.1195E+02	0.1640E+02	0.1015E-03
0.1725E+02	0.1320E+03	0.1725E+02	0.2130E+01	0.1725E+02	0.1975E-04
0.1825E+02	0.2035E+02	0.1825E+02	0.0	0.1825E+02	0.0
0.1925E+02	0.0	0.1925E+02	0.0	0.1925E+02	0.0
0.2025E+02	0.0	0.2025E+02	0.0	0.2025E+02	0.0
0.2100E+02	0.0	0.2100E+02	0.0	0.2100E+02	0.0

TIME STEP= 10 TIME=0.743553E-03 SEC

Y=0.27000E+02

Y=0.28000E+02

Y=0.29000E+02

Y=0.30000E+02

Y=0.30750E+02

X	P	X	P	X	P	X	P	X	P
0.1100E+02	0.8094E-11	0.1100E+02	0.1259E+00	0.1100E+02	0.9760E+03	0.1100E+02	0.1688E+04	0.1100E+02	0.1688E+04
0.1160E+02	0.3641E-05	0.1160E+02	0.6397E+02	0.1160E+02	0.2620E+04	0.1160E+02	0.2436E+04	0.1160E+02	0.2436E+04
0.1220E+02	0.1799E-02	0.1220E+02	0.2621E+03	0.1220E+02	0.2524E+04	0.1220E+02	0.1722E+04	0.1220E+02	0.1722E+04
0.1280E+02	0.3144E-01	0.1280E+02	0.3215E+03	0.1280E+02	0.2644E+04	0.1280E+02	0.2606E+04	0.1280E+02	0.2649E+04
0.1340E+02	0.1162E+00	0.1340E+02	0.2780E+03	0.1340E+02	0.2557E+04	0.1340E+02	0.2178E+04	0.1340E+02	0.2624E+04
0.1400E+02	0.8905E+00	0.1400E+02	0.4566E+03	0.1400E+02	0.2656E+04	0.1400E+02	0.2626E+04	0.1400E+02	0.2626E+04
0.1460E+02	0.2798E+01	0.1460E+02	0.4644E+03	0.1460E+02	0.2613E+04	0.1460E+02	0.2302E+04	0.1460E+02	0.2613E+04
0.1520E+02	0.4415E+01	0.1520E+02	0.5493E+03	0.1520E+02	0.2418E+04	0.1520E+02	0.1798E+04	0.1520E+02	0.2509E+04
0.1580E+02	0.4596E+01	0.1580E+02	0.5694E+03	0.1580E+02	0.2101E+04	0.1580E+02	0.1327E+04	0.1580E+02	0.2216E+04
0.1640E+02	0.3608E+01	0.1640E+02	0.4625E+03	0.1640E+02	0.1629E+04	0.1640E+02	0.9476E+03	0.1640E+02	0.1741E+04
0.1725E+02	0.3743E+00	0.1725E+02	0.2619E+03	0.1725E+02	0.9121E+03	0.1725E+02	0.5702E+03	0.1725E+02	0.9861E+03
0.1825E+02	0.0	0.1825E+02	0.1072E+02	0.1825E+02	0.3329E+03	0.1825E+02	0.3058E+03	0.1825E+02	0.3622E+03
0.1925E+02	0.0	0.1925E+02	0.0	0.1925E+02	0.0	0.1925E+02	0.0	0.1925E+02	0.0
0.2025E+02	0.0	0.2025E+02	0.0	0.2025E+02	0.0	0.2025E+02	0.0	0.2025E+02	0.0
0.2100E+02	0.0	0.2100E+02	0.0	0.2100E+02	0.0	0.2100E+02	0.0	0.2100E+02	0.0

Y=0.31750E+02

Y=0.32750E+02

Y=0.33750E+02

Y=

X	P	X	P	X	P
0.1100E+02	0.5219E+01	0.1100E+02	0.1028E-07	0.1100E+02	0.2379E-22
0.1160E+02	0.5096E+03	0.1160E+02	0.8261E-03	0.1160E+02	0.1967E-14
0.1220E+02	0.9277E+03	0.1220E+02	0.1052E+00	0.1220E+02	0.6080E-10
0.1280E+02	0.8449E+03	0.1280E+02	0.7742E+00	0.1280E+02	0.3556E-07
0.1340E+02	0.9385E+03	0.1340E+02	0.1634E+01	0.1340E+02	0.1237E-05
0.1400E+02	0.9819E+03	0.1400E+02	0.7007E+01	0.1400E+02	0.8322E-05
0.1460E+02	0.1032E+04	0.1460E+02	0.1527E+02	0.1460E+02	0.2654E-02
0.1520E+02	0.1098E+04	0.1520E+02	0.1905E+02	0.1520E+02	0.1067E-01
0.1580E+02	0.1005E+04	0.1580E+02	0.2673E+02	0.1580E+02	0.3368E-04
0.1640E+02	0.7733E+03	0.1640E+02	0.3271E+02	0.1640E+02	0.1015E-03
0.1725E+02	0.4234E+03	0.1725E+02	0.5400E+01	0.1725E+02	0.1975E-04
0.1825E+02	0.2035E+02	0.1825E+02	0.1255E-01	0.1825E+02	0.0
0.1925E+02	0.0	0.1925E+02	0.0	0.1925E+02	0.0
0.2025E+02	0.0	0.2025E+02	0.0	0.2025E+02	0.0
0.2100E+02	0.0	0.2100E+02	0.0	0.2100E+02	0.0

ORIGINAL PAGE IS
OF POOR QUALITY

TIME STEP= 11 TIME=0.873301E-03 SEC

Y=0.27000E+02

Y=0.28000E+02

Y=0.29000E+02

Y=0.30000E+02

Y=0.30750E+02

X	P	X	P	X	P	X	P	X	P
0.1100E+02	0.8094E-11	0.1100E+02	0.1259E+00	0.1100E+02	0.9760E+03	0.1100E+02	0.1688E+04	0.1100E+02	0.1688E+04
0.1160E+02	0.3641E-05	0.1160E+02	0.6397E+02	0.1160E+02	0.2620E+04	0.1160E+02	0.2436E+04	0.1160E+02	0.2436E+04
0.1220E+02	0.1799E-02	0.1220E+02	0.2621E+03	0.1220E+02	0.2524E+04	0.1220E+02	0.1722E+04	0.1220E+02	0.1722E+04
0.1280E+02	0.3144E-01	0.1280E+02	0.3215E+03	0.1280E+02	0.2644E+04	0.1280E+02	0.2606E+04	0.1280E+02	0.2649E+04
0.1340E+02	0.1162E+00	0.1340E+02	0.2780E+03	0.1340E+02	0.2557E+04	0.1340E+02	0.2178E+04	0.1340E+02	0.2624E+04
0.1400E+02	0.8995E+00	0.1400E+02	0.4566E+03	0.1400E+02	0.2656E+04	0.1400E+02	0.2626E+04	0.1400E+02	0.2626E+04
0.1460E+02	0.2798E+01	0.1460E+02	0.4644E+03	0.1460E+02	0.2613E+04	0.1460E+02	0.2306E+04	0.1460E+02	0.2613E+04
0.1520E+02	0.4415E+01	0.1520E+02	0.5507E+03	0.1520E+02	0.2418E+04	0.1520E+02	0.1805E+04	0.1520E+02	0.2509E+04
0.1580E+02	0.5960E+01	0.1580E+02	0.5725E+03	0.1580E+02	0.2105E+04	0.1580E+02	0.1333E+04	0.1580E+02	0.2219E+04
0.1640E+02	0.9039E+01	0.1640E+02	0.4659E+03	0.1640E+02	0.1634E+04	0.1640E+02	0.9529E+03	0.1640E+02	0.1746E+04
0.1725E+02	0.8508E+01	0.1725E+02	0.2643E+03	0.1725E+02	0.9170E+03	0.1725E+02	0.5740E+03	0.1725E+02	0.9911E+03
0.1825E+02	0.9169E-01	0.1825E+02	0.9726E+02	0.1825E+02	0.3354E+03	0.1825E+02	0.3081E+03	0.1825E+02	0.3648E+03
0.1925E+02	0.0	0.1925E+02	0.0	0.1925E+02	0.0	0.1925E+02	0.0	0.1925E+02	0.0
0.2025E+02	0.0	0.2025E+02	0.0	0.2025E+02	0.0	0.2025E+02	0.0	0.2025E+02	0.0
0.2100E+02	0.0	0.2100E+02	0.0	0.2100E+02	0.0	0.2100E+02	0.0	0.2100E+02	0.0

Y=0.31750E+02

Y=0.32750E+02

Y=0.33750E+02

Y=

X	P	X	P	X	P
0.1100E+02	0.5219E+01	0.1100E+02	0.1028E-07	0.1100E+02	0.2379E-22
0.1160E+02	0.5096E+03	0.1160E+02	0.8261E-03	0.1160E+02	0.1967E-14
0.1220E+02	0.9277E+03	0.1220E+02	0.1052E+00	0.1220E+02	0.8080E-10
0.1280E+02	0.8449E+03	0.1260E+02	0.7742E+00	0.1280E+02	0.3556E-07
0.1340E+02	0.9385E+03	0.1340E+02	0.1634E+01	0.1340E+02	0.3745E-05
0.1400E+02	0.9819E+03	0.1400E+02	0.7007E+01	0.1400E+02	0.2303E-03
0.1460E+02	0.1032E+04	0.1460E+02	0.1527E+02	0.1460E+02	0.2654E-02
0.1520E+02	0.1100E+04	0.1520E+02	0.1905E+02	0.1520E+02	0.1067E-01
0.1580E+02	0.1009E+04	0.1580E+02	0.2701E+02	0.1580E+02	0.2164E-01
0.1640E+02	0.7778E+03	0.1640E+02	0.3313E+02	0.1640E+02	0.2750E-01
0.1725E+02	0.4267E+03	0.1725E+02	0.2592E+02	0.1725E+02	0.2359E-03
0.1825E+02	0.1541E+03	0.1825E+02	0.4369E+00	0.1825E+02	0.0
0.1925E+02	0.0	0.1925E+02	0.0	0.1925E+02	0.0
0.2025E+02	0.0	0.2025E+02	0.0	0.2025E+02	0.0
0.2100E+02	0.0	0.2100E+02	0.0	0.2100E+02	0.0

ORIGINAL PAGE IS
OF POOR QUALITY

TIME STEP= 12 TIME=0.962933E-03 SEC

Y=0.27000E+02		Y=0.28000E+02		Y=0.29000E+02		Y=0.30000E+02		Y=0.30750E+02	
X	P	X	P	X	P	X	P	X	P
0.1100E+02	0.8094E-11	0.1100E+02	0.1259E+00	0.1100E+02	0.9760E+03	0.1100E+02	0.1688E+04	0.1100E+02	0.1688E+04
0.1160E+02	0.3641E-05	0.1160E+02	0.6397E+02	0.1160E+02	0.2620E+04	0.1160E+02	0.2436E+04	0.1160E+02	0.2436E+04
0.1220E+02	0.1799E-02	0.1220E+02	0.2621E+03	0.1220E+02	0.2524E+04	0.1220E+02	0.1722E+04	0.1220E+02	0.1722E+04
0.1280E+02	0.3144E-01	0.1280E+02	0.3215E+03	0.1280E+02	0.2644E+04	0.1280E+02	0.2606E+04	0.1280E+02	0.2649E+04
0.1340E+02	0.1162E+00	0.1340E+02	0.2780E+03	0.1340E+02	0.2557E+04	0.1340E+02	0.2178E+04	0.1340E+02	0.2624E+04
0.1400E+02	0.8995E+00	0.1400E+02	0.4566E+03	0.1400E+02	0.2656E+04	0.1400E+02	0.2626E+04	0.1400E+02	0.2626E+04
0.1460E+02	0.2798E+01	0.1460E+02	0.4644E+03	0.1460E+02	0.2613E+04	0.1460E+02	0.2306E+04	0.1460E+02	0.2613E+04
0.1520E+02	0.4415E+01	0.1520E+02	0.5507E+03	0.1520E+02	0.2594E+04	0.1520E+02	0.2561E+04	0.1520E+02	0.2561E+04
0.1580E+02	0.5960E+01	0.1580E+02	0.5725E+03	0.1580E+02	0.2583E+04	0.1580E+02	0.2210E+04	0.1580E+02	0.2219E+04
0.1640E+02	0.9039E+01	0.1640E+02	0.5294E+03	0.1640E+02	0.2371E+04	0.1640E+02	0.1546E+04	0.1640E+02	0.1746E+04
0.1725E+02	0.8508E+01	0.1725E+02	0.3720E+03	0.1725E+02	0.1505E+04	0.1725E+02	0.8234E+03	0.1725E+02	0.9911E+03
0.1825E+02	0.8861E+00	0.1825E+02	0.1181E+03	0.1825E+02	0.4772E+03	0.1825E+02	0.3639E+03	0.1825E+02	0.3648E+03
0.1925E+02	0.0	0.1925E+02	0.2051E+02	0.1925E+02	0.8169E+02	0.1925E+02	0.1557E+03	0.1925E+02	0.1557E+03
0.2025E+02	0.0	0.2025E+02	0.0	0.2025E+02	0.0	0.2025E+02	0.0	0.2025E+02	0.0
0.2100E+02	0.0	0.2100E+02	0.0	0.2100E+02	0.0	0.2100E+02	0.0	0.2100E+02	0.0

Y=0.31750E+02

Y=0.32750E+02

Y=0.33750E+02

Y=

X	P	X	P	X	P
0.1100E+02	0.5219E+01	0.1100E+02	0.1028E-07	0.1100E+02	0.2379E-22
0.1160E+02	0.5096E+03	0.1160E+02	0.8261E-03	0.1160E+02	0.1967E-14
0.1220E+02	0.9277E+03	0.1220E+02	0.1052E+00	0.1220E+02	0.8080E-10
0.1280E+02	0.8449E+03	0.1280E+02	0.7742E+00	0.1280E+02	0.3556E-07
0.1340E+02	0.9385E+03	0.1340E+02	0.1634E+01	0.1340E+02	0.3745E-05
0.1400E+02	0.9819E+03	0.1400E+02	0.7007E+01	0.1400E+02	0.2303E-03
0.1460E+02	0.1032E+04	0.1460E+02	0.1527E+02	0.1460E+02	0.2654E-02
0.1520E+02	0.1100E+04	0.1520E+02	0.1905E+02	0.1520E+02	0.1067E-01
0.1580E+02	0.1082E+04	0.1580E+02	0.2701E+02	0.1580E+02	0.2164E-01
0.1640E+02	0.1184E+04	0.1640E+02	0.3313E+02	0.1640E+02	0.2750E-01
0.1725E+02	0.7183E+03	0.1725E+02	0.2592E+02	0.1725E+02	0.2209E-01
0.1825E+02	0.2180E+03	0.1825E+02	0.1164E+02	0.1825E+02	0.3595E-05
0.1925E+02	0.3707E+02	0.1925E+02	0.0	0.1925E+02	0.0
0.2025E+02	0.0	0.2025E+02	0.0	0.2025E+02	0.0
0.2100E+02	0.0	0.2100E+02	0.0	0.2100E+02	0.0

ORIGINAL PAGE IS
OF POOR QUALITY

TIME STEP= 13 TIME=0.970919E-03 SEC

Y=0.27000E+02		Y=0.28000E+02		Y=0.29000E+02		Y=0.30000E+02		Y=0.30750E+02	
X	P	X	P	X	P	X	P	X	P
0.1100E+02	0.8094E-11	0.1100E+02	0.1259E+00	0.1100E+02	0.9760E+03	0.1100E+02	0.1688E+04	0.1100E+02	0.1688E+04
0.1160E+02	0.3641E-05	0.1160E+02	0.6397E+02	0.1160E+02	0.2620E+04	0.1160E+02	0.2436E+04	0.1160E+02	0.2436E+04
0.1220E+02	0.1799E-02	0.1220E+02	0.2621E+03	0.1220E+02	0.2524E+04	0.1220E+02	0.1722E+04	0.1220E+02	0.1722E+04
0.1280E+02	0.3144E-01	0.1280E+02	0.3215E+03	0.1280E+02	0.2644E+04	0.1280E+02	0.2606E+04	0.1280E+02	0.2649E+04
0.1340E+02	0.1162E+00	0.1340E+02	0.2780E+03	0.1340E+02	0.2557E+04	0.1340E+02	0.2178E+04	0.1340E+02	0.2624E+04
0.1400E+02	0.8995E+00	0.1400E+02	0.4566E+03	0.1400E+02	0.2656E+04	0.1400E+02	0.2626E+04	0.1400E+02	0.2626E+04
0.1460E+02	0.2798E+01	0.1460E+02	0.4644E+03	0.1460E+02	0.2613E+04	0.1460E+02	0.2306E+04	0.1460E+02	0.2613E+04
0.1520E+02	0.4415E+01	0.1520E+02	0.5507E+03	0.1520E+02	0.2594E+04	0.1520E+02	0.2561E+04	0.1520E+02	0.2561E+04
0.1580E+02	0.5960E+01	0.1580E+02	0.5725E+03	0.1580E+02	0.2583E+04	0.1580E+02	0.2210E+04	0.1580E+02	0.2219E+04
0.1640E+02	0.9039E+01	0.1640E+02	0.5294E+03	0.1640E+02	0.2371E+04	0.1640E+02	0.1546E+04	0.1640E+02	0.1746E+04
0.1725E+02	0.8508E+01	0.1725E+02	0.3720E+03	0.1725E+02	0.1864E+04	0.1725E+02	0.1864E+04	0.1725E+02	0.1864E+04
0.1825E+02	0.8861E+00	0.1825E+02	0.1181E+03	0.1825E+02	0.6178E+03	0.1825E+02	0.6178E+03	0.1825E+02	0.6178E+03
0.1925E+02	0.0	0.1925E+02	0.2051E+02	0.1925E+02	0.8169E+02	0.1925E+02	0.1557E+03	0.1925E+02	0.1557E+03
0.2025E+02	0.0	0.2025E+02	0.0	0.2025E+02	0.0	0.2025E+02	0.0	0.2025E+02	0.0
0.2100E+02	0.0	0.2100E+02	0.0	0.2100E+02	0.0	0.2100E+02	0.0	0.2100E+02	0.0

Y=0.31750E+02

Y=0.32750E+02

Y=0.33750E+02

Y=

X	P	X	P	X	P
0.1100E+02	0.5219E+01	0.1100E+02	0.1028E-07	0.1100E+02	0.2379E-22
0.1160E+02	0.5096E+03	0.1160E+02	0.8261E-03	0.1160E+02	0.1967E-14
0.1220E+02	0.9277E+03	0.1220E+02	0.1052E+00	0.1220E+02	0.8080E-10
0.1280E+02	0.8449E+03	0.1280E+02	0.7742E+00	0.1280E+02	0.3556E-07
0.1340E+02	0.9385E+03	0.1340E+02	0.1634E+01	0.1340E+02	0.3745E-05
0.1400E+02	0.9819E+03	0.1400E+02	0.7007E+01	0.1400E+02	0.2303E-03
0.1460E+02	0.1032E+04	0.1460E+02	0.1527E+02	0.1460E+02	0.2654E-02
0.1520E+02	0.1100E+04	0.1520E+02	0.1905E+02	0.1520E+02	0.1067E-01
0.1580E+02	0.1082E+04	0.1580E+02	0.2701E+02	0.1580E+02	0.2164E-01
0.1640E+02	0.1184E+04	0.1640E+02	0.3313E+02	0.1640E+02	0.2750E-01
0.1725E+02	0.7183E+03	0.1725E+02	0.2592E+02	0.1725E+02	0.2209E-01
0.1825E+02	0.2228E+03	0.1825E+02	0.1164E+02	0.1825E+02	0.3595E-05
0.1925E+02	0.3707E+02	0.1925E+02	0.0	0.1925E+02	0.0
0.2025E+02	0.0	0.2025E+02	0.0	0.2025E+02	0.0
0.2100E+02	0.0	0.2100E+02	0.0	0.2100E+02	0.0

ORIGINAL PAGE IS
OF POOR QUALITY

TIME STEP= 14 TIME=0.100438E-02 SEC

Y=0.27000E+02		Y=0.28000E+02		Y=0.29000E+02		Y=0.30000E+02		Y=0.30750E+02	
X	P	X	P	X	P	X	P	X	P
0.1100E+02	0.8094E-11	0.1100E+02	0.1259E+00	0.1100E+02	0.9760E+03	0.1100E+02	0.1688E+04	0.1100E+02	0.1688E+04
0.1160E+02	0.3641E-05	0.1160E+02	0.6397E+02	0.1160E+02	0.2620E+04	0.1160E+02	0.2436E+04	0.1160E+02	0.2436E+04
0.1220E+02	0.1799E-02	0.1220E+02	0.2621E+03	0.1220E+02	0.2524E+04	0.1220E+02	0.1722E+04	0.1220E+02	0.1722E+04
0.1280E+02	0.3144E-01	0.1280E+02	0.3215E+03	0.1280E+02	0.2644E+04	0.1280E+02	0.2606E+04	0.1280E+02	0.2649E+04
0.1340E+02	0.1162E+00	0.1340E+02	0.2780E+03	0.1340E+02	0.2557E+04	0.1340E+02	0.2178E+04	0.1340E+02	0.2624E+04
0.1400E+02	0.8995E+00	0.1400E+02	0.4566E+03	0.1400E+02	0.2656E+04	0.1400E+02	0.2626E+04	0.1400E+02	0.2626E+04
0.1460E+02	0.2798E+01	0.1460E+02	0.4644E+03	0.1460E+02	0.2613E+04	0.1460E+02	0.2306E+04	0.1460E+02	0.2613E+04
0.1520E+02	0.4415E+01	0.1520E+02	0.5507E+03	0.1520E+02	0.2594E+04	0.1520E+02	0.2561E+04	0.1520E+02	0.2561E+04
0.1580E+02	0.5960E+01	0.1580E+02	0.5725E+03	0.1580E+02	0.2583E+04	0.1580E+02	0.2210E+04	0.1580E+02	0.2219E+04
0.1640E+02	0.9039E+01	0.1640E+02	0.5294E+03	0.1640E+02	0.2371E+04	0.1640E+02	0.1546E+04	0.1640E+02	0.1746E+04
0.1725E+02	0.8508E+01	0.1725E+02	0.3720E+03	0.1725E+02	0.1974E+04	0.1725E+02	0.1974E+04	0.1725E+02	0.1974E+04
0.1825E+02	0.4323E+01	0.1825E+02	0.1181E+03	0.1825E+02	0.6836E+03	0.1825E+02	0.6836E+03	0.1825E+02	0.6836E+03
0.1925E+02	0.0	0.1925E+02	0.2051E+02	0.1925E+02	0.1767E+03	0.1925E+02	0.1767E+03	0.1925E+02	0.1767E+03
0.2025E+02	0.0	0.2025E+02	0.0	0.2025E+02	0.0	0.2025E+02	0.0	0.2025E+02	0.0
0.2100E+02	0.0	0.2100E+02	0.0	0.2100E+02	0.0	0.2100E+02	0.0	0.2100E+02	0.0

Y=0.31750E+02

Y=0.32750E+02

Y=0.33750E+02

Y=

X	P	X	P	X	P
0.1100E+02	0.5219E+01	0.1100E+02	0.1028E-07	0.1100E+02	0.2379E-22
0.1160E+02	0.5096E+03	0.1160E+02	0.8261E-03	0.1160E+02	0.1967E-14
0.1220E+02	0.9277E+03	0.1220E+02	0.1052E+00	0.1220E+02	0.8080E-10
0.1280E+02	0.8449E+03	0.1280E+02	0.7742E+00	0.1280E+02	0.3556E-07
0.1340E+02	0.9385E+03	0.1340E+02	0.1634E+01	0.1340E+02	0.3745E-05
0.1400E+02	0.9819E+03	0.1400E+02	0.7007E+01	0.1400E+02	0.2303E-03
0.1460E+02	0.1032E+04	0.1460E+02	0.1527E+02	0.1460E+02	0.2654E-02
0.1520E+02	0.1100E+04	0.1520E+02	0.1905E+02	0.1520E+02	0.1067E-01
0.1580E+02	0.1082E+04	0.1580E+02	0.2701E+02	0.1580E+02	0.2164E-01
0.1640E+02	0.1184E+04	0.1640E+02	0.3313E+02	0.1640E+02	0.4424E-01
0.1725E+02	0.7183E+03	0.1725E+02	0.2592E+02	0.1725E+02	0.2209E-01
0.1825E+02	0.2589E+03	0.1825E+02	0.1164E+02	0.1825E+02	0.1401E-03
0.1925E+02	0.3707E+02	0.1925E+02	0.6936E-03	0.1925E+02	0.0
0.2025E+02	0.0	0.2025E+02	0.0	0.2025E+02	0.0
0.2100E+02	0.0	0.2100E+02	0.0	0.2100E+02	0.0

TIME STEP= 15 TIME=0.128215E-02 SEC

Y=0.27000E+02

Y=0.28000E+02

Y=0.29000E+02

Y=0.30000E+02

Y=0.30750E+02

X	P	X	P	X	P	X	P	X	P
0.1100E+02	0.0	0.1100E+02	0.0	0.1100E+02	0.0	0.1100E+02	0.4596E-01	0.1100E+02	0.4596E-01
0.1160E+02	0.0	0.1160E+02	0.0	0.1160E+02	0.0	0.1160E+02	0.5234E+00	0.1160E+02	0.5234E+00
0.1220E+02	0.0	0.1220E+02	0.3767E-16	0.1220E+02	0.0	0.1220E+02	0.0	0.1220E+02	0.0
0.1280E+02	0.0	0.1280E+02	0.0	0.1280E+02	0.0	0.1280E+02	0.0	0.1280E+02	0.0
0.1340E+02	0.0	0.1340E+02	0.0	0.1340E+02	0.0	0.1340E+02	0.6472E+01	0.1340E+02	0.6472E+01
0.1400E+02	0.6349E-22	0.1400E+02	0.0	0.1400E+02	0.0	0.1400E+02	0.0	0.1400E+02	0.0
0.1460E+02	0.0	0.1460E+02	0.0	0.1460E+02	0.0	0.1460E+02	0.0	0.1460E+02	0.0
0.1520E+02	0.0	0.1520E+02	0.0	0.1520E+02	0.3020E+01	0.1520E+02	0.3020E+01	0.1520E+02	0.3020E+01
0.1580E+02	0.0	0.1580E+02	0.5293E-16	0.1580E+02	0.0	0.1580E+02	0.0	0.1580E+02	0.0
0.1640E+02	0.1710E-16	0.1640E+02	0.0	0.1640E+02	0.0	0.1640E+02	0.0	0.1640E+02	0.0
0.1725E+02	0.0	0.1725E+02	0.0	0.1725E+02	0.0	0.1725E+02	0.0	0.1725E+02	0.0
0.1825E+02	0.1936E-03	0.1825E+02	0.2196E-09	0.1825E+02	0.2041E+00	0.1825E+02	0.2041E+00	0.1825E+02	0.2041E+00
0.1925E+02	0.2430E+00	0.1925E+02	0.1824E-01	0.1925E+02	0.9292E-01	0.1925E+02	0.9554E+01	0.1925E+02	0.9554E+01
0.2025E+02	0.5118E-05	0.2025E+02	0.2064E+01	0.2025E+02	0.4883E+02	0.2025E+02	0.8568E+02	0.2025E+02	0.6582E+02
0.2100E+02	0.0	0.2100E+02	0.0	0.2100E+02	0.0	0.2100E+02	0.0	0.2100E+02	0.0

Y=0.31750E+02

Y=0.32750E+02

Y=0.33750E+02

Y=

X	P	X	P	X	P
0.1100E+02	0.0	0.1100E+02	0.0	0.1100E+02	0.0
0.1160E+02	0.0	0.1160E+02	0.0	0.1160E+02	0.0
0.1220E+02	0.0	0.1220E+02	0.0	0.1220E+02	0.0
0.1280E+02	0.0	0.1280E+02	0.0	0.1280E+02	0.0
0.1340E+02	0.0	0.1340E+02	0.0	0.1340E+02	0.3107E-11
0.1400E+02	0.0	0.1400E+02	0.2398E-19	0.1400E+02	0.0
0.1460E+02	0.0	0.1460E+02	0.0	0.1460E+02	0.1078E-19
0.1520E+02	0.0	0.1520E+02	0.0	0.1520E+02	0.3154E-12
0.1580E+02	0.0	0.1580E+02	0.8140E-27	0.1580E+02	0.0
0.1640E+02	0.0	0.1640E+02	0.0	0.1640E+02	0.0
0.1725E+02	0.0	0.1725E+02	0.0	0.1725E+02	0.8617E-18
0.1825E+02	0.9930E-09	0.1825E+02	0.1228E-12	0.1825E+02	0.8359E-03
0.1925E+02	0.3604E-01	0.1925E+02	0.1044E+01	0.1925E+02	0.5668E-03
0.2025E+02	0.3682E+01	0.2025E+02	0.1215E+00	0.2025E+02	0.0
0.2100E+02	0.0	0.2100E+02	0.0	0.2100E+02	0.0

ORIGINAL PAGE IS
OF POOR QUALITY

TIME STEP= 17 TIME=0.183769E-02 SEC

Y=0.27000E+02		Y=0.28000E+02		Y=0.29000E+02		Y=0.30000E+02		Y=0.30750E+02	
X	P	X	P	X	P	X	P	X	P
0.1100E+02	0.0	0.1100E+02	0.0	0.1100E+02	0.0	0.1100E+02	0.1034E-02	0.1100E+02	0.1034E-02
0.1160E+02	0.0	0.1160E+02	0.0	0.1160E+02	0.0	0.1160E+02	0.9199E-02	0.1160E+02	0.9199E-02
0.1220E+02	0.0	0.1220E+02	0.0	0.1220E+02	0.0	0.1220E+02	0.0	0.1220E+02	0.0
0.1280E+02	0.0	0.1280E+02	0.0	0.1280E+02	0.1242E-04	0.1280E+02	0.1242E-04	0.1280E+02	0.1242E-04
0.1340E+02	0.0	0.1340E+02	0.0	0.1340E+02	0.2758E-03	0.1340E+02	0.2758E-03	0.1340E+02	0.2758E-03
0.1400E+02	0.0	0.1400E+02	0.0	0.1400E+02	0.0	0.1400E+02	0.0	0.1400E+02	0.0
0.1460E+02	0.0	0.1460E+02	0.0	0.1460E+02	0.0	0.1460E+02	0.0	0.1460E+02	0.0
0.1520E+02	0.0	0.1520E+02	0.0	0.1520E+02	0.0	0.1520E+02	0.0	0.1520E+02	0.0
0.1580E+02	0.0	0.1580E+02	0.0	0.1580E+02	0.0	0.1580E+02	0.0	0.1580E+02	0.0
0.1640E+02	0.0	0.1640E+02	0.0	0.1640E+02	0.0	0.1640E+02	0.0	0.1640E+02	0.0
0.1725E+02	0.0	0.1725E+02	0.0	0.1725E+02	0.0	0.1725E+02	0.0	0.1725E+02	0.0
0.1825E+02	0.0	0.1825E+02	0.0	0.1825E+02	0.0	0.1825E+02	0.0	0.1825E+02	0.0
0.1925E+02	0.0	0.1925E+02	0.0	0.1925E+02	0.0	0.1925E+02	0.0	0.1925E+02	0.0
0.2025E+02	0.6407E-22	0.2025E+02	0.2879E-17	0.2025E+02	0.1083E-01	0.2025E+02	0.1083E-01	0.2025E+02	0.1083E-01
0.2100E+02	0.2918E-06	0.2100E+02	0.5584E-07	0.2100E+02	0.3600E-02	0.2100E+02	0.4272E+00	0.2100E+02	0.4272E+00

Y=0.31750E+02

Y=0.32750E+02

Y=0.33750E+02

Y=

X	P	X	P	X	P
0.1100E+02	0.0	0.1100E+02	0.0	0.1100E+02	0.0
0.1160E+02	0.0	0.1160E+02	0.0	0.1160E+02	0.0
0.1220E+02	0.0	0.1220E+02	0.0	0.1220E+02	0.0
0.1280E+02	0.0	0.1280E+02	0.0	0.1280E+02	0.0
0.1340E+02	0.0	0.1340E+02	0.0	0.1340E+02	0.0
0.1400E+02	0.0	0.1400E+02	0.0	0.1400E+02	0.0
0.1460E+02	0.0	0.1460E+02	0.0	0.1460E+02	0.0
0.1520E+02	0.0	0.1520E+02	0.0	0.1520E+02	0.0
0.1580E+02	0.0	0.1580E+02	0.0	0.1580E+02	0.0
0.1640E+02	0.0	0.1640E+02	0.0	0.1640E+02	0.0
0.1725E+02	0.0	0.1725E+02	0.0	0.1725E+02	0.0
0.1825E+02	0.0	0.1825E+02	0.0	0.1825E+02	0.0
0.1925E+02	0.0	0.1925E+02	0.0	0.1925E+02	0.0
0.2025E+02	0.1280E-16	0.2025E+02	0.1975E-20	0.2025E+02	0.3391E-10
0.2100E+02	0.1120E-06	0.2100E+02	0.1274E-05	0.2100E+02	0.2276E-04

TIME STEP= 19 TIME=0.239324E-02 SEC

Y=0.29000E+02

Y=0.30000E+02

Y=0.30750E+02

Y=

X	P	X	P	X	P
0.1100E+02	0.1134E-08	0.1100E+02	0.1134E-08	0.1100E+02	0.1134E-08
0.1160E+02	0.0	0.1160E+02	0.0	0.1160E+02	0.0
0.1220E+02	0.0	0.1220E+02	0.0	0.1220E+02	0.0
0.1280E+02	0.0	0.1280E+02	0.1014E-16	0.1280E+02	0.0
0.1340E+02	0.0	0.1340E+02	0.0	0.1340E+02	0.0
0.1400E+02	0.0	0.1400E+02	0.0	0.1400E+02	0.0
0.1460E+02	0.0	0.1460E+02	0.0	0.1460E+02	0.0
0.1520E+02	0.0	0.1520E+02	0.0	0.1520E+02	0.0
0.1580E+02	0.0	0.1580E+02	0.0	0.1580E+02	0.0
0.1640E+02	0.0	0.1640E+02	0.0	0.1640E+02	0.0
0.1725E+02	0.0	0.1725E+02	0.0	0.1725E+02	0.0
0.1825E+02	0.0	0.1825E+02	0.0	0.1825E+02	0.0
0.1925E+02	0.0	0.1925E+02	0.0	0.1925E+02	0.0
0.2025E+02	0.0	0.2025E+02	0.0	0.2025E+02	0.0
0.2100E+02	0.0	0.2100E+02	0.0	0.2100E+02	0.0

TIME STEP= 21 TIME=0.412041E-02 SEC

ALL NODE PRESSURES ARE ZERO

ORIGINAL PAGE IS
OF POOR QUALITY

TIME STEP= 53 TIME=0.505014E-01 SEC

ALL NODE PRESSURES ARE ZERO

TIME=0.181667E-03 SEC

DISPLACEMENTS AND BENDING STRESSES VS. RADIAL STATION

R	DISPLACEMENTS		RADIAL BENDING STRESS		
	IN-PLANE	OUT-OF-PLANE***LED-EDG	CHD-PNT	TRL-EDG	
0.27000E+02	0.38396E-02	-94973E-02 **	-92376E+03	-92376E+03	
0.28000E+02	0.29056E-02	-86260E-02 **	-84432E+03	-84432E+03	
0.29000E+02	0.19716E-02	-77548E-02 **	-73765E+03	-73765E+03	
0.30000E+02	0.10377E-02	-68835E-02 **	-67062E+03	-67062E+03	
0.30750E+02	0.33718E-03	-62300E-02 **	-61936E+03	-61936E+03	
0.31750E+02	-59680E-03	-53588E-02 **	-46211E+03	-46211E+03	
0.32750E+02	-15308E-02	-44875E-02 **	-30928E+03	-30928E+03	
0.33750E+02	-24647E-02	-36162E-02 **	-16801E+03	-16801E+03	

DISPLACEMENTS VS. CHORDWISE LOCATION
AT IMPACT RADIUS

X	IN-PLANE	OUT-OF-PLANE
0.0	0.13742E-01	-30523E-01
0.60000E+00	0.12452E-01	-28121E-01
0.12000E+01	0.10821E-01	-25087E-01
0.18000E+01	0.91905E-02	-22053E-01
0.24000E+01	0.75599E-02	-19019E-01
0.30000E+01	0.59294E-02	-15985E-01
0.36000E+01	0.42988E-02	-12951E-01
0.42000E+01	0.26682E-02	-99174E-02
0.48000E+01	0.10377E-02	-68835E-02
0.54000E+01	-59289E-03	-38496E-02
0.62500E+01	-29028E-02	0.44848E-03
0.72500E+01	-56205E-02	0.55050E-02
0.82500E+01	-83380E-02	0.10562E-01
0.92500E+01	-11056E-01	0.15618E-01
0.10000E+02	-13434E-01	0.20043E-01

STRESSES VS. CHORDWISE LOCATION
AT IMPACT RADIUS

STRESS-X				STRESS-Y				SHEAR-XY			
X	*R=0.2900E+02	*R=0.3000E+02	*R=0.3075E+02	*R=0.2900E+02	*R=0.3000E+02	*R=0.3075E+02	*R=0.2900E+02	*R=0.3000E+02	*R=0.3075E+02	*R=0.2900E+02	*R=0.3000E+02
0.0	0.1546E+04	0.1431E+04	0.1343E+04	-7377E+03	-6706E+03	-6194E+03	0.1102E+04	0.1102E+04	0.1101E+04	0.1102E+04	0.1102E+04
0.6000E+00	0.1546E+04	0.1431E+04	0.1343E+04	-7377E+03	-6706E+03	-6194E+03	0.1102E+04	0.1102E+04	0.1101E+04	0.1102E+04	0.1102E+04
0.1200E+01	0.1546E+04	0.1431E+04	0.1343E+04	-7377E+03	-6706E+03	-6194E+03	0.1102E+04	0.1102E+04	0.1101E+04	0.1102E+04	0.1102E+04
0.1800E+01	0.1546E+04	0.1431E+04	0.1343E+04	-7377E+03	-6706E+03	-6194E+03	0.1102E+04	0.1102E+04	0.1101E+04	0.1102E+04	0.1102E+04
0.2400E+01	0.1546E+04	0.1431E+04	0.1343E+04	-7377E+03	-6706E+03	-6194E+03	0.1102E+04	0.1102E+04	0.1101E+04	0.1102E+04	0.1102E+04
0.3000E+01	0.1546E+04	0.1431E+04	0.1343E+04	-7377E+03	-6706E+03	-6194E+03	0.1102E+04	0.1102E+04	0.1101E+04	0.1102E+04	0.1102E+04
0.3600E+01	0.1546E+04	0.1431E+04	0.1343E+04	-7377E+03	-6706E+03	-6194E+03	0.1102E+04	0.1102E+04	0.1101E+04	0.1102E+04	0.1102E+04
0.4200E+01	0.1546E+04	0.1431E+04	0.1343E+04	-7377E+03	-6706E+03	-6194E+03	0.1102E+04	0.1102E+04	0.1101E+04	0.1102E+04	0.1102E+04
0.4800E+01	0.1546E+04	0.1431E+04	0.1343E+04	-7377E+03	-6706E+03	-6194E+03	0.1102E+04	0.1102E+04	0.1101E+04	0.1102E+04	0.1102E+04
0.5400E+01	0.1546E+04	0.1431E+04	0.1343E+04	-7377E+03	-6706E+03	-6194E+03	0.1102E+04	0.1102E+04	0.1101E+04	0.1102E+04	0.1102E+04

0.6250E+01 * 0.1546E+04 * 0.1431E+04 * 0.1343E+04 * -.7377E+03 * -.6706E+03 * -.6194E+03 * 0.1102E+04 * 0.1102E+04 * 0.1101E+04
 0.7250E+01 * 0.1546E+04 * 0.1431E+04 * 0.1343E+04 * -.7377E+03 * -.6706E+03 * -.6194E+03 * 0.1102E+04 * 0.1102E+04 * 0.1101E+04
 0.8250E+01 * 0.1546E+04 * 0.1431E+04 * 0.1343E+04 * -.7377E+03 * -.6706E+03 * -.6194E+03 * 0.1102E+04 * 0.1102E+04 * 0.1101E+04
 0.9250E+01 * 0.1546E+04 * 0.1431E+04 * 0.1343E+04 * -.7377E+03 * -.6706E+03 * -.6194E+03 * 0.1102E+04 * 0.1102E+04 * 0.1101E+04
 0.1000E+02 * 0.1546E+04 * 0.1431E+04 * 0.1343E+04 * -.7377E+03 * -.6706E+03 * -.6194E+03 * 0.1102E+04 * 0.1102E+04 * 0.1101E+04

TIME=0.293143E-03 SEC

DISPLACEMENTS AND BENDING STRESSES VS. RADIAL STATION

R	DISPLACEMENTS		RADIAL BENDING STRESS		
	IN-PLANE	OUT-OF-PLANE***LED-EDG	CHD-FNT	TRL-EDG	
0.27000E+02	0.11612E-01	-.27797E-01 **	-.27163E+04	-.27163E+04	-.27163E+04
0.28000E+02	0.89131E-02	-.25282E-01 **	-.24721E+04	-.24721E+04	-.24721E+04
0.29000E+02	0.62145E-02	-.22768E-01 **	-.21562E+04	-.21562E+04	-.21562E+04
0.30000E+02	0.35159E-02	-.20253E-01 **	-.19576E+04	-.19576E+04	-.19576E+04
0.30750E+02	0.14920E-02	-.18367E-01 **	-.18058E+04	-.18058E+04	-.18058E+04
0.31750E+02	-.12066E-02	-.15852E-01 **	-.13400E+04	-.13400E+04	-.13400E+04
0.32750E+02	-.39051E-02	-.13337E-01 **	-.88745E+03	-.88745E+03	-.88745E+03
0.33750E+02	-.66037E-02	-.10822E-01 **	-.46949E+03	-.46949E+03	-.46949E+03

DISPLACEMENTS VS. CHORDWISE LOCATION AT IMPACT RADIUS

X	IN-PLANE	OUT-OF-PLANE
0.0	0.39496E-01	-.87165E-01
0.60000E+00	0.35840E-01	-.80366E-01
0.12000E+01	0.31223E-01	-.71779E-01
0.18000E+01	0.26605E-01	-.63191E-01
0.24000E+01	0.21987E-01	-.54604E-01
0.30000E+01	0.17369E-01	-.46016E-01
0.36000E+01	0.12751E-01	-.37428E-01
0.42000E+01	0.81337E-02	-.28841E-01
0.48000E+01	0.35159E-02	-.20253E-01
0.54000E+01	-.11019E-02	-.11665E-01
0.62500E+01	-.76437E-02	0.50079E-03
0.72500E+01	-.15340E-01	0.14814E-01
0.82500E+01	-.23036E-01	0.29127E-01
0.92500E+01	-.30733E-01	0.43439E-01
0.10000E+02	-.37467E-01	0.55963E-01

STRESSES VS. CHORDWISE LOCATION AT IMPACT RADIUS

X	STRESS-X			STRESS-Y			SHEAR-XY		
	*R=0.2900E+02	*R=0.3000E+02	*R=0.3075E+02	*R=0.2900E+02	*R=0.3000E+02	*R=0.3075E+02	*R=0.2900E+02	*R=0.3000E+02	*R=0.3075E+02
0.0	* 0.4515E+04	* 0.4175E+04	* 0.3917E+04	* -.2156E+04	* -.1958E+04	* -.1806E+04	* 0.3103E+04	* 0.3103E+04	* 0.3102E+04
0.6000E+00	* 0.4515E+04	* 0.4175E+04	* 0.3917E+04	* -.2156E+04	* -.1958E+04	* -.1806E+04	* 0.3103E+04	* 0.3103E+04	* 0.3102E+04
0.1200E+01	* 0.4515E+04	* 0.4175E+04	* 0.3917E+04	* -.2156E+04	* -.1958E+04	* -.1806E+04	* 0.3103E+04	* 0.3103E+04	* 0.3102E+04
0.1800E+01	* 0.4515E+04	* 0.4175E+04	* 0.3917E+04	* -.2156E+04	* -.1958E+04	* -.1806E+04	* 0.3103E+04	* 0.3103E+04	* 0.3102E+04
0.2400E+01	* 0.4515E+04	* 0.4175E+04	* 0.3917E+04	* -.2156E+04	* -.1958E+04	* -.1806E+04	* 0.3103E+04	* 0.3103E+04	* 0.3102E+04
0.3000E+01	* 0.4515E+04	* 0.4175E+04	* 0.3917E+04	* -.2156E+04	* -.1958E+04	* -.1806E+04	* 0.3103E+04	* 0.3103E+04	* 0.3102E+04
0.3600E+01	* 0.4515E+04	* 0.4175E+04	* 0.3917E+04	* -.2156E+04	* -.1958E+04	* -.1806E+04	* 0.3103E+04	* 0.3103E+04	* 0.3102E+04
0.4200E+01	* 0.4515E+04	* 0.4175E+04	* 0.3917E+04	* -.2156E+04	* -.1958E+04	* -.1806E+04	* 0.3103E+04	* 0.3103E+04	* 0.3102E+04

0.4800E+01 * 0.4515E+04 * 0.4175E+04 * 0.3917E+04 * -.2156E+04 * -.1958E+04 * -.1806E+04 * 0.3103E+04 * 0.3103E+04 * 0.3102E+04
 0.5400E+01 * 0.4515E+04 * 0.4175E+04 * 0.3917E+04 * -.2156E+04 * -.1958E+04 * -.1806E+04 * 0.3103E+04 * 0.3103E+04 * 0.3102E+04
 0.6250E+01 * 0.4515E+04 * 0.4175E+04 * 0.3917E+04 * -.2156E+04 * -.1958E+04 * -.1806E+04 * 0.3103E+04 * 0.3103E+04 * 0.3102E+04
 0.7250E+01 * 0.4515E+04 * 0.4175E+04 * 0.3917E+04 * -.2156E+04 * -.1958E+04 * -.1806E+04 * 0.3103E+04 * 0.3103E+04 * 0.3102E+04
 0.8250E+01 * 0.4515E+04 * 0.4175E+04 * 0.3917E+04 * -.2156E+04 * -.1958E+04 * -.1806E+04 * 0.3103E+04 * 0.3103E+04 * 0.3102E+04
 0.9250E+01 * 0.4515E+04 * 0.4175E+04 * 0.3917E+04 * -.2156E+04 * -.1958E+04 * -.1806E+04 * 0.3103E+04 * 0.3103E+04 * 0.3102E+04
 0.1000E+02 * 0.4515E+04 * 0.4175E+04 * 0.3917E+04 * -.2156E+04 * -.1958E+04 * -.1806E+04 * 0.3103E+04 * 0.3103E+04 * 0.3102E+04

TIME=0.504719E-03 SEC

DISPLACEMENTS AND BENDING STRESSES VS. RADIAL STATION

R	DISPLACEMENTS		RADIAL BENDING STRESS		
	IN-PLANE	OUT-OF-PLANE***LED-EDG	CHD-PNT	TRL-EDG	
0.2700E+02	0.47263E-01	-.98679E-01 **	-.99224E+04	-.99224E+04	-.99224E+04
0.2800E+02	0.38198E-01	-.90341E-01 **	-.88456E+04	-.88456E+04	-.88456E+04
0.2900E+02	0.29132E-01	-.82003E-01 **	-.76535E+04	-.76535E+04	-.76535E+04
0.3000E+02	0.20067E-01	-.73664E-01 **	-.69043E+04	-.69043E+04	-.69043E+04
0.3075E+02	0.13268E-01	-.67411E-01 **	-.63314E+04	-.63314E+04	-.63314E+04
0.3175E+02	0.42026E-02	-.59073E-01 **	-.45733E+04	-.45733E+04	-.45733E+04
0.3275E+02	-.48626E-02	-.50735E-01 **	-.28672E+04	-.28672E+04	-.28672E+04
0.3375E+02	-.13928E-01	-.42396E-01 **	-.12980E+04	-.12980E+04	-.12980E+04

DISPLACEMENTS VS. CHORDWISE LOCATION
AT IMPACT RADIUS

X	IN-PLANE	OUT-OF-PLANE
0.0	0.12707E+00	-.27201E+00
0.6000E+00	0.11619E+00	-.25186E+00
0.1200E+01	0.10246E+00	-.22640E+00
0.1800E+01	0.88729E-01	-.20095E+00
0.2400E+01	0.74997E-01	-.17549E+00
0.3000E+01	0.61264E-01	-.15003E+00
0.3600E+01	0.47532E-01	-.12458E+00
0.4200E+01	0.33799E-01	-.99121E-01
0.4800E+01	0.20067E-01	-.73664E-01
0.5400E+01	0.63345E-02	-.48208E-01
0.6250E+01	-.13120E-01	-.12145E-01
0.7250E+01	-.36007E-01	0.30283E-01
0.8250E+01	-.58894E-01	0.72711E-01
0.9250E+01	-.81782E-01	0.11514E+00
0.1000E+02	-.10181E+00	0.15226E+00

STRESSES VS. CHORDWISE LOCATION
AT IMPACT RADIUS

X	STRESS-X				STRESS-Y				SHEAR-XY			
	NR=0.2900E+02	NR=0.3000E+02	NR=0.3075E+02	NR=0.2900E+02	NR=0.3000E+02	NR=0.3075E+02	NR=0.2900E+02	NR=0.3000E+02	NR=0.3075E+02			
0.0	* 0.1577E+05	* 0.1453E+05	* 0.1358E+05	* -.7654E+04	* -.6904E+04	* -.6331E+04	* 0.8916E+04	* 0.8915E+04	* 0.8913E+04			
0.6000E+00	* 0.1577E+05	* 0.1453E+05	* 0.1358E+05	* -.7654E+04	* -.6904E+04	* -.6331E+04	* 0.8916E+04	* 0.8915E+04	* 0.8913E+04			
0.1200E+01	* 0.1577E+05	* 0.1453E+05	* 0.1358E+05	* -.7654E+04	* -.6904E+04	* -.6331E+04	* 0.8916E+04	* 0.8915E+04	* 0.8913E+04			
0.1800E+01	* 0.1577E+05	* 0.1453E+05	* 0.1358E+05	* -.7654E+04	* -.6904E+04	* -.6331E+04	* 0.8916E+04	* 0.8915E+04	* 0.8913E+04			
0.2400E+01	* 0.1577E+05	* 0.1453E+05	* 0.1358E+05	* -.7654E+04	* -.6904E+04	* -.6331E+04	* 0.8916E+04	* 0.8915E+04	* 0.8913E+04			
0.3000E+01	* 0.1577E+05	* 0.1453E+05	* 0.1358E+05	* -.7654E+04	* -.6904E+04	* -.6331E+04	* 0.8916E+04	* 0.8915E+04	* 0.8913E+04			

0.3600E+01	* 0.1577E+05	* 0.1453E+05	* 0.1358E+05	* -.7654E+04	* -.6904E+04	* -.6331E+04	* 0.8916E+04	* 0.8915E+04	* 0.8913E+04
0.4200E+01	* 0.1577E+05	* 0.1453E+05	* 0.1358E+05	* -.7654E+04	* -.6904E+04	* -.6331E+04	* 0.8916E+04	* 0.8915E+04	* 0.8913E+04
0.4800E+01	* 0.1577E+05	* 0.1453E+05	* 0.1358E+05	* -.7654E+04	* -.6904E+04	* -.6331E+04	* 0.8916E+04	* 0.8915E+04	* 0.8913E+04
0.5400E+01	* 0.1577E+05	* 0.1453E+05	* 0.1358E+05	* -.7654E+04	* -.6904E+04	* -.6331E+04	* 0.8916E+04	* 0.8915E+04	* 0.8913E+04
0.6250E+01	* 0.1577E+05	* 0.1453E+05	* 0.1358E+05	* -.7654E+04	* -.6904E+04	* -.6331E+04	* 0.8916E+04	* 0.8915E+04	* 0.8913E+04
0.7250E+01	* 0.1577E+05	* 0.1453E+05	* 0.1358E+05	* -.7654E+04	* -.6904E+04	* -.6331E+04	* 0.8916E+04	* 0.8915E+04	* 0.8913E+04
0.8250E+01	* 0.1577E+05	* 0.1453E+05	* 0.1358E+05	* -.7654E+04	* -.6904E+04	* -.6331E+04	* 0.8916E+04	* 0.8915E+04	* 0.8913E+04
0.9250E+01	* 0.1577E+05	* 0.1453E+05	* 0.1358E+05	* -.7654E+04	* -.6904E+04	* -.6331E+04	* 0.8916E+04	* 0.8915E+04	* 0.8913E+04
0.1000E+02	* 0.1577E+05	* 0.1453E+05	* 0.1358E+05	* -.7654E+04	* -.6904E+04	* -.6331E+04	* 0.8916E+04	* 0.8915E+04	* 0.8913E+04

TIME=0.548717E-03 SEC

DISPLACEMENTS AND BENDING STRESSES VS. RADIAL STATION

R	DISPLACEMENTS		RADIAL BENDING STRESS		
	IN-PLANE	OUT-OF-PLANE***LED-EDG	CHD-FNT	TRL-EDG	
0.27000E+02	0.56903E-01	-.11976E+00 **	-.12111E+05	-.12111E+05	
0.28000E+02	0.48052E-01	-.10980E+00 **	-.10753E+05	-.10753E+05	
0.29000E+02	0.37201E-01	-.99841E-01 **	-.92890E+04	-.92890E+04	
0.30000E+02	0.26350E-01	-.89882E-01 **	-.83690E+04	-.83690E+04	
0.30750E+02	0.18211E-01	-.82413E-01 **	-.76655E+04	-.76655E+04	
0.31750E+02	0.73602E-02	-.72454E-01 **	-.55066E+04	-.55066E+04	
0.32750E+02	-.34909E-02	-.62495E-01 **	-.34119E+04	-.34119E+04	
0.33750E+02	-.14342E-01	-.52536E-01 **	-.14868E+04	-.14868E+04	

DISPLACEMENTS VS. CHORDWISE LOCATION AT IMPACT RADIUS

X	IN-PLANE	OUT-OF-PLANE
0.0	0.15110E+00	-.32096E+00
0.60000E+00	0.13842E+00	-.29748E+00
0.12000E+01	0.12241E+00	-.26783E+00
0.18000E+01	0.10640E+00	-.23817E+00
0.24000E+01	0.90391E-01	-.20851E+00
0.30000E+01	0.74381E-01	-.17885E+00
0.36000E+01	0.58371E-01	-.14920E+00
0.42000E+01	0.42360E-01	-.11954E+00
0.48000E+01	0.26350E-01	-.89882E-01
0.54000E+01	0.10339E-01	-.60225E-01
0.62500E+01	-.12342E-01	-.18210E-01
0.72500E+01	-.39026E-01	0.31219E-01
0.82500E+01	-.65710E-01	0.80648E-01
0.92500E+01	-.92394E-01	0.13008E+00
0.10000E+02	-.11574E+00	0.17333E+00

STRESSES VS. CHORDWISE LOCATION AT IMPACT RADIUS

X	STRESS-X				STRESS-Y				SHEAR-XY			
	*R=0.2900E+02	*R=0.3000E+02	*R=0.3075E+02	*R=0.2900E+02	*R=0.3000E+02	*R=0.3075E+02	*R=0.2900E+02	*R=0.3000E+02	*R=0.3075E+02	*R=0.2900E+02	*R=0.3000E+02	*R=0.3075E+02
0.0	* 0.1908E+05	* 0.1756E+05	* 0.1641E+05	* -.9289E+04	* -.8369E+04	* -.7666E+04	* 0.1031E+05	* 0.1030E+05	* 0.1030E+05	* 0.1031E+05	* 0.1030E+05	* 0.1030E+05
0.6000E+00	* 0.1908E+05	* 0.1756E+05	* 0.1641E+05	* -.9289E+04	* -.8369E+04	* -.7666E+04	* 0.1031E+05	* 0.1030E+05	* 0.1030E+05	* 0.1031E+05	* 0.1030E+05	* 0.1030E+05
0.1200E+01	* 0.1908E+05	* 0.1756E+05	* 0.1641E+05	* -.9289E+04	* -.8369E+04	* -.7666E+04	* 0.1031E+05	* 0.1030E+05	* 0.1030E+05	* 0.1031E+05	* 0.1030E+05	* 0.1030E+05
0.1800E+01	* 0.1908E+05	* 0.1756E+05	* 0.1641E+05	* -.9289E+04	* -.8369E+04	* -.7666E+04	* 0.1031E+05	* 0.1030E+05	* 0.1030E+05	* 0.1031E+05	* 0.1030E+05	* 0.1030E+05

ORIGINAL PAGE IS
OF POOR QUALITY

0.2400E+01 * 0.1908E+05 * 0.1756E+05 * 0.1641E+05 * -.9289E+04 * -.8369E+04 * -.7666E+04 * 0.1031E+05 * 0.1030E+05 * 0.1030E+05
 0.3000E+01 * 0.1908E+05 * 0.1756E+05 * 0.1641E+05 * -.9289E+04 * -.8369E+04 * -.7666E+04 * 0.1031E+05 * 0.1030E+05 * 0.1030E+05
 0.3600E+01 * 0.1908E+05 * 0.1756E+05 * 0.1641E+05 * -.9289E+04 * -.8369E+04 * -.7666E+04 * 0.1031E+05 * 0.1030E+05 * 0.1030E+05
 0.4200E+01 * 0.1908E+05 * 0.1756E+05 * 0.1641E+05 * -.9289E+04 * -.8369E+04 * -.7666E+04 * 0.1031E+05 * 0.1030E+05 * 0.1030E+05
 0.4800E+01 * 0.1908E+05 * 0.1756E+05 * 0.1641E+05 * -.9289E+04 * -.8369E+04 * -.7666E+04 * 0.1031E+05 * 0.1030E+05 * 0.1030E+05
 0.5400E+01 * 0.1908E+05 * 0.1756E+05 * 0.1641E+05 * -.9289E+04 * -.8369E+04 * -.7666E+04 * 0.1031E+05 * 0.1030E+05 * 0.1030E+05
 0.6250E+01 * 0.1908E+05 * 0.1756E+05 * 0.1641E+05 * -.9289E+04 * -.8369E+04 * -.7666E+04 * 0.1031E+05 * 0.1030E+05 * 0.1030E+05
 0.7250E+01 * 0.1908E+05 * 0.1756E+05 * 0.1641E+05 * -.9289E+04 * -.8369E+04 * -.7666E+04 * 0.1031E+05 * 0.1030E+05 * 0.1030E+05
 0.8250E+01 * 0.1908E+05 * 0.1756E+05 * 0.1641E+05 * -.9289E+04 * -.8369E+04 * -.7666E+04 * 0.1031E+05 * 0.1030E+05 * 0.1030E+05
 0.9250E+01 * 0.1908E+05 * 0.1756E+05 * 0.1641E+05 * -.9289E+04 * -.8369E+04 * -.7666E+04 * 0.1031E+05 * 0.1030E+05 * 0.1030E+05
 0.1000E+02 * 0.1908E+05 * 0.1756E+05 * 0.1641E+05 * -.9289E+04 * -.8369E+04 * -.7666E+04 * 0.1031E+05 * 0.1030E+05 * 0.1030E+05

TIME=0.719889E-03 SEC

DISPLACEMENTS AND BENDING STRESSES VS. RADIAL STATION

R	DISPLACEMENTS		RADIAL BENDING STRESS		
	IN-PLANE	OUT-OF-PLANE***LED-EDG	CHD-PNT	TRL-EDG	
0.27000E+02	0.12069E+00	-.22341E+00 **	-.23048E+05	-.23048E+05	-.23048E+05
0.28000E+02	0.10171E+00	-.20606E+00 **	-.20181E+05	-.20181E+05	-.20181E+05
0.29000E+02	0.82737E-01	-.18872E+00 **	-.17342E+05	-.17342E+05	-.17342E+05
0.30000E+02	0.63761E-01	-.17137E+00 **	-.15557E+05	-.15557E+05	-.15557E+05
0.30750E+02	0.49528E-01	-.15837E+00 **	-.14192E+05	-.14192E+05	-.14192E+05
0.31750E+02	0.30552E-01	-.14102E+00 **	-.10003E+05	-.10003E+05	-.10003E+05
0.32750E+02	0.11575E-01	-.12368E+00 **	-.59414E+04	-.59414E+04	-.59414E+04
0.33750E+02	-.74008E-02	-.10633E+00 **	-.22167E+04	-.22167E+04	-.22167E+04

DISPLACEMENTS VS. CHORDWISE LOCATION
AT IMPACT RADIUS

X	IN-PLANE	OUT-OF-PLANE
0.0	0.26268E+00	-.53888E+00
0.60000E+00	0.24247E+00	-.50153E+00
0.12000E+01	0.21694E+00	-.45437E+00
0.18000E+01	0.19141E+00	-.40720E+00
0.24000E+01	0.16588E+00	-.36004E+00
0.30000E+01	0.14035E+00	-.31287E+00
0.36000E+01	0.11482E+00	-.26571E+00
0.42000E+01	0.89290E-01	-.21854E+00
0.48000E+01	0.63761E-01	-.17137E+00
0.54000E+01	0.38231E-01	-.12421E+00
0.62500E+01	0.20643E-02	-.57390E-01
0.72500E+01	-.40485E-01	0.21220E-01
0.82500E+01	-.83034E-01	0.99830E-01
0.92500E+01	-.12558E+00	0.17844E+00
0.10000E+02	-.16281E+00	0.24722E+00

STRESSES VS. CHORDWISE LOCATION
AT IMPACT RADIUS

X	STRESS-X				STRESS-Y				SHEAR-XY			
	*R=0.2900E+02	*R=0.3000E+02	*R=0.3075E+02	*R=0.2900E+02	*R=0.3000E+02	*R=0.3075E+02	*R=0.2900E+02	*R=0.3000E+02	*R=0.3075E+02	*R=0.2900E+02	*R=0.3000E+02	*R=0.3075E+02
0.0	* 0.3524E+05	* 0.3236E+05	* 0.3017E+05	* -.1734E+05	* -.1556E+05	* -.1419E+05	* 0.1586E+05	* 0.1586E+05	* 0.1586E+05	* 0.1586E+05	* 0.1586E+05	* 0.1586E+05
0.6000E+00	* 0.3524E+05	* 0.3236E+05	* 0.3017E+05	* -.1734E+05	* -.1556E+05	* -.1419E+05	* 0.1586E+05	* 0.1586E+05	* 0.1586E+05	* 0.1586E+05	* 0.1586E+05	* 0.1586E+05

0.1200E+01	* 0.3524E+05	* 0.3236E+05	* 0.3017E+05	* -.1734E+05	* -.1556E+05	* -.1419E+05	* 0.1586E+05	* 0.1586E+05	* 0.1586E+05
0.1800E+01	* 0.3524E+05	* 0.3236E+05	* 0.3017E+05	* -.1734E+05	* -.1556E+05	* -.1419E+05	* 0.1586E+05	* 0.1586E+05	* 0.1586E+05
0.2400E+01	* 0.3524E+05	* 0.3236E+05	* 0.3017E+05	* -.1734E+05	* -.1556E+05	* -.1419E+05	* 0.1586E+05	* 0.1586E+05	* 0.1586E+05
0.3000E+01	* 0.3524E+05	* 0.3236E+05	* 0.3017E+05	* -.1734E+05	* -.1556E+05	* -.1419E+05	* 0.1586E+05	* 0.1586E+05	* 0.1586E+05
0.3600E+01	* 0.3524E+05	* 0.3236E+05	* 0.3017E+05	* -.1734E+05	* -.1556E+05	* -.1419E+05	* 0.1586E+05	* 0.1586E+05	* 0.1586E+05
0.4200E+01	* 0.3524E+05	* 0.3236E+05	* 0.3017E+05	* -.1734E+05	* -.1556E+05	* -.1419E+05	* 0.1586E+05	* 0.1586E+05	* 0.1586E+05
0.4800E+01	* 0.3524E+05	* 0.3236E+05	* 0.3017E+05	* -.1734E+05	* -.1556E+05	* -.1419E+05	* 0.1586E+05	* 0.1586E+05	* 0.1586E+05
0.5400E+01	* 0.3524E+05	* 0.3236E+05	* 0.3017E+05	* -.1734E+05	* -.1556E+05	* -.1419E+05	* 0.1586E+05	* 0.1586E+05	* 0.1586E+05
0.6250E+01	* 0.3524E+05	* 0.3236E+05	* 0.3017E+05	* -.1734E+05	* -.1556E+05	* -.1419E+05	* 0.1586E+05	* 0.1586E+05	* 0.1586E+05
0.7250E+01	* 0.3524E+05	* 0.3236E+05	* 0.3017E+05	* -.1734E+05	* -.1556E+05	* -.1419E+05	* 0.1586E+05	* 0.1586E+05	* 0.1586E+05
0.8250E+01	* 0.3524E+05	* 0.3236E+05	* 0.3017E+05	* -.1734E+05	* -.1556E+05	* -.1419E+05	* 0.1586E+05	* 0.1586E+05	* 0.1586E+05
0.9250E+01	* 0.3524E+05	* 0.3236E+05	* 0.3017E+05	* -.1734E+05	* -.1556E+05	* -.1419E+05	* 0.1586E+05	* 0.1586E+05	* 0.1586E+05
0.1000E+02	* 0.3524E+05	* 0.3236E+05	* 0.3017E+05	* -.1734E+05	* -.1556E+05	* -.1419E+05	* 0.1586E+05	* 0.1586E+05	* 0.1586E+05

TIME=0.873301E-03 SEC

DISPLACEMENTS AND BENDING STRESSES VS. RADIAL STATION

R	DISPLACEMENTS		RADIAL BENDING STRESS		
	IN-PLANE	OUT-OF-PLANE***LED-EDG	CHD-PNT	TRL-EDG	
0.2700E+02	0.19245E+00	-.33549E+00 **	-.35205E+05	-.35205E+05	-.35205E+05
0.2800E+02	0.16593E+00	-.31118E+00 **	-.30595E+05	-.30595E+05	-.30595E+05
0.2900E+02	0.13941E+00	-.26687E+00 **	-.26230E+05	-.26230E+05	-.26230E+05
0.3000E+02	0.11289E+00	-.26256E+00 **	-.23486E+05	-.23486E+05	-.23486E+05
0.3075E+02	0.92993E-01	-.24433E+00 **	-.21388E+05	-.21388E+05	-.21388E+05
0.3175E+02	0.66471E-01	-.22002E+00 **	-.14946E+05	-.14946E+05	-.14946E+05
0.3275E+02	0.39948E-01	-.19572E+00 **	-.87017E+04	-.87017E+04	-.87017E+04
0.3375E+02	0.13426E-01	-.17141E+00 **	-.29788E+04	-.29788E+04	-.29788E+04

DISPLACEMENTS VS. CHORDWISE LOCATION AT IMPACT RADIUS

X	IN-PLANE	OUT-OF-PLANE
0.0	0.38104E+00	-.75760E+00
0.60000E+00	0.35379E+00	-.70730E+00
0.12000E+01	0.31938E+00	-.64377E+00
0.18000E+01	0.28496E+00	-.58023E+00
0.24000E+01	0.25055E+00	-.51670E+00
0.30000E+01	0.21613E+00	-.45316E+00
0.36000E+01	0.18172E+00	-.38963E+00
0.42000E+01	0.14730E+00	-.32610E+00
0.48000E+01	0.11289E+00	-.26256E+00
0.54000E+01	0.78470E-01	-.19903E+00
0.62500E+01	0.29716E-01	-.10902E+00
0.72500E+01	-.27643E-01	-.31321E-02
0.82500E+01	-.85001E-01	0.10276E+00
0.92500E+01	-.14236E+00	0.20865E+00
0.10000E+02	-.19255E+00	0.30130E+00

ORIGINAL PAGE IS
OF POOR QUALITY

STRESSES VS. CHORDWISE LOCATION AT IMPACT RADIUS

X	STRESS-X			STRESS-Y			SHEAR-XY		
	*R=0.2900E+02	*R=0.3000E+02	*R=0.3075E+02	*R=0.2900E+02	*R=0.3000E+02	*R=0.3075E+02	*R=0.2900E+02	*R=0.3000E+02	*R=0.3075E+02

0.0	* 0.5257E+05	* 0.4820E+05	* 0.4488E+05	* -.2623E+05	* -.2349E+05	* -.2139E+05	* 0.2090E+05	* 0.2090E+05	* 0.2090E+05
0.6000E+00	* 0.5257E+05	* 0.4820E+05	* 0.4488E+05	* -.2623E+05	* -.2349E+05	* -.2139E+05	* 0.2090E+05	* 0.2090E+05	* 0.2090E+05
0.1200E+01	* 0.5257E+05	* 0.4820E+05	* 0.4488E+05	* -.2623E+05	* -.2349E+05	* -.2139E+05	* 0.2090E+05	* 0.2090E+05	* 0.2090E+05
0.1800E+01	* 0.5257E+05	* 0.4820E+05	* 0.4488E+05	* -.2623E+05	* -.2349E+05	* -.2139E+05	* 0.2090E+05	* 0.2090E+05	* 0.2090E+05
0.2400E+01	* 0.5257E+05	* 0.4820E+05	* 0.4488E+05	* -.2623E+05	* -.2349E+05	* -.2139E+05	* 0.2090E+05	* 0.2090E+05	* 0.2090E+05
0.3000E+01	* 0.5257E+05	* 0.4820E+05	* 0.4488E+05	* -.2623E+05	* -.2349E+05	* -.2139E+05	* 0.2090E+05	* 0.2090E+05	* 0.2090E+05
0.3600E+01	* 0.5257E+05	* 0.4820E+05	* 0.4488E+05	* -.2623E+05	* -.2349E+05	* -.2139E+05	* 0.2090E+05	* 0.2090E+05	* 0.2090E+05
0.4200E+01	* 0.5257E+05	* 0.4820E+05	* 0.4488E+05	* -.2623E+05	* -.2349E+05	* -.2139E+05	* 0.2090E+05	* 0.2090E+05	* 0.2090E+05
0.4800E+01	* 0.5257E+05	* 0.4820E+05	* 0.4488E+05	* -.2623E+05	* -.2349E+05	* -.2139E+05	* 0.2090E+05	* 0.2090E+05	* 0.2090E+05
0.5400E+01	* 0.5257E+05	* 0.4820E+05	* 0.4488E+05	* -.2623E+05	* -.2349E+05	* -.2139E+05	* 0.2090E+05	* 0.2090E+05	* 0.2090E+05
0.6250E+01	* 0.5257E+05	* 0.4820E+05	* 0.4488E+05	* -.2623E+05	* -.2349E+05	* -.2139E+05	* 0.2090E+05	* 0.2090E+05	* 0.2090E+05
0.7250E+01	* 0.5257E+05	* 0.4820E+05	* 0.4488E+05	* -.2623E+05	* -.2349E+05	* -.2139E+05	* 0.2090E+05	* 0.2090E+05	* 0.2090E+05
0.8250E+01	* 0.5257E+05	* 0.4820E+05	* 0.4488E+05	* -.2623E+05	* -.2349E+05	* -.2139E+05	* 0.2090E+05	* 0.2090E+05	* 0.2090E+05
0.9250E+01	* 0.5257E+05	* 0.4820E+05	* 0.4488E+05	* -.2623E+05	* -.2349E+05	* -.2139E+05	* 0.2090E+05	* 0.2090E+05	* 0.2090E+05
0.1000E+02	* 0.5257E+05	* 0.4820E+05	* 0.4488E+05	* -.2623E+05	* -.2349E+05	* -.2139E+05	* 0.2090E+05	* 0.2090E+05	* 0.2090E+05

TIME=0.970919E-03 SEC

DISPLACEMENTS AND BENDING STRESSES VS. RADIAL STATION

R	DISPLACEMENTS		RADIAL BENDING STRESS		
	IN-PLANE	OUT-OF-PLANE***LED-EDG	CHD-FNT	TRL-EDG	
0.27000E+02	0.24026E+00	-.40807E+00 **	-.43256E+05	-.43256E+05	-.43256E+05
0.28000E+02	0.20970E+00	-.37987E+00 **	-.37520E+05	-.37520E+05	-.37520E+05
0.29000E+02	0.17913E+00	-.35168E+00 **	-.32166E+05	-.32166E+05	-.32166E+05
0.30000E+02	0.14857E+00	-.32349E+00 **	-.28800E+05	-.28800E+05	-.28800E+05
0.30750E+02	0.12565E+00	-.30234E+00 **	-.26227E+05	-.26227E+05	-.26227E+05
0.31750E+02	0.95091E-01	-.27415E+00 **	-.18326E+05	-.18326E+05	-.18326E+05
0.32750E+02	0.64530E-01	-.24596E+00 **	-.10665E+05	-.10665E+05	-.10665E+05
0.33750E+02	0.33969E-01	-.21777E+00 **	-.36422E+04	-.36422E+04	-.36422E+04

DISPLACEMENTS VS. CHORDWISE LOCATION AT IMPACT RADIUS

X	IN-PLANE	OUT-OF-PLANE
0.0	0.46217E+00	-.90295E+00
0.60000E+00	0.43031E+00	-.84408E+00
0.12000E+01	0.39006E+00	-.76971E+00
0.18000E+01	0.34981E+00	-.69534E+00
0.24000E+01	0.30957E+00	-.62097E+00
0.30000E+01	0.26932E+00	-.54660E+00
0.36000E+01	0.22907E+00	-.47223E+00
0.42000E+01	0.18882E+00	-.39786E+00
0.48000E+01	0.14857E+00	-.32349E+00
0.54000E+01	0.10832E+00	-.24912E+00
0.62500E+01	0.51307E-01	-.14376E+00
0.72500E+01	-.15774E-01	-.19813E-01
0.82500E+01	-.82854E-01	0.10414E+00
0.92500E+01	-.14993E+00	0.22809E+00
0.10000E+02	-.20863E+00	0.33654E+00

STRESSES VS. CHORDWISE LOCATION AT IMPACT RADIUS

TIME=0.128215E-02 SEC

DISPLACEMENTS AND BENDING STRESSES VS. RADIAL STATION

DISPLACEMENTS		RADIAL BENDING STRESS		
R	IN-PLANE	OUT-OF-PLANE***LED-EDG	CHD-PNT	TRL-EDG
0.27800E+02	0.37774E+00	-.59590E+00 **	-.67170E+05	-.67170E+05
0.28000E+02	0.34467E+00	-.56435E+00 **	-.58216E+05	-.58216E+05
0.29000E+02	0.31169E+00	-.53281E+00 **	-.50137E+05	-.50137E+05
0.30000E+02	0.27853E+00	-.50126E+00 **	-.45059E+05	-.45059E+05
0.30750E+02	0.25373E+00	-.47760E+00 **	-.41174E+05	-.41174E+05
0.31750E+02	0.22065E+00	-.44606E+00 **	-.29251E+05	-.29251E+05
0.32750E+02	0.18759E+00	-.41451E+00 **	-.17674E+05	-.17674E+05
0.33750E+02	0.15452E+00	-.38297E+00 **	-.70159E+04	-.70159E+04

DISPLACEMENTS VS. CHORDWISE LOCATION AT IMPACT RADIUS

	X	IN-PLANE	OUT-OF-PLANE
	0.0	0.69756E+00	-.12826E+01
	0.60000E+00	0.65498E+00	-.12032E+01
	0.12000E+01	0.60121E+00	-.11029E+01
	0.18000E+01	0.54743E+00	-.10027E+01
	0.24000E+01	0.49365E+00	-.90238E+00
	0.30000E+01	0.43987E+00	-.80210E+00
	0.36000E+01	0.38609E+00	-.70182E+00
	0.42000E+01	0.33231E+00	-.60154E+00
	0.48000E+01	0.27853E+00	-.50126E+00
	0.54000E+01	0.22475E+00	-.40098E+00
	0.62500E+01	0.14856E+00	-.25892E+00
	0.72500E+01	0.58930E-01	-.91787E-01
	0.82500E+01	-.30702E-01	0.75347E-01
	0.92500E+01	-.12033E+00	0.24248E+00
	0.10000E+02	-.19876E+00	0.36872E+00

STRESSES VS. CHORDWISE LOCATION

AT IMPACT RADIUS

X	STRESS-X			STRESS-Y			SHEAR-XY		
	*R=0.2900E+02	*R=0.3000E+02	*R=0.3075E+02	*R=0.2900E+02	*R=0.3000E+02	*R=0.3075E+02	*R=0.2900E+02	*R=0.3000E+02	*R=0.3075E+02
0.0	* 0.9079E+05	* 0.8319E+05	* 0.7741E+05	* -.5014E+05	* -.4506E+05	* -.4117E+05	* 0.3319E+05	* 0.3319E+05	* 0.3318E+05
0.6000E+00	* 0.9079E+05	* 0.8319E+05	* 0.7741E+05	* -.5014E+05	* -.4506E+05	* -.4117E+05	* 0.3319E+05	* 0.3319E+05	* 0.3318E+05
0.1200E+01	* 0.9079E+05	* 0.8319E+05	* 0.7741E+05	* -.5014E+05	* -.4506E+05	* -.4117E+05	* 0.3319E+05	* 0.3319E+05	* 0.3318E+05
0.1800E+01	* 0.9079E+05	* 0.8319E+05	* 0.7741E+05	* -.5014E+05	* -.4506E+05	* -.4117E+05	* 0.3319E+05	* 0.3319E+05	* 0.3318E+05
0.2400E+01	* 0.9079E+05	* 0.8319E+05	* 0.7741E+05	* -.5014E+05	* -.4506E+05	* -.4117E+05	* 0.3319E+05	* 0.3319E+05	* 0.3318E+05
0.3000E+01	* 0.9079E+05	* 0.8319E+05	* 0.7741E+05	* -.5014E+05	* -.4506E+05	* -.4117E+05	* 0.3319E+05	* 0.3319E+05	* 0.3318E+05
0.3600E+01	* 0.9079E+05	* 0.8319E+05	* 0.7741E+05	* -.5014E+05	* -.4506E+05	* -.4117E+05	* 0.3319E+05	* 0.3319E+05	* 0.3318E+05
0.4200E+01	* 0.9079E+05	* 0.8319E+05	* 0.7741E+05	* -.5014E+05	* -.4506E+05	* -.4117E+05	* 0.3319E+05	* 0.3319E+05	* 0.3318E+05
0.4800E+01	* 0.9079E+05	* 0.8319E+05	* 0.7741E+05	* -.5014E+05	* -.4506E+05	* -.4117E+05	* 0.3319E+05	* 0.3319E+05	* 0.3318E+05
0.5400E+01	* 0.9079E+05	* 0.8319E+05	* 0.7741E+05	* -.5014E+05	* -.4506E+05	* -.4117E+05	* 0.3319E+05	* 0.3319E+05	* 0.3318E+05
0.6250E+01	* 0.9079E+05	* 0.8319E+05	* 0.7741E+05	* -.5014E+05	* -.4506E+05	* -.4117E+05	* 0.3319E+05	* 0.3319E+05	* 0.3318E+05
0.7250E+01	* 0.9079E+05	* 0.8319E+05	* 0.7741E+05	* -.5014E+05	* -.4506E+05	* -.4117E+05	* 0.3319E+05	* 0.3319E+05	* 0.3318E+05
0.8250E+01	* 0.9079E+05	* 0.8319E+05	* 0.7741E+05	* -.5014E+05	* -.4506E+05	* -.4117E+05	* 0.3319E+05	* 0.3319E+05	* 0.3318E+05
0.9250E+01	* 0.9079E+05	* 0.8319E+05	* 0.7741E+05	* -.5014E+05	* -.4506E+05	* -.4117E+05	* 0.3319E+05	* 0.3319E+05	* 0.3318E+05
0.1000E+02	* 0.9079E+05	* 0.8319E+05	* 0.7741E+05	* -.5014E+05	* -.4506E+05	* -.4117E+05	* 0.3319E+05	* 0.3319E+05	* 0.3318E+05

TIME=0.183769E-02 SEC

DISPLACEMENTS AND BENDING STRESSES VS. RADIAL STATION

R	DISPLACEMENTS		RADIAL BENDING STRESS		
	IN-PLANE	OUT-OF-PLANE***LED-EDG	CHD-PNT	TRL-EDG	
0.27000E+02	0.45261E+00	-.59108E+00 **	-.89500E+05	-.89500E+05	
0.28000E+02	0.47267E+00	-.60576E+00 **	-.78546E+05	-.78546E+05	
0.29000E+02	0.49273E+00	-.62045E+00 **	-.69297E+05	-.69297E+05	
0.30000E+02	0.51279E+00	-.63514E+00 **	-.63483E+05	-.63483E+05	
0.30750E+02	0.52783E+00	-.64616E+00 **	-.59034E+05	-.59034E+05	
0.31750E+02	0.54789E+00	-.66084E+00 **	-.45381E+05	-.45381E+05	
0.32750E+02	0.56795E+00	-.67553E+00 **	-.32039E+05	-.32039E+05	
0.33750E+02	0.58801E+00	-.69022E+00 **	-.19473E+05	-.19473E+05	

DISPLACEMENTS VS. CHORDWISE LOCATION AT IMPACT RADIUS

X	IN-PLANE	OUT-OF-PLANE
0.0	0.87154E+00	-.13476E+01
0.60000E+00	0.83509E+00	-.12752E+01
0.12000E+01	0.78905E+00	-.11838E+01
0.18000E+01	0.74300E+00	-.10924E+01
0.24000E+01	0.69696E+00	-.10009E+01
0.30000E+01	0.65092E+00	-.90947E+00
0.36000E+01	0.60487E+00	-.81803E+00
0.42000E+01	0.55883E+00	-.72658E+00
0.48000E+01	0.51279E+00	-.63514E+00
0.54000E+01	0.46674E+00	-.54370E+00
0.62500E+01	0.40152E+00	-.41415E+00
0.72500E+01	0.32478E+00	-.26175E+00
0.82500E+01	0.24804E+00	-.10934E+00
0.92500E+01	0.17130E+00	0.43061E-01
0.10000E+02	0.10415E+00	0.17641E+00

STRESSES VS. CHORDWISE LOCATION
AT IMPACT RADIUS

X	STRESS-X				STRESS-Y				SHEAR-XY			
	*R=0.2900E+02	*R=0.3000E+02	*R=0.3075E+02	*R=0.2900E+02	*R=0.3000E+02	*R=0.3075E+02	*R=0.2900E+02	*R=0.3000E+02	*R=0.3075E+02	*R=0.2900E+02	*R=0.3000E+02	*R=0.3075E+02
0.0	* 0.7473E+05	* 0.6858E+05	* 0.6391E+05	* -.6930E+05	* -.6348E+05	* -.5903E+05	* 0.3494E+05	* 0.3493E+05	* 0.3493E+05	* 0.3494E+05	* 0.3493E+05	* 0.3493E+05
0.6000E+00	* 0.7473E+05	* 0.6858E+05	* 0.6391E+05	* -.6930E+05	* -.6348E+05	* -.5903E+05	* 0.3494E+05	* 0.3493E+05	* 0.3493E+05	* 0.3494E+05	* 0.3493E+05	* 0.3493E+05
0.1200E+01	* 0.7473E+05	* 0.6858E+05	* 0.6391E+05	* -.6930E+05	* -.6348E+05	* -.5903E+05	* 0.3494E+05	* 0.3493E+05	* 0.3493E+05	* 0.3494E+05	* 0.3493E+05	* 0.3493E+05
0.1800E+01	* 0.7473E+05	* 0.6858E+05	* 0.6391E+05	* -.6930E+05	* -.6348E+05	* -.5903E+05	* 0.3494E+05	* 0.3493E+05	* 0.3493E+05	* 0.3494E+05	* 0.3493E+05	* 0.3493E+05
0.2400E+01	* 0.7473E+05	* 0.6858E+05	* 0.6391E+05	* -.6930E+05	* -.6348E+05	* -.5903E+05	* 0.3494E+05	* 0.3493E+05	* 0.3493E+05	* 0.3494E+05	* 0.3493E+05	* 0.3493E+05
0.3000E+01	* 0.7473E+05	* 0.6858E+05	* 0.6391E+05	* -.6930E+05	* -.6348E+05	* -.5903E+05	* 0.3494E+05	* 0.3493E+05	* 0.3493E+05	* 0.3494E+05	* 0.3493E+05	* 0.3493E+05
0.3600E+01	* 0.7473E+05	* 0.6858E+05	* 0.6391E+05	* -.6930E+05	* -.6348E+05	* -.5903E+05	* 0.3494E+05	* 0.3493E+05	* 0.3493E+05	* 0.3494E+05	* 0.3493E+05	* 0.3493E+05
0.4200E+01	* 0.7473E+05	* 0.6858E+05	* 0.6391E+05	* -.6930E+05	* -.6348E+05	* -.5903E+05	* 0.3494E+05	* 0.3493E+05	* 0.3493E+05	* 0.3494E+05	* 0.3493E+05	* 0.3493E+05
0.4800E+01	* 0.7473E+05	* 0.6858E+05	* 0.6391E+05	* -.6930E+05	* -.6348E+05	* -.5903E+05	* 0.3494E+05	* 0.3493E+05	* 0.3493E+05	* 0.3494E+05	* 0.3493E+05	* 0.3493E+05
0.5400E+01	* 0.7473E+05	* 0.6858E+05	* 0.6391E+05	* -.6930E+05	* -.6348E+05	* -.5903E+05	* 0.3494E+05	* 0.3493E+05	* 0.3493E+05	* 0.3494E+05	* 0.3493E+05	* 0.3493E+05
0.6250E+01	* 0.7473E+05	* 0.6858E+05	* 0.6391E+05	* -.6930E+05	* -.6348E+05	* -.5903E+05	* 0.3494E+05	* 0.3493E+05	* 0.3493E+05	* 0.3494E+05	* 0.3493E+05	* 0.3493E+05
0.7250E+01	* 0.7473E+05	* 0.6858E+05	* 0.6391E+05	* -.6930E+05	* -.6348E+05	* -.5903E+05	* 0.3494E+05	* 0.3493E+05	* 0.3493E+05	* 0.3494E+05	* 0.3493E+05	* 0.3493E+05
0.8250E+01	* 0.7473E+05	* 0.6858E+05	* 0.6391E+05	* -.6930E+05	* -.6348E+05	* -.5903E+05	* 0.3494E+05	* 0.3493E+05	* 0.3493E+05	* 0.3494E+05	* 0.3493E+05	* 0.3493E+05
0.9250E+01	* 0.7473E+05	* 0.6858E+05	* 0.6391E+05	* -.6930E+05	* -.6348E+05	* -.5903E+05	* 0.3494E+05	* 0.3493E+05	* 0.3493E+05	* 0.3494E+05	* 0.3493E+05	* 0.3493E+05
0.1000E+02	* 0.7473E+05	* 0.6858E+05	* 0.6391E+05	* -.6930E+05	* -.6348E+05	* -.5903E+05	* 0.3494E+05	* 0.3493E+05	* 0.3493E+05	* 0.3494E+05	* 0.3493E+05	* 0.3493E+05

TIME=0.239324E-02 SEC

DISPLACEMENTS AND BENDING STRESSES VS. RADIAL STATION

R	DISPLACEMENTS		RADIAL BENDING STRESS		
	IN-PLANE	OUT-OF-PLANE**LED-EDG	CHD-PNT	TRL-EDG	
0.27000E+02	0.38976E+00	-.28413E+00 **	-.84357E+05	-.84357E+05	-.84357E+05
0.28000E+02	0.59595E+00	-.38314E+00 **	-.75138E+05	-.75138E+05	-.75138E+05
0.29000E+02	0.62215E+00	-.48216E+00 **	-.68461E+05	-.68461E+05	-.68461E+05
0.30000E+02	0.73834E+00	-.58117E+00 **	-.64266E+05	-.64266E+05	-.64266E+05
0.30750E+02	0.82549E+00	-.65543E+00 **	-.61050E+05	-.61050E+05	-.61050E+05
0.31750E+02	0.94168E+00	-.75445E+00 **	-.51190E+05	-.51190E+05	-.51190E+05
0.32750E+02	0.10579E+01	-.85346E+00 **	-.41411E+05	-.41411E+05	-.41411E+05
0.33750E+02	0.11741E+01	-.95247E+00 **	-.31760E+05	-.31760E+05	-.31760E+05

DISPLACEMENTS VS. CHORDWISE LOCATION
AT IMPACT RADIUS

X	IN-PLANE	OUT-OF-PLANE
0.0	0.75681E+00	-.72541E+00
0.60000E+00	0.75493E+00	-.71076E+00
0.12000E+01	0.75256E+00	-.69224E+00
0.18000E+01	0.75019E+00	-.67373E+00
0.24000E+01	0.74782E+00	-.65522E+00
0.30000E+01	0.74545E+00	-.63671E+00
0.36000E+01	0.74308E+00	-.61820E+00
0.42000E+01	0.74071E+00	-.59968E+00
0.48000E+01	0.73834E+00	-.58117E+00
0.54000E+01	0.73597E+00	-.56266E+00
0.62500E+01	0.73262E+00	-.53643E+00
0.72500E+01	0.72867E+00	-.50558E+00
0.82500E+01	0.72472E+00	-.47472E+00
0.92500E+01	0.72077E+00	-.44387E+00
0.10000E+02	0.71731E+00	-.41687E+00

STRESSES VS. CHORDWISE LOCATION
AT IMPACT RADIUS

X	STRESS-X			STRESS-Y			SHEAR-XY		
	*R=0.2900E+02	*R=0.3000E+02	*R=0.3075E+02	*R=0.2900E+02	*R=0.3000E+02	*R=0.3075E+02	*R=0.2900E+02	*R=0.3000E+02	*R=0.3075E+02
0.0	* 0.1039E+05	* 0.9781E+04	* 0.9327E+04	* -.6846E+05	* -.6427E+05	* -.6105E+05	* 0.1691E+05	* 0.1690E+05	* 0.1690E+05
0.6000E+00	* 0.1039E+05	* 0.9781E+04	* 0.9327E+04	* -.6846E+05	* -.6427E+05	* -.6105E+05	* 0.1691E+05	* 0.1690E+05	* 0.1690E+05
0.1200E+01	* 0.1039E+05	* 0.9781E+04	* 0.9327E+04	* -.6846E+05	* -.6427E+05	* -.6105E+05	* 0.1691E+05	* 0.1690E+05	* 0.1690E+05
0.1800E+01	* 0.1039E+05	* 0.9781E+04	* 0.9327E+04	* -.6846E+05	* -.6427E+05	* -.6105E+05	* 0.1691E+05	* 0.1690E+05	* 0.1690E+05
0.2400E+01	* 0.1039E+05	* 0.9781E+04	* 0.9327E+04	* -.6846E+05	* -.6427E+05	* -.6105E+05	* 0.1691E+05	* 0.1690E+05	* 0.1690E+05
0.3000E+01	* 0.1039E+05	* 0.9781E+04	* 0.9327E+04	* -.6846E+05	* -.6427E+05	* -.6105E+05	* 0.1691E+05	* 0.1690E+05	* 0.1690E+05
0.3600E+01	* 0.1039E+05	* 0.9781E+04	* 0.9327E+04	* -.6846E+05	* -.6427E+05	* -.6105E+05	* 0.1691E+05	* 0.1690E+05	* 0.1690E+05
0.4200E+01	* 0.1039E+05	* 0.9781E+04	* 0.9327E+04	* -.6846E+05	* -.6427E+05	* -.6105E+05	* 0.1691E+05	* 0.1690E+05	* 0.1690E+05
0.4800E+01	* 0.1039E+05	* 0.9781E+04	* 0.9327E+04	* -.6846E+05	* -.6427E+05	* -.6105E+05	* 0.1691E+05	* 0.1690E+05	* 0.1690E+05
0.5400E+01	* 0.1039E+05	* 0.9781E+04	* 0.9327E+04	* -.6846E+05	* -.6427E+05	* -.6105E+05	* 0.1691E+05	* 0.1690E+05	* 0.1690E+05
0.6250E+01	* 0.1039E+05	* 0.9781E+04	* 0.9327E+04	* -.6846E+05	* -.6427E+05	* -.6105E+05	* 0.1691E+05	* 0.1690E+05	* 0.1690E+05
0.7250E+01	* 0.1039E+05	* 0.9781E+04	* 0.9327E+04	* -.6846E+05	* -.6427E+05	* -.6105E+05	* 0.1691E+05	* 0.1690E+05	* 0.1690E+05
0.8250E+01	* 0.1039E+05	* 0.9781E+04	* 0.9327E+04	* -.6846E+05	* -.6427E+05	* -.6105E+05	* 0.1691E+05	* 0.1690E+05	* 0.1690E+05
0.9250E+01	* 0.1039E+05	* 0.9781E+04	* 0.9327E+04	* -.6846E+05	* -.6427E+05	* -.6105E+05	* 0.1691E+05	* 0.1690E+05	* 0.1690E+05
0.1000E+02	* 0.1039E+05	* 0.9781E+04	* 0.9327E+04	* -.6846E+05	* -.6427E+05	* -.6105E+05	* 0.1691E+05	* 0.1690E+05	* 0.1690E+05

TIME=0.412041E-02 SEC

DISPLACEMENTS AND BENDING STRESSES VS. RADIAL STATION

R	DISPLACEMENTS		RADIAL BENDING STRESS		
	IN-PLANE	OUT-OF-PLANE***LED-EDG	CHD-PNT	TRL-EDG	
0.27000E+02	0.39630E+00	-.57051E-01 **	-.18851E+05	-.18851E+05	
0.28000E+02	0.55482E+00	-.19548E+00 **	-.14989E+05	-.14989E+05	
0.29000E+02	0.71334E+00	-.33391E+00 **	-.13623E+05	-.13623E+05	
0.30000E+02	0.87186E+00	-.47234E+00 **	-.12761E+05	-.12761E+05	
0.30750E+02	0.99075E+00	-.57616E+00 **	-.12099E+05	-.12099E+05	
0.31750E+02	0.11493E+01	-.71459E+00 **	-.10057E+05	-.10057E+05	
0.32750E+02	0.13078E+01	-.85301E+00 **	-.79688E+04	-.79688E+04	
0.33750E+02	0.14663E+01	-.99144E+00 **	-.58435E+04	-.58435E+04	

DISPLACEMENTS VS. CHORDWISE LOCATION
AT IMPACT RADIUS

X	IN-PLANE	OUT-OF-PLANE
0.0	0.31715E+00	0.38321E+00
0.60000E+00	0.37351E+00	0.29628E+00
0.12000E+01	0.44470E+00	0.18648E+00
0.18000E+01	0.51589E+00	0.76681E-01
0.24000E+01	0.58709E+00	-.33122E-01
0.30000E+01	0.65828E+00	-.14293E+00
0.36000E+01	0.72947E+00	-.25273E+00
0.42000E+01	0.80067E+00	-.36253E+00
0.48000E+01	0.87186E+00	-.47234E+00
0.54000E+01	0.94305E+00	-.58214E+00
0.62500E+01	0.10439E+01	-.73769E+00
0.72500E+01	0.11626E+01	-.92070E+00
0.82500E+01	0.12812E+01	-.11037E+01
0.92500E+01	0.13999E+01	-.12867E+01

0.10000E+02 0.15037E+01 -1.4468E+01

STRESSES VS. CHORDWISE LOCATION
AT IMPACT RADIUS

X	STRESS-X				STRESS-Y				SHEAR-XY			
	*R=0.2900E+02	*R=0.3000E+02	*R=0.3075E+02	*R=0.2900E+02	*R=0.3000E+02	*R=0.3075E+02	*R=0.2900E+02	*R=0.3000E+02	*R=0.3075E+02	*R=0.2900E+02	*R=0.3000E+02	*R=0.3075E+02
0.0	* 0.2767E+05	* 0.2578E+05	* 0.2435E+05	* -1.362E+05	* -1.276E+05	* -1.210E+05	* -1.3097E+05	* -1.3097E+05	* -1.3097E+05	* -1.3097E+05	* -1.3097E+05	* -1.3097E+05
0.6000E+00	* 0.2767E+05	* 0.2578E+05	* 0.2435E+05	* -1.362E+05	* -1.276E+05	* -1.210E+05	* -1.3097E+05	* -1.3097E+05	* -1.3097E+05	* -1.3097E+05	* -1.3097E+05	* -1.3097E+05
0.1200E+01	* 0.2767E+05	* 0.2578E+05	* 0.2435E+05	* -1.362E+05	* -1.276E+05	* -1.210E+05	* -1.3097E+05	* -1.3097E+05	* -1.3097E+05	* -1.3097E+05	* -1.3097E+05	* -1.3097E+05
0.1800E+01	* 0.2767E+05	* 0.2578E+05	* 0.2435E+05	* -1.362E+05	* -1.276E+05	* -1.210E+05	* -1.3097E+05	* -1.3097E+05	* -1.3097E+05	* -1.3097E+05	* -1.3097E+05	* -1.3097E+05
0.2400E+01	* 0.2767E+05	* 0.2578E+05	* 0.2435E+05	* -1.362E+05	* -1.276E+05	* -1.210E+05	* -1.3097E+05	* -1.3097E+05	* -1.3097E+05	* -1.3097E+05	* -1.3097E+05	* -1.3097E+05
0.3000E+01	* 0.2767E+05	* 0.2578E+05	* 0.2435E+05	* -1.362E+05	* -1.276E+05	* -1.210E+05	* -1.3097E+05	* -1.3097E+05	* -1.3097E+05	* -1.3097E+05	* -1.3097E+05	* -1.3097E+05
0.3600E+01	* 0.2767E+05	* 0.2578E+05	* 0.2435E+05	* -1.362E+05	* -1.276E+05	* -1.210E+05	* -1.3097E+05	* -1.3097E+05	* -1.3097E+05	* -1.3097E+05	* -1.3097E+05	* -1.3097E+05
0.4200E+01	* 0.2767E+05	* 0.2578E+05	* 0.2435E+05	* -1.362E+05	* -1.276E+05	* -1.210E+05	* -1.3097E+05	* -1.3097E+05	* -1.3097E+05	* -1.3097E+05	* -1.3097E+05	* -1.3097E+05
0.4800E+01	* 0.2767E+05	* 0.2578E+05	* 0.2435E+05	* -1.362E+05	* -1.276E+05	* -1.210E+05	* -1.3097E+05	* -1.3097E+05	* -1.3097E+05	* -1.3097E+05	* -1.3097E+05	* -1.3097E+05
0.5400E+01	* 0.2767E+05	* 0.2578E+05	* 0.2435E+05	* -1.362E+05	* -1.276E+05	* -1.210E+05	* -1.3097E+05	* -1.3097E+05	* -1.3097E+05	* -1.3097E+05	* -1.3097E+05	* -1.3097E+05
0.6250E+01	* 0.2767E+05	* 0.2578E+05	* 0.2435E+05	* -1.362E+05	* -1.276E+05	* -1.210E+05	* -1.3097E+05	* -1.3097E+05	* -1.3097E+05	* -1.3097E+05	* -1.3097E+05	* -1.3097E+05
0.7250E+01	* 0.2767E+05	* 0.2578E+05	* 0.2435E+05	* -1.362E+05	* -1.276E+05	* -1.210E+05	* -1.3097E+05	* -1.3097E+05	* -1.3097E+05	* -1.3097E+05	* -1.3097E+05	* -1.3097E+05
0.8250E+01	* 0.2767E+05	* 0.2578E+05	* 0.2435E+05	* -1.362E+05	* -1.276E+05	* -1.210E+05	* -1.3097E+05	* -1.3097E+05	* -1.3097E+05	* -1.3097E+05	* -1.3097E+05	* -1.3097E+05
0.9250E+01	* 0.2767E+05	* 0.2578E+05	* 0.2435E+05	* -1.362E+05	* -1.276E+05	* -1.210E+05	* -1.3097E+05	* -1.3097E+05	* -1.3097E+05	* -1.3097E+05	* -1.3097E+05	* -1.3097E+05
0.1000E+02	* 0.2767E+05	* 0.2578E+05	* 0.2435E+05	* -1.362E+05	* -1.276E+05	* -1.210E+05	* -1.3097E+05	* -1.3097E+05	* -1.3097E+05	* -1.3097E+05	* -1.3097E+05	* -1.3097E+05

TIME=0.701923E-02 SEC

DISPLACEMENTS AND BENDING STRESSES VS. RADIAL STATION

R	DISPLACEMENTS		RADIAL BENDING STRESS		
	IN-PLANE	OUT-OF-PLANE***LED-EDG	CHD-PNT	TRL-EDG	
0.27000E+02	0.18350E-01	0.93241E-01 ** 0.57434E+04	0.57434E+04	0.57434E+04	
0.28000E+02	0.69533E-01	0.35989E-01 ** 0.61610E+04	0.61610E+04	0.61610E+04	
0.29000E+02	0.12072E+00	-2.1263E-01 ** 0.55578E+04	0.55578E+04	0.55578E+04	
0.30000E+02	0.17190E+00	-7.8515E-01 ** 0.51831E+04	0.51831E+04	0.51831E+04	
0.30750E+02	0.21029E+00	-1.2145E+00 ** 0.48889E+04	0.48889E+04	0.48889E+04	
0.31750E+02	0.26147E+00	-1.7871E+00 ** 0.40085E+04	0.40085E+04	0.40085E+04	
0.32750E+02	0.31265E+00	-2.3596E+00 ** 0.31468E+04	0.31468E+04	0.31468E+04	
0.33750E+02	0.36384E+00	-2.9321E+00 ** 0.23192E+04	0.23192E+04	0.23192E+04	

DISPLACEMENTS VS. CHORDWISE LOCATION
AT IMPACT RADIUS

X	IN-PLANE	OUT-OF-PLANE
0.0	-1.7049E+00	0.48128E+00
0.60000E+00	-1.3570E+00	0.42440E+00
0.12000E+01	-9.1758E-01	0.35255E+00
0.18000E+01	-4.7815E-01	0.28071E+00
0.24000E+01	-3.8722E-02	0.20886E+00
0.30000E+01	0.40071E-01	0.13702E+00
0.36000E+01	0.84014E-01	0.65174E-01
0.42000E+01	0.12796E+00	-6.6700E-02
0.48000E+01	0.17190E+00	-7.8515E-01
0.54000E+01	0.21584E+00	-1.5036E+00
0.62500E+01	0.27810E+00	-2.5214E+00
0.72500E+01	0.35133E+00	-3.7188E+00

ORIGINAL PAGE IS
OF POOR QUALITY

0.82500E+01	0.42457E+00	-.49162E+00
0.92500E+01	0.49781E+00	-.61136E+00
0.10000E+02	0.56189E+00	-.71614E+00

STRESSES VS. CHORDWISE LOCATION AT IMPACT RADIUS

X	STRESS-X			STRESS-Y			SHEAR-XY		
	*R=0.2900E+02	*R=0.3000E+02	*R=0.3075E+02	*R=0.2900E+02	*R=0.3000E+02	*R=0.3075E+02	*R=0.2900E+02	*R=0.3000E+02	*R=0.3075E+02
0.0	*-.9349E+04	*-.8771E+04	*-.8331E+04	*0.5558E+04	*0.5183E+04	*0.4889E+04	*-.2430E+05	*-.2430E+05	*-.2429E+05
0.6000E+00	*-.9349E+04	*-.8771E+04	*-.8331E+04	*0.5558E+04	*0.5183E+04	*0.4889E+04	*-.2430E+05	*-.2430E+05	*-.2429E+05
0.1200E+01	*-.9349E+04	*-.8771E+04	*-.8331E+04	*0.5558E+04	*0.5183E+04	*0.4889E+04	*-.2430E+05	*-.2430E+05	*-.2429E+05
0.1800E+01	*-.9349E+04	*-.8771E+04	*-.8331E+04	*0.5558E+04	*0.5183E+04	*0.4889E+04	*-.2430E+05	*-.2430E+05	*-.2429E+05
0.2400E+01	*-.9349E+04	*-.8771E+04	*-.8331E+04	*0.5558E+04	*0.5183E+04	*0.4889E+04	*-.2430E+05	*-.2430E+05	*-.2429E+05
0.3000E+01	*-.9349E+04	*-.8771E+04	*-.8331E+04	*0.5558E+04	*0.5183E+04	*0.4889E+04	*-.2430E+05	*-.2430E+05	*-.2429E+05
0.3600E+01	*-.9349E+04	*-.8771E+04	*-.8331E+04	*0.5558E+04	*0.5183E+04	*0.4889E+04	*-.2430E+05	*-.2430E+05	*-.2429E+05
0.4200E+01	*-.9349E+04	*-.8771E+04	*-.8331E+04	*0.5558E+04	*0.5183E+04	*0.4889E+04	*-.2430E+05	*-.2430E+05	*-.2429E+05
0.4800E+01	*-.9349E+04	*-.8771E+04	*-.8331E+04	*0.5558E+04	*0.5183E+04	*0.4889E+04	*-.2430E+05	*-.2430E+05	*-.2429E+05
0.5400E+01	*-.9349E+04	*-.8771E+04	*-.8331E+04	*0.5558E+04	*0.5183E+04	*0.4889E+04	*-.2430E+05	*-.2430E+05	*-.2429E+05
0.6250E+01	*-.9349E+04	*-.8771E+04	*-.8331E+04	*0.5558E+04	*0.5183E+04	*0.4889E+04	*-.2430E+05	*-.2430E+05	*-.2429E+05
0.7250E+01	*-.9349E+04	*-.8771E+04	*-.8331E+04	*0.5558E+04	*0.5183E+04	*0.4889E+04	*-.2430E+05	*-.2430E+05	*-.2429E+05
0.8250E+01	*-.9349E+04	*-.8771E+04	*-.8331E+04	*0.5558E+04	*0.5183E+04	*0.4889E+04	*-.2430E+05	*-.2430E+05	*-.2429E+05
0.9250E+01	*-.9349E+04	*-.8771E+04	*-.8331E+04	*0.5558E+04	*0.5183E+04	*0.4889E+04	*-.2430E+05	*-.2430E+05	*-.2429E+05
0.1000E+02	*-.9349E+04	*-.8771E+04	*-.8331E+04	*0.5558E+04	*0.5183E+04	*0.4889E+04	*-.2430E+05	*-.2430E+05	*-.2429E+05

TIME=0.991804E-02 SEC

DISPLACEMENTS AND BENDING STRESSES VS. RADIAL STATION

R	DISPLACEMENTS		RADIAL BENDING STRESS		
	IN-PLANE	OUT-OF-PLANE***LED-EDG	CHD-PNT	TRL-EDG	
0.27000E+02	-.11660E-02	-.26894E+00 **	-.16854E+05	-.16854E+05	
0.28000E+02	-.14138E+00	-.13046E+00 **	-.14213E+05	-.14213E+05	
0.29000E+02	-.28159E+00	0.80197E-02 **	-.11115E+05	-.11115E+05	
0.30000E+02	-.42180E+00	0.14650E+00 **	-.91737E+04	-.91737E+04	
0.30750E+02	-.52696E+00	0.25036E+00 **	-.76805E+04	-.76805E+04	
0.31750E+02	-.66717E+00	0.38884E+00 **	-.31242E+04	-.31242E+04	
0.32750E+02	-.80738E+00	0.52732E+00 **	0.12241E+04	0.12241E+04	
0.33750E+02	-.94759E+00	0.66580E+00 **	0.50500E+04	0.50500E+04	

DISPLACEMENTS VS. CHORDWISE LOCATION AT IMPACT RADIUS

X	IN-PLANE	OUT-OF-PLANE
0.0	0.97765E-01	-.63594E+00
0.60000E+00	0.44975E-01	-.55644E+00
0.12000E+01	-.21707E-01	-.45602E+00
0.18000E+01	-.68389E-01	-.35560E+00
0.24000E+01	-.15507E+00	-.25519E+00
0.30000E+01	-.22175E+00	-.15476E+00
0.36000E+01	-.28844E+00	-.54339E-01
0.42000E+01	-.35512E+00	0.46080E-01
0.48000E+01	-.42180E+00	0.14650E+00
0.54000E+01	-.48848E+00	0.24692E+00

0.62500E+01	-.58295E+00	0.38918E+00
0.72500E+01	-.69409E+00	0.55655E+00
0.82500E+01	-.80522E+00	0.72392E+00
0.92500E+01	-.91636E+00	0.89126E+00
0.10000E+02	-.10136E+01	0.10377E+01

STRESSES VS. CHORDWISE LOCATION AT IMPACT RADIUS

X	STRESS-X			STRESS-Y			SHEAR-XY		
	*R=0.2900E+02	*R=0.3000E+02	*R=0.3075E+02	*R=0.2900E+02	*R=0.3000E+02	*R=0.3075E+02	*R=0.2900E+02	*R=0.3000E+02	*R=0.3075E+02
0.0	* 0.2888E+05	* 0.2586E+05	* 0.2355E+05	* -.1112E+05	* -.9174E+04	* -.7681E+04	* 0.2532E+05	* 0.2531E+05	* 0.2531E+05
0.6000E+00	* 0.2888E+05	* 0.2586E+05	* 0.2355E+05	* -.1112E+05	* -.9174E+04	* -.7681E+04	* 0.2532E+05	* 0.2531E+05	* 0.2531E+05
0.1200E+01	* 0.2888E+05	* 0.2586E+05	* 0.2355E+05	* -.1112E+05	* -.9174E+04	* -.7681E+04	* 0.2532E+05	* 0.2531E+05	* 0.2531E+05
0.1800E+01	* 0.2888E+05	* 0.2586E+05	* 0.2355E+05	* -.1112E+05	* -.9174E+04	* -.7681E+04	* 0.2532E+05	* 0.2531E+05	* 0.2531E+05
0.2400E+01	* 0.2888E+05	* 0.2586E+05	* 0.2355E+05	* -.1112E+05	* -.9174E+04	* -.7681E+04	* 0.2532E+05	* 0.2531E+05	* 0.2531E+05
0.3000E+01	* 0.2888E+05	* 0.2586E+05	* 0.2355E+05	* -.1112E+05	* -.9174E+04	* -.7681E+04	* 0.2532E+05	* 0.2531E+05	* 0.2531E+05
0.3600E+01	* 0.2888E+05	* 0.2586E+05	* 0.2355E+05	* -.1112E+05	* -.9174E+04	* -.7681E+04	* 0.2532E+05	* 0.2531E+05	* 0.2531E+05
0.4200E+01	* 0.2888E+05	* 0.2586E+05	* 0.2355E+05	* -.1112E+05	* -.9174E+04	* -.7681E+04	* 0.2532E+05	* 0.2531E+05	* 0.2531E+05
0.4800E+01	* 0.2888E+05	* 0.2586E+05	* 0.2355E+05	* -.1112E+05	* -.9174E+04	* -.7681E+04	* 0.2532E+05	* 0.2531E+05	* 0.2531E+05
0.5400E+01	* 0.2888E+05	* 0.2586E+05	* 0.2355E+05	* -.1112E+05	* -.9174E+04	* -.7681E+04	* 0.2532E+05	* 0.2531E+05	* 0.2531E+05
0.6250E+01	* 0.2888E+05	* 0.2586E+05	* 0.2355E+05	* -.1112E+05	* -.9174E+04	* -.7681E+04	* 0.2532E+05	* 0.2531E+05	* 0.2531E+05
0.7250E+01	* 0.2888E+05	* 0.2586E+05	* 0.2355E+05	* -.1112E+05	* -.9174E+04	* -.7681E+04	* 0.2532E+05	* 0.2531E+05	* 0.2531E+05
0.8250E+01	* 0.2888E+05	* 0.2586E+05	* 0.2355E+05	* -.1112E+05	* -.9174E+04	* -.7681E+04	* 0.2532E+05	* 0.2531E+05	* 0.2531E+05
0.9250E+01	* 0.2888E+05	* 0.2586E+05	* 0.2355E+05	* -.1112E+05	* -.9174E+04	* -.7681E+04	* 0.2532E+05	* 0.2531E+05	* 0.2531E+05
0.1000E+02	* 0.2888E+05	* 0.2586E+05	* 0.2355E+05	* -.1112E+05	* -.9174E+04	* -.7681E+04	* 0.2532E+05	* 0.2531E+05	* 0.2531E+05

TIME=0.128169E-01 SEC

DISPLACEMENTS AND BENDING STRESSES VS. RADIAL STATION

R	DISPLACEMENTS		RADIAL BENDING STRESS		
	IN-PLANE	OUT-OF-PLANE ***LED-EDG	CHD-PNT	TRL-EDG	
0.27000E+02	-.33029E+00	0.19874E+00 **	0.75674E+05	0.75674E+05	0.75674E+05
0.28000E+02	-.44965E+00	0.30739E+00 **	0.66837E+05	0.66837E+05	0.66837E+05
0.29000E+02	-.56901E+00	0.41604E+00 **	0.60926E+05	0.60926E+05	0.60926E+05
0.30000E+02	-.68637E+00	0.52469E+00 **	0.57210E+05	0.57210E+05	0.57210E+05
0.30750E+02	-.77788E+00	0.60618E+00 **	0.54365E+05	0.54365E+05	0.54365E+05
0.31750E+02	-.89724E+00	0.71483E+00 **	0.45632E+05	0.45632E+05	0.45632E+05
0.32750E+02	-.10166E+01	0.82348E+00 **	0.36973E+05	0.36973E+05	0.36973E+05
0.33750E+02	-.11360E+01	0.93213E+00 **	0.28418E+05	0.28418E+05	0.28418E+05

ORIGINAL PAGE IS
OF POOR QUALITY

DISPLACEMENTS VS. CHORDWISE LOCATION AT IMPACT RADIUS

X	IN-PLANE	OUT-OF-PLANE
0.0	-.55520E+00	0.39634E+00
0.60000E+00	-.56873E+00	0.40938E+00
0.12000E+01	-.58582E+00	0.42585E+00
0.18000E+01	-.60291E+00	0.44232E+00
0.24000E+01	-.62000E+00	0.45880E+00
0.30000E+01	-.63769E+00	0.47527E+00
0.36000E+01	-.65418E+00	0.49175E+00
0.42000E+01	-.67127E+00	0.50822E+00

0.48000E+01	-.68837E+00	0.52469E+00
0.54000E+01	-.70546E+00	0.54117E+00
0.62500E+01	-.72967E+00	0.56450E+00
0.72500E+01	-.75815E+00	0.59196E+00
0.82500E+01	-.78664E+00	0.61942E+00
0.92500E+01	-.81512E+00	0.64687E+00
0.10000E+02	-.84005E+00	0.67090E+00

STRESSES VS. CHORDWISE LOCATION AT IMPACT RADIUS

X	STRESS-X			STRESS-Y			SHEAR-XY		
	*R=0.2900E+02	*R=0.3000E+02	*R=0.3075E+02	*R=0.2900E+02	*R=0.3000E+02	*R=0.3075E+02	*R=0.2900E+02	*R=0.3000E+02	*R=0.3075E+02
0.0	* 0.3675E+04	* 0.3409E+04	* 0.3196E+04	* 0.6093E+05	* 0.5721E+05	* 0.5436E+05	* -.3207E+04	* -.3207E+04	* -.3206E+04
0.6000E+00	* 0.3675E+04	* 0.3409E+04	* 0.3196E+04	* 0.6093E+05	* 0.5721E+05	* 0.5436E+05	* -.3207E+04	* -.3207E+04	* -.3206E+04
0.1200E+01	* 0.3675E+04	* 0.3409E+04	* 0.3196E+04	* 0.6093E+05	* 0.5721E+05	* 0.5436E+05	* -.3207E+04	* -.3207E+04	* -.3206E+04
0.1800E+01	* 0.3675E+04	* 0.3409E+04	* 0.3196E+04	* 0.6093E+05	* 0.5721E+05	* 0.5436E+05	* -.3207E+04	* -.3207E+04	* -.3206E+04
0.2400E+01	* 0.3675E+04	* 0.3409E+04	* 0.3196E+04	* 0.6093E+05	* 0.5721E+05	* 0.5436E+05	* -.3207E+04	* -.3207E+04	* -.3206E+04
0.3000E+01	* 0.3675E+04	* 0.3409E+04	* 0.3196E+04	* 0.6093E+05	* 0.5721E+05	* 0.5436E+05	* -.3207E+04	* -.3207E+04	* -.3206E+04
0.3600E+01	* 0.3675E+04	* 0.3409E+04	* 0.3196E+04	* 0.6093E+05	* 0.5721E+05	* 0.5436E+05	* -.3207E+04	* -.3207E+04	* -.3206E+04
0.4200E+01	* 0.3675E+04	* 0.3409E+04	* 0.3196E+04	* 0.6093E+05	* 0.5721E+05	* 0.5436E+05	* -.3207E+04	* -.3207E+04	* -.3206E+04
0.4800E+01	* 0.3675E+04	* 0.3409E+04	* 0.3196E+04	* 0.6093E+05	* 0.5721E+05	* 0.5436E+05	* -.3207E+04	* -.3207E+04	* -.3206E+04
0.5400E+01	* 0.3675E+04	* 0.3409E+04	* 0.3196E+04	* 0.6093E+05	* 0.5721E+05	* 0.5436E+05	* -.3207E+04	* -.3207E+04	* -.3206E+04
0.6250E+01	* 0.3675E+04	* 0.3409E+04	* 0.3196E+04	* 0.6093E+05	* 0.5721E+05	* 0.5436E+05	* -.3207E+04	* -.3207E+04	* -.3206E+04
0.7250E+01	* 0.3675E+04	* 0.3409E+04	* 0.3196E+04	* 0.6093E+05	* 0.5721E+05	* 0.5436E+05	* -.3207E+04	* -.3207E+04	* -.3206E+04
0.8250E+01	* 0.3675E+04	* 0.3409E+04	* 0.3196E+04	* 0.6093E+05	* 0.5721E+05	* 0.5436E+05	* -.3207E+04	* -.3207E+04	* -.3206E+04
0.9250E+01	* 0.3675E+04	* 0.3409E+04	* 0.3196E+04	* 0.6093E+05	* 0.5721E+05	* 0.5436E+05	* -.3207E+04	* -.3207E+04	* -.3206E+04
0.1000E+02	* 0.3675E+04	* 0.3409E+04	* 0.3196E+04	* 0.6093E+05	* 0.5721E+05	* 0.5436E+05	* -.3207E+04	* -.3207E+04	* -.3206E+04

TIME=0.157157E-01 SEC

DISPLACEMENTS AND BENDING STRESSES VS. RADIAL STATION

R	DISPLACEMENTS		RADIAL BENDING STRESS		
	IN-PLANE	OUT-OF-PLANE***LED-EDG	CHD-PNT	TRL-EDG	
0.27000E+02	0.14056E+00	0.22743E-01 ** -.28102E+05	-.28102E+05		-.28102E+05
0.28000E+02	0.20670E+00	-.33820E-01 ** -.23873E+05	-.23873E+05		-.23873E+05
0.29000E+02	0.27284E+00	-.90382E-01 ** -.22000E+05	-.22000E+05		-.22000E+05
0.30000E+02	0.33898E+00	-.14694E+00 ** -.20823E+05	-.20823E+05		-.20823E+05
0.30750E+02	0.38859E+00	-.18937E+00 ** -.19918E+05	-.19918E+05		-.19918E+05
0.31750E+02	0.45473E+00	-.24593E+00 ** -.17146E+05	-.17146E+05		-.17146E+05
0.32750E+02	0.52087E+00	-.30249E+00 ** -.14365E+05	-.14365E+05		-.14365E+05
0.33750E+02	0.58701E+00	-.35905E+00 ** -.11513E+05	-.11513E+05		-.11513E+05

DISPLACEMENTS VS. CHORDWISE LOCATION AT IMPACT RADIUS

X	IN-PLANE	OUT-OF-PLANE
0.0	0.68892E-01	0.32166E+00
0.60000E+00	0.96334E-01	0.27405E+00
0.12000E+01	0.13100E+00	0.21391E+00
0.18000E+01	0.16566E+00	0.15377E+00
0.24000E+01	0.20033E+00	0.93624E-01
0.30000E+01	0.23499E+00	0.33482E-01

0.36000E+01	0.26966E+00	-.26660E-01
0.42000E+01	0.30432E+00	-.86802E-01
0.48000E+01	0.33898E+00	-.14694E+00
0.54000E+01	0.37365E+00	-.20709E+00
0.62500E+01	0.42276E+00	-.29229E+00
0.72500E+01	0.48053E+00	-.39252E+00
0.82500E+01	0.53830E+00	-.49276E+00
0.92500E+01	0.59608E+00	-.59300E+00
0.10000E+02	0.64663E+00	-.68070E+00

STRESSES VS. CHORDWISE LOCATION AT IMPACT RADIUS

X	STRESS-X			STRESS-Y			SHEAR-XY		
	*R=0.2900E+02	*R=0.3000E+02	*R=0.3075E+02	*R=0.2900E+02	*R=0.3000E+02	*R=0.3075E+02	*R=0.2900E+02	*R=0.3000E+02	*R=0.3075E+02
0.0	* -.2595E+05	* -.2422E+05	* -.2290E+05	* -.2200E+05	* -.2082E+05	* -.1992E+05	* -.1873E+05	* -.1872E+05	* -.1872E+05
0.6000E+00	* -.2595E+05	* -.2422E+05	* -.2290E+05	* -.2200E+05	* -.2082E+05	* -.1992E+05	* -.1873E+05	* -.1872E+05	* -.1872E+05
0.1200E+01	* -.2595E+05	* -.2422E+05	* -.2290E+05	* -.2200E+05	* -.2082E+05	* -.1992E+05	* -.1873E+05	* -.1872E+05	* -.1872E+05
0.1800E+01	* -.2595E+05	* -.2422E+05	* -.2290E+05	* -.2200E+05	* -.2082E+05	* -.1992E+05	* -.1873E+05	* -.1872E+05	* -.1872E+05
0.2400E+01	* -.2595E+05	* -.2422E+05	* -.2290E+05	* -.2200E+05	* -.2082E+05	* -.1992E+05	* -.1873E+05	* -.1872E+05	* -.1872E+05
0.3000E+01	* -.2595E+05	* -.2422E+05	* -.2290E+05	* -.2200E+05	* -.2082E+05	* -.1992E+05	* -.1873E+05	* -.1872E+05	* -.1872E+05
0.3600E+01	* -.2595E+05	* -.2422E+05	* -.2290E+05	* -.2200E+05	* -.2082E+05	* -.1992E+05	* -.1873E+05	* -.1872E+05	* -.1872E+05
0.4200E+01	* -.2595E+05	* -.2422E+05	* -.2290E+05	* -.2200E+05	* -.2082E+05	* -.1992E+05	* -.1873E+05	* -.1872E+05	* -.1872E+05
0.4800E+01	* -.2595E+05	* -.2422E+05	* -.2290E+05	* -.2200E+05	* -.2082E+05	* -.1992E+05	* -.1873E+05	* -.1872E+05	* -.1872E+05
0.5400E+01	* -.2595E+05	* -.2422E+05	* -.2290E+05	* -.2200E+05	* -.2082E+05	* -.1992E+05	* -.1873E+05	* -.1872E+05	* -.1872E+05
0.6250E+01	* -.2595E+05	* -.2422E+05	* -.2290E+05	* -.2200E+05	* -.2082E+05	* -.1992E+05	* -.1873E+05	* -.1872E+05	* -.1872E+05
0.7250E+01	* -.2595E+05	* -.2422E+05	* -.2290E+05	* -.2200E+05	* -.2082E+05	* -.1992E+05	* -.1873E+05	* -.1872E+05	* -.1872E+05
0.8250E+01	* -.2595E+05	* -.2422E+05	* -.2290E+05	* -.2200E+05	* -.2082E+05	* -.1992E+05	* -.1873E+05	* -.1872E+05	* -.1872E+05
0.9250E+01	* -.2595E+05	* -.2422E+05	* -.2290E+05	* -.2200E+05	* -.2082E+05	* -.1992E+05	* -.1873E+05	* -.1872E+05	* -.1872E+05
0.1000E+02	* -.2595E+05	* -.2422E+05	* -.2290E+05	* -.2200E+05	* -.2082E+05	* -.1992E+05	* -.1873E+05	* -.1872E+05	* -.1872E+05

TIME=0.186145E-01 SEC

DISPLACEMENTS AND BENDING STRESSES VS. RADIAL STATION

R	DISPLACEMENTS		RADIAL BENDING STRESS		
	IN-PLANE	OUT-OF-PLANE***LED-EDG	CHD-PNT	TRL-EDG	
0.27000E+02	0.25773E+00	-.19832E+00 **	-.44022E+05	-.44022E+05	-.44022E+05
0.28000E+02	0.35375E+00	-.29426E+00 **	-.38984E+05	-.38984E+05	-.38984E+05
0.29000E+02	0.44976E+00	-.39020E+00 **	-.35179E+05	-.35179E+05	-.35179E+05
0.30000E+02	0.54578E+00	-.48613E+00 **	-.32784E+05	-.32784E+05	-.32784E+05
0.30750E+02	0.61779E+00	-.55808E+00 **	-.30957E+05	-.30957E+05	-.30957E+05
0.31750E+02	0.71381E+00	-.65402E+00 **	-.25332E+05	-.25332E+05	-.25332E+05
0.32750E+02	0.80983E+00	-.74996E+00 **	-.19781E+05	-.19781E+05	-.19781E+05
0.33750E+02	0.90585E+00	-.84589E+00 **	-.14419E+05	-.14419E+05	-.14419E+05

DISPLACEMENTS VS. CHORDWISE LOCATION AT IMPACT RADIUS

X	IN-PLANE	OUT-OF-PLANE
0.0	0.44682E+00	-.45210E+00
0.60000E+00	0.45687E+00	-.45556E+00
0.12000E+01	0.46957E+00	-.45992E+00
0.18000E+01	0.48228E+00	-.46429E+00

0.24000E+01	0.49498E+00	- .46866E+00
0.30000E+01	0.50768E+00	- .47303E+00
0.36000E+01	0.52038E+00	- .47740E+00
0.42000E+01	0.53308E+00	- .48176E+00
0.48000E+01	0.54578E+00	- .48613E+00
0.54000E+01	0.55848E+00	- .49050E+00
0.62500E+01	0.57648E+00	- .49669E+00
0.72500E+01	0.59764E+00	- .50397E+00
0.82500E+01	0.61881E+00	- .51125E+00
0.92500E+01	0.63998E+00	- .51853E+00
0.10000E+02	0.65850E+00	- .52490E+00

STRESSES VS. CHORDWISE LOCATION AT IMPACT RADIUS

X	STRESS-X				STRESS-Y				SHEAR-XY			
	*R=0.2900E+02	*R=0.3000E+02	*R=0.3075E+02	*R=0.2900E+02	*R=0.3000E+02	*R=0.3075E+02	*R=0.2900E+02	*R=0.3000E+02	*R=0.3075E+02			
0.0	* 0.2887E+05	* 0.2686E+05	* 0.2535E+05	* -.3518E+05	* -.3278E+05	* -.3096E+05	* 0.6183E+04	* 0.6181E+04	* 0.6180E+04			
0.6000E+00	* 0.2887E+05	* 0.2686E+05	* 0.2535E+05	* -.3518E+05	* -.3278E+05	* -.3096E+05	* 0.6183E+04	* 0.6181E+04	* 0.6180E+04			
0.1200E+01	* 0.2887E+05	* 0.2686E+05	* 0.2535E+05	* -.3518E+05	* -.3278E+05	* -.3096E+05	* 0.6183E+04	* 0.6181E+04	* 0.6180E+04			
0.1800E+01	* 0.2887E+05	* 0.2686E+05	* 0.2535E+05	* -.3518E+05	* -.3278E+05	* -.3096E+05	* 0.6183E+04	* 0.6181E+04	* 0.6180E+04			
0.2400E+01	* 0.2887E+05	* 0.2686E+05	* 0.2535E+05	* -.3518E+05	* -.3278E+05	* -.3096E+05	* 0.6183E+04	* 0.6181E+04	* 0.6180E+04			
0.3000E+01	* 0.2887E+05	* 0.2686E+05	* 0.2535E+05	* -.3518E+05	* -.3278E+05	* -.3096E+05	* 0.6183E+04	* 0.6181E+04	* 0.6180E+04			
0.3600E+01	* 0.2887E+05	* 0.2686E+05	* 0.2535E+05	* -.3518E+05	* -.3278E+05	* -.3096E+05	* 0.6183E+04	* 0.6181E+04	* 0.6180E+04			
0.4200E+01	* 0.2887E+05	* 0.2686E+05	* 0.2535E+05	* -.3518E+05	* -.3278E+05	* -.3096E+05	* 0.6183E+04	* 0.6181E+04	* 0.6180E+04			
0.4800E+01	* 0.2887E+05	* 0.2686E+05	* 0.2535E+05	* -.3518E+05	* -.3278E+05	* -.3096E+05	* 0.6183E+04	* 0.6181E+04	* 0.6180E+04			
0.5400E+01	* 0.2887E+05	* 0.2686E+05	* 0.2535E+05	* -.3518E+05	* -.3278E+05	* -.3096E+05	* 0.6183E+04	* 0.6181E+04	* 0.6180E+04			
0.6250E+01	* 0.2887E+05	* 0.2686E+05	* 0.2535E+05	* -.3518E+05	* -.3278E+05	* -.3096E+05	* 0.6183E+04	* 0.6181E+04	* 0.6180E+04			
0.7250E+01	* 0.2887E+05	* 0.2686E+05	* 0.2535E+05	* -.3518E+05	* -.3278E+05	* -.3096E+05	* 0.6183E+04	* 0.6181E+04	* 0.6180E+04			
0.8250E+01	* 0.2887E+05	* 0.2686E+05	* 0.2535E+05	* -.3518E+05	* -.3278E+05	* -.3096E+05	* 0.6183E+04	* 0.6181E+04	* 0.6180E+04			
0.9250E+01	* 0.2887E+05	* 0.2686E+05	* 0.2535E+05	* -.3518E+05	* -.3278E+05	* -.3096E+05	* 0.6183E+04	* 0.6181E+04	* 0.6180E+04			
0.1000E+02	* 0.2887E+05	* 0.2686E+05	* 0.2535E+05	* -.3518E+05	* -.3278E+05	* -.3096E+05	* 0.6183E+04	* 0.6181E+04	* 0.6180E+04			

TIME=0.215133E-01 SEC

DISPLACEMENTS AND BENDING STRESSES VS. RADIAL STATION

R	DISPLACEMENTS			RADIAL BENDING STRESS		
	IN-PLANE	OUT-OF-PLANE**LED-EDG	CHD-PNT	TRL-EDG		
0.27000E+02	0.61188E-01	-.68930E-01 ** 0.11510E+05	0.11510E+05	0.11510E+05		
0.28000E+02	0.75653E-01	-.82111E-01 ** 0.96758E+04	0.96758E+04	0.96758E+04		
0.29000E+02	0.90118E-01	-.95290E-01 ** 0.89649E+04	0.89649E+04	0.89649E+04		
0.30000E+02	0.10458E+00	-.10847E+00 ** 0.85199E+04	0.85199E+04	0.85199E+04		
0.30750E+02	0.11543E+00	-.11835E+00 ** 0.81767E+04	0.81767E+04	0.81767E+04		
0.31750E+02	0.12990E+00	-.13153E+00 ** 0.71316E+04	0.71316E+04	0.71316E+04		
0.32750E+02	0.14456E+00	-.14471E+00 ** 0.60978E+04	0.60978E+04	0.60978E+04		
0.33750E+02	0.15883E+00	-.15789E+00 ** 0.50258E+04	0.50258E+04	0.50258E+04		

DISPLACEMENTS VS. CHORDWISE LOCATION AT IMPACT RADIUS

X	IN-PLANE	OUT-OF-PLANE
0.0	0.15319E+00	-.25159E+00
0.60000E+00	0.14825E+00	-.23705E+00

0.12000E+01	0.14201E+00	-21868E+00
0.18000E+01	0.13577E+00	-20031E+00
0.24000E+01	0.12954E+00	-18194E+00
0.30000E+01	0.12330E+00	-16357E+00
0.36000E+01	0.11706E+00	-14521E+00
0.42000E+01	0.11082E+00	-12684E+00
0.48000E+01	0.10458E+00	-10847E+00
0.54000E+01	0.98344E-01	-90102E-01
0.62500E+01	0.89507E-01	-64080E-01
0.72500E+01	0.79110E-01	-33467E-01
0.82500E+01	0.68712E-01	-28534E-02
0.92500E+01	0.58315E-01	0.27760E-01
0.10000E+02	0.49217E-01	0.54546E-01

STRESSES VS. CHORDWISE LOCATION
AT IMPACT RADIUS

X	STRESS-X				STRESS-Y				SHEAR-XY			
	*R=0.2900E+02	*R=0.3000E+02	*R=0.3075E+02	*R=0.3000E+02	*R=0.2900E+02	*R=0.3000E+02	*R=0.3075E+02	*R=0.3000E+02	*R=0.2900E+02	*R=0.3000E+02	*R=0.3075E+02	*R=0.3000E+02
0.0	* 0.3703E+05	* 0.3462E+05	* 0.3280E+05	* 0.3280E+05	* 0.8965E+04	* 0.8520E+04	* 0.8177E+04	* 0.8177E+04	* 0.8785E+04	* 0.8783E+04	* 0.8781E+04	* 0.8781E+04
0.6000E+00	* 0.3703E+05	* 0.3462E+05	* 0.3280E+05	* 0.3280E+05	* 0.8965E+04	* 0.8520E+04	* 0.8177E+04	* 0.8177E+04	* 0.8785E+04	* 0.8783E+04	* 0.8781E+04	* 0.8781E+04
0.1200E+01	* 0.3703E+05	* 0.3462E+05	* 0.3280E+05	* 0.3280E+05	* 0.8965E+04	* 0.8520E+04	* 0.8177E+04	* 0.8177E+04	* 0.8785E+04	* 0.8783E+04	* 0.8781E+04	* 0.8781E+04
0.1800E+01	* 0.3703E+05	* 0.3462E+05	* 0.3280E+05	* 0.3280E+05	* 0.8965E+04	* 0.8520E+04	* 0.8177E+04	* 0.8177E+04	* 0.8785E+04	* 0.8783E+04	* 0.8781E+04	* 0.8781E+04
0.2400E+01	* 0.3703E+05	* 0.3462E+05	* 0.3280E+05	* 0.3280E+05	* 0.8965E+04	* 0.8520E+04	* 0.8177E+04	* 0.8177E+04	* 0.8785E+04	* 0.8783E+04	* 0.8781E+04	* 0.8781E+04
0.3000E+01	* 0.3703E+05	* 0.3462E+05	* 0.3280E+05	* 0.3280E+05	* 0.8965E+04	* 0.8520E+04	* 0.8177E+04	* 0.8177E+04	* 0.8785E+04	* 0.8783E+04	* 0.8781E+04	* 0.8781E+04
0.3600E+01	* 0.3703E+05	* 0.3462E+05	* 0.3280E+05	* 0.3280E+05	* 0.8965E+04	* 0.8520E+04	* 0.8177E+04	* 0.8177E+04	* 0.8785E+04	* 0.8783E+04	* 0.8781E+04	* 0.8781E+04
0.4200E+01	* 0.3703E+05	* 0.3462E+05	* 0.3280E+05	* 0.3280E+05	* 0.8965E+04	* 0.8520E+04	* 0.8177E+04	* 0.8177E+04	* 0.8785E+04	* 0.8783E+04	* 0.8781E+04	* 0.8781E+04
0.4800E+01	* 0.3703E+05	* 0.3462E+05	* 0.3280E+05	* 0.3280E+05	* 0.8965E+04	* 0.8520E+04	* 0.8177E+04	* 0.8177E+04	* 0.8785E+04	* 0.8783E+04	* 0.8781E+04	* 0.8781E+04
0.5400E+01	* 0.3703E+05	* 0.3462E+05	* 0.3280E+05	* 0.3280E+05	* 0.8965E+04	* 0.8520E+04	* 0.8177E+04	* 0.8177E+04	* 0.8785E+04	* 0.8783E+04	* 0.8781E+04	* 0.8781E+04
0.6250E+01	* 0.3703E+05	* 0.3462E+05	* 0.3280E+05	* 0.3280E+05	* 0.8965E+04	* 0.8520E+04	* 0.8177E+04	* 0.8177E+04	* 0.8785E+04	* 0.8783E+04	* 0.8781E+04	* 0.8781E+04
0.7250E+01	* 0.3703E+05	* 0.3462E+05	* 0.3280E+05	* 0.3280E+05	* 0.8965E+04	* 0.8520E+04	* 0.8177E+04	* 0.8177E+04	* 0.8785E+04	* 0.8783E+04	* 0.8781E+04	* 0.8781E+04
0.8250E+01	* 0.3703E+05	* 0.3462E+05	* 0.3280E+05	* 0.3280E+05	* 0.8965E+04	* 0.8520E+04	* 0.8177E+04	* 0.8177E+04	* 0.8785E+04	* 0.8783E+04	* 0.8781E+04	* 0.8781E+04
0.9250E+01	* 0.3703E+05	* 0.3462E+05	* 0.3280E+05	* 0.3280E+05	* 0.8965E+04	* 0.8520E+04	* 0.8177E+04	* 0.8177E+04	* 0.8785E+04	* 0.8783E+04	* 0.8781E+04	* 0.8781E+04
0.1000E+02	* 0.3703E+05	* 0.3462E+05	* 0.3280E+05	* 0.3280E+05	* 0.8965E+04	* 0.8520E+04	* 0.8177E+04	* 0.8177E+04	* 0.8785E+04	* 0.8783E+04	* 0.8781E+04	* 0.8781E+04

TIME=0.244121E-01 SEC

DISPLACEMENTS AND BENDING STRESSES VS. RADIAL STATION

R	DISPLACEMENTS		RADIAL BENDING STRESS		
	IN-PLANE	OUT-OF-PLANE***LED-EDG	CHD-PNT	TRL-EDG	
0.27000E+02	-11515E+00	0.10322E+00 ** 0.49779E+04	0.49779E+04	0.49779E+04	
0.28000E+02	-16981E+00	0.16170E+00 ** 0.48937E+04	0.48937E+04	0.48937E+04	
0.29000E+02	-22446E+00	0.22018E+00 ** 0.42977E+04	0.42977E+04	0.42977E+04	
0.30000E+02	-27912E+00	0.27665E+00 ** 0.39187E+04	0.39187E+04	0.39187E+04	
0.30750E+02	-32011E+00	0.32251E+00 ** 0.36370E+04	0.36370E+04	0.36370E+04	
0.31750E+02	-37476E+00	0.38098E+00 ** 0.27497E+04	0.27497E+04	0.27497E+04	
0.32750E+02	-42942E+00	0.43946E+00 ** 0.18780E+04	0.18780E+04	0.18780E+04	
0.33750E+02	-48408E+00	0.49793E+00 ** 0.10948E+04	0.10948E+04	0.10948E+04	

DISPLACEMENTS VS. CHORDWISE LOCATION
AT IMPACT RADIUS

X IN-PLANE OUT-OF-PLANE

0.0	-24081E+00	0.32853E+00
0.60000E+00	-24470E+00	0.32346E+00
0.12000E+01	-24962E+00	0.31706E+00
0.18000E+01	-25453E+00	0.31066E+00
0.24000E+01	-25945E+00	0.30425E+00
0.30000E+01	-26437E+00	0.29785E+00
0.36000E+01	-26928E+00	0.29145E+00
0.42000E+01	-27420E+00	0.28505E+00
0.48000E+01	-27912E+00	0.27865E+00
0.54000E+01	-28403E+00	0.27225E+00
0.62500E+01	-29100E+00	0.26318E+00
0.72500E+01	-29920E+00	0.25251E+00
0.82500E+01	-30739E+00	0.24185E+00
0.92500E+01	-31559E+00	0.23118E+00
0.10000E+02	-32276E+00	0.22184E+00

STRESSES VS. CHORDWISE LOCATION AT IMPACT RADIUS

X	STRESS-X			STRESS-Y			SHEAR-XY		
	*R=0.2900E+02	*R=0.3000E+02	*R=0.3075E+02	*R=0.2900E+02	*R=0.3000E+02	*R=0.3075E+02	*R=0.2900E+02	*R=0.3000E+02	*R=0.3075E+02
0.0	*-3742E+05	*-3501E+05	*-3318E+05	*0.4298E+04	*0.3919E+04	*0.3637E+04	*-7571E+04	*-7569E+04	*-7567E+04
0.6000E+00	*-3742E+05	*-3501E+05	*-3318E+05	*0.4298E+04	*0.3919E+04	*0.3637E+04	*-7571E+04	*-7569E+04	*-7567E+04
0.1200E+01	*-3742E+05	*-3501E+05	*-3318E+05	*0.4298E+04	*0.3919E+04	*0.3637E+04	*-7571E+04	*-7569E+04	*-7567E+04
0.1800E+01	*-3742E+05	*-3501E+05	*-3318E+05	*0.4298E+04	*0.3919E+04	*0.3637E+04	*-7571E+04	*-7569E+04	*-7567E+04
0.2400E+01	*-3742E+05	*-3501E+05	*-3318E+05	*0.4298E+04	*0.3919E+04	*0.3637E+04	*-7571E+04	*-7569E+04	*-7567E+04
0.3000E+01	*-3742E+05	*-3501E+05	*-3318E+05	*0.4298E+04	*0.3919E+04	*0.3637E+04	*-7571E+04	*-7569E+04	*-7567E+04
0.3600E+01	*-3742E+05	*-3501E+05	*-3318E+05	*0.4298E+04	*0.3919E+04	*0.3637E+04	*-7571E+04	*-7569E+04	*-7567E+04
0.4200E+01	*-3742E+05	*-3501E+05	*-3318E+05	*0.4298E+04	*0.3919E+04	*0.3637E+04	*-7571E+04	*-7569E+04	*-7567E+04
0.4800E+01	*-3742E+05	*-3501E+05	*-3318E+05	*0.4298E+04	*0.3919E+04	*0.3637E+04	*-7571E+04	*-7569E+04	*-7567E+04
0.5400E+01	*-3742E+05	*-3501E+05	*-3318E+05	*0.4298E+04	*0.3919E+04	*0.3637E+04	*-7571E+04	*-7569E+04	*-7567E+04
0.6250E+01	*-3742E+05	*-3501E+05	*-3318E+05	*0.4298E+04	*0.3919E+04	*0.3637E+04	*-7571E+04	*-7569E+04	*-7567E+04
0.7250E+01	*-3742E+05	*-3501E+05	*-3318E+05	*0.4298E+04	*0.3919E+04	*0.3637E+04	*-7571E+04	*-7569E+04	*-7567E+04
0.8250E+01	*-3742E+05	*-3501E+05	*-3318E+05	*0.4298E+04	*0.3919E+04	*0.3637E+04	*-7571E+04	*-7569E+04	*-7567E+04
0.9250E+01	*-3742E+05	*-3501E+05	*-3318E+05	*0.4298E+04	*0.3919E+04	*0.3637E+04	*-7571E+04	*-7569E+04	*-7567E+04
0.1000E+02	*-3742E+05	*-3501E+05	*-3318E+05	*0.4298E+04	*0.3919E+04	*0.3637E+04	*-7571E+04	*-7569E+04	*-7567E+04

TIME=0.273109E-01 SEC

DISPLACEMENTS AND BENDING STRESSES VS. RADIAL STATION

R	DISPLACEMENTS		RADIAL BENDING STRESS	
	IN-PLANE	OUT-OF-PLANE**LED-EDG	CHD-PNT	TRL-EDG
0.27000E+02	-31290E+00	0.19413E+00 ** 0.35796E+05	0.35796E+05	0.35796E+05
0.28000E+02	-39396E+00	0.25945E+00 ** 0.31391E+05	0.31391E+05	0.31391E+05
0.29000E+02	-47503E+00	0.32478E+00 ** 0.28284E+05	0.28284E+05	0.28284E+05
0.30000E+02	-55610E+00	0.39011E+00 ** 0.26330E+05	0.26330E+05	0.26330E+05
0.30750E+02	-61690E+00	0.43910E+00 ** 0.24831E+05	0.24831E+05	0.24831E+05
0.31750E+02	-69796E+00	0.50443E+00 ** 0.20235E+05	0.20235E+05	0.20235E+05
0.32750E+02	-77903E+00	0.56976E+00 ** 0.15674E+05	0.15674E+05	0.15674E+05
0.33750E+02	-86010E+00	0.63509E+00 ** 0.11228E+05	0.11228E+05	0.11228E+05

DISPLACEMENTS VS. CHORDWISE LOCATION AT IMPACT RADIUS

X	IN-PLANE	OUT-OF-PLANE
0.0	-.47957E+00	0.33444E+00
0.60000E+00	-.48735E+00	0.34009E+00
0.12000E+01	-.49717E+00	0.34724E+00
0.18000E+01	-.50699E+00	0.35438E+00
0.24000E+01	-.51681E+00	0.36153E+00
0.30000E+01	-.52663E+00	0.36867E+00
0.36000E+01	-.53645E+00	0.37582E+00
0.42000E+01	-.54628E+00	0.38296E+00
0.48000E+01	-.55610E+00	0.39011E+00
0.54000E+01	-.56592E+00	0.39725E+00
0.62500E+01	-.57983E+00	0.40739E+00
0.72500E+01	-.59620E+00	0.41928E+00
0.82500E+01	-.61257E+00	0.43119E+00
0.92500E+01	-.62894E+00	0.44310E+00
0.10000E+02	-.64326E+00	0.45352E+00

STRESSES VS. CHORDWISE LOCATION
AT IMPACT RADIUS

X	STRESS-X			STRESS-Y			SHEAR-XY		
	*R=0.2900E+02	*R=0.3000E+02	*R=0.3075E+02	*R=0.2900E+02	*R=0.3000E+02	*R=0.3075E+02	*R=0.2900E+02	*R=0.3000E+02	*R=0.3075E+02
0.0	*-.3226E+05	*-.3000E+05	*-.2828E+05	*0.2828E+05	*0.2633E+05	*0.2483E+05	*-.3331E+04	*-.3330E+04	*-.3330E+04
0.6000E+00	*-.3226E+05	*-.3000E+05	*-.2828E+05	*0.2828E+05	*0.2633E+05	*0.2483E+05	*-.3331E+04	*-.3330E+04	*-.3330E+04
0.1200E+01	*-.3226E+05	*-.3000E+05	*-.2828E+05	*0.2828E+05	*0.2633E+05	*0.2483E+05	*-.3331E+04	*-.3330E+04	*-.3330E+04
0.1800E+01	*-.3226E+05	*-.3000E+05	*-.2828E+05	*0.2828E+05	*0.2633E+05	*0.2483E+05	*-.3331E+04	*-.3330E+04	*-.3330E+04
0.2400E+01	*-.3226E+05	*-.3000E+05	*-.2828E+05	*0.2828E+05	*0.2633E+05	*0.2483E+05	*-.3331E+04	*-.3330E+04	*-.3330E+04
0.3000E+01	*-.3226E+05	*-.3000E+05	*-.2828E+05	*0.2828E+05	*0.2633E+05	*0.2483E+05	*-.3331E+04	*-.3330E+04	*-.3330E+04
0.3600E+01	*-.3226E+05	*-.3000E+05	*-.2828E+05	*0.2828E+05	*0.2633E+05	*0.2483E+05	*-.3331E+04	*-.3330E+04	*-.3330E+04
0.4200E+01	*-.3226E+05	*-.3000E+05	*-.2828E+05	*0.2828E+05	*0.2633E+05	*0.2483E+05	*-.3331E+04	*-.3330E+04	*-.3330E+04
0.4800E+01	*-.3226E+05	*-.3000E+05	*-.2828E+05	*0.2828E+05	*0.2633E+05	*0.2483E+05	*-.3331E+04	*-.3330E+04	*-.3330E+04
0.5400E+01	*-.3226E+05	*-.3000E+05	*-.2828E+05	*0.2828E+05	*0.2633E+05	*0.2483E+05	*-.3331E+04	*-.3330E+04	*-.3330E+04
0.6250E+01	*-.3226E+05	*-.3000E+05	*-.2828E+05	*0.2828E+05	*0.2633E+05	*0.2483E+05	*-.3331E+04	*-.3330E+04	*-.3330E+04
0.7250E+01	*-.3226E+05	*-.3000E+05	*-.2828E+05	*0.2828E+05	*0.2633E+05	*0.2483E+05	*-.3331E+04	*-.3330E+04	*-.3330E+04
0.8250E+01	*-.3226E+05	*-.3000E+05	*-.2828E+05	*0.2828E+05	*0.2633E+05	*0.2483E+05	*-.3331E+04	*-.3330E+04	*-.3330E+04
0.9250E+01	*-.3226E+05	*-.3000E+05	*-.2828E+05	*0.2828E+05	*0.2633E+05	*0.2483E+05	*-.3331E+04	*-.3330E+04	*-.3330E+04
0.1000E+02	*-.3226E+05	*-.3000E+05	*-.2828E+05	*0.2828E+05	*0.2633E+05	*0.2483E+05	*-.3331E+04	*-.3330E+04	*-.3330E+04

TIME=0.302097E-01 SEC

DISPLACEMENTS AND BENDING STRESSES VS. RADIAL STATION

R	DISPLACEMENTS			RADIAL BENDING STRESS		
	IN-PLANE	CUT-OF-PLANE***LED-EDG		CHD-PNT	TRL-EDG	
0.27000E+02	0.14668E+00	-.13697E+00	**-.12667E+05	-.12667E+05	-.12667E+05	
0.28000E+02	0.16321E+00	-.14404E+00	**-.11402E+05	-.11402E+05	-.11402E+05	
0.29000E+02	0.17954E+00	-.15112E+00	**-.10084E+05	-.10084E+05	-.10084E+05	
0.30000E+02	0.19587E+00	-.15819E+00	**-.92564E+04	-.92564E+04	-.92564E+04	
0.30750E+02	0.20812E+00	-.16349E+00	**-.86191E+04	-.86191E+04	-.86191E+04	
0.31750E+02	0.22445E+00	-.17057E+00	**-.66709E+04	-.66709E+04	-.66709E+04	
0.32750E+02	0.24078E+00	-.17764E+00	**-.47477E+04	-.47477E+04	-.47477E+04	
0.33750E+02	0.25712E+00	-.18471E+00	**-.29183E+04	-.29183E+04	-.29183E+04	

ORIGINAL PAGE IS
OF POOR QUALITY

DISPLACEMENTS VS. CHORDWISE LOCATION
AT IMPACT RADIUS

X	IN-PLANE	OUT-OF-PLANE
0.0	0.28705E+00	-.34584E+00
0.60000E+00	0.27779E+00	-.32678E+00
0.12000E+01	0.26609E+00	-.30269E+00
0.18000E+01	0.25438E+00	-.27861E+00
0.24000E+01	0.24268E+00	-.25452E+00
0.30000E+01	0.23098E+00	-.23044E+00
0.36000E+01	0.21928E+00	-.20636E+00
0.42000E+01	0.20758E+00	-.18227E+00
0.48000E+01	0.19587E+00	-.15819E+00
0.54000E+01	0.18417E+00	-.13411E+00
0.62500E+01	0.16759E+00	-.99987E-01
0.72500E+01	0.14809E+00	-.59847E-01
0.82500E+01	0.12859E+00	-.19707E-01
0.92500E+01	0.10908E+00	0.20432E-01
0.10000E+02	0.92016E-01	0.55554E-01

STRESSES VS. CHORDWISE LOCATION
AT IMPACT RADIUS

X	STRESS-X	STRESS-Y	SHEAR-XY
0.0	*R=0.2900E+02 * 0.3000E+02 * 0.3075E+02	*R=0.2900E+02 * 0.3000E+02 * 0.3075E+02	*R=0.2900E+02 * 0.3000E+02 * 0.3075E+02
0.6000E+00	* 0.2863E+05 * 0.2663E+05 * 0.2511E+05	* -.1008E+05 * -.9256E+04 * -.8619E+04	* 0.1055E+05 * 0.1055E+05 * 0.1055E+05
0.1200E+01	* 0.2863E+05 * 0.2663E+05 * 0.2511E+05	* -.1008E+05 * -.9256E+04 * -.8619E+04	* 0.1055E+05 * 0.1055E+05 * 0.1055E+05
0.1800E+01	* 0.2863E+05 * 0.2663E+05 * 0.2511E+05	* -.1008E+05 * -.9256E+04 * -.8619E+04	* 0.1055E+05 * 0.1055E+05 * 0.1055E+05
0.2400E+01	* 0.2863E+05 * 0.2663E+05 * 0.2511E+05	* -.1008E+05 * -.9256E+04 * -.8619E+04	* 0.1055E+05 * 0.1055E+05 * 0.1055E+05
0.3000E+01	* 0.2863E+05 * 0.2663E+05 * 0.2511E+05	* -.1008E+05 * -.9256E+04 * -.8619E+04	* 0.1055E+05 * 0.1055E+05 * 0.1055E+05
0.3600E+01	* 0.2863E+05 * 0.2663E+05 * 0.2511E+05	* -.1008E+05 * -.9256E+04 * -.8619E+04	* 0.1055E+05 * 0.1055E+05 * 0.1055E+05
0.4200E+01	* 0.2863E+05 * 0.2663E+05 * 0.2511E+05	* -.1008E+05 * -.9256E+04 * -.8619E+04	* 0.1055E+05 * 0.1055E+05 * 0.1055E+05
0.4800E+01	* 0.2863E+05 * 0.2663E+05 * 0.2511E+05	* -.1008E+05 * -.9256E+04 * -.8619E+04	* 0.1055E+05 * 0.1055E+05 * 0.1055E+05
0.5400E+01	* 0.2863E+05 * 0.2663E+05 * 0.2511E+05	* -.1008E+05 * -.9256E+04 * -.8619E+04	* 0.1055E+05 * 0.1055E+05 * 0.1055E+05
0.6250E+01	* 0.2863E+05 * 0.2663E+05 * 0.2511E+05	* -.1008E+05 * -.9256E+04 * -.8619E+04	* 0.1055E+05 * 0.1055E+05 * 0.1055E+05
0.7250E+01	* 0.2863E+05 * 0.2663E+05 * 0.2511E+05	* -.1008E+05 * -.9256E+04 * -.8619E+04	* 0.1055E+05 * 0.1055E+05 * 0.1055E+05
0.8250E+01	* 0.2863E+05 * 0.2663E+05 * 0.2511E+05	* -.1008E+05 * -.9256E+04 * -.8619E+04	* 0.1055E+05 * 0.1055E+05 * 0.1055E+05
0.9250E+01	* 0.2863E+05 * 0.2663E+05 * 0.2511E+05	* -.1008E+05 * -.9256E+04 * -.8619E+04	* 0.1055E+05 * 0.1055E+05 * 0.1055E+05
0.1000E+02	* 0.2863E+05 * 0.2663E+05 * 0.2511E+05	* -.1008E+05 * -.9256E+04 * -.8619E+04	* 0.1055E+05 * 0.1055E+05 * 0.1055E+05

TIME=0.331085E-01 SEC

DISPLACEMENTS AND BENDING STRESSES VS. RADIAL STATION

R	DISPLACEMENTS	RADIAL BENDING STRESS
	IN-PLANE	OUT-OF-PLANE***LED-EDG
0.27000E+02	0.18395E+00	-.67796E-01 ** -.25494E+05
0.28000E+02	0.27732E+00	-.15719E+00 ** -.22653E+05
0.29000E+02	0.37069E+00	-.24658E+00 ** -.20855E+05
0.30000E+02	0.46406E+00	-.33598E+00 ** -.19722E+05
0.30750E+02	0.53408E+00	-.40302E+00 ** -.18858E+05
0.31750E+02	0.62745E+00	-.49242E+00 ** -.16195E+05
0.32750E+02	0.72082E+00	-.58181E+00 ** -.13526E+05
0.33750E+02	0.81418E+00	-.67120E+00 ** -.10845E+05
		CHD-PNT
		TRL-EDG
		-.25494E+05
		-.22653E+05
		-.20855E+05
		-.19722E+05
		-.18858E+05
		-.16195E+05
		-.13526E+05
		-.10845E+05

DISPLACEMENTS VS. CHORDWISE LOCATION
AT IMPACT RADIUS

X	IN-PLANE	OUT-OF-PLANE
0.0	0.28131E+00	-.12225E+00
0.60000E+00	0.29988E+00	-.14397E+00
0.12000E+01	0.32333E+00	-.17140E+00
0.18000E+01	0.34679E+00	-.19883E+00
0.24000E+01	0.37024E+00	-.22626E+00
0.30000E+01	0.39369E+00	-.25369E+00
0.36000E+01	0.41715E+00	-.28112E+00
0.42000E+01	0.44060E+00	-.30855E+00
0.48000E+01	0.46406E+00	-.33598E+00
0.54000E+01	0.48751E+00	-.36341E+00
0.62500E+01	0.52074E+00	-.40227E+00
0.72500E+01	0.55983E+00	-.44798E+00
0.82500E+01	0.59892E+00	-.49370E+00
0.92500E+01	0.63801E+00	-.53942E+00
0.10000E+02	0.67221E+00	-.57942E+00

STRESSES VS. CHORDWISE LOCATION
AT IMPACT RADIUS

X	STRESS-X			STRESS-Y			SHEAR-XY		
	*R=0.2900E+02	*R=0.3000E+02	*R=0.3075E+02	*R=0.2900E+02	*R=0.3000E+02	*R=0.3075E+02	*R=0.2900E+02	*R=0.3000E+02	*R=0.3075E+02
0.0	* 0.1081E+05	* 0.1028E+05	* 0.9889E+04	* -.2085E+05	* -.1972E+05	* -.1886E+05	* -.2628E+04	* -.2628E+04	* -.2627E+04
0.6000E+00	* 0.1081E+05	* 0.1028E+05	* 0.9889E+04	* -.2085E+05	* -.1972E+05	* -.1886E+05	* -.2628E+04	* -.2628E+04	* -.2627E+04
0.1200E+01	* 0.1081E+05	* 0.1028E+05	* 0.9889E+04	* -.2085E+05	* -.1972E+05	* -.1886E+05	* -.2628E+04	* -.2628E+04	* -.2627E+04
0.1800E+01	* 0.1081E+05	* 0.1028E+05	* 0.9889E+04	* -.2085E+05	* -.1972E+05	* -.1886E+05	* -.2628E+04	* -.2628E+04	* -.2627E+04
0.2400E+01	* 0.1081E+05	* 0.1028E+05	* 0.9889E+04	* -.2085E+05	* -.1972E+05	* -.1886E+05	* -.2628E+04	* -.2628E+04	* -.2627E+04
0.3000E+01	* 0.1081E+05	* 0.1028E+05	* 0.9889E+04	* -.2085E+05	* -.1972E+05	* -.1886E+05	* -.2628E+04	* -.2628E+04	* -.2627E+04
0.3600E+01	* 0.1081E+05	* 0.1028E+05	* 0.9889E+04	* -.2085E+05	* -.1972E+05	* -.1886E+05	* -.2628E+04	* -.2628E+04	* -.2627E+04
0.4200E+01	* 0.1081E+05	* 0.1028E+05	* 0.9889E+04	* -.2085E+05	* -.1972E+05	* -.1886E+05	* -.2628E+04	* -.2628E+04	* -.2627E+04
0.4800E+01	* 0.1081E+05	* 0.1028E+05	* 0.9889E+04	* -.2085E+05	* -.1972E+05	* -.1886E+05	* -.2628E+04	* -.2628E+04	* -.2627E+04
0.5400E+01	* 0.1081E+05	* 0.1028E+05	* 0.9889E+04	* -.2085E+05	* -.1972E+05	* -.1886E+05	* -.2628E+04	* -.2628E+04	* -.2627E+04
0.6250E+01	* 0.1081E+05	* 0.1028E+05	* 0.9889E+04	* -.2085E+05	* -.1972E+05	* -.1886E+05	* -.2628E+04	* -.2628E+04	* -.2627E+04
0.7250E+01	* 0.1081E+05	* 0.1028E+05	* 0.9889E+04	* -.2085E+05	* -.1972E+05	* -.1886E+05	* -.2628E+04	* -.2628E+04	* -.2627E+04
0.8250E+01	* 0.1081E+05	* 0.1028E+05	* 0.9889E+04	* -.2085E+05	* -.1972E+05	* -.1886E+05	* -.2628E+04	* -.2628E+04	* -.2627E+04
0.9250E+01	* 0.1081E+05	* 0.1028E+05	* 0.9889E+04	* -.2085E+05	* -.1972E+05	* -.1886E+05	* -.2628E+04	* -.2628E+04	* -.2627E+04
0.1000E+02	* 0.1081E+05	* 0.1028E+05	* 0.9889E+04	* -.2085E+05	* -.1972E+05	* -.1886E+05	* -.2628E+04	* -.2628E+04	* -.2627E+04

TIME=0.360073E-01 SEC

DISPLACEMENTS AND BENDING STRESSES VS. RADIAL STATION

R	DISPLACEMENTS		RADIAL BENDING STRESS		
	IN-PLANE	OUT-OF-PLANE***LED-EDG	CHD-PNT	TRL-EDG	
0.27000E+02	0.86047E-02	0.41158E-01 **	-.76767E+04	-.76767E+04	
0.28000E+02	0.46539E-01	0.22826E-03 **	-.68244E+04	-.68244E+04	
0.29000E+02	0.84472E-01	-.40701E-01 **	-.65411E+04	-.65411E+04	
0.30000E+02	0.12241E+00	-.81631E-01 **	-.63613E+04	-.63613E+04	
0.30750E+02	0.15086E+00	-.11233E+00 **	-.62273E+04	-.62273E+04	
0.31750E+02	0.18879E+00	-.15326E+00 **	-.58061E+04	-.58061E+04	
0.32750E+02	0.22672E+00	-.19419E+00 **	-.53680E+04	-.53680E+04	

0.33750E+02 0.26466E+00 -23512E+00 ** -48636E+04 -48636E+04 -48636E+04

DISPLACEMENTS VS. CHORDWISE LOCATION
AT IMPACT RADIUS

X	IN-PLANE	OUT-OF-PLANE
0.0	-74963E-02	0.10820E+00
0.60000E+00	0.57024E-02	0.88914E-01
0.12000E+01	0.22374E-01	0.64551E-01
0.18000E+01	0.39046E-01	0.40188E-01
0.24000E+01	0.55718E-01	0.15824E-01
0.30000E+01	0.72390E-01	-85398E-02
0.36000E+01	0.89062E-01	-32904E-01
0.42000E+01	0.10573E+00	-57267E-01
0.48000E+01	0.12241E+00	-81631E-01
0.54000E+01	0.13908E+00	-10599E+00
0.62500E+01	0.16270E+00	-14051E+00
0.72500E+01	0.19048E+00	-18112E+00
0.82500E+01	0.21827E+00	-22172E+00
0.92500E+01	0.24606E+00	-26233E+00
0.10000E+02	0.27037E+00	-29786E+00

STRESSES VS. CHORDWISE LOCATION
AT IMPACT RADIUS

X	STRESS-X	STRESS-Y	SHEAR-XY
0.0	*R=0.2900E+02 *R=0.3000E+02 *R=0.3075E+02	*R=0.2900E+02 *R=0.3000E+02 *R=0.3075E+02	*R=0.2900E+02 *R=0.3000E+02 *R=0.3075E+02
0.6000E+00	* -1239E+05 * -1139E+05 * -1063E+05	* -6541E+04 * -6361E+04 * -6227E+04	* -5993E+04 * -5992E+04 * -5992E+04
0.1200E+01	* -1239E+05 * -1139E+05 * -1063E+05	* -6541E+04 * -6361E+04 * -6227E+04	* -5993E+04 * -5992E+04 * -5992E+04
0.1800E+01	* -1239E+05 * -1139E+05 * -1063E+05	* -6541E+04 * -6361E+04 * -6227E+04	* -5993E+04 * -5992E+04 * -5992E+04
0.2400E+01	* -1239E+05 * -1139E+05 * -1063E+05	* -6541E+04 * -6361E+04 * -6227E+04	* -5993E+04 * -5992E+04 * -5992E+04
0.3000E+01	* -1239E+05 * -1139E+05 * -1063E+05	* -6541E+04 * -6361E+04 * -6227E+04	* -5993E+04 * -5992E+04 * -5992E+04
0.3600E+01	* -1239E+05 * -1139E+05 * -1063E+05	* -6541E+04 * -6361E+04 * -6227E+04	* -5993E+04 * -5992E+04 * -5992E+04
0.4200E+01	* -1239E+05 * -1139E+05 * -1063E+05	* -6541E+04 * -6361E+04 * -6227E+04	* -5993E+04 * -5992E+04 * -5992E+04
0.4800E+01	* -1239E+05 * -1139E+05 * -1063E+05	* -6541E+04 * -6361E+04 * -6227E+04	* -5993E+04 * -5992E+04 * -5992E+04
0.5400E+01	* -1239E+05 * -1139E+05 * -1063E+05	* -6541E+04 * -6361E+04 * -6227E+04	* -5993E+04 * -5992E+04 * -5992E+04
0.6250E+01	* -1239E+05 * -1139E+05 * -1063E+05	* -6541E+04 * -6361E+04 * -6227E+04	* -5993E+04 * -5992E+04 * -5992E+04
0.7250E+01	* -1239E+05 * -1139E+05 * -1063E+05	* -6541E+04 * -6361E+04 * -6227E+04	* -5993E+04 * -5992E+04 * -5992E+04
0.8250E+01	* -1239E+05 * -1139E+05 * -1063E+05	* -6541E+04 * -6361E+04 * -6227E+04	* -5993E+04 * -5992E+04 * -5992E+04
0.9250E+01	* -1239E+05 * -1139E+05 * -1063E+05	* -6541E+04 * -6361E+04 * -6227E+04	* -5993E+04 * -5992E+04 * -5992E+04
0.1000E+02	* -1239E+05 * -1139E+05 * -1063E+05	* -6541E+04 * -6361E+04 * -6227E+04	* -5993E+04 * -5992E+04 * -5992E+04

TIME=0.389062E-01 SEC

DISPLACEMENTS AND BENDING STRESSES VS. RADIAL STATION

R	DISPLACEMENTS	RADIAL BENDING STRESS
0.27000E+02	IN-PLANE	CHD-PNT
0.28000E+02	-177466E-01	0.12717E+05
0.29000E+02	-14329E+00	0.11222E+05
0.30000E+02	-20910E+00	0.10436E+05
0.30000E+02	-27492E+00	0.20891E+00 ** 0.99378E+04
0.30750E+02	-32429E+00	0.26065E+00 ** 0.95630E+04
		0.95630E+04

0.31750E+02	-.39011E+00	0.32963E+00	** 0.83948E+04	0.83948E+04	0.83948E+04
0.32750E+02	-.45593E+00	0.39861E+00	** 0.72201E+04	0.72201E+04	0.72201E+04
0.33750E+02	-.52175E+00	0.46760E+00	** 0.60232E+04	0.60232E+04	0.60232E+04

DISPLACEMENTS VS. CHORDWISE LOCATION
AT IMPACT RADIUS

X	IN-PLANE	OUT-OF-PLANE
0.0	-.90709E-01	-.32766E-01
0.60000E+00	-.10943E+00	-.82104E-02
0.12000E+01	-.13307E+00	0.22807E-01
0.18000E+01	-.15671E+00	0.53824E-01
0.24000E+01	-.18035E+00	0.84842E-01
0.30000E+01	-.20400E+00	0.11586E+00
0.36000E+01	-.22764E+00	0.14688E+00
0.42000E+01	-.25128E+00	0.17790E+00
0.48000E+01	-.27492E+00	0.20891E+00
0.54000E+01	-.29857E+00	0.23993E+00
0.62500E+01	-.33206E+00	0.28387E+00
0.72500E+01	-.37147E+00	0.33557E+00
0.82500E+01	-.41087E+00	0.38727E+00
0.92500E+01	-.45028E+00	0.43896E+00
0.10000E+02	-.48475E+00	0.48420E+00

STRESSES VS. CHORDWISE LOCATION
AT IMPACT RADIUS

X	STRESS-X	STRESS-Y	SHEAR-XY
0.0	* -.6990E+03 * -.8066E+03 * -.8947E+03	* 0.1044E+05 * 0.9938E+04 * 0.9563E+04	* 0.6318E+04 * 0.6317E+04 * 0.6316E+04
0.6000E+00	* -.6990E+03 * -.8066E+03 * -.8947E+03	* 0.1044E+05 * 0.9938E+04 * 0.9563E+04	* 0.6318E+04 * 0.6317E+04 * 0.6316E+04
0.1200E+01	* -.6990E+03 * -.8066E+03 * -.8947E+03	* 0.1044E+05 * 0.9938E+04 * 0.9563E+04	* 0.6318E+04 * 0.6317E+04 * 0.6316E+04
0.1800E+01	* -.6990E+03 * -.8066E+03 * -.8947E+03	* 0.1044E+05 * 0.9938E+04 * 0.9563E+04	* 0.6318E+04 * 0.6317E+04 * 0.6316E+04
0.2400E+01	* -.6990E+03 * -.8066E+03 * -.8947E+03	* 0.1044E+05 * 0.9938E+04 * 0.9563E+04	* 0.6318E+04 * 0.6317E+04 * 0.6316E+04
0.3000E+01	* -.6990E+03 * -.8066E+03 * -.8947E+03	* 0.1044E+05 * 0.9938E+04 * 0.9563E+04	* 0.6318E+04 * 0.6317E+04 * 0.6316E+04
0.3600E+01	* -.6990E+03 * -.8066E+03 * -.8947E+03	* 0.1044E+05 * 0.9938E+04 * 0.9563E+04	* 0.6318E+04 * 0.6317E+04 * 0.6316E+04
0.4200E+01	* -.6990E+03 * -.8066E+03 * -.8947E+03	* 0.1044E+05 * 0.9938E+04 * 0.9563E+04	* 0.6318E+04 * 0.6317E+04 * 0.6316E+04
0.4800E+01	* -.6990E+03 * -.8066E+03 * -.8947E+03	* 0.1044E+05 * 0.9938E+04 * 0.9563E+04	* 0.6318E+04 * 0.6317E+04 * 0.6316E+04
0.5400E+01	* -.6990E+03 * -.8066E+03 * -.8947E+03	* 0.1044E+05 * 0.9938E+04 * 0.9563E+04	* 0.6318E+04 * 0.6317E+04 * 0.6316E+04
0.6250E+01	* -.6990E+03 * -.8066E+03 * -.8947E+03	* 0.1044E+05 * 0.9938E+04 * 0.9563E+04	* 0.6318E+04 * 0.6317E+04 * 0.6316E+04
0.7250E+01	* -.6990E+03 * -.8066E+03 * -.8947E+03	* 0.1044E+05 * 0.9938E+04 * 0.9563E+04	* 0.6318E+04 * 0.6317E+04 * 0.6316E+04
0.8250E+01	* -.6990E+03 * -.8066E+03 * -.8947E+03	* 0.1044E+05 * 0.9938E+04 * 0.9563E+04	* 0.6318E+04 * 0.6317E+04 * 0.6316E+04
0.9250E+01	* -.6990E+03 * -.8066E+03 * -.8947E+03	* 0.1044E+05 * 0.9938E+04 * 0.9563E+04	* 0.6318E+04 * 0.6317E+04 * 0.6316E+04
0.1000E+02	* -.6990E+03 * -.8066E+03 * -.8947E+03	* 0.1044E+05 * 0.9938E+04 * 0.9563E+04	* 0.6318E+04 * 0.6317E+04 * 0.6316E+04

TIME=0.418050E-01 SEC

DISPLACEMENTS AND BENDING STRESSES VS. RADIAL STATION

R	DISPLACEMENTS	RADIAL BENDING STRESS
	IN-PLANE	OUT-OF-PLANE***LED-EDG
0.27000E+02	-.21656E+00	0.11188E+00 ** 0.31933E+05
0.28000E+02	-.28852E+00	0.17479E+00 ** 0.27952E+05
0.29000E+02	-.36047E+00	0.23770E+00 ** 0.25380E+05

0.30000E+02	-43242E+00	0.30060E+00	** 0.23763E+05	0.23763E+05	0.23763E+05
0.30750E+02	-48639E+00	0.34779E+00	** 0.22524E+05	0.22524E+05	0.22524E+05
0.31750E+02	-55834E+00	0.41069E+00	** 0.18721E+05	0.18721E+05	0.18721E+05
0.32750E+02	-63030E+00	0.47360E+00	** 0.14942E+05	0.14942E+05	0.14942E+05
0.33750E+02	-70225E+00	0.53651E+00	** 0.11221E+05	0.11221E+05	0.11221E+05

DISPLACEMENTS VS. CHORDWISE LOCATION
AT IMPACT RADIUS

X	IN-PLANE	OUT-OF-PLANE
0.0	-31166E+00	0.15261E+00
0.60000E+00	-32393E+00	0.16765E+00
0.12000E+01	-33943E+00	0.18664E+00
0.18000E+01	-35493E+00	0.20564E+00
0.24000E+01	-37042E+00	0.22463E+00
0.30000E+01	-38592E+00	0.24362E+00
0.36000E+01	-40142E+00	0.26262E+00
0.42000E+01	-41692E+00	0.28161E+00
0.48000E+01	-43242E+00	0.30060E+00
0.54000E+01	-44792E+00	0.31960E+00
0.62500E+01	-46988E+00	0.34651E+00
0.72500E+01	-49571E+00	0.37816E+00
0.82500E+01	-52155E+00	0.40982E+00
0.92500E+01	-54738E+00	0.44148E+00
0.10000E+02	-56998E+00	0.46917E+00

STRESSES VS. CHORDWISE LOCATION
AT IMPACT RADIUS

X	STRESS-X	STRESS-Y	SHEAR-XY
0.0	*R=0.2900E+02 * -1.101E+05 * -1.025E+05 * -9671E+04	*R=0.2900E+02 *R=0.3000E+02 *R=0.3075E+02 * 0.2538E+05 * 0.2376E+05 * 0.2252E+05	*R=0.2900E+02 *R=0.3000E+02 *R=0.3075E+02 * 0.1821E+04 * 0.1820E+04 * 0.1820E+04
0.6000E+00	* -1.101E+05 * -1.025E+05 * -9671E+04	* 0.2538E+05 * 0.2376E+05 * 0.2252E+05	* 0.1821E+04 * 0.1820E+04 * 0.1820E+04
0.1200E+01	* -1.101E+05 * -1.025E+05 * -9671E+04	* 0.2538E+05 * 0.2376E+05 * 0.2252E+05	* 0.1821E+04 * 0.1820E+04 * 0.1820E+04
0.1800E+01	* -1.101E+05 * -1.025E+05 * -9671E+04	* 0.2538E+05 * 0.2376E+05 * 0.2252E+05	* 0.1821E+04 * 0.1820E+04 * 0.1820E+04
0.2400E+01	* -1.101E+05 * -1.025E+05 * -9671E+04	* 0.2538E+05 * 0.2376E+05 * 0.2252E+05	* 0.1821E+04 * 0.1820E+04 * 0.1820E+04
0.3000E+01	* -1.101E+05 * -1.025E+05 * -9671E+04	* 0.2538E+05 * 0.2376E+05 * 0.2252E+05	* 0.1821E+04 * 0.1820E+04 * 0.1820E+04
0.3600E+01	* -1.101E+05 * -1.025E+05 * -9671E+04	* 0.2538E+05 * 0.2376E+05 * 0.2252E+05	* 0.1821E+04 * 0.1820E+04 * 0.1820E+04
0.4200E+01	* -1.101E+05 * -1.025E+05 * -9671E+04	* 0.2538E+05 * 0.2376E+05 * 0.2252E+05	* 0.1821E+04 * 0.1820E+04 * 0.1820E+04
0.4800E+01	* -1.101E+05 * -1.025E+05 * -9671E+04	* 0.2538E+05 * 0.2376E+05 * 0.2252E+05	* 0.1821E+04 * 0.1820E+04 * 0.1820E+04
0.5400E+01	* -1.101E+05 * -1.025E+05 * -9671E+04	* 0.2538E+05 * 0.2376E+05 * 0.2252E+05	* 0.1821E+04 * 0.1820E+04 * 0.1820E+04
0.6250E+01	* -1.101E+05 * -1.025E+05 * -9671E+04	* 0.2538E+05 * 0.2376E+05 * 0.2252E+05	* 0.1821E+04 * 0.1820E+04 * 0.1820E+04
0.7250E+01	* -1.101E+05 * -1.025E+05 * -9671E+04	* 0.2538E+05 * 0.2376E+05 * 0.2252E+05	* 0.1821E+04 * 0.1820E+04 * 0.1820E+04
0.8250E+01	* -1.101E+05 * -1.025E+05 * -9671E+04	* 0.2538E+05 * 0.2376E+05 * 0.2252E+05	* 0.1821E+04 * 0.1820E+04 * 0.1820E+04
0.9250E+01	* -1.101E+05 * -1.025E+05 * -9671E+04	* 0.2538E+05 * 0.2376E+05 * 0.2252E+05	* 0.1821E+04 * 0.1820E+04 * 0.1820E+04
0.1000E+02	* -1.101E+05 * -1.025E+05 * -9671E+04	* 0.2538E+05 * 0.2376E+05 * 0.2252E+05	* 0.1821E+04 * 0.1820E+04 * 0.1820E+04

TIME=0.447038E-01 SEC

DISPLACEMENTS AND BENDING STRESSES VS. RADIAL STATION

R	DISPLACEMENTS	RADIAL BENDING STRESS
0.27000E+02	IN-PLANE OUT-OF-PLANE***LED-EDG	CHD-PNT TRL-EDG
	0.75809E-01 -24173E-01 ** -17831E+05	-17831E+05 -17831E+05

0.28000E+02	0.10653E+00	-.51367E-01 **	-.15568E+05	-.15568E+05	-.15568E+05
0.29000E+02	0.13725E+00	-.78560E-01 **	-.14251E+05	-.14251E+05	-.14251E+05
0.30000E+02	0.16797E+00	-.10575E+00 **	-.13424E+05	-.13424E+05	-.13424E+05
0.30750E+02	0.19101E+00	-.12615E+00 **	-.12789E+05	-.12789E+05	-.12789E+05
0.31750E+02	0.22173E+00	-.15334E+00 **	-.10843E+05	-.10843E+05	-.10843E+05
0.32750E+02	0.25245E+00	-.18053E+00 **	-.89059E+04	-.89059E+04	-.89059E+04
0.33750E+02	0.28317E+00	-.20773E+00 **	-.69689E+04	-.69689E+04	-.69689E+04

DISPLACEMENTS VS. CHORDWISE LOCATION
AT IMPACT RADIUS

X	IN-PLANE	OUT-OF-PLANE
0.0	0.96182E-01	0.49810E-02
0.60000E+00	0.10348E+00	-.62705E-02
0.12000E+01	0.11269E+00	-.20482E-01
0.18000E+01	0.12190E+00	-.34694E-01
0.24000E+01	0.13111E+00	-.48906E-01
0.30000E+01	0.14033E+00	-.63117E-01
0.36000E+01	0.14954E+00	-.77329E-01
0.42000E+01	0.15875E+00	-.91541E-01
0.48000E+01	0.16797E+00	-.10575E+00
0.54000E+01	0.17718E+00	-.11997E+00
0.62500E+01	0.19023E+00	-.14010E+00
0.72500E+01	0.20559E+00	-.16379E+00
0.82500E+01	0.22094E+00	-.18747E+00
0.92500E+01	0.23630E+00	-.21116E+00
0.10000E+02	0.24974E+00	-.23188E+00

ORIGINAL PAGE IS
OF POOR QUALITY

STRESSES VS. CHORDWISE LOCATION
AT IMPACT RADIUS

X	STRESS-X	STRESS-Y	SHEAR-XY
0.0	*R=0.2900E+02 *R=0.3000E+02 *R=0.3075E+02 *R=0.2900E+02 *R=0.3000E+02 *R=0.3075E+02 *R=0.2900E+02 *R=0.3000E+02 *R=0.3075E+02		
0.6000E+00	* -.7152E+04 * -.6668E+04 * -.6299E+04 * -.1425E+05 * -.1342E+05 * -.1279E+05 * -.3179E+04 * -.3178E+04 * -.3177E+04		
0.1200E+01	* -.7152E+04 * -.6668E+04 * -.6299E+04 * -.1425E+05 * -.1342E+05 * -.1279E+05 * -.3179E+04 * -.3178E+04 * -.3177E+04		
0.1800E+01	* -.7152E+04 * -.6668E+04 * -.6299E+04 * -.1425E+05 * -.1342E+05 * -.1279E+05 * -.3179E+04 * -.3178E+04 * -.3177E+04		
0.2400E+01	* -.7152E+04 * -.6668E+04 * -.6299E+04 * -.1425E+05 * -.1342E+05 * -.1279E+05 * -.3179E+04 * -.3178E+04 * -.3177E+04		
0.3000E+01	* -.7152E+04 * -.6668E+04 * -.6299E+04 * -.1425E+05 * -.1342E+05 * -.1279E+05 * -.3179E+04 * -.3178E+04 * -.3177E+04		
0.3600E+01	* -.7152E+04 * -.6668E+04 * -.6299E+04 * -.1425E+05 * -.1342E+05 * -.1279E+05 * -.3179E+04 * -.3178E+04 * -.3177E+04		
0.4200E+01	* -.7152E+04 * -.6668E+04 * -.6299E+04 * -.1425E+05 * -.1342E+05 * -.1279E+05 * -.3179E+04 * -.3178E+04 * -.3177E+04		
0.4800E+01	* -.7152E+04 * -.6668E+04 * -.6299E+04 * -.1425E+05 * -.1342E+05 * -.1279E+05 * -.3179E+04 * -.3178E+04 * -.3177E+04		
0.5400E+01	* -.7152E+04 * -.6668E+04 * -.6299E+04 * -.1425E+05 * -.1342E+05 * -.1279E+05 * -.3179E+04 * -.3178E+04 * -.3177E+04		
0.6250E+01	* -.7152E+04 * -.6668E+04 * -.6299E+04 * -.1425E+05 * -.1342E+05 * -.1279E+05 * -.3179E+04 * -.3178E+04 * -.3177E+04		
0.7250E+01	* -.7152E+04 * -.6668E+04 * -.6299E+04 * -.1425E+05 * -.1342E+05 * -.1279E+05 * -.3179E+04 * -.3178E+04 * -.3177E+04		
0.8250E+01	* -.7152E+04 * -.6668E+04 * -.6299E+04 * -.1425E+05 * -.1342E+05 * -.1279E+05 * -.3179E+04 * -.3178E+04 * -.3177E+04		
0.9250E+01	* -.7152E+04 * -.6668E+04 * -.6299E+04 * -.1425E+05 * -.1342E+05 * -.1279E+05 * -.3179E+04 * -.3178E+04 * -.3177E+04		
0.1000E+02	* -.7152E+04 * -.6668E+04 * -.6299E+04 * -.1425E+05 * -.1342E+05 * -.1279E+05 * -.3179E+04 * -.3178E+04 * -.3177E+04		

TIME=0.476026E-01 SEC

DISPLACEMENTS AND BENDING STRESSES VS. RADIAL STATION

DISPLACEMENTS

RADIAL BENDING STRESS

R	IN-PLANE	OUT-OF-PLANE**LED-EDG	CHD-PNT	TRL-EDG
0.27000E+02	0.15848E+00	- .71601E-01 ** - .16796E+05	- .16790E+05	- .16790E+05
0.28000E+02	0.22881E+00	- .13765E+00 ** - .14946E+05	- .14946E+05	- .14946E+05
0.29000E+02	0.29913E+00	- .20370E+00 ** - .13693E+05	- .13693E+05	- .13693E+05
0.30000E+02	0.36946E+00	- .26974E+00 ** - .12903E+05	- .12903E+05	- .12903E+05
0.30750E+02	0.42220E+00	- .31928E+00 ** - .12300E+05	- .12300E+05	- .12300E+05
0.31750E+02	0.49253E+00	- .38532E+00 ** - .10442E+05	- .10442E+05	- .10442E+05
0.32750E+02	0.56285E+00	- .45137E+00 ** - .85810E+04	- .85810E+04	- .85810E+04
0.33750E+02	0.63318E+00	- .51742E+00 ** - .67286E+04	- .67286E+04	- .67286E+04

DISPLACEMENTS VS. CHORDWISE LOCATION
AT IMPACT RADIUS

X	IN-PLANE	OUT-OF-PLANE
0.0	0.24672E+00	- .14044E+00
0.60000E+00	0.25919E+00	- .15358E+00
0.12000E+01	0.27494E+00	- .17017E+00
0.18000E+01	0.29070E+00	- .18677E+00
0.24000E+01	0.30645E+00	- .20336E+00
0.30000E+01	0.32220E+00	- .21996E+00
0.36000E+01	0.33795E+00	- .23655E+00
0.42000E+01	0.35370E+00	- .25315E+00
0.48000E+01	0.36946E+00	- .26974E+00
0.54000E+01	0.38521E+00	- .28634E+00
0.62500E+01	0.40752E+00	- .30985E+00
0.72500E+01	0.43378E+00	- .33751E+00
0.82500E+01	0.46003E+00	- .36516E+00
0.92500E+01	0.48628E+00	- .39282E+00
0.10000E+02	0.50926E+00	- .41702E+00

STRESSES VS. CHORDWISE LOCATION
AT IMPACT RADIUS

X	STRESS-X	STRESS-Y	SHEAR-XY
0.0	*R=0.2900E+02 * 0.1691E+05 * 0.1590E+05 * 0.1514E+05	*R=0.2900E+02 * 0.3000E+02 * 0.3075E+02	*R=0.2900E+02 * 0.3000E+02 * 0.3075E+02
0.6000E+00	* 0.1691E+05 * 0.1590E+05 * 0.1514E+05	* - .1369E+05 * - .1290E+05 * - .1230E+05	* - .4395E+03 * - .4396E+03 * - .4397E+03
0.1200E+01	* 0.1691E+05 * 0.1590E+05 * 0.1514E+05	* - .1369E+05 * - .1290E+05 * - .1230E+05	* - .4395E+03 * - .4396E+03 * - .4397E+03
0.1800E+01	* 0.1691E+05 * 0.1590E+05 * 0.1514E+05	* - .1369E+05 * - .1290E+05 * - .1230E+05	* - .4395E+03 * - .4396E+03 * - .4397E+03
0.2400E+01	* 0.1691E+05 * 0.1590E+05 * 0.1514E+05	* - .1369E+05 * - .1290E+05 * - .1230E+05	* - .4395E+03 * - .4396E+03 * - .4397E+03
0.3000E+01	* 0.1691E+05 * 0.1590E+05 * 0.1514E+05	* - .1369E+05 * - .1290E+05 * - .1230E+05	* - .4395E+03 * - .4396E+03 * - .4397E+03
0.3600E+01	* 0.1691E+05 * 0.1590E+05 * 0.1514E+05	* - .1369E+05 * - .1290E+05 * - .1230E+05	* - .4395E+03 * - .4396E+03 * - .4397E+03
0.4200E+01	* 0.1691E+05 * 0.1590E+05 * 0.1514E+05	* - .1369E+05 * - .1290E+05 * - .1230E+05	* - .4395E+03 * - .4396E+03 * - .4397E+03
0.4800E+01	* 0.1691E+05 * 0.1590E+05 * 0.1514E+05	* - .1369E+05 * - .1290E+05 * - .1230E+05	* - .4395E+03 * - .4396E+03 * - .4397E+03
0.5400E+01	* 0.1691E+05 * 0.1590E+05 * 0.1514E+05	* - .1369E+05 * - .1290E+05 * - .1230E+05	* - .4395E+03 * - .4396E+03 * - .4397E+03
0.6250E+01	* 0.1691E+05 * 0.1590E+05 * 0.1514E+05	* - .1369E+05 * - .1290E+05 * - .1230E+05	* - .4395E+03 * - .4396E+03 * - .4397E+03
0.7250E+01	* 0.1691E+05 * 0.1590E+05 * 0.1514E+05	* - .1369E+05 * - .1290E+05 * - .1230E+05	* - .4395E+03 * - .4396E+03 * - .4397E+03
0.8250E+01	* 0.1691E+05 * 0.1590E+05 * 0.1514E+05	* - .1369E+05 * - .1290E+05 * - .1230E+05	* - .4395E+03 * - .4396E+03 * - .4397E+03
0.9250E+01	* 0.1691E+05 * 0.1590E+05 * 0.1514E+05	* - .1369E+05 * - .1290E+05 * - .1230E+05	* - .4395E+03 * - .4396E+03 * - .4397E+03
0.1000E+02	* 0.1691E+05 * 0.1590E+05 * 0.1514E+05	* - .1369E+05 * - .1290E+05 * - .1230E+05	* - .4395E+03 * - .4396E+03 * - .4397E+03

TIME=0.505014E-01 SEC

DISPLACEMENTS AND BENDING STRESSES VS. RADIAL STATION

ORIGINAL PAGE IS
OF POOR QUALITY

DISPLACEMENTS

R	IN-PLANE	OUT-OF-PLANE***LED-EDG	RADIAL BENDING STRESS	CHD-PNT	TRL-EDG
0.27000E+02	0.42755E-01	-.34927E-01 ** -.40075E+04	-.40075E+04	-.40075E+04	-.40075E+04
0.28000E+02	0.60821E-01	-.53295E-01 ** -.36811E+04	-.36811E+04	-.36811E+04	-.36811E+04
0.29000E+02	0.78867E-01	-.71664E-01 ** -.33163E+04	-.33163E+04	-.33163E+04	-.33163E+04
0.30000E+02	0.96953E-01	-.90032E-01 ** -.30860E+04	-.30860E+04	-.30860E+04	-.30860E+04
0.30750E+02	0.11050E+00	-.10381E+00 ** -.29116E+04	-.29116E+04	-.29116E+04	-.29116E+04
0.31750E+02	0.12657E+00	-.12218E+00 ** -.23709E+04	-.23709E+04	-.23709E+04	-.23709E+04
0.32750E+02	0.14663E+00	-.14055E+00 ** -.18364E+04	-.18364E+04	-.18364E+04	-.18364E+04
0.33750E+02	0.16470E+00	-.15891E+00 ** -.13271E+04	-.13271E+04	-.13271E+04	-.13271E+04

DISPLACEMENTS VS. CHORDWISE LOCATION AT IMPACT RADIUS

X	IN-PLANE	OUT-OF-PLANE
0.0	0.85907E-01	-.10400E+00
0.60000E+00	0.87029E-01	-.10258E+00
0.12000E+01	0.88447E-01	-.10079E+00
0.16000E+01	0.89864E-01	-.98997E-01
0.24000E+01	0.91282E-01	-.97204E-01
0.30000E+01	0.92700E-01	-.95411E-01
0.36000E+01	0.94117E-01	-.93618E-01
0.42000E+01	0.95535E-01	-.91825E-01
0.48000E+01	0.96953E-01	-.90032E-01
0.54000E+01	0.98370E-01	-.88239E-01
0.62500E+01	0.10038E+00	-.85699E-01
0.72500E+01	0.10274E+00	-.82710E-01
0.82500E+01	0.10510E+00	-.79722E-01
0.92500E+01	0.10747E+00	-.76733E-01
0.10000E+02	0.10953E+00	-.74118E-01

STRESSES VS. CHORDWISE LOCATION AT IMPACT RADIUS

X	STRESS-X	STRESS-Y	SHEAR-XY
0.0	*R=0.2900E+02 *R=0.3000E+02 *R=0.3075E+02	*R=0.2900E+02 *R=0.3000E+02 *R=0.3075E+02	*R=0.2900E+02 *R=0.3000E+02 *R=0.3075E+02
0.0	* 0.9763E+04 * 0.9137E+04 * 0.8662E+04	* -.3316E+04 * -.3086E+04 * -.2912E+04	* 0.2334E+04 * 0.2333E+04 * 0.2333E+04
0.6000E+00	* 0.9763E+04 * 0.9137E+04 * 0.8662E+04	* -.3316E+04 * -.3086E+04 * -.2912E+04	* 0.2334E+04 * 0.2333E+04 * 0.2333E+04
0.1200E+01	* 0.9763E+04 * 0.9137E+04 * 0.8662E+04	* -.3316E+04 * -.3086E+04 * -.2912E+04	* 0.2334E+04 * 0.2333E+04 * 0.2333E+04
0.1800E+01	* 0.9763E+04 * 0.9137E+04 * 0.8662E+04	* -.3316E+04 * -.3086E+04 * -.2912E+04	* 0.2334E+04 * 0.2333E+04 * 0.2333E+04
0.2400E+01	* 0.9763E+04 * 0.9137E+04 * 0.8662E+04	* -.3316E+04 * -.3086E+04 * -.2912E+04	* 0.2334E+04 * 0.2333E+04 * 0.2333E+04
0.3000E+01	* 0.9763E+04 * 0.9137E+04 * 0.8662E+04	* -.3316E+04 * -.3086E+04 * -.2912E+04	* 0.2334E+04 * 0.2333E+04 * 0.2333E+04
0.3600E+01	* 0.9763E+04 * 0.9137E+04 * 0.8662E+04	* -.3316E+04 * -.3086E+04 * -.2912E+04	* 0.2334E+04 * 0.2333E+04 * 0.2333E+04
0.4200E+01	* 0.9763E+04 * 0.9137E+04 * 0.8662E+04	* -.3316E+04 * -.3086E+04 * -.2912E+04	* 0.2334E+04 * 0.2333E+04 * 0.2333E+04
0.4800E+01	* 0.9763E+04 * 0.9137E+04 * 0.8662E+04	* -.3316E+04 * -.3086E+04 * -.2912E+04	* 0.2334E+04 * 0.2333E+04 * 0.2333E+04
0.5400E+01	* 0.9763E+04 * 0.9137E+04 * 0.8662E+04	* -.3316E+04 * -.3086E+04 * -.2912E+04	* 0.2334E+04 * 0.2333E+04 * 0.2333E+04
0.6250E+01	* 0.9763E+04 * 0.9137E+04 * 0.8662E+04	* -.3316E+04 * -.3086E+04 * -.2912E+04	* 0.2334E+04 * 0.2333E+04 * 0.2333E+04
0.7250E+01	* 0.9763E+04 * 0.9137E+04 * 0.8662E+04	* -.3316E+04 * -.3086E+04 * -.2912E+04	* 0.2334E+04 * 0.2333E+04 * 0.2333E+04
0.8250E+01	* 0.9763E+04 * 0.9137E+04 * 0.8662E+04	* -.3316E+04 * -.3086E+04 * -.2912E+04	* 0.2334E+04 * 0.2333E+04 * 0.2333E+04
0.9250E+01	* 0.9763E+04 * 0.9137E+04 * 0.8662E+04	* -.3316E+04 * -.3086E+04 * -.2912E+04	* 0.2334E+04 * 0.2333E+04 * 0.2333E+04
0.1000E+02	* 0.9763E+04 * 0.9137E+04 * 0.8662E+04	* -.3316E+04 * -.3086E+04 * -.2912E+04	* 0.2334E+04 * 0.2333E+04 * 0.2333E+04

APPENDIX H

COMPILED LISTING OF SOURCE PROGRAM AND SUBROUTINES

(PAGES 252-287)

```

0001      C      INITIALIZE THE PROBLEM
0002      2002  FORMAT(1H,7HENTERED)
0003      COMMON/XMID/ XCEN1(25),XCEN2(25)
0004      COMMON/BLADE/ XO(25),YO(25),THETA(24),XM(25)
0005      COMMON/AR/ XNODE(25,25),YNODE(25),MAX(25),PRESS(25,25),
0006      1AANODE(25,25),PPL(25,25),PVL(25,25),PRSS(25,25)
0007      COMMON/MODE/ BET(10),VKI(10),WI(10),GI(10),FI(10),FDI(10),GDI(10),
0008      1AA(10),B5(10),PI(10),QI(10),Q(10),QD(10),QDI(10),WO(10),PH2(3,625,
0009      110),PP(625,2),DEF(2,625),VEL(2,625),STRSS(3,625),SH2(3,625,10)
0010      COMMON/LK/VDT(6,1000),ISLIDE(6,1000),GAMMA(6),VR(6,1000),
0011      1ALPHA(6),ISPLIT(6),GAMMA1(1000),GAMMA2(1000),
0012      1SPPL(1000),PO(1000),LAMD11(1000),LAMD21(1000),FIMP2D(1000
0013      1),FIMP3D(1000),DIST(1000),SPPL(1000)
0014      COMMON/VARBLI/NA(1000),RM1(1000),RM2(1000),ITSLD(1000),GMALI(1000)
0015      1,VR1(1000),ALPL1(1000),ISPLT(1000),VDTL1(1000),WMI(1000)
0016      COMMON/L/I(6),RM(6),XI(6),YI(6),IHIT(6),RL(6),X(6),Y(6),WM(6)
0017      COMMON/PRNT/NJ3(25),DEFBI(1000,25),DEFBO(1000,25),CODI(1000,25),
0018      1CODO(1000,25),SIGMB1(1000,25,3),SIGMB2(1000,25,3),SIGMA1(1000,3,
0019      125),SIGMA2(1000,3,25),TIMEP(1000)
0020      DIMENSION HIMODE(10),VMI(10),XO(25),YO(25),INDEX(25),
0021      1XI(6),YI(6),DETL(6),CL(6),ADVNC(6),GBK1K(6
0022      1),IBACK(6),XNEAR(6),DFB(6),DELTA(6),DMAX(6),
0023      1SDFB(6),PIFORC(25,25),POFORC(25,25),DR(10),CLO(6)
0024      REAL LAMD11,LAMD21
0025      READ(5,*)V,RIMP,TSTOP,ALPHA0,XOCL,YOCL,NR,NN,NM,NVA,IPDEL,DEN,ISYM
0026      IF(ISYM.EQ.1)GO TO 2001
0027      READ(5,*) (RL(M),M=1,3),(CL(M),M=1,3),(WM(L),L=1,3)
0028      RH(1)=(RL(1)-2*RL(2)+2*RL(3))*2
0029      RM(2)=(RL(2)-2*RL(3))*2
0030      RH(3)=2*RL(3)
0031      DETL(3)=0.
0032      DETL(2)=(CL(3)-CL(2))/2
0033      DETL(1)=(CL(3)-CL(1))/2
0034      DO 2003 L=4,6
0035      ML=L-3
0036      RL(L)=RL(ML)
0037      RM(L)=RM(ML)
0038      CL(L)=CL(ML)
0039      DETL(L)=DETL(ML)
0040      RH(L)=RH(ML)
0041      2003  CONTINUE
0042      GO TO 2004
0043      2001  READ(5,*)(RL(M),M=1,NVA),(RM(L),L=1,NVA)
0044      READ(5,*)(CL(M),M=1,NVA),(DETL(M),M=1,NVA),(WM(L),L=1,NVA)
0045      2004  READ(5,*)(MAX(I3),I3=1,NR)
0046      READ(5,*)(NJ3(I3),I3=1,NR)
0047      READ(5,*)(VMI(I6),I6=1,NM)
0048      READ(5,*)(DR(I6),I6=1,NM)

```

ORIGINAL PAGE IS
OF POOR QUALITY

```

0036      READ(5,*)(WO(I6),I6=1,NM)
0037      DO 6005 I=1,NVA
0038      6005  CL0(I)=CL(I)
0039      WRITE(6,2002)
0040      DO 199 I6=1,NM
0041      READ(5,*)((PH2(J6,K6,I6),K6=1,NN),J6=1,2)
0042      199  CONTINUE
0043      DO 299 I6=1,NM
0044      READ(5,*)((SH2(J6,K6,I6),K6=1,NN),J6=1,3)
0045      299  CONTINUE
0046      DO 399 I3=1,NR
0047      LIM=MAX(I3)
0048      READ(5,*)YNODE(I3),(XNODE(I3,J3),J3=1,LIM)
0049      399  CONTINUE
0050      C      ZERO OUT THE MODAL COEFFICIENTS
0051      DO 801 I6=1,NM
0052      801  Q(I6)=0.
0053      C      SEARCH FOR THE HIGHEST NATURAL FREQUENCY
0054      DO 46 J6=1,NM
0055      DO 46 I6=1,NM
0056      HIMODE(I6)=WO(I6)
0057      IF(I6.EQ.1) GO TO 46
0058      IF(HIMODE(I6).GE.HIMODE(I6-1)) GO TO 46
0059      H6=HIMODE(I6)
0060      HIMODE(I6)=HIMODE(I6-1)
0061      HIMODE(I6-1)=H6
0061      46  CONTINUE
0062      C      CALCULATE THE PRESSURE AREA FOR EACH NODE
0063      DO 7 I3=1,NR
0064      LIM=MAX(I3)
0065      DO 8 J3=1,LIM
0066      XL=XNODE(I3,J3-1)
0067      IF(J3-1.LT.1)XL=XNODE(I3,J3)
0068      XR=XNODE(I3,J3+1)
0069      IF(J3+1.GT.LIM)XR=XNODE(I3,J3)
0070      RA=YNODE(I3+1)
0071      IF(I3+1.GT.NR)RA=YNODE(I3)
0072      RB=YNODE(I3-1)
0073      IF(I3-1.LT.1)RB=YNODE(I3)
0074      AANODE(I3,J3)=(XR-XL)*(RA-RB)/4.
0075      8  CONTINUE
0075      7  CONTINUE
0076      C      CALCULATE THE PARAMETERS FOR MODAL ANALYSIS
0077      DO 400 I6=1,NM
0078      BET(I6)=DR(I6)*WO(I6)
0079      VKI(I6)=VMI(I6)*WO(I6)**2
0079      400  WI(I6)=SQRT(ABS(WO(I6)**2-BET(I6)**2))

```

```

00000490
00000500
00000510
00000520
00000530
00000540
00000550
00000560
00000570
00000580
00000590
00000600
00000610
00000620
00000630
00000640
00000650
00000660
00000670
00000680
00000690
00000700
00000710
00000720
00000730
00000740
00000750
00000760
00000770
00000780
00000790
00000800
00000810
00000820
00000830
00000840
00000850
00000860
00000870
00000880
00000890
00000900
00000910
00000920
00000930
00000940
00000950
00000960

```

```

0080      C      FIND WHICH RADIUS OF THE BLADE IS THE IMPACT RADIUS
0081      DO 110 I3=1,NR
0082      YIMP=YNODE(I3)
0083      IF(YIMP.EQ.RIMP)I7=I3
0084      110      CONTINUE
0085      NSTAT=MAX(I7)
0086      NSTAF=NSTAT-1
0087      READ(5,*)(XO(JC),JC=1,NSTAT),(YO(JC),JC=1,NSTAT)
0088      DO 180 J5=1,NSTAT
0089      180      XM(J5)=XNODE(I7,J5)
0090      C      LOCATE THE MID POINTS OF THE BLADE SEGMENTS
0091      XCEN1(1)=XM(1)
0092      NST=NSTAF-1
0093      DO 413 JC=1,NST
0094      IF(JC.EQ.1)GO TO 414
0095      XCEN1(JC)=XCEN2(JC-1)
0096      414      XCEN2(JC)=(XM(JC+2)+XM(JC+1))/2.
0097      IF(JC.EQ.(NSTAF-1))XCEN2(JC)=XM(JC+2)
0098      413      CONTINUE
0099      C      ESTABLISH THE INITIAL COORDINATES OF THE BLADE
0100      DO 101 JC=1,NSTAT
0101      XO(JC)=XO(JC)
0102      YO(JC)=YO(JC)
0103      I=0
0104      ITPRNT=1
0105      TIME=0.
0106      IFV=0
0107      IFSLD=0
0108      IIFLG=0
0109      C      ***** PRINT INITIAL CONDITIONS *****
0110      DIMENSION ICNTL(6),ICNTM(10),ICNTN(625),ICNTR(25)
0111      DO 2005 J=1,NVA
0112      2005      ICNTL(J)=J
0113      DO 2006 J=1,NH
0114      2006      ICNTM(J)=J
0115      DO 2007 J=1,NN
0116      2007      ICNTN(J)=J
0117      DO 2008 J=1,NR
0118      2008      ICNTR(J)=J
0119      WRITE(6,2010)V,RIMP,TSTOP,ALPHA0,XOCL,YOCL,NR,NN,NH,NVA,IPDEL,
0120      IDEN,ISYM
0121      2010      FORMAT(1H1,57HV,RIMP,TSTOP,ALPHA0,XOCL,YOCL,NR,NN,NH,NVA,IPDEL,
0122      1,ISYM,71H,6(E12.6,1H,),5(I3,1H,),E12.6,1H,,I3)
0123      WRITE(6,2011)(ICNTL(J),J=1,NVA)
0124      2011      FORMAT(1H0,2HRL,1X,6(I2,1H,))
0125      WRITE(6,2012)(RL(J),J=1,NVA)
0126      2012      FORMAT(1H,6(E12.6,1H,))
0127      WRITE(6,2013)(ICNTL(J),J=1,NVA)

```

00000970
00000980
00000990
00001000
00001010
00001020
00001030
00001040
00001050
00001060
00001070
00001080
00001090
00001100
00001110
00001120
00001130
00001140
00001150
00001160
00001170
00001180
00001190
00001200
00001210
00001220
00001230
00001240
00001250
00001260
00001270
00001280
00001290
00001300
00001310
00001320
00001330
00001340
00001350
00001360
00001370
00001380
00001390
00001400
00001410
00001420
00001430
00001440

```

0122      2013 FORMAT(1H0,2HRM,1X,6(I2,1H,))
0123      WRITE(6,2012)(RM(J),J=1,NVA)
0124      WRITE(6,2014)(ICNTL(J),J=1,NVA)
0125      2014 FORMAT(1H0,2HCL,1X,6(I2,1H,))
0126      WRITE(6,2012)(CL(J),J=1,NVA)
0127      WRITE(6,2015)(ICNTL(J),J=1,NVA)
0128      2015 FORMAT(1H0,5HDELT,1X,6(I2,1H,))
0129      WRITE(6,2012)(DELT(J),J=1,NVA)
0130      WRITE(6,2016)(ICNTL(J),J=1,NVA)
0131      2016 FORMAT(1H0,2HWM,1X,6(I2,1H,))
0132      WRITE(6,2012)(WM(J),J=1,NVA)
0133      WRITE(6,2017)(ICNTR(J),J=1,NR)
0134      2017 FORMAT(1H0,3HMAX,1X,25(I2,1H,))
0135      WRITE(6,2018)(MAX(J),J=1,NR)
0136      2018 FORMAT(1H ,25(I3,1H,))
0137      WRITE(6,2019)(ICNTR(J),J=1,NR)
0138      2019 FORMAT(1H0,3HNJ3,1X,25(I2,1H,))
0139      WRITE(6,2018)(NJ3(J),J=1,NR)
0140      WRITE(6,2020)(ICNTH(J),J=1,NM)
0141      2020 FORMAT(1H0,3HVM,1X,10(I2,1H,))
0142      WRITE(6,2021)(VMI(J),J=1,NM)
0143      2021 FORMAT(1H ,10(E11.5,1H,))
0144      WRITE(6,2022)(ICNTH(J),J=1,NM)
0145      2022 FORMAT(1H0,2HDR,1X,10(I2,1H,))
0146      WRITE(6,2021)(DR(J),J=1,NM)
0147      WRITE(6,2023)(ICNTH(J),J=1,NM)
0148      2023 FORMAT(1H0,2HWO,1X,10(I2,1H,))
0149      WRITE(6,2021)(WO(J),J=1,NM)
0150      DO 2024 I6=1,NM
0151      DO 2024 J6=1,2
0152      WRITE(6,2025)J6,I6,J6,NM,I6
0153      2025 FORMAT(1H0,4HPH2(I2,3H,1,,I2,11H) THRU PH2(I2,1H,,I3,1H,,I2,1H))
0154      WRITE(6,2026)(PH2(J6,K6,I6),K6=1,NM)
0155      2026 FORMAT(1H0,63(/1H ,10(E11.5,1H,)))
0156      2024 CONTINUE
0157      DO 2027 I6=1,NM
0158      DO 2027 J6=1,3
0159      WRITE(6,2028)J6,I6,J6,NM,I6
0160      2028 FORMAT(1H0,4HSH2(I2,3H,1,,I2,11H) THRU SH2(I2,1H,,I3,1H,,I2,1H))
0161      WRITE(6,2029)(SH2(J6,K6,I6),K6=1,NM)
0162      2029 FORMAT(1H0,63(/1H ,10(E11.5,1H,)))
0163      2027 CONTINUE
0164      WRITE(6,1049)
0165      1049 FORMAT(1H1,53X,26HPLANFORM GEOMETRY OF BLADE)
0166      DO 1100 I3=1,NR
0167      LIM=MAX(I3)
0168      WRITE(6,1050)YNODE(I3)
0169      1050 FORMAT(/1H0,I30(1H*),/1H ,60X,2HY=,F9.4)

```

```

00001450
00001460
00001470
00001480
00001490
00001500
00001510
00001520
00001530
00001540
00001550
00001560
00001570
00001580
00001590
00001600
00001610
00001620
00001630
00001640
00001650
00001660
00001670
00001680
00001690
00001700
00001710
00001720
00001730
00001740
00001750
00001760
00001770
00001780
00001790
00001800
00001810
00001820
00001830
00001840
00001850
00001860
00001870
00001880
00001890
00001900
00001910
00001920

```

0170	LIMP=LIM-10	00001930
0171	IF(LIMP.LE.0)LIN1=LIM	00001940
0172	IF(LIMP.GT.0)LIN1=10	00001950
0173	KN=1	00001960
0174	LIMP=LIM-LIN1	00001970
0175	IF(LIMP.LE.0)GO TO 1001	00001980
0176	KN=2	00001990
0177	LIMP1=LIMP-10	00002000
0178	IF(LIMP1.LE.0)LIN2=LIMP	00002010
0179	IF(LIMP1.GT.0)LIN2=10	00002020
0180	LIMP=LIMP-LIN2	00002030
0181	IF(LIMP.LE.0)GO TO 1001	00002040
0182	KN=3	00002050
0183	LIN3=LIMP	00002060
0184	1001 DO 1002 NLIN=1,KN	00002070
0185	IF(NLIN.EQ.1)GO TO 1003	00002080
0186	IF(NLIN.EQ.2)GO TO 1004	00002090
0187	IF(NLIN.EQ.3)GO TO 1005	00002100
0188	1003 KN1=LIN1	00002110
0189	DO 1006 IXX=1,LIN1	00002120
0190	1006 INDEX(IXX)=IXX	00002130
0191	WRITE(6,1051)(INDEX(IXX),IXX=1,LIN1)	00002140
0192	1051 FORMAT(/1H ,3X,10(1HX,I2,8X))	00002150
0193	WRITE(6,1052)(XNODE(I3,J3),J3=1,LIN1)	00002160
0194	1052 FORMAT(/1H ,10(F9.4,2X))	00002170
0195	GO TO 1002	00002180
0196	1004 KN1=LIN2+10	00002190
0197	DO 1007 IXX=11,KN1	00002200
0198	1007 INDEX(IXX)=IXX	00002210
0199	WRITE(6,1051)(INDEX(IXX),IXX=11,KN1)	00002220
0200	WRITE(6,1052)(XNODE(I3,J3),J3=11,KN1)	00002230
0201	GO TO 1002	00002240
0202	1005 KN1=LIN3+20	00002250
0203	DO 1008 IXX=21,KN1	00002260
0204	1008 INDEX(IXX)=IXX	00002270
0205	WRITE(6,1053)(INDEX(IXX),IXX=21,KN1)	00002280
0206	1053 FORMAT(/1H ,3X,5(1HX,I2,8X))	00002290
0207	WRITE(6,1052)(XNODE(I3,J3),J3=21,KN1)	00002300
0208	1002 CONTINUE	00002310
0209	1100 CONTINUE	00002320
0210	WRITE(6,1054)	00002330
0211	1054 FORMAT(/1H0,51X,29HINITIAL BLADE CAMBER GEOMETRY,/1H ,57X, 117HAT IMPACT STATION,/1H ,39X,4HNODE,4X,19HIN-PLANE COORDINATE, 14X,23HOUT OF PLANE COORDINATE)	00002340
0212	DO 1009 JC=1,NSTAT	00002350
0213	WRITE(6,1055)JC,XO(JC),YO(JC)	00002360
0214	1055 FORMAT(1H ,40X,I2,9X,F10.5,16X,F10.5)	00002370
0215	1009 CONTINUE	00002380
		00002390
		00002400

```

0216      WRITE(6,1056)
0217      1056 FORMAT(/1H0,58X,16HMISSILE GEOMETRY,/1H0,44X,7HSECTION,2X,
0218          19HTHICKNESS,2X,5HWIDTH,4X,6HLENGTH,3X,6HOFFSET,/)
0219      DO 1010 L=1,NVA
0220      WRITE(6,1057)L,RM(L),WM(L),CL(L),DELTL(L)
0221      1057 FORMAT(1H ,47X,I1,4X,4(3X,F6.3))
0222      1010 CONTINUE
0223      WRITE(6,1058)
0224      1058 FORMAT(/1H0,60X,10HMODAL DATA,/1H0,31X,4HMODE,2X,
0225          113HFREQ(RAD/SEC),4X,10HMODAL MASS,6X,15HMODAL STIFFNESS,3X,
0226          113HDAMPING RATIO)
0227      DO 1011 I6=1,NM
0228      WRITE(6,1059)I6,W0(I6),VMI(I6),VKI(I6),DR(I6)
0229      1059 FORMAT(1H ,32X,I2,3X,E12.6,3(5X,E12.6))
0230      1011 CONTINUE
0231      WRITE(6,1060)IV,ALPHA0,DEN,X0CL,Y0CL,RIMP
0232      1060 FORMAT(/1H0,77X,9HCHORDWISE,/1H ,25X,6HIMPACT,10X,6HIMPACT,9X,
0233          17HMISSILE,12X,18HIMPACT COORDINATES,12X,6HIMPACT,/1H ,22X,
0234          16HVELOCITY,9X,5HANGLE,10X,7HDENSITY,9X,8HIN-PLANE,6X,
0235          112HOUT-OF-PLANE,7X,6HRADIUS,/1H0,16X,6(4X,E12.6))
0236      C
0237      C *****
0238      C ESTABLISH THE INCREMENTAL ENTRY POINT OF THE PROGRAM
0239      800 I=I+1
0240      C
0241      C FIND THE ANGLE OF THE BLADE CHORD AND THE ANGLE OF THE BIRD WITH
0242      C TO THE X-AXIS
0243      THETA0=ACOS((X0(NSTAT)-X0(1))/(SQRT((X0(NSTAT)-X0(1))**2+(Y0(NSTA
0244      1T)-Y0(1))**2)))
0245      IF((Y0(5)-Y0(1)).LT.0.)THETA0=-THETA0
0246      IF(I.GT.1)GO TO 121
0247      BETA=THETA0-ALPHA0
0248      C
0249      C FIND THE BLADE SEGMENT ANGLES
0250      121 DO 21 JC=1,NSTAF
0251      THETA(JC)=ACOS((X0(JC+1)-X0(JC))/(SQRT((X0(JC+1)-X0(JC))**2+(Y0(JC
0252      1+1)-Y0(JC))**2)))
0253      IF((Y0(JC+1)-Y0(JC)).LT.0.)THETA(JC)=-THETA(JC)
0254      21 CONTINUE
0255      C
0256      C FIND THE FORWARD AND AFT POINTS OF THE BIRD SECTIONS
0257      DO 20 L=1,NVA
0258      IF(I.GT.1)GO TO 19
0259      X(L)=X0CL+RL(L)*SIN(BETA)-DELTL(L)*COS(BETA)
0260      Y(L)=Y0CL-RL(L)*COS(BETA)-DELTL(L)*SIN(BETA)
0261      X1(L)=X(L)-CL(L)*COS(BETA)
0262      Y1(L)=Y(L)-CL(L)*SIN(BETA)
0263      GO TO 20
0264      19 IF(II(L).GT.1) GO TO 20
0265      IF(II(L).EQ.0) VDT(L,I-1)=0.
0266      ADVNCE(L)=V*DT-VDT(L,I-1)
0267      X(L)=X(L)+ADVNCE(L)*COS(BETA)

```


0250		Y(L)=Y(L)+ADVNC(L)*SIN(BETA)	00002880
0251		X1(L)=X1(L)+V*DT*COS(BETA)	00002890
0252		Y1(L)=Y1(L)+V*DT*SIN(BETA)	00002900
0253		ACL=CL(L)	00002910
0254		CL(L)=CL(L)-VDT(L,I-1)	00002920
0255		IF((CL(L)/ACL).LE..01)II(L)=2	00002930
0256		IF(ABS(CL(L)/CLO(L)).LT..01)II(L)=2	00002940
0257	20	CONTINUE	00002950
	C	FIND THE INITIAL CONTACT POINTS OF THE BIRD	00002960
0258		IT=0	00002970
0259		DO 30 L=1,NVA	00002980
0260		IF(I.EQ.1)GO TO 11	00002990
0261		IF(II(L).GT.1)GO TO 30	00003000
0262	11	BKBIK(L)=0.	00003010
0263		IBACK(L)=0	00003020
0264		DO 3100 JC=1,NSTAF	00003030
0265		ISLIDE(L,I)=0	00003040
0266		UAK1=(Y0(JC+1)-Y1(L))*COS(BETA)-(X0(JC+1)-X1(L))*SIN(BETA)	00003050
0267		AIK1=(X0(JC)-X1(L))*SIN(BETA)-(Y0(JC)-Y1(L))*COS(BETA)	00003060
0268		IF(THETA(JC).GE.0..AND.UAK1.GE.0..AND.AIK1.GE.0.) GO TO 31	00003070
0269		IF(THETA(JC).LT.0..AND.UAK1.LE.0..AND.AIK1.LE.0.) GO TO 31	00003080
0270		IHIT(L)=0	00003090
0271		GO TO 3100	00003100
0272	31	BKBIK(L)=(X(L)-X0(JC+1))*(Y(L)-Y0(JC))-(X(L)-X0(JC))*(Y(L)-Y0(JC+100003110	00003120
0273		1))	00003130
0274		IHIT(L)=JC	00003140
0275		IF(THETA(JC).GE.0..AND.BKBIK(L).GE.0.)IBACK(L)=1	00003150
	C	IF(THETA(JC).LT.0..AND.BKBIK(L).LE.0.)IBACK(L)=1	00003160
	C	CHECK WHETHER THE IMPACT ANGLE IS SHALLOW ENOUGH TO CONSTITUTE	00003170
0276		SLIDING ALONG THE BLADE	00003180
0277		IF(ABS(THETA(JC)-BETA).GE.1.7E-3) GO TO 32	00003190
	C	IF(ABS(3.141592654-ABS(THETA(JC)-BETA)).GE.1.7E-3)GO TO 32	00003200
0278		SLIDING	00003210
	C	ISLIDE(L,I)=1	00003220
0279		CHECK WHETHER THE BLADE ANGLE IS CLOSE TO 90 DEGREES	00003230
0280		PPII=3.141592654	00003240
	C	IF(ABS(PPII/2.-ABS(THETA(JC))).GE.1.7E-3) GO TO 33	00003250
0281		THE BLADE ANGLE IS CLOSE TO 90 DEGREES	00003260
		YI(L)=Y(L)	00003270
0282		XI(L)=(Y(L)-Y0(JC))*COTAN(THETA(JC))+X0(JC)	00003280
0283		XNEAR(L)=XM(JC)	00003290
0284		GO TO 34	00003300
	C	THE BLADE ANGLE IS NOT 90 DEGREES	00003310
0285	33	XI(L)=X(L)	00003320
0286		YI(L)=(X(L)-X0(JC))*TAN(THETA(JC))+Y0(JC)	00003330
0287		XNEAR(L)=XM(JC)	00003340
0288	34	DFB(L)=0.	00003350
0289		DELTA(L)=((XI(L)-X0(JC))*2+(YI(L)-Y0(JC))*2)**.5	

ORIGINAL PAGE IS
OF POOR QUALITY

	C	CHECK WHETHER THE SLIDE IS GOING FROM MODE N TO N+1 AND WHETHER TH	00003360
	C	FORWARD POINT OF THE BIRD SECTION IS BEYOND THE END NODE OF THE	00003370
	C	SEGMENT	
0290		IF((THETA(JC).LT.0..AND.YI(L).LE.Y0(JC+1)).OR.(THETA(JC).GE.0..AND	00003380
		1.YI(L).GE.Y0(JC+1))) GO TO 35	00003390
0291		IF((THETA(JC).LT.0..AND.YI(L).GE.Y0(JC)).OR.(THETA(JC).GE.0..AND	00003400
		1YI(L).LE.Y0(JC)))GO TO 36	00003410
0292		GAMMA(L)=XNEAR(L)+DELTA(L)	00003420
0293		GO TO 40	00003430
0294	35	XI(L)=X0(JC+1)	00003440
0295		YI(L)=Y0(JC+1)	00003450
0296		XNEAR(L)=XM(JC+1)	00003460
0297		IHIT(L)=JC+1	00003470
0298		ISLIDE(L,K)=0	00003480
0299		DELTA(L)=0.	00003490
0300		GO TO 38	00003500
0301	36	XI(L)=X0(JC)	00003510
0302		YI(L)=Y0(JC)	00003520
0303		XNEAR(L)=XM(JC-1)	00003530
0304		IHIT(L)=JC-1	00003540
0305		ISLIDE(L,K)=0	00003550
0306		DELTA(L)=((X0(JC)-X0(JC-1))*2+(Y0(JC)-Y0(JC-1))*2)**.5	00003560
0307	38	DFB(L)=((X(L)-XI(L))*2+(Y(L)-YI(L))*2)**.5	00003570
0308		IF(DFB(L).LT.1.0E-5)GO TO 340	00003580
0309		DALPHA=ACOS((X(L)-XI(L))/DFB(L))	00003590
0310		DFB(L)=ABS(DFB(L)*COS(BETA-DALPHA))	00003600
0311		GAMMA(L)=XNEAR(L)+DELTA(L)	00003610
0312		GO TO 40	00003620
0313	340	DFB(L)=0.	00003630
0314		GAMMA(L)=XNEAR(L)+DELTA(L)	00003640
0315		GO TO 40	00003650
	C	IMPACT ANGLE IS NOT SHALLOW	00003660
0316	32	XI(L)=(((Y(L)-Y0(JC))*COS(BETA)-X(L)*SIN(BETA))*COS(THETA(JC))	00003670
		1+X0(JC)*SIN(THETA(JC))*COS(BETA))/SIN(THETA(JC)-BETA)	00003680
	C	CHECK WHETHER THE BLADE SEGMENT ANGLE IS CLOSE TO 90 DEGREES	00003690
0317		PPII=3.141592654	00003700
0318		IF(ABS(PPII/2.-ABS(THETA(JC))).LT.1.7E-3)GO TO 37	00003710
0319	C	BLADE SEGMENT ANGLE IS NOT 90 DEGREES	00003720
		YI(L)=(XI(L)-X0(JC))*TAN(THETA(JC))+Y0(JC)	00003730
0320		GO TO 39	00003740
	C	BLADE SEGMENT ANGLE IS CLOSE TO 90 DEGREES-USE TAN(BETA)	00003750
0321	37	YI(L)=(XI(L)-X(L))*TAN(BETA)+Y(L)	00003760
	C	FIND XNEAR,DELTA AND DFB	00003770
0322	39	XNEAR(L)=XM(JC)	00003780
0323		DELTA(L)=((X0(JC)-XI(L))*2+(Y0(JC)-YI(L))*2)**.5	00003790
0324		GAMMA(L)=XNEAR(L)+DELTA(L)	00003800
0325		DFB(L)=((XI(L)-X(L))*2+(YI(L)-Y(L))*2)**.5	00003810
	C	IF THIS BIRD SECTION'S FORWARD POINT IS IN BACK OF THE BLADE FIND	00003820
			00003830

0326	C	OUT IF IT IS THE GREATEST DISTANCE BEHIND THE BLADE	00003840
0327	40	IF(IBACK(L).EQ.0)GO TO 30	00003850
0328		IT=IT+1	00003860
0329		DMAX(IT)=DFB(L)	00003870
0330		IF(IT.EQ.1)GO TO 30	00003880
0331		IF(DMAX(IT).GE.DMAX(IT-1))GO TO 30	00003890
0332		DJ7=DMAX(IT)	00003900
0333		DMAX(IT)=DMAX(IT-1)	00003910
0334		DMAX(IT-1)=DM7	00003920
0335		GO TO 30	00003930
0336	3100	CONTINUE	00003940
0337	30	CONTINUE	00003950
		PPII=3.141592654	00003960
	C	RESET THE POSITION OF THE BIRD SO THAT THE BIRD SECTION CLOSEST TO	00003970
	C	THE BLADE WILL HIT FIRST	00003980
0338		DO 41 L=1,NVA	00003990
0339		IF(I.EQ.1) GO TO 12	00004000
0340		IF(II(L).GT.1) GO TO 41	00004010
0341	12	IF(IHIT(L).EQ.0)GO TO 41	00004020
	C	IF ALL OF THE FORWARD POINTS ARE IN FRONT OF THE BLADE THE BIRD WI	00004030
	C	HAVE TO BE MOVED TOWARD THE BLADE	00004040
0342		IF(IT.EQ.0)GO TO 42	00004050
	C	FORWARD POINTS BEHIND THE BLADE-MOVE THE BIRD BACK	00004060
0343		X(L)=X(L)-DMAX(IT)*COS(BETA)	00004070
0344		Y(L)=Y(L)-DMAX(IT)*SIN(BETA)	00004080
0345		DFB(L)=((XI(L)-X(L))**2+(YI(L)-Y(L))**2)**.5	00004090
0346		GO TO 41	00004100
	C	ALL FORWARD POINTS ARE IN FRONT OF THE BLADE	00004110
0347	42	SDFB(L)=DFB(L)	00004120
0348		IF(L.EQ.1) GO TO 41	00004130
0349		IF(SDFB(L).LE.SDFB(L-1)) GO TO 41	00004140
0350		DJ7=SDFB(L)	00004150
0351		SDFB(L)=SDFB(L-1)	00004160
0352		SDFB(L-1)=DJ7	00004170
0353	41	CONTINUE	00004180
	C	IF ALL FORWARD POINTS ARE IN FRONT OF THE BLADE MOVE THE BIRD TOWA	00004190
	C	THE BLADE	00004200
0354		IF(IT.GT.0)GO TO 43	00004210
0355		DO 44 L=1,NVA	00004220
0356		IF(I.EQ.1) GO TO 13	00004230
0357		IF(II(L).GT.1)GO TO 44	00004240
0358	13	X(L)=X(L)+SDFB(NVA)*COS(BETA)	00004250
0359		Y(L)=Y(L)+SDFB(NVA)*SIN(BETA)	00004260
0360	44	DFB(L)=((XI(L)-X(L))**2+(YI(L)-Y(L))**2)**.5	00004270
	C	TEST FOR WHICH BIRD SECTIONS WILL IMPACT ON THE BLADE AND SET I	00004280
	C	IF IMPACT WILL OCCUR DURING THIS TIME STEP	00004290
0361	43	DO 45 L=1,NVA	00004300
0362		IF(IHIT(L).EQ.0) GO TO 45	00004310


```

0363      IF(I.EQ.1)II(L)=0                                00004320
0364      IF(II(L).GT.1)GO TO 45                             00004330
0365      IF(DFB(L).LT..01)II(L)=1                          00004340
0366      45 CONTINUE                                       00004350
           C SET THE TIME STEP TO ONE TENTH THE HIGHEST NATURAL PERIOD DURING T 00004360
           C TIME THAT THE BIRD IS IMPACTING                00004370
0367      CONST=2.*PPII/(10.*HIMODE(NM))                    00004380
           C IF THE BIRD HAS COMPLETELY IMPACTED SET THE TIME STEP TO ONE TENTH 00004390
           C LOWEST NATURAL PERIOD                          00004400
0368      IF(IFV.GT.0)CONST=2.*PPII/(10.*HIMODE(1))          00004410
0369      DT=CONST                                           00004420
           C CALCULATE THE RELATIVE IMPACT VELOCITY AND ANGLE-CHANGE DT IF VREL 00004430
           C IS GREATER THAN THE LENGTH OF THE IMPACTING BIRD SECTION          00004440
0370      DO 47 L=1,NVA                                     00004450
0371      JK=IHIT(L)                                         00004460
0372      IF(IHIT(L).EQ.0)GO TO 47                          00004470
0373      IF(II(L).GT.1)GO TO 47                          00004480
0374      IF(I.EQ.1)GO TO 48                               00004490
0375      J9=I8-1                                           00004500
0376      DO 203 JB=1,NSTAF                                 00004510
0377      J9=J9+1                                           00004520
0378      IF(JB.EQ.IHIT(L))JT=J9                          00004530
0379      203 CONTINUE                                     00004540
0380      IF(ABS(PPII/2.-ABS(THETA(IHIT(L))))).GE.PPII/12.)GO TO 49 00004550
0381      OMEGA=(VEL(1,JT+1)-VEL(1,JT))/(Y0(JK+1)-Y0(JK)) 00004560
0382      GO TO 50                                           00004570
0383      49 OMEGA=(VEL(2,JT+1)-VEL(2,JT))/(X0(JK+1)-X0(JK)) 00004580
0384      50 XID=VEL(1,JT)-(YI(L)-Y0(IHIT(L)))*OMEGA      00004590
0385      YID=VEL(2,JT)+(XI(L)-X0(IHIT(L)))*OMEGA          00004600
0386      GO TO 51                                           00004610
0387      48 XID=0.                                          00004620
0388      YID=0.                                          00004630
0389      51 VI=XID*COS(BETA)+YID*SIN(BETA)                00004640
0390      VB=XID*COS(THETA(IHIT(L)))+YID*SIN(THETA(IHIT(L))) 00004650
0391      VX1=(V-VI)*COS(BETA)-VB*COS(THETA(IHIT(L)))      00004660
0392      VY1=(V-VI)*SIN(BETA)-VB*SIN(THETA(IHIT(L)))      00004670
0393      VR(L,I)=(VX1**2+VY1**2)**.5                      00004680
0394      ALPHA(L)=ACOS((VX1*COS(THETA(IHIT(L)))+VY1*SIN(THETA(IHIT(L))))/ 00004690
           1VR(L,I))                                       00004700
0395      ISPLIT(L)=1                                        00004710
0396      IF(ALPHA(L).LE.PPII/2.)GO TO 56                  00004720
0397      ALPHA(L)=PPII-ALPHA(L)                            00004730
0398      ISPLIT(L)=-1                                       00004740
0399      56 IF(II(L).EQ.0)GO TO 52                         00004750
           C CHECK WHETHER VREL*DT IS GREATER THAN THE LENGTH OF IMPACTING BIRD 00004760
           C SECTION AND SHORTEN DT IF IT IS                00004770
0400      DT1=CL(L)/VR(L,I)                                00004780
0401      IF(DT1.LT.DT)DT=DT1                             00004790

```

0402		GO TO 47	00004800
	C	CHECK WHETHER VREL*DT IS GREATER THAN DFB FOR BIRD SECTIONS NOT IN CONTACT WITH THE BLADE YET	00004810
0403	52	DT1=DFB(L)/VR(L,I)	00004820
0404		IF(DT1.GE.DT)GO TO 47	00004830
0405		IF(DT1.LT.DT/2.)GO TO 53	00004840
0406		DT=DT1	00004850
0407		GO TO 47	00004860
	C	IF THIS BIRD SECTION WILL TAKE LESS THAN ONE HALF THIS TIME STEP	00004870
	C	IMPACT THEN IMPACT IT DURING THIS TIME STEP	00004880
0408	53	II(L)=1	00004890
0409	47	CONTINUE	00004900
	C	FOR EACH BIRD SECTION CALCULATE THE LENGTH OF THE SECTION THAT WILL IMPACT DURING THIS TIME STEP	00004910
	C	DO 54 L=1,NVA	00004920
0410		IF(IHIT(L).EQ.0)GO TO 55	00004930
0411		IF(II(L).GT.1)GO TO 55	00004940
0412		IF(II(L).EQ.0)GO TO 55	00004950
0413		VDT(L,I)=VR(L,I)*DT-DFB(L)	00004960
0414		GO TO 54	00004970
0415	55	VDT(L,I)=0.	00004980
0416	54	CONTINUE	00004990
0417			00005000
	C	NODAL LOADS	00005010
	C	ZERO OUT THE PRESSURES AND IN-PLANE AND OUT OF-PLANE FORCES ON ALL	00005020
0418		DO 61 I3=1,NR	00005030
0419		LIM=MAX(I3)	00005040
0420		DO 61 J3=1,LIM	00005050
0421		PRESS(I3,J3)=0.	00005060
0422		PIFORC(I3,J3)=0.	00005070
0423		FRSS(I3,J3)=0.	00005080
0424		PPL(I3,J3)=0	00005090
0425		PVL(I3,J3)=0	00005100
0426	61	POFORC(I3,J3)=0.	00005110
	C	CALCULATE THE INITIAL IMPACT FORCE FOR BIRD SECTIONS HITTING THE BLADE DURING THIS TIME STEP	00005120
0427		IF(IFSLO.EQ.1.OR.IIFLG.EQ.1)GO TO 57	00005130
0428		CALL PINIT(L1,NVA,BETA,JCL,XNERL1,DLTALL,I8,NSTAF,PPII,E,F,IG,AL,R1,S,DEN,I,V,I7,DT,RIMP,NSTAT)	00005140
0429	57	IF(IFSLO.EQ.1.OR.IIFLG.EQ.1)GO TO 58	00005150
0430		IF(NA(I).EQ.0.AND.ITSLO(I).EQ.7)GO TO 60	00005160
0431		IF(NA(I).EQ.0.AND.ITSLO(I).LT.7)GO TO 59	00005170
0432		IF(ALPL1(I).LT.1.7E-3)GO TO 59	00005180
0433		KFIN=I	00005190
0434		GO TO 58	00005200
0435	59	IFSLO=1	00005210
0436		KFIN=I-1	00005220
0437		GO TO 58	00005230
0438	60	IIFLG=1	00005240
			00005250
			00005260
			00005270

 ORIGINAL PAGE IS
OF POOR QUALITY

```

0439      KFIN=I-1
          C      CALCULATE THE NODE PRESSURES FOR EACH BIRD SECTION THAT HAS IMPACT
          C      IN A PREVIOUS TIME STEP
0440      58 DO 64 K=1,KFIN
          C      THIS BIRD SECTION HAS IMPACTED THE BLADE AND SQUASHED
          C      -IF THE BIRD SECTION CAME ON THE BLADE DURING THIS TIME STEP
          C      -FIND THE X-COORDINATE OF THE CENTER OF THE CLOSED LOOP (SPP1)
          C      -AND SET THE VALUE OF DIST-PRESSURES ARE NOT CALCULATED FOR
          C      -THE FIRST TIME STEP OF IMPACT
0441      65 IF(K.LT.I)GO TO 72
0442      SPP1(K)=SPP(K)+(LAMD11(K)-LAMD21(K))/2.
0443      IF((GMAL1(K)-SPP(K)).LT.0.)SPP1(K)=SPP(K)+(LAMD21(K)-
          C      LAMD11(K))/2.
0444      DIST(K)=(LAMD11(K)+LAMD21(K))/2.
0445      GO TO 64
0446      72 A=RIMP+(WH1(K)-RMI(K))/2.
0447      B=RIMP-(WH1(K)-RMI(K))/2.
0448      IF((A-B).GT.0.)GO TO 7200
0449      A=RIMP
0450      B=RIMP
0451      7200 DIST(K)=DIST(K)+VRL1(K)*DT/2.
          C      CALCULATE THE PRESSURE DISTRIBUTION DUE TO THIS BIRD SECTION
0452      CALL PRESUR(NR,A,B,DIST(K),ISPLT(K),SPP(K),SPP1(K),VDTLI(
          C      IK),GAMMA1(K),GAMMA2(K),PO(K),RMI(K),ALPLI(K),VRL1(K),DEN,
          C      INSTAT,IIFLG)
0453      64 CONTINUE
          C      CALCULATE THE IN-PLANE AND OUT OF PLANE FORCES ON EACH NODE
0454      62 IS=0
0455      FV=0.
0456      DO 73 I3=1,NR
0457      LIM=MAX(I3)
0458      DO 74 J3=1,LIM
          C      -FIND WHICH BLADE SEGMENT ANGLE SHOULD BE USED WITH THIS NODE AND
          C      -CALCULATE THE IN-PLANE AND OUT OF-PLANE FORCES ON THIS NODE USING
          C      -THE CORRECT ANGLE
0459      SECT=XH(NSTAT)-XH(I)
0460      CAMLIM=XNODE(I3,1)
0461      DO 75 JC=1,NSTAF
0462      WIDTH=(XH(JC+1)-XH(JC))*(XNODE(I3,LIM)-XNODE(I3,1))/SECT
0463      CAMLIM=CAMLIM+WIDTH
0464      IF(XNODE(I3,J3).GT.CAMLIM.OR.XNODE(I3,J3).LT.(CAMLIM-WIDTH))GO
          C      TO 75
0465      ANGLE=THETA(JC)
0466      IF(J3.NE.1.AND.J3.NE.LIM)ANGLE=(THETA(JC)+THETA(JC+1))/2.
0467      PIPORC(I3,J3)=PRSS(I3,J3)*AANODE(I3,J3)*SIN(ANGLE)
0468      POPORC(I3,J3)=-PRSS(I3,J3)*AANODE(I3,J3)*COS(ANGLE)
0469      75 CONTINUE
0470      IS=IS+1

```

```

0471      PP(I5,1)=PIFORC(I3,J3)
0472      PP(I5,2)=POFORC(I3,J3)
0473      IF(I3.EQ.I7.AND.J3.EQ.1)I8=I5
0474      FV=FV+PP(I5,1)+PP(I5,2)
0475      74 CONTINUE
0476      73 CONTINUE
C
C      -CALCULATE THE MODAL RESPONSE DURING THIS TIME STEP
C      -USING THE RESULTS OF THE PREVIOUS TIME STEP AS
C      -INITIAL CONDITIONS
0477      CALL MODAL(NM,NSTAT,HN,I8,FV,DT)
C
C      -CALCULATE THE NEW COORDINATES OF THE NODES DESCRIBING
C      -THE BLADE SHAPE AT THE IMPACTED RADIAL STATION
0476      I9=I8
0479      DO 445 JB=1,NSTAT
0480      X0(JB)=X0(JB)+DEF(1,I9)
0481      Y0(JB)=Y0(JB)+DEF(2,I9)
0482      I9=I9+1
0483      445 CONTINUE
C
C      -CALCULATE THE TOTAL ELAPSED TIME
0484      TIME=TIME+DT
0485      III=0
0486      DO 1200 L=1,NVA
0487      IF(II(L).GT.1.OR.IHIT(L).EQ.0)III=III+1
0488      1200 CONTINUE
0489      IF(IFV.EQ.1)GO TO 202
0490      IF(III.EQ.6)GO TO 202
0491      CALL PRINTP(I,TIME,NR)
0492      202 IF(I.EQ.1)GO TO 200
0493      IF(TIME GE.TSTOP)GO TO 200
0494      IF(I.EQ.ITPRNT)GO TO 200
0495      GO TO 201
0496      200 CALL PRINTV(I,TIME,IPDEL,ITPRNT,NR,IJPRNT,I7)
0497      IF(III.LT.6)GO TO 201
0498      CALL PRINTP(I,TIME,NR)
C
C      -CHECK WHETHER THE ENTIRE LENGTH OF THE BIRD HAS IMPACTED
0499      201 IF(FV.EQ.0.) GO TO 77
0500      IF(TIME.LT.TSTOP) GO TO 800
0501      WRITE(6,600)TIM
0502      600 FORMAT(1H1,29X,
C      1) IMPACT BLADE C. DURATION OF PROBLEM TOO SHORT FOR MISSILE TO
C      1) ELI,53X,'ELAPSED TIME=',1X,E11.5,1X'SEC'
0503      GO TO 998
0504      77 IF(IFV.EQ.1) GO TO 78
0505      IF(I.EQ.1)GO TO 78
0506      IFV=1
0507      TELAPS=TIME-DT
0508      WRITE(6,601)TELAPS
0509      601 FORMAT(1H0,35X,47HTIME ELAPSED FOR MISSILE TO FULLY IMPACT BLADE=,00006230

```

ORIGINAL PAGE IS
OF POOR QUALITY

FORTRAN IV G1 RELEASE 2.0

MAIN

DATE = 79012

08/33/03

PAGE 0014

0510
0511
0512
0513

11X,E11.5,1X,3HSEC)
78 IF(TIME.LT.YSTOP)GO TO 800
998 CALL PRINTR(I7,NSTAT,NR,IJPRNT)
999 STOP
END

00006240
00006250
00006260
00006270
00006280


```

C *****00006290
C ***** SUBROUTINES *****00006300
C *****00006310
0001 SUBROUTINE P3D(A,ALPHA,PO,GAMDA1,GAMDA2,TLOAD) 00006320
0002 DIMENSION ALOAD(2),XR(2),YR(2) 00006330
0003 R=(GAMDA1+GAMDA2)/2. 00006340
0004 DIFF=(GAMDA1-GAMDA2)/2. 00006350
0005 DELY=R/25. 00006360
0006 DO 10 N=1,2 00006370
0007 ALOAD(N)=0. 00006380
0008 SIGN=-1. 00006390
0009 IF(N.EQ.2)SIGN=1. 00006400
0010 DO 11 IR=1,25 00006410
0011 YR(1)=IR*DELY 00006420
0012 YR(2)=YR(1)-DELY 00006430
0013 XR(1)=SIGN*((R**2-YR(1)**2)**.5) 00006440
0014 XR(2)=SIGN*((R**2-YR(2)**2)**.5) 00006450
0015 DELX=ABS(XR(1)/25.) 00006460
0016 VTLOAD=0. 00006470
0017 DO 12 IX=1,2 00006480
0018 DO 13 IY=1,2 00006490
0019 IF(IX.EQ.2.AND.IY.EQ.1)GO TO 13 00006500
0020 R1=((XR(IX)+DIFF)**2+YR(IY)**2)**.5 00006510
0021 IF(R1.LT.1.E-5)GO TO 20 00006520
0022 COSPSI=(XR(IX)+DIFF)/R1 00006530
0023 GO TO 21 00006540
0024 20 COSPSI=1. 00006550
0025 21 GAMMA2=(4./3.)*A*A*((SIN(ALPHA)/(1.-COSPSI*COS(ALPHA))**2)*((1.- 00006560
I(COSPSI*COS(ALPHA))**2)**.5)*SIN(ALPHA)) 00006570
0026 IF((R1*R1/GAMMA2).LE.20.)GO TO 30 00006580
0027 P=0. 00006590
0028 GO TO 31 00006600
0029 30 P=PO*(2.-EXP(-R1*R1/GAMMA2))*EXP(-R1*R1/GAMMA2) 00006610
0030 31 VTLOAD=VTLOAD+P 00006620
0031 13 CONTINUE 00006630
0032 12 CONTINUE 00006640
0033 VTLOAD=0. 00006650
0034 DO 14 IQ=1,25 00006660
0035 DO 14 II=1,2 00006670
0036 DO 15 IY=1,2 00006680
0037 JQ=IQ 00006690
0038 IF(II.EQ.2)JQ=IQ-1 00006700
0039 MULT=1 00006710
0040 IF(II.EQ.IY)MULT=2 00006720
0041 X=XR(1)-SIGN*JQ*DELX 00006730
0042 R1=((X+DIFF)**2+YR(IY)**2)**.5 00006740
0043 IF(R1.LT.1.E-5)GO TO 22 00006750
0044 COSPSI=(X+DIFF)/R1 00006760

```

0045		GO TO 23	00006770
0046	22	COSPSI=1.	00006780
0047	23	GAMMA2=(4./3.)*A*A*((SIN(ALPHA)/(1.-COSPSI*COS(ALPHA))**2)*	00006790
		1*((1.-(COSPSI*COS(ALPHA))**2)**.5)*SIN(ALPHA))	00006800
0048		IF((R1*R1/GAMMA2).LE.20.)GO TO 40	00006810
0049		P=0.	00006820
0050		GO TO 15	00006830
0051	40	P=PO*(2.-EXP(-R1*R1/GAMMA2))*EXP(-R1*R1/GAMMA2)	00006840
0052	15	VLOAD=VLOAD+MULT*P	00006850
0053	14	CONTINUE	00006860
0054		ALOAD(N)=ALOAD(N)+(VTLOAD+VLOAD)*DELX*DELY/6.	00006870
0055	11	CONTINUE	00006880
0056	10	CONTINUE	00006890
0057		TLOAD=0.	00006900
0058		DO 16 N=1,2	00006910
0059	16	TLOAD=TLOAD+ALOAD(N)	00006920
0060		RETURN	00006930
0061		END	00006940

```

C *****00006950
0001 SUBROUTINE LAMDA1(GAMDA1,DEL,G1,G2,F,I,ALPHA,BESTL,ISPLT,SP,X1,X2)00006960
0002 K=0
0003 IF(ABS(2.*GAMDA1/G2).GT.20.)GO TO 10 00006970
0004 IF(ABS(2.*DEL/G2).GT.20.)GO TO 10 00006980
0005 E111=EXP(-GAMDA1/G1) 00006990
0006 E121=EXP(-DEL/G1) 00007000
0007 E122=EXP(-DEL/G2) 00007010
0008 E211=EXP(-2.*GAMDA1/G1) 00007020
0009 E221=EXP(-2.*DEL/G1) 00007030
0010 E222=EXP(-2.*DEL/G2) 00007040
0011 GAMDA2=GAMDA1 00007050
0012 1 K=K+1 00007060
0013 IF(K.EQ.1)GO TO 2 00007070
0014 GAMDA2=BESTL 00007080
0015 IF(ABS(2.*GAMDA2/G2).GT.20.)GO TO 10 00007090
0016 2 E112=EXP(GAMDA2/G2) 00007100
0017 E212=EXP(2.*GAMDA2/G2) 00007110
0018 A1=(G1/4.)*E211*((2.*(GAMDA1-F)+G1)*(E221-1.))+2.*DEL*E221 00007120
0019 1+2.*G1*E111*((GAMDA1-F+G1)*(1.-E121)-DEL*E121) 00007130
0020 A2=(G2/4.)*((2.*(GAMDA2+F)+G2)*(E222-1.))+2.*DEL*E222+2.*G2*E112* 00007140
0021 1((GAMDA2+F+G2)*(1.-E122)-DEL*E122)-E212*A1 00007150
0022 A3=2.*E112*((GAMDA2+F)*(E122-1.)+DEL*E122)-((GAMDA2+F)*(E222-1.)) 00007160
0023 1+DEL*E222) 00007170
0024 BESTL=GAMDA2-A2/A3 00007180
0025 TEST=ABS(1.-BESTL/GAMDA2) 00007190
0026 IF(K.EQ.200)GO TO 3 00007200
0027 IF(TEST.LE.1.0E-3)GO TO 4 00007210
0028 GO TO 1 00007220
0029 3 TESP=100.*TEST 00007230
0030 WRITE(6,5)TESP,I,ALPHA 00007240
0031 5 FORMAT(1H0,67HWARNING: CONVERGENCE TEST FOR LAMDA2 NOT SATISFIED--00007260
0032 1PERCENT ERROR= ,F8.3,1H0,44X,11HTIME STEP= ,I5,4X,14HIMPACT ANGLE00007270
0033 1= ,F7.4,1X,3HRAD) 00007280
0034 GO TO 4 00007290
0035 10 IF(ISPLT.EQ.1)BESTL=0.0 00007300
0036 IF(ISPLT.EQ.-1)BESTL=0.0 00007310
0037 4 RETURN 00007320
0038 END 00007330

```

0001	C	*****	00007340
		SUBROUTINE CAMBER(XNODE,YNODE,A,B,ISPLIT,RM,ALPHA,SPP,VDI,COSFEE,	00007350
0002		1VR,DEN,NSTAT,PRESSC)	
	C	IF(YNODE.GT.A.OR.YNODE.LT.B)GO TO 511	00007360
	C	-CALCULATE THE SQUASHED BIRD THICKNESS	00007370
0003		-FOR A 2D JET	00007380
0004		IF(ISPLIT.EQ.-1)GO TO 512	00007390
0005		THICK=RM*(1.+COS(ALPHA))/2.	00007400
0006		IF((XNODE-SPP).LT.0.)THICK=RM*(1.-COS(ALPHA))/2.	00007410
0007		GO TO 513	00007420
0008	512	THICK=RM*(1.-COS(ALPHA))/2.	00007430
0009		IF((XNODE-SPP).LT.0.)THICK=RM*(1.+COS(ALPHA))/2.	00007440
		GO TO 513	00007450
	C	-CALCULATE THE SQUASHED BIRD THICKNESS	00007460
	C	-FOR A 3D JET	00007470
0010	511	HSD=VDI*(RM**2)/(4.*((DIST+VDI)**2-DIST**2))	00007480
0011		THICK=HSD*(1.+COS(ALPHA)-2.*COS(ALPHA)*(ACOS(COSFEE))/3.141592654)	00007490
	C	-FIND WHICH BLADE CURVATURE REGION	00007500
	C	-THIS NODE FALLS WITHIN	00007510
0012	513	CALL REGION(XNODE,NSTAT,JC1)	00007520
	C	-FIND THE VALUE OF ONE OVER THE RADIUS OF CURVATURE	00007530
0013		CALL INCURV(JC1,P1)	00007540
0014		VEL=VR	00007550
0015		IF(YNODE.GT.A.OR.YNODE.LT.B)VEL=VR*COSFEE	00007560
0016		PRESSC=PI*THICK*DEN*(VEL**2)	00007570
0017		PRESSC=0.	00007580
0018		RETURN	00007590
0019		END	00007600
			00007610

FORTRAN IV G1 RELEASE 2.0

MAIN

DATE = 79012

08/33/03

PAGE 0001

	C	*****	00007620
0001		SUBROUTINE REGION(XNODE,NSTAT,JCI)	00007630
0002		COMMON/XMID/ XCEN1(25),XCEN2(25)	00007640
0003		NST=NSTAT-2	00007650
0004		DO 514 KJ=1,NST	00007660
0005		IF(XNODE.LT.XCEN1(KJ).OR.XNODE.GE.XCEN2(KJ))GO TO 514	00007670
0006		JCI=KJ	00007680
0007	514	CONTINUE	00007690
0008		RETURN	00007700
0009		END	00007710

0001	C	*****	00007720
0002		SUBROUTINE INCURV(JC1,P1)	00007730
0003		COMMON/BLADE/X0(25),Y0(25),THETA(24),XM(25)	00007740
		XMID1=X0(JC1)+COS(THETA(JC1))*((X0(JC1+1)-X0(JC1))*2+(Y0(JC1+1)-	00007750
0004		Y0(JC1))*2)**2)/2.	00007760
		YMID1=Y0(JC1)+SIN(THETA(JC1))*((X0(JC1+1)-X0(JC1))*2+(Y0(JC1+1)-	00007770
		Y0(JC1))*2)**2)/2.	00007780
0005		XMID2=X0(JC1+1)+COS(THETA(JC1+1))*((X0(JC1+2)-X0(JC1+1))*2+	00007790
		1(Y0(JC1+2)-Y0(JC1+1))*2)**2)/2.	00007800
0006		YMID2=Y0(JC1+1)+SIN(THETA(JC1+1))*((X0(JC1+2)-X0(JC1+1))*2+	00007810
		1(Y0(JC1+2)-Y0(JC1+1))*2)**2)/2.	00007820
0007		DELPHI=THETA(JC1+1)-THETA(JC1)	00007830
0008		IF(DELPHI.LT.1.7E-5)GO TO 501	00007840
0009		CHORD=SQRT((XMID1-XMID2)**2+(YMID1-YMID2)**2)	00007850
0010		RCURV=CHORD/(2.*SIN(DELPHI/2.))	00007860
0011		P1=1./RCURV	00007870
0012		GO TO 500	00007880
0013	501	P1=0.	00007890
0014	500	RETURN	00007900
0015		END	00007910

```

0001      C *****00007920
          SUBROUTINE PRESUR(NR,A,B,DIST,ISPLIT,SPP,SPP1,VDI,GAMMA1,GAMMA2,P000007930
0002      1,RM,ALPHA,VR,DEN,NSTAT,IIFLG)
          COMMON/AR/ XNODE(25,25),YNODE(25),MAX(25),PRESS(25,25),
          1AANODE(25,25),PPL(25,25),PVL(25,25),FRSS(25,25)
0003      DO 501 I3=1,NR
0004      LIM=MAX(I3)
0005      DO 502 J3=1,LIM
0006      IF(YNODE(I3).GE.A.OR.YNODE(I3).LE.B)GO TO 503
0007      IF(ISPLIT.EQ.-1)GO TO 504

          C      2D JET
          C      FLOW FROM NODE N TO N+1--ISPLIT=1
0008      DOT=XNODE(I3,J3)-SPP1
0009      IF(DOT.LT.0.)DOT=-DOT
0010      IF(DOT.GT.(DIST+VDI))GO TO 502
0011      IF(DOT.LT.DIST.AND.IIFLG.EQ.1)GO TO 502
0012      XDOT=XNODE(I3,J3)-SPP
0013      507 IF(XDOT.LT.0.)GO TO 5000
0014      IF((XDOT/GAMMA1).GT.75.)GO TO 600
0015      FEXP=EXP(-XDOT/GAMMA1)
0016      GO TO 601
0017      5000 IF(ABS(XDOT/GAMMA2).GT.75.)GO TO 600
0018      FEXP=EXP(XDOT/GAMMA2)
0019      GO TO 601
0020      600 FEXP=0.
0021      601 PPL(I3,J3)=P0*FEXP*(2.-FEXP)
0022      IF(PRESS(I3,J3).LT.PPL(I3,J3))PRESS(I3,J3)=PPL(I3,J3)
0023      GO TO 506

          C      FLOW FROM NODE N+1 TO N--ISPLIT=-1
0024      504 DOT=SPP1-XNODE(I3,J3)
0025      IF(DOT.LT.0.)DOT=-DOT
0026      IF(DOT.GT.(DIST+VDI))GO TO 502
0027      IF(DOT.LT.DIST.AND.IIFLG.EQ.1)GO TO 502
0028      XDOT=SPP-XNODE(I3,J3)
0029      GO TO 507

          C      3D JET
          C      FLOW FROM NODE N TO N+1--ISPLIT=1
0030      503 SIGN=1.
0031      IF(ISPLIT.EQ.-1)SIGN=-1.
0032      IF(YNODE(I3).LE.B)GO TO 509
0033      DOT=((XNODE(I3,J3)-SPP1)**2+(YNODE(I3)-A)**2)**.5
0034      IF(DOT.GT.(DIST+VDI))GO TO 502
0035      IF(DOT.LT.DIST.AND.IIFLG.EQ.1)GO TO 502
0036      XDOT=XNODE(I3,J3)-SPP
0037      RDOT=((XNODE(I3,J3)-SPP)**2+(YNODE(I3)-A)**2)**.5
0038      510 IF(RDOT.LT.1.E-3)GO TO 700
0039      COSFEE=(XNODE(I3,J3)-SPP)*SIGN/RDOT
0040      GO TO 701

```

```

0041      700 COSFEE=1.                                00008400
0042      701 Y2=((RM*SIN(ALPHA)/(1.-COSFEE*COS(ALPHA)))**2)*SIN(ALPHA)* 00008410
          1((1.-(COSFEE*COS(ALPHA)))**2)**.5)/3.          00008420
0043      IF(ABS((RDOT**2)/Y2).GT.75.)GO TO 600          00008430
0044      FEXP=EXP(-(RDOT**2)/Y2)                        00008440
0045      PPL(I3,J3)=P0*FEXP*(2.-FEXP)                   00008450
0046      IF(PRESS(I3,J3).LT.PPL(I3,J3))PRESS(I3,J3)=PPL(I3,J3) 00008460
0047      GO TO 506
0048      509 DOT=((XNODE(I3,J3)-SPP1)**2+(YNODE(I3)-B)**2)**.5 00008470
0049      IF(DOT.GT.(DIST+VDT))GO TO 502                  00008480
0050      IF(DOT.LT.DIST.AND.IIFLG.EQ.1)GO TO 502         00008490
0051      RDOT=((XNODE(I3,J3)-SPP)**2+(YNODE(I3)-B)**2)**.5 00008500
0052      XDOT=XNODE(I3,J3)-SPP                          00008510
0053      GO TO 510                                       00008520
          C
          C      ADD ON THE PRESSURE EFFECTS DUE TO      00008530
          C      BLADE CAMBER                            00008540
0054      506 CALL CAMBER(XNODE(I3,J3),YNODE(I3),A,B,ISPLIT,RM,ALPHA,SPP,VDT, 00008550
          1COSFEE,VR,DEN,NSTAT,PRESSC)                  00008560
0055      IF(PVL(I3,J3).LT.PRESSC)PVL(I3,J3)=PRESSC     00008570
0056      PRESS(I3,J3)=PRESS(I3,J3)+PVL(I3,J3)          00008580
0057      IF(DOT.LT.DIST)GO TO 502                      00008590
0058      PRSS(I3,J3)=PRESS(I3,J3)                      00008600
0059      502 CONTINUE                                  00008610
0060      501 CONTINUE                                  00008620
0061      RETURN                                         00008630
0062      END                                           00008640
          00008650

```



```

0001      C *****00008660
0002      SUBROUTINE MODAL(NM,NSTAT,NN,I8,FV,T) 00008670
      COMMON/MODE/BET(10),VKI(10),WI(10),GI(10),FI(10),FDI(10),GDI(10), 00008680
      1AA(10),BB(10),PI(10),QI(10),Q(10),QD(10),QDI(10),WO(10),PH2(3,625,00008690
      110),PP(625,2),DEF(2,625),VEL(2,625),STRSS(3,625),SH2(3,625,10) 00008700
      C      IF FV=0 THIS IS FREE VIBRATION 00008710
      C      CALCULATE THE PARAMETERS 00008720
0003      DO 420 I6=1,NN
0004      C3=EXP(-BET(I6)*T) 00008730
0005      GI(I6)=C3*SIN(WI(I6)*T)/WI(I6) 00008740
0006      FI(I6)=C3*COS(WI(I6)*T)+BET(I6)*GI(I6) 00008750
0007      FDI(I6)=-GI(I6)*WO(I6)**2 00008760
0008      GDI(I6)=C3*(COS(WI(I6)*T)-(BET(I6)/WI(I6))*SIN(WI(I6)*T)) 00008770
0009      AA(I6)=(1.-FI(I6))/VKI(I6) 00008780
0010      BB(I6)=-FDI(I6)/VKI(I6) 00008790
      420      00008800
      C      ZERO OUT THE DEFLECTIONS 00008810
      C      STRESSES AND VELOCITIES 00008820
0011      150 DO 430 JB=1,NN 00008830
0012      DEF(1,JB)=0. 00008840
0013      DEF(2,JB)=0. 00008850
0014      STRSS(1,JB)=0. 00008860
0015      STRSS(2,JB)=0. 00008870
0016      STRSS(3,JB)=0. 00008880
0017      VEL(1,JB)=0. 00008890
0018      430 VEL(2,JB)=0. 00008900
0019      DO 440 I6=1,NN 00008910
0020      PI(I6)=0. 00008920
      C      CALCULATE THE GENERALIZED FORCE 00008930
      C      FOR EACH MODE 00008940
0021      DO 450 K6=1,NN 00008950
0022      450 PI(I6)=PI(I6)+PH2(1,K6,I6)*PP(K6,1)+PH2(2,K6,I6)*PP(K6,2) 00008960
      C      CALCULATE THE MODAL COEFFICIENTS 00008970
      C      AND THEIR TIME DERIVATIVES 00008980
0023      QI(I6)=FI(I6)*Q(I6)+GI(I6)*QD(I6)+AA(I6)*PI(I6) 00008990
0024      QDI(I6)=FDI(I6)*Q(I6)+GDI(I6)*QD(I6)+BB(I6)*PI(I6) 00009000
0025      Q(I6)=QI(I6) 00009010
0026      QD(I6)=QDI(I6) 00009020
0027      DO 460 JB=1,NN 00009030
0028      DEF(1,JB)=DEF(1,JB)+PH2(1,JB,I6)*QI(I6) 00009040
0029      DEF(2,JB)=DEF(2,JB)+PH2(2,JB,I6)*QI(I6) 00009050
0030      STRSS(1,JB)=STRSS(1,JB)+SH2(1,JB,I6)*QI(I6) 00009060
0031      STRSS(2,JB)=STRSS(2,JB)+SH2(2,JB,I6)*QI(I6) 00009070
0032      STRSS(3,JB)=STRSS(3,JB)+SH2(3,JB,I6)*QI(I6) 00009080
0033      VEL(1,JB)=VEL(1,JB)+PH2(1,JB,I6)*QDI(I6) 00009090
0034      VEL(2,JB)=VEL(2,JB)+PH2(2,JB,I6)*QDI(I6) 00009100
0035      460 CONTINUE 00009110
0036      440 CONTINUE 00009120
0037      RETURN 00009130

```

FORTTRAN IV G1 RELEASE 2.0

MODAL

DATE = 79012

08/33/03

PAGE 0002

0038

END

00009140

```

0001 C ***** PRESSURE PRINTOUT *****00009150
0002 SUBROUTINE PRINTP(I,TIME,NR)
0003 COMMON/AR/XNODE(25,25),YNODE(25),MAX(25),PRESS(25,25),
1AANCDE(25,25),PPL(25,25),PVL(25,25),PRSS(25,25),
DIMENSION MAXL(5)
C FIND OUT WHICH RADIAL STATIONS
C BORDER THE PRESSURE DISTRIBUTION
C -II3 IS THE LOWER RADIAL STATION
C -IK3 IS THE UPPER RADIAL STATION
0004 II3=0
0005 IK3=0
0006 DO 10 I4=1,NR
0007 K3=NR+1-I4
0008 LIM1=MAX(I4)
0009 LIM2=MAX(K3)
0010 DO 15 J3=1,LIM1
0011 IF(II3.GT.0)GO TO 15
0012 IF(PRESS(I4,J3).EQ.0.)GO TO 15
0013 II3=I4
0014 15 CONTINUE
0015 DO 20 L3=1,LIM2
0016 IF(IK3.GT.0)GO TO 20
0017 IF(PRESS(K3,L3).EQ.0.)GO TO 20
0018 IK3=K3
0019 20 CONTINUE
0020 10 CONTINUE
C PRINT THE TIME STEP AND THE TIME
0021 IF(I.EQ.1)GO TO 500
0022 WRITE(6,100)I,TIME
0023 100 FORMAT(1H1,47X,10HTIME STEP=,I4,2X,5HTIME=,E12.6,1X,3HSEC)
C IF NO NODAL LOADS PRINT NO PRESSURES
C AND RETURN TO MAIN PROGRAM
0024 IF(II3.GT.0)GO TO 30
0025 WRITE(6,101)
0026 101 FORMAT(1H0,52X,27HALL NODE PRESSURES ARE ZERO)
0027 GO TO 500
C FIND OUT HOW MANY RADIAL STATIONS
C WILL HAVE TO BE PRINTED
0028 30 ITY=IK3-II3+1
0029 DO 35 KK=1,5
0030 IF((ITY-5).LE.0)GO TO 31
0031 MAXL(KK)=5
0032 ITOTL=KK
0033 ITY=ITY-5
0034 GO TO 35
0035 31 MAXL(KK)=ITY
0036 ITOTL=KK
0037 GO TO 40

```

ORIGINAL PAGE IS
OF POOR QUALITY

0038	35	CONTINUE	00009630
	C	ITOTL CONTAINS THE THE TOTAL NUMBER	00009640
	C	OF GROUPS OF FIVE RADIAL STATIONS	00009650
	C	THAT WILL BE PRINTED ACROSS A PAGE	00009660
	C	FOR EACH GROUP PRINTED ACROSS A PAGE	00009670
	C	MAXL CONTAINS THE NUMBER OF RADIAL	00009680
	C	STATIONS THAT WILL BE PRINTED ACROSS	00009690
0039	40	IS=I13	00009700
0040		DO 50 I1=1,ITOTL	00009710
0041		IE=IS+MAXL(I1)-1	00009720
	C	PRINT THE HEADINGS	00009730
0042		WRITE(6,102)(YNODE(IY),IY=IS,IE)	00009740
0043	102	FORMAT(//1H0,8X,2HY=,E11.5,4(13X,2HY=,E11.5))	00009750
0044		WRITE(6,202)	00009760
0045	202	FORMAT(//)	00009770
0046		ICF=MAXL(I1)	00009780
0047		DO 60 IC=1,ICF	00009790
0048		IF(IC.EQ.1)GO TO 61	00009800
0049		IF(IC.EQ.2)GO TO 62	00009810
0050		IF(IC.EQ.3)GO TO 63	00009820
0051		IF(IC.EQ.4)GO TO 64	00009830
0052		WRITE(6,1035)	00009840
0053	1035	FORMAT(1H+,108X,1HX,11X,1HP)	00009850
0054		GO TO 60	00009860
0055	61	WRITE(6,1031)	00009870
0056	1031	FORMAT(1H+,4X,1HX,11X,1HP)	00009880
0057		GO TO 60	00009890
0058	62	WRITE(6,1032)	00009900
0059	1032	FORMAT(1H+,30X,1HX,11X,1HP)	00009910
0060		GO TO 60	00009920
0061	63	WRITE(6,1033)	00009930
0062	1033	FORMAT(1H+,56X,1HX,11X,1HP)	00009940
0063		GO TO 60	00009950
0064	64	WRITE(6,1034)	00009960
0065	1034	FORMAT(1H+,82X,1HX,11X,1HP)	00009970
0066	60	CONTINUE	00009980
0067		DO 70 J3=1,25	00009990
0068		WRITE(6,105)	00010000
0069	105	FORMAT(/)	00010010
0070		IPF=MAXL(I1)	00010020
0071		DO 80 IP=1,IPF	00010030
0072		I3=IS+IP-1	00010040
0073		LIM=MAX(I3)	00010050
0074		IF(J3.GT.LIM)GO TO 80	00010060
0075		IF(IP.EQ.1)GO TO 81	00010070
0076		IF(IP.EQ.2)GO TO 82	00010080
0077		IF(IP.EQ.3)GO TO 83	00010090
0078		IF(IP.EQ.4)GO TO 84	00010100

0079		WRITE(6,1045)XNODE(I3,J3),PRESS(I3,J3)	00010110
0080	1045	FORMAT(1H+,105X,2(2X,E10.4))	00010120
0081		GO TO 80	00010130
0082	81	WRITE(6,1041)XNODE(I3,J3),PRESS(I3,J3)	00010140
0083	1041	FORMAT(1H+,1X,2(2X,E10.4))	00010150
0084		GO TO 80	00010160
0085	82	WRITE(6,1042)XNODE(I3,J3),PRESS(I3,J3)	00010170
0086	1042	FORMAT(1H+,27X,2(2X,E10.4))	00010180
0087		GO TO 80	00010190
0088	83	WRITE(6,1043)XNODE(I3,J3),PRESS(I3,J3)	00010200
0089	1043	FORMAT(1H+,53X,2(2X,E10.4))	00010210
0090		GO TO 80	00010220
0091	84	WRITE(6,1044)XNODE(I3,J3),PRESS(I3,J3)	00010230
0092	1044	FORMAT(1H+,79X,2(2X,E10.4))	00010240
0093	80	CONTINUE	00010250
0094	70	CONTINUE	00010260
0095		IS=IE+1	00010270
0096	50	CONTINUE	00010280
0097	500	RETURN	00010290
0098		END	00010300

0001	C	*****	00010310
0002		SUBROUTINE PRINTV(I,TIME,IPDEL,ITPRNT,NR,IJPRNT,I7)	00010320
		COMMON/MODE/DUMMY(20150),DEF(2,625),VEL(2,625),STRSS(3,625),	00010330
0003		ISH2(3,625,10)	00010340
		COMMON/PRNT/NJ3(25),DEFBI(1000,25),DEFBO(1000,25),CODI(1000,25),	00010350
		ICODO(1000,25),SIGMB1(1000,25,3),SIGMB2(1000,25,3),SIGMA1(1000,3,	00010360
		125),SIGMA2(1000,3,25),TIMEP(1000)	00010370
0004		COMMON/AR/XNODE(25,25),YNODE(25),MAX(25),PRESS(25,25),	00010380
		1AANODE(25,25),PPL(25,25),PVL(25,25),PRSS(25,25)	00010390
0005		ITPRNT=ITPRNT+IPDEL	00010400
0006		IJPRNT=(ITPRNT-1)/IPDEL	00010410
0007		TIMEP(IJPRNT)=TIME	00010420
0008		J5=0	00010430
0009		DO 10 I3=1,NR	00010440
0010		LIM=MAX(I3)	00010450
0011		NXPRNT=NJ3(I3)	00010460
0012		DO 20 J3=1,LIM	00010470
0013		J5=J5+1	00010480
0014		IF(J3.NE.NXPRNT)GO TO 21	00010490
0015		DEFBI(IJPRNT,I3)=DEF(1,J5)	00010500
0016		DEFBO(IJPRNT,I3)=DEF(2,J5)	00010510
0017	21	IF(I3.NE.I7)GO TO 20	00010520
0018		CODI(IJPRNT,J3)=DEF(1,J5)	00010530
0019		CODO(IJPRNT,J3)=DEF(2,J5)	00010540
0020	20	CONTINUE	00010550
0021	10	CONTINUE	00010560
0022		I5=0	00010570
0023		I4=0	00010575
0024		DO 30 I3=1,NR	00010580
0025		LIM=MAX(I3)	00010590
0026		NSPRNT=NJ3(I3)	00010600
0027		IC=0	00010610
0028		IFLG=0	00010630
0029		DO 40 J3=1,LIM	00010640
0030		I5=I5+1	00010650
0031		IF((J3.NE.1).AND.(J3.NE.LIM).AND.(J3.NE.NSPRNT))GO TO 41	00010660
0032		IC=IC+1	00010670
0033		IF(IC.EQ.1) SIGMB1(IJPRNT,I3,1)=STRSS(2,I5)	00010680
0034		IF(IC.EQ.2) SIGMB1(IJPRNT,I3,2)=STRSS(2,I5)	00010690
0035		IF(IC.EQ.3) SIGMB1(IJPRNT,I3,3)=STRSS(2,I5)	00010700
0036	41	IF((I3.NE.I7-1).AND.(I3.NE.I7).AND.(I3.NE.I7+1))GO TO 40	00010710
0037		IF(IFLG.EQ.1)GO TO 42	00010720
0038		I4=I4+1	00010730
0039	42	SIGMA1(IJPRNT,I4,J3)=STRSS(1,I5)	00010740
0040		SIGMA2(IJPRNT,I4,J3)=STRSS(2,I5)	00010750
0041		SIGMB2(IJPRNT,J3,I4)=STRSS(3,I5)	00010760
0042		IFLG=1	00010770
0043	40	CONTINUE	00010780

FORTRAN IV G1 RELEASE 2.0

PRINTV

DATE = 79012

08/33/03

PAGE 0002

0044 30 CONTINUE
0045 RETURN
0046 END

00010790
00010800
00010810

```

0001      C *****00010820
0002      SUBROUTINE PRINTR(I7,NSTAT,NR,IJPRNT)00010830
0003      COMMON/AR/XNODE(25,25),YNODE(25),MAXI(25),PRESS(25,25),00010840
0004      1AANODE(25,25),PPL(25,25),PVL(25,25),PRSS(25,25)00010850
0005      COMMON/PRNT/NJ3(25),DEFBI(1000,25),DEFBO(1000,25),CODI(1000,25),00010860
0006      ICODO(1000,25),SIGMB1(1000,25,3),SIGMB2(1000,25,3),SIGMA1(1000,3,00010870
0007      125),SIGMA2(1000,3,25),TIMEP(1000)00010880
0008      DIMENSION R(3),STRS1(3,25),STRS2(3,25),X(25),STRS3(3,25)00010890
0009      DO 10 IT=1,IJPRNT00010900
0010      WRITE(6,100)TIMEP(IT)00010910
0011      100 FORMAT(/1H0,56X,5HTIME=,E12.6,1X,3HSEC,/,1H ,39X,53HDISPLACEMENTS00010920
0012      1 AND BENDING STRESSES VS. RADIAL STATION,/,1H ,26X,13HDISPLACEMENT00010930
0013      1S,18X,21HRADIAL BENDING STRESS,/,1H ,9X,1HR,9X,8HIN-PLANE,7X,00010940
0014      112HOUT-OF-PLANE,3H***,7HLED-EDG,8X,7HCHD-PNT,8X,7HTRL-EDG)00010950
0015      DO 11 I3=1,NR00010960
0016      WRITE(6,101)YNODE(I3),DEFBI(IT,I3),DEFBO(IT,I3),(SIGMB1(IT,I3,IV),00010970
0017      1IV=1,3)00010980
0018      101 FORMAT(1H ,3(4X,E11.5),1X,2H**.,1X,E11.5,2(4X,E11.5))00010990
0019      CONTINUE00011000
0020      DO 30 K=1,300011010
0021      IF(K.EQ.2)GO TO 3200011020
0022      I8=I7+100011030
0023      IF(K.EQ.1)I8=I7-100011040
0024      IF(I8.LT.1)GO TO 3100011050
0025      IF(I8.GT.NR)GO TO 3100011060
0026      R(K)=YNODE(I8)00011070
0027      LIM1=MAX(I8)00011080
0028      LIM2=LIM1-100011090
0029      DO 40 J3=1,NSTAT00011100
0030      IF(XNODE(I7,J3).LT.XNODE(I8,1).OR.XNODE(I7,J3).GT.XNODE(I8,LIM1))00011110
0031      GO TO 4100011120
0032      DO 50 J4=1,LIM200011130
0033      IF(XNODE(I7,J3).LT.XNODE(I8,J4).OR.XNODE(I7,J3).GT.XNODE(I8,J4+1))00011140
0034      GO TO 5000011150
0035      STRS1(K,J3)=(SIGMA1(IT,K,J4+1)-SIGMA1(IT,K,J4))*(XNODE(I7,J3)-00011160
0036      1XNODE(I8,J4))/(XNODE(I8,J4+1)-XNODE(I8,J4))+SIGMA1(IT,K,J4)00011170
0037      STRS2(K,J3)=(SIGMA2(IT,K,J4+1)-SIGMA2(IT,K,J4))*(XNODE(I7,J3)-00011180
0038      1XNODE(I8,J4))/(XNODE(I8,J4+1)-XNODE(I8,J4))+SIGMA2(IT,K,J4)00011190
0039      STRS3(K,J3)=(SIGMB2(IT,J4+1,K)-SIGMB2(IT,J4,K))*(XNODE(I7,J3)-00011200
0040      1XNODE(I8,J4))/(XNODE(I8,J4+1)-XNODE(I8,J4))+SIGMB2(IT,J4,K)00011210
0041      CONTINUE00011220
0042      GO TO 4000011230
0043      41 STRS1(K,J3)=0.00011240
0044      STRS2(K,J3)=0.00011250
0045      STRS3(K,J3)=0.00011260
0046      CONTINUE00011270
0047      GO TO 3000011280
0048      31 R(K)=0.00011290

```


0036		DO 45 J3=1,NSTAT	00011300
0037		STRS1(K,J3)=0.	00011310
0038		STRS2(K,J3)=0.	00011320
0039	45	STRS3(K,J3)=0.	00011330
0040		GO TO 30	00011340
0041	32	R(K)=YNODE(I7)	00011350
0042		DO 33 J3=1,NSTAT	00011360
0043		STRS1(2,J3)=SIGMA1(IT,2,J3)	00011370
0044		STRS2(2,J3)=SIGMA2(IT,2,J3)	00011380
0045		STRS3(2,J3)=SIGMA2(IT,J3,2)	00011390
0046	33	X(J3)=XNODE(I7,J3)-XNODE(I7,1)	00011400
0047	30	CONTINUE	00011410
0048		WRITE(6,104)	00011420
0049	104	FORMAT(/1H0,47X,36HDISPLACEMENTS VS. CHORDWISE LOCATION, 1/1H ,57X,16HAT IMPACT RADIUS,/1H ,50X,1HX,9X,8HIN-PLANE, 16X,12HOUT-OF-PLANE)	00011430 00011440
0050		DO 60 J3=1,NSTAT	00011450
0051		WRITE(6,105)X(J3),CODI(IT,J3),CODO(IT,J3)	00011460
0052	103	FORMAT(1H ,41X,3(4X,E11.5))	00011470
0053	60	CONTINUE	00011480
0054		WRITE(6,102)(R(JK),JK=1,3),(R(JL),JL=1,3),(R(JM),JM=1,3)	00011490
0055	102	FORMAT(/1H0,50X,31HSTRESSES VS. CHORDWISE LOCATION, 1/1H ,57X,16HAT IMPACT RADIUS,/1H ,27X,8HSTRESS-X,32X,8HSTRESS-Y, 132X,8Hshear-XY,/1H ,4X,1HX,6X,3(3H*R=,E10.4),2(1X,3(3H*R=,E10.4)))	00011500 00011510 00011520 00011530
0056		DO 61 J3=1,NSTAT	00011540
0057		WRITE(6,105)X(J3),(STRS1(KL,J3),KL=1,3),(STRS2(KL,J3),KL=1,3), 1(STRS3(KL,J3),KL=1,3)	00011550 00011560
0058	105	FORMAT(1H ,E10.4,3(1X,3(1H*,1X,E10.4,1X)))	00011570
0059	61	CONTINUE	00011580
0060	10	CONTINUE	00011590
0061		RETURN	00011600
0062		END	00011610

ORIGINAL PAGE IS
OF POOR QUALITY

```

0001      C *****00011620
          SUBROUTINE PINIT(L1,NVA,BETA,JC1,XNERL1,DLTALL,I8,NSTAF,PPII,E,F, 00011630
          1G,AL,R1,S,DEN,I,V,I7,DT,RIMP,NSTAT) 00011640
0002      COMMON/VARBLI/NA(1000),RM1(1000),RM2(1000),ITSLD(1000),GMALL(1000)00011650
          1,VRL1(1000),ALPL1(1000),ISPLT(1000),VDTL1(1000),WM1(1000) 00011660
0003      COMMON/L/II(6),RM(6),XI(6),YI(6),IHIT(6),RL(6),X(6),Y(6),WM(6) 00011670
0004      COMMON/LK/VDT(6,1000),ISLIDE(6,1000),GAMMA(6),VR(6,1000), 00011680
          1ALPHA(6),ISPLIT(6),GAMMA1(1000),GAMMA2(1000),SPP(1000),PO(1000), 00011690
          1LAM011(1000),LAM021(1000),FIMP2D(1000),FIMP3D(1000),DIST(1000), 00011700
          1SPP1(1000) 00011710
0005      COMMON/BLADE/X0(25),Y0(25),THETA(24),XM(25) 00011720
0006      COMMON/AR/XNODE(25,25),YNODE(25),MAX(25),PRESS(25,25), 00011730
          1AANODE(25,25),PPL(25,25),PVL(25,25),PRSS(25,25) 00011740
0007      COMMON/MODE/DUMMY(21400),VEL(2,625),STRSS(3,625),SH2(3,625,10) 00011750
0008      REAL LAM011,LAM021 00011760
0009      NA(I)=0 00011770
0010      L1=0 00011780
0011      RM1(I)=0. 00011790
0012      RM2(I)=0. 00011800
0013      ITSLD(I)=7 00011810
0014      DO 10 I=1,NVA 00011820
0015      IF(L.GT.ITSLD(I))GO TO 20 00011830
0016      IF(II(L).NE.1)GO TO 10 00011840
0017      IF(ISLIDE(L,I).EQ.1)GO TO 20 00011850
0018      RM1(I)=RM1(I)+RM(L) 00011860
0019      NA(I)=NA(I)+1 00011870
0020      IF(NA(I).GT.1)GO TO 11 00011880
0021      L1=L 00011890
0022      WM1(I)=WM(L) 00011900
0023      GO TO 10 00011910
0024      11 IF(WM(L).GT.WM1(I))WM1(I)=WM(L) 00011920
0025      GO TO 10 00011930
0026      20 IF(ITSLD(I).EQ.7)ITSLD(I)=L 00011940
0027      RM2(I)=RM2(I)+RM(L) 00011950
0028      10 CONTINUE 00011960
0029      IF(NA(I).EQ.0)GO TO 100 00011970
0030      A=RIMP+(WM1(I)-RM1(I))/2. 00011980
0031      B=RIMP-(WM1(I)-RM1(I))/2. 00011990
0032      IF((A-B).GT.0.)GO TO 7200 00012000
0033      A=RIMP 00012010
0034      B=RIMP 00012020
0035      7200 DL=A-B 00012030
0036      RL1=(RM1(I)-RM(L1))/2. 00012040
0037      RL1=RL1 00012050
0038      XIT1=XI(L1) 00012060
0039      YIT1=YI(L1) 00012070
0040      JC1=IHIT(L1) 00012080
0041      32 Z=RL1/SIN(THETA(JC1)-BETA) 00012090

```

```

0042      D=((X0(JC1+1)-XIT1)**2+(Y0(JC1+1)-YIT1)**2)**.5      00012100
0043      IF(Z.LE.D)GO TO 31      00012110
0044      JC1=JC1+1      00012120
0045      XIT1=X0(JC1)      00012130
0046      YIT1=Y0(JC1)      00012140
0047      RL1=RL1-D*SIN(THETA(JC1-1)-BETA)      00012150
0048      GO TO 32      00012160
0049      31 XIT1=XIT1+Z*COS(THETA(JC1))      00012170
0050      YIT1=YIT1+Z*SIN(THETA(JC1))      00012180
0051      XNERL1=XM(JC1)      00012190
0052      DLTAL1=((X0(JC1)-XIT1)**2+(Y0(JC1)-YIT1)**2)**.5      00012200
0053      GHAL1(I)=XNERL1+DLTAL1      00012210
0054      DO 33 KL=1,NVA      00012220
0055      RK1=RL(L1)-RL(KL)-RM(KL)/2.      00012230
0056      RK2=RL(L1)-RL(KL)+RM(KL)/2.      00012240
0057      IF((RK1.LE.RLL).AND.(RK2.GT.RLL))KIM=KL      00012250
0058      33 CONTINUE      00012260
0059      RV=RL(L1)-RL(KIM)-RLL      00012270
0060      XKM=X(KIM)+RV*SIN(BETA)      00012280
0061      YKM=Y(KIM)-RV*COS(BETA)      00012290
0062      DFBL1=((XKM-XIT1)**2+(YKM-YIT1)**2)**.5      00012300
0063      IF(I.EQ.1)GO TO 35      00012310
0064      J9=I8-1      00012320
0065      DO 36 JB=1,NSTAF      00012330
0066      J9=J9+1      00012340
0067      IF(JB.EQ.JC1)JT=J9      00012350
0068      36 CONTINUE      00012360
0069      IF(ABS(PPII/2.-ABS(THETA(JC1)))>.GE.PPII/12.)GO TO 37      00012370
0070      OMEGA=(VEL(1,JT+1)-VEL(1,JT))/(Y0(JC1+1)-Y0(JC1))      00012380
0071      GO TO 38      00012390
0072      37 OMEGA=(VEL(2,JT+1)-VEL(2,JT))/(X0(JC1+1)-X0(JC1))      00012400
0073      38 XID=VEL(1,JT)-(YIT1-Y0(JC1))*OMEGA      00012410
0074      YID=VEL(2,JT)+(XIT1-X0(JC1))*OMEGA      00012420
0075      GO TO 39      00012430
0076      35 XID=0.      00012440
0077      YID=0.      00012450
0078      39 VI=XID*COS(BETA)+YID*SIN(BETA)      00012460
0079      VB=XID*COS(THETA(JC1))+YID*SIN(THETA(JC1))      00012470
0080      VX1=(V-VI)*COS(BETA)-VB*COS(THETA(JC1))      00012480
0081      VY1=(V-VI)*SIN(BETA)-VB*SIN(THETA(JC1))      00012490
0082      VRL1(I)=(VX1**2+VY1**2)**.5      00012500
0083      ALPL1(I)=ACOS((VX1*COS(THETA(JC1))+VY1*SIN(THETA(JC1)))/      00012510
      1VRL1(I))      00012520
0084      ISPLT(I)=1      00012530
0085      IF(ALPL1(I).LE.PPII/2.)GO TO 40      00012540
0086      ALPL1(I)=PPII-ALPL1(I)      00012550
0087      ISPLT(I)=-1      00012560
0088      40 VDTL1(I)=VRL1(I)*DT      00012570

```

ORIGINAL PAGE IS
OF POOR QUALITY

```

0089      IF(ALPL1(I).LT.1.7E-3)GO TO 100
          C      CALCULATE THE PARAMETERS ASSOCIATED WITH THE FLUID JET MODEL
0090      ELJ=RM1(I)*COTAN(ALPL1(I))/2.
0091      F=14.*RM1(I)*(1.-2.*ALPL1(I)/PPII)*SIN(ALPL1(I))/9.
0092      GLJ=RM1(I)*(COTAN(ALPL1(I))+28.*(1.-2.*ALPL1(I)/PPII)*SIN(ALPL1(
          I))/9.)/2.
0093      IF(ABS(PPII/2.-ABS(ALPL1(I))).GE.1.E-3)GO TO 200
0094      ELJ=0.
0095      F=0.
0096      GLJ=0.
0097      200 FACTOR=(PPII/2.-ALPL1(I))
0098      IF(FACTOR.GE.1.7E-3)GO TO 59
0099      RATIO=1.
0100      GO TO 60
0101      59 RATIO=FACTOR/SIN(FACTOR)
0102      60 AL=(28.*RM1(I)*RATIO/(9.*PPII))*SIN(ALPL1(I))*(1.+SIN(ALPL1(I)
          1)
0103      A2F=DL*RM1(I)*(1.+COS(ALPL1(I)))/2.
0104      A3F=PPII*(RM1(I)**2)*(1.-ALPL1(I)/PPII+SIN(2.*ALPL1(I))/
          I(2.*PPII))/4.
0105      E3J=4.*COTAN(ALPL1(I))/(3.*PPII*(1.+SQRT(SIN(ALPL1(I)))))
0106      F3J=(2.3*(1.-2.*ALPL1(I)/PPII)*(1.-(1.-2.*ALPL1(I)/PPII)**27)
          1+.1*SIN(2.*ALPL1(I)))*RM1(I)/2.
0107      G3J=E3J+F3J
0108      E=(E3J*A3F+ELJ*A2F)/(A3F+A2F)
0109      G=(G3J*A3F+GLJ*A2F)/(A3F+A2F)
0110      R1=AL*COTAN(ALPL1(I))/2.)
0111      S=AL*(RM1(I)/2.)*((COTAN(ALPL1(I))**2)
          PHI=S/R1
0112      GAMMA1(I)=4.*RM1(I)*(1.-ALPL1(I)/PPII)*SIN(ALPL1(I))/3.
0113      GAMMA2(I)=4.*RM1(I)*ALPL1(I)*SIN(ALPL1(I))/(3.*PPII)
0114      LAMD11(I)=AL-R1*SIN(ALPL1(I)-PHI)+F
0115      IF(PHI.GT.ALPL1(I))LAMD11(I)=AL+S-R1*ALPL1(I)+F
0116      IF(THETA(JC1).LE.PPII/2..AND.ALPL1(I).LE.PPII/2.)SPP(I)=
          1GMAL1(I)-G
0117      IF(THETA(JC1).LE.PPII/2..AND.ALPL1(I).GT.PPII/2.)SPP(I)=
          1GMAL1(I)+G
0118      IF(THETA(JC1).GT.PPII/2..AND.ALPL1(I).LE.PPII/2.)SPP(I)=
          1GMAL1(I)-G
0119      IF(THETA(JC1).GT.PPII/2..AND.ALPL1(I).GT.PPII/2.)SPP(I)=
          1GMAL1(I)+G
0120      IF(ISPLT(I).EQ.1.AND.GMAL1(I)-E.LT.XM(1)) GO TO 58
0121      IF(ISPLT(I).EQ.-1.AND.GMAL1(I)+E.GT.XM(NSTAT))GO TO 58
0122      CALL LAMBDX(LAMD11(I),VDY1(I),GAMMA1(I),GAMMA2(I),F,I,ALPL1
          1(I),BESTL,ISPLT(I),SPP(I),XM(1),XM(NSTAT))
0123      LAMD21(I)=BESTL
0124      C      CALCULATE THE VALUE OF THE IMPACT FORCE FOR THE 2D AND 3D JET
0125      IF(ABS(LAMD11(I)/GAMMA1(I)).LE.20.)GO TO 581

```

0126		EX1=0.	
0127		GO TO 582	00013060
0128	581	EX1=EXP(-LAMD11(I)/GAMMA1(I))	00013070
0129	582	IF(ABS(LAMD21(I)/GAMMA2(I)).LE.20.)GO TO 583	00013080
0130		EX2=0.	00013090
0131		GO TO 584	00013100
0132	583	EX2=EXP(-LAMD21(I)/GAMMA2(I))	00013110
0133	584	P0(I)=.5+DEN*VRL1(I)**2	00013120
0134		FIMP2D(I)=(P0(I)/2.)*(GAMMA1(I)*(3.+EX1*(EX1-4.))+GAMMA2(I)* (3.+EX2*(EX2-4.)))*(A-B)	00013130
0135		CALL P3D(RM1(I),ALPL1(I),P0(I),LAMD11(I),LAMD21(I),TLOAD)	00013140
0136		FIMP3D(I)=TLOAD	00013150
0137		GO TO 167	00013160
0138	58	FIMP2D(I)=0.	00013170
0139		FIMP3D(I)=0.	00013180
	C	SUM UP THE TOTAL IMPACT FORCE	00013190
0140	167	FIMP=FIMP2D(I)+FIMP3D(I)	00013200
	C	FIND OUT BETWEEN WHICH 2 NODES THE IMPACT OCCURS-IF THE IMPACT FOR	00013210
	C	IS ZERO-USE THE VALUE OF GAMMA IF IT(L) IS NOT GREATER THAN 1	00013220
	C	-USE THE MID-POINT OF THE BLADE IF II(L) IS 2	00013230
0141		IF(FIMP.EQ.0.)GO TO 163	00013240
0142		IF((SPP(I)-GMAL1(I)).LE.0.)SFIMP=GMAL1(I)-E	00013250
0143		IF((SPP(I)-GMAL1(I)).GT.0.)SFIMP=GMAL1(I)+E	00013260
0144		GO TO 164	00013270
0145	163	SFIMP=GMAL1(I)	00013280
	C	DISTRIBUTE THE FORCE BETWEEN THE TWO CLOSEST NODES AS PRESSURE	00013290
0146	164	MAXM1=MAX(I7)-1	00013300
0147		DO 166 J3=1,MAXM1	00013310
0148		XMA=SFIMP-XNODE(I7,J3)	00013320
0149		XMB=XNODE(I7,J3+1)-SFIMP	00013330
0150		IF(XMA.LT.0..OR.XMB.LT.0.)GO TO 166	00013340
0151		PRSS(I7,J3)=PRSS(I7,J3)+XMB*FIMP/(AANODE(I7,J3)*(XMA+XMB))	00013350
0152		PRSS(I7,J3+1)=PRSS(I7,J3+1)+XMA*FIMP/(AANODE(I7,J3+1)*(XMA+XMB))	00013360
0153		GO TO 100	00013370
0154	166	CONTINUE	00013380
0155	100	RETURN	00013410
0156		END	00013420
			00013430
			00013440